SIZE-FRACTIONATION OF AIRBORNE PARTICULATE MATTER AND PARTICIPATORY CITIZEN APPROACHES FOR AIR POLLUTION CONTROL AND HEALTH RISK ASSESSMENT

Anja Ilenič

Doctoral Dissertation
Jožef Stefan International Postgraduate School
Ljubljana, Slovenia

Supervisor: Prof. Dr. Janez Ščančar, Jožef Stefan International Postgraduate School and Jožef Stefan Institute, Ljubljana, Slovenia
Co-Supervisor: Dr. Alenka Mauko Pranjić, Slovenian National Building and Civil Engineering Institute, Ljubljana, Slovenia

Evaluation Board:
Assist. Prof. Dr. Janja Vidmar, Chair, Jožef Stefan International Postgraduate School and Jožef Stefan Institute, Ljubljana, Slovenia
Prof. Dr. Aleksander Zidanšek, Member, Jožef Stefan International Postgraduate School and Jožef Stefan Institute, Ljubljana, Slovenia
Prof. Dr. Prashant Kumar, Member, University of Surrey, United Kingdom

MEDNARODNA PODIPLOMSKA ŠOLA JOŽEFA STEFANA
JOŽEF STEFAN INTERNATIONAL POSTGRADUATE SCHOOL



Anja Ilenič

SIZE-FRACTIONATION OF AIRBORNE PARTICULATE MATTER AND PARTICIPATORY CITIZEN APPROACHES FOR AIR POLLUTION CONTROL AND HEALTH RISK ASSESSMENT

Doctoral Dissertation

VELIKOSTNO FRAKCIONIRANJE TRDNIH DELCEV V ZRAKU IN VKLJUČEVANJE DRŽAVLJANOV V NADZOR ONESNAŽENOSTI ZRAKA TER OCENO ZDRAVSTVENIH TVEGANJ

Doktorska disertacija

Supervisor: Prof. Dr. Janez Ščančar

Co-Supervisor: Dr. Alenka Mauko Pranjić

Ljubljana, Slovenia, February 2026

Acknowledgments

First and foremost, I would like to thank my supervisor, Prof. Dr. Janez Ščančar (Jožef Stefan International Postgraduate School, Jožef Stefan Institute) and my co-supervisor Dr. Alenka Mauko Pranjić (Slovenian National Building and Civil Engineering Institute), for their guidance from the initial topic proposal to the final manuscript. Thank you for believing in my abilities, your support and for sharing your extensive knowledge, which helped me navigate both academic and personal challenges throughout this journey.

Next, I extend my sincere appreciation to Prof. Dr. Radmila Milačič Ščančar (Jožef Stefan International Postgraduate School, Jožef Stefan Institute), whose continuous encouragement, scientific insights and optimism have been invaluable throughout my research.

My gratitude goes to the members of the evaluation board – Assist. Prof. Dr. Janja Vidmar (Jožef Stefan International Postgraduate School, Jožef Stefan Institute), Prof. Dr. Aleksander Zidanšek (Jožef Stefan International Postgraduate School, Jožef Stefan Institute) and Prof. Dr. Prashant Kumar (University of Surrey) for reviewing and evaluating my work.

I would like to thank Assist. Prof. Dr. Ana Mladenovič (Slovenian National Building and Civil Engineering Institute) for initially offering me the opportunity to pursue this PhD on such an important and meaningful topic, and Dr. Primož Oprčkal for supporting the continuation of this research. I am also grateful to other colleagues at ZAG: Dr. Marija Đurić for all her help with ICP-MS analyses and for brightening even the longest days in the laboratory, Dr. Sara Seršen for her assistance with PM sample collection, Dr. Mateja Košir, Dr. Mateja Štefančič and Dr. Vesna Zalar Serjun for help with SEM analyses, Žan Hauptman for all encouragements, Luka Škrlep for preparing protective gear for the instrumental setups, Matej Michelizza for help with 3D printing the framework structure of the low cost sensor, Mojca Škerl for last-minute lending of laboratory equipment, Uroš Ristić and Matjaž Hlebš for designing the metal cages for the PM sampling units, as well as anyone I may have unintentionally missed.

Next, I would like to thank Brigita Kozolc and Jure Jakše (National Laboratory of Health, Environment and Food), as well as Dr. Taja Verovšek (Jožef Stefan Institute), for all their assistance with the PAH analyses.

I would also like to express my sincere gratitude to Prof. Dr. Nina Zupančič (University of Ljubljana, Faculty of Natural Sciences and Engineering, ZRC SAZU Ivan Rakovec Institute of Palaeontology) for her patience and guidance in answering my seemingly endless questions regarding statistical analysis.

I would like to thank Mustafa Selimović, Janez Pečarič and Jožef Dšuban for their assistance with the installation of the PM sampling setups. I am also grateful to Petra Ilenič for adding a touch of fun to the PM sample collection. The one-year nationwide monitoring would not have been possible without the confirmed permits from municipalities, institutes and individuals, who allowed the setup installation on their premises. In particular, I would like to thank Dr. Katja Klun (National Institute of Biology), Assist. Prof. Dr. Irena Bačlija Brajnik (University of Ljubljana, Faculty of

Social Sciences, Municipality Dobrova – Polhov Gradec), Angelca Dokl Mir, Boris Gomiunik, Bernardka Ryan, Bogomir Rola and Tadej Fister (City Municipality Murska Sobota), Borut Hojnik (Nigrad, komunalno podjetje d.o.o.), Irena Kozar and Saša Bricman Rantuša (City Municipality of Maribor) as well as the Pavlič family (Bojan, Dana, Ana and Maša).

I am also grateful to the cycling volunteers who supported the citizen-led campaigns conducted in Ljubljana and Maribor, collecting $PM_{2.5}$ data, and to the Maribor and Ljubljana Cycling Associations. Special thanks to Blaž Gamse for his assistance.
I would like to express my sincere gratitude to Prof. Prashant Kumar for welcoming me twice at the University of Surrey as part of the research exchange, for his guidance, generosity and for making me feel at home while sharing invaluable knowledge and wisdom on air quality. Special thanks also to Dr. Ana Paula Mendes Emygdio and all other colleagues at the Global Centre for Clean Air Research (GCARE).

I am grateful for the financial support that enabled my research, international exchanges, conferences and publications. This includes support from the Slovenian National Building and Civil Engineering Institute, the Slovenian Research Agency's programme group P2-0273 and Developmental Funding Pillar, supporting the project SLO-CAPTURE (SLOvenian Commuters' Assessment of air Pollutants in Traffic related URban Environments), as well as funding from EIT Urban Mobility under Subgrant Agreement No. SGA22368. I also thank the Erasmus+ programme and the PROM programme under the Polish National Agency for Academic Exchange (NAWA), which enabled two research visits to the United Kingdom and one to Poland.

Last, but certainly not least, I want to thank the people who stood by me through every high and low. Your love and support made all the difference. In the end, such achievements matter far less if you cannot share them with those you love.

Abstract

Urban air pollution, with particulate matter (PM) classified as one of the most problematic primary pollutants, is characterised by wide spatio-temporal variability. Even at relatively low concentrations, PM poses significant health and environmental risks due to its high toxicity per unit mass, ability to penetrate deep into lung tissue and prolonged atmospheric residing times. Its size, chemical composition, hygroscopicity and optical properties strongly influence its toxicity, atmospheric distribution and behaviour within the human respiratory system, with negative effects more closely associated with (ultra)fine particles. Therefore, a comprehensive understanding of size-fractionated PM, particularly (ultra)fine fractions, is essential for hazard mitigation and the improvement of regulatory air pollution control strategies, yet available data remain limited. Combining gravimetric, size-fractionating PM sampling solutions with low-cost mobile sensors (LCS) can complement national air quality monitoring networks, overcoming the limitations of sparsely distributed stations and providing valuable insights into commuters' exposure, thereby improving the safety of most vulnerable traffic groups, such as cyclists and pedestrians. To address these challenges, an affordable, portable sampling device capable of collecting size-fractionated PM (PM_{10}, $PM_{2.5}$, $PM_{0.1}$ and $PM_{<0.1}$) was developed, together with optimised and validated analytical methods for the determination of metal(oid)s and polycyclic aromatic hydrocarbons (PAHs). The applicability of the device was further successfully demonstrated in a nationwide, systematic one-year study in Slovenia, at five pedestrian and cycling microenvironments (Dobrova, Ljubljana, Maribor, Murska Sobota, Piran), differing in size, population and traffic density. In parallel, two citizen-led campaigns were conducted in Ljubljana and Maribor, using bicycle-mounted LCS. The quality of the acquired data and sensor performance was evaluated in both controlled laboratory and co-location field environments. The overall aim was: i) to assess the seasonal and spatial distribution of PM-bound pollutants, ii) to conduct source apportionment analysis, iii) to evaluate the toxic potential and possible health and environmental risk implications, and iv) to highlight the importance of individual behavioural patterns in mitigating urban air pollution.

Povzetek

Onesnaženost zraka v urbanih okoljih, pri čemer so trdni delci (PM) opredeljeni kot eno izmed najbolj problematičnih primarnih onesnažil, zaznamuje velika prostorska in časovna spremenljivost. Tudi pri sorazmerno nizkih koncentracijah predstavljajo povišane koncentracije PM resno tveganje za zdravje in okolje zaradi visoke potencialne strupenosti na enoto mase, sposobnosti prodora globoko v pljučna tkiva ter dolgega zadrževanja v atmosferi. Velikost, kemijska sestava, higroskopnost in optične lastnosti močno vplivajo na njihovo strupenost, atmosfersko razporeditev ter obnašanje v človeškem dihalnem sistemu, pri čemer so ti učinki še posebej izraziti pri (ultra)finih delcih. Celovito razumevanje velikostno frakcioniranih PM, zlasti (ultra)finih delcev, je ključno za zmanjšanje tveganj in izboljšanje zakonskih okvirov za nadzor onesnaženosti zraka, vendar pa so razpoložljivi podatki še vedno omejeni. Integracija gravimetričnih metod vzorčenja PM po velikostnih frakcijah z nizkocenovnimi mobilnimi senzorji (LCS) lahko nadgradi državno mrežo za spremljanje kakovosti zraka, odpravi vrzeli razpršenih statičnih merilnih postaj in omogoči celovitejši vpogled v dinamično izpostavljenost potnikov, s posledično izboljšano varnostjo najbolj ranljivih skupin v prometu, kot so kolesarji in pešci. Za reševanje tega izziva je bil razvit cenovno dostopen prenosni vzorčevalnik, sestavljen iz kaskadnega sistema filtrov za lovljenje PM (PM_{10}, $PM_{2,5}$, $PM_{0,1}$ in $PM_{<0,1}$) skupaj z optimiziranimi in validiranimi analitskimi tehnikami za določanje koncentracij elementov (pol)kovin in policikličnih aromatskih ogljikovodikov (PAO). Uporabnost vzorčevalnika je bila uspešno dokazana v sistematični enoletni nacionalni študiji, izvedeni na petih slovenskih mikrolokacijah, namenjenih pešcem in kolesarjem (Dobrova, Ljubljana, Maribor, Murska Sobota, Piran), ki so se razlikovale po velikosti, številu prebivalcev in gostoti prometa. Vzporedno sta bili v Ljubljani in Mariboru izvedeni tudi dve pobudi občanske znanosti, ki sta vključevali LCS, nameščene na krmila koles. Zanesljivost podatkov in delovanje LCS sta bila predhodno ocenjena z laboratorijskimi in terenskimi preizkusi. Glavni cilji raziskave so bili: i) oceniti sezonsko in prostorsko razporeditev onesnažil, vezanih na PM, ii) identificirati potencialne vire v okolju, iii) oceniti potencialna tveganja za zdravje in okolje, ter iv) poudariti pomen individualnih vedenjskih vzorcev pri zmanjševanju urbanega onesnaženja zraka.

Contents

List of Figures **xv**

List of Tables **xvii**

Abbreviations **xix**

Symbols **xxiii**

1 Introduction **1**
1.1 Air Pollution 1
1.1.1 Air pollutants 1
1.1.2 Brief history of air pollution 2
1.1.3 Effects of air pollution on health, environment and economy 3
1.1.4 Air pollution prevention 4
1.2 Particulate Matter 6
1.2.1 Particulate matter-bound metal(oid)s 7
1.2.2 Particulate matter-bound polycyclic aromatic hydrocarbons 8
1.3 Aerosol Particulate Monitoring 9
1.4 Characterisation Methods 12
1.4.1 Inductively coupled plasma mass spectrometry 12
1.4.2 Gas chromatography mass spectrometry 13
1.4.3 Scanning electron microscopy 15

2 Research Aims and Hypothesis **17**

3 Scientific Publications **19**
3.1 Article 1: Innovative Sampling Device for Size-Fractionating Airborne Particulate Matter for Improved Air Pollution Control of Metal(oid)s and Polycyclic Aromatic Hydrocarbons 19
3.2 Article 2: Size-Fractionated Airborne Particulate Matter-Bound Metal(oid)s and Polycyclic Aromatic Hydrocarbons in Urban Pedestrian and Cycling Microenvironments: Seasonal Trends, Source Apportionment and Health Risk Assessment 46
3.3 Article 3: Can Low-Cost Sensors (LCS) Enhance Air Quality Monitoring for Personal Pollution Exposure Assessment? 105
3.4 Article 4: Fine Particulate Matter ($PM_{2.5}$) Exposure Assessment Among Active Daily Commuters to Induce Behaviour Change to Reduce Air Pollution 127
3.5 Article 5: Advances in Sampling and Analytical Approaches for the Determination of Metal(oid)s and Polycyclic Aromatic Hydrocarbons Bound to Size-Fractionated Airborne Particulate Matter: A Review 142

4 Conclusions **193**

References **197**

Bibliography **225**

Biography **229**

List of Figures

Figure 1: Schematic presentation of size-fractionated PM. 7
Figure 2: Comparison of PM fractions in the atmosphere and selected studies. 10
Figure 3: Schematic diagram of ICP-MS setup 13
Figure 4: Schematic diagram of GC-MS setup 14
Figure 5: Schematic diagram of SEM setup. 15

List of Tables

Table 1: Legal air quality standards and WHO guidelines for PM_{10} and $PM_{2.5}$ monitoring.5

Abbreviations

AAS	... Atomic absorption spectroscopy
Acc	... Accuracy
ANOVA	... Analysis of variance
APCS	... Absolute principal component score
AQD	... Air quality directive
AQG	... Air quality guidelines
AQI	... Air quality index
AQMS	... Air quality monitoring station
ARSO	... Slovenian Environment Agency
ASE	... Accelerated solvent extraction
AT	... Averaging time
BaP_{eq}	... Carcinogenic equivalent concentration of BaP
BC	... Black carbon
BSE	... Backscattered electrons
BTA	... Backward trajectory analysis
BW	... Body weight
CMB	... Chemical mass balance
CMC	... Crustal matter contribution
COD	... Coefficient of divergences
CPF	... Conditional probability function
CRM	... Certified reference material
CWT	... Concentration weighted trajectory
DAD	... Dermal absorption dose
DB	... Dobrova
DQO	... Data quality objectives
DR	... Diagnostic ratios
EC	... Elemental carbon
ED	... Exposure duration
EDX	... Energy dispersive X-ray microanalyser
ED-XRF	... Energy dispersive X-ray fluorescence
EEA	... European Environment Agency
EF	... Exposure frequency
ENF	... Enrichment factor
EL	... Elevated level airborne particulate matter sampler
Er	... Error
ETAAS	... Electrothermal atomic absorption spectrometry
EU	... European Union
FA	... Factor analysis
FAAS	... Flame atomic absorption spectroscopy
FGF	... Fiberglass fabric filters
GC-FID	... Gas chromatography coupled with the flame ionisation detector

GC-MS	... Gas chromatography coupled with mass spectrometry
GC-MS/MS	... Gas chromatography coupled to a triple quadrupole mass spectrometer
GC-Q-TOF-MS	... Gas chromatography coupled with quadrupole time-of flight mass spectrometry system
GFF	... Glass fiber filters
GIS	... Geographic information system
GL	... Ground level airborne particulate matter sampler
GPS	... Global positioning system
HCA	... Hierarchical component analysis
HI	... Hazard index
HMW PAH	... High-molecular weight polycyclic aromatic hydrocarbon
HP	... Heating period
HOP	... Hot plate
HPLC	... High performance liquid chromatography
HPLC/FLD	... High-pressure liquid chromatography with programmable fluorescence detection
HQ	... Hazard quotient
HVS	... High-volume airborne particulate matter sampler
IARC	... International Agency for Research on Cancer
ICP-MS	... Inductively coupled plasma mass spectrometry
ICP-OES	... Inductively coupled plasma atomic emission spectroscopy
ILCR	... Incremental lifetime cancer risk
IPS	... International Postgraduate School
IR	... Inhalation rate
ISO	... International Organisation for Standardisation
JSI	... Jožef Stefan Institute
LADD	... Lifetime daily exposure dose
LC-FLD	... Liquid chromatography with fluorescent detector
LCS	... Low-cost sensor
LJ	... Ljubljana
LLE	... Liquid-liquid extraction
LLEX	... Loss of life expectancy
LMW PAH	... Low-molecular weight polycyclic aromatic hydrocarbons
LOD	... Limit of detection
LOQ	... Limit of quantification
LRM	... Linear regression models
LVS	... Low-volume airborne particulate matter sampler
MAD	... Microwave assisted digestion
MB	... Maribor
MRA	... Multivariate regression analysis
MS	... Murska Sobota
MSD	... Mass selective detector
MSE	... Mechanical shaking extraction
MVS	... Medium-volume airborne particulate matter sampler
n/a	... Not applicable
NCF	... Nitrocellulose membrane filters
NHP	... Non-heating period
NIST	... National Institute of Standards and Technology
nr	... Not reported

OECD	... The Organisation for Economic Cooperation and Development
OM	... Organic matter
OPC	... Optical particle counter
PAH	... Polycyclic aromatic hydrocarbons
PBL	... Planetary boundary layer
PCA	... Principal component analysis
PF	... Polycarbonate filter
PGE	... Platinum group elements
PIXE	... Proton induced X-ray emission
PM	... Particulate matter
$PM_{<0.1}$	... Particulate matter with aerodynamic diameter smaller than 0.1 µm, captured in ultrapure water trap
$PM_{0.1}$	... Particulate matter with aerodynamic diameter smaller than 0.1 µm
PM_{1}	... Particulate matter with aerodynamic diameter smaller than 1 µm
$PM_{2.5}$	... Particulate matter with aerodynamic diameter smaller than 2.5 µm
PM_{10}	... Particulate matter with aerodynamic diameter smaller than 10 µm
PMF	... Positive matrix factorisation
PR	... Piran
Prec	... Precision
PSCF	... Potential source contribution function
PTFE	... Polytetrafluoroethylene filter
QA/QC	... Quality assurance quality control
QFF	... Quartz fiber filter
RC	... Relative abundance marker of an individual polycyclic aromatic hydrocarbon to the carcinogenic marker benzo(a)pyrene
RE	... Roadside enrichment
Rec	... Recovery
RfC	... Reference concentration
RfD	... Reference dose
RH	... Relative humidity
RHT	... Rush hour time
RMSE	... Root mean square error
RSD	... Relative standard deviation
SDG	... Sustainable development goal
SE	... Secondary electrons
SEM	... Scanning electron microscopy
SF-ICP-MS	... Sector field inductively coupled plasma mass spectrometry
SIST	... Slovenian Institute for Standardisation
SOE	... Soxhlet extraction
SOM	... Self-organising maps
SPS30	... Sensirion SPS30
SPS-SW1	... Standard reference material for measuring elements in surface waters
SRM	... Standard reference material
SURS	... Statistical Office of the Republic of Slovenia
TD-GC-MS	... Thermal desorption gas chromatography mass spectrometry
TSP	... Total suspended particles
TXRF	... Total reflection X-ray fluorescence spectroscopy
UAE	... Ultrasound assisted extraction
UFP	... Ultrafine particle
UN	... United Nations

Unc	... Uncertainty
UNMIX	... UNMIX multivariate receptor model US EPA
US EPA	... United States Environmental Protection Agency
VOC	... Volatile organic compound
VSL	... Value of a statistical life
WHO	... World Health Organisation
WRF-Chem	... Weather research and forecasting model with chemistry
XPS	... X-ray photoelectron spectroscopy
XRF	... X-ray fluorescence
ZAG	... Slovenian National Building and Civil Engineering Institute

Symbols

%	... Percentage
$^{\circ}$C	... Celsius
µCi	... Microcurie
µg m^{-3}	... Microgram per cubic metre
µg mL^{-1}	... Microgram per millilitre
µL	... Microliter
µm	... Micrometre
^{14}C	... Carbon-14
Å	... Angstrom (10^{-10} metre)
Ace	... Acetone (C_3H_6O)
Ar	... Argon
As	... Arsenic
a_w	... Water activity
Ba	... Barium
BaA	... Benzo(a)anthracene
BaP	... Benzo(a)pyrene
BbF	... Benzo(b)fluoranthene
Beq	... Becquerel
BghiP	... Benzo(ghi)perylene
BkF	... Benzo(k)fluoranthene
Br^-	... Bromine
C_3H_8O	... Isopropyl alcohol
Cd	... Cadmium
Ce	... Cerium
Ch	... Chrysene
CH_2Cl_2	... Methylene chloride
Chx	... Cyclohexane
Cl^-	... Chlorine
Co	... Cobalt
CO	... Carbon monoxide
CO_2	... Carbon dioxide
Cr	... Chromium
Cu	... Copper
DCM	... Dichloromethane
Eth	... Diethyl ether
Fl	... Fluoranthene
g	... Gram

g cm^{-3} ... Gram per cubic centimetre
Ge ... Germanium
h ... Hour
H_2O ... Water
H_2O_2 ... Hydrogen peroxide
H_2SO_4 ... Sulfuric acid
H_3BO_3 ... Boric acid
HCl ... Hydrochloric acid
$HClO_4$ ... Perchloric acid
HF ... Hydrofluoric acid
HNO_3 ... Nitric acid
Hx ... Hexane (C_6H_{14})
IP ... Indeno(1,2,3-cd)pyrene
Ir ... Iridium
K ... Kelvin
kg ... Kilogram
km h^{-1} ... Kilometre per hour
kV ... Kilovolt
L min^{-1} ... Litres per minute
L s^{-1} ... Litres per second
La ... Lanthanum
m ... Metre
m/z ... Mass-to-charge ratio
m^3 h^{-1} ... Cubic metres per hour
m^3 min^{-1} ... Cubic meters per minute
mbar ... Millibar
MeCN ... Acetonitrile
MeOH ... Methanol
mg ... Milligram
mg kg^{-1} ... Milligram per kilogram
mg L^{-1} ... Milligram per litre
mg m^{-3} ... Milligram per cubic metre
mg mL^{-1} ... Milligram per millilitre
MgO_3Si ... Activated magnesium silicate (Strata FL-PR Florisil)
MHz ... Megahertz
min ... Minute
mL ... Millilitre
mm ... Millimetre
Mo ... Molybdenum
mol L^{-1} ... Mole per litre
N_2 ... Nitrogen
Na_2SO_4 ... Sodium sulphate
NaOH ... Sodium hydroxide
ng m^{-3} ... Nanogram per cubic metre
NH_3 ... Ammonia
Ni ... Nickel
nm ... Nanometre
NO ... Nitric oxide
NO_2 ... Nitrogen dioxide
NO_x ... Nitrogen oxides (NO, NO_2)
O_3 ... Ozone

Pyr ... Pyrene
Pa ... Pascal
Pb ... Lead
Pd ... Palladium
Pet Eth ... Petroleum ether
Pt ... Platinum
R^2 ... Coefficient of determination
Rh ... Rhodium
rpm ... Rotations per minute
s ... Second
SO_2 ... Sulfur dioxide
T ... Temperature
Tl ... Thallium
Tol ... Toluene
V ... Vanadium
W ... Watt
Zn ... Zinc
δ ... Percentage discrepancy between LCS and AQMS
κ ... Particle hygroscopicity depending on particle composition (1.65 g cm^{-3})

Chapter 1

Introduction

1.1 Air Pollution

Outdoor air pollution is considered one of the greatest global challenges of the 21st century. It refers to any substance emitted into the air from natural or anthropogenic sources, which is either unnatural in the atmosphere or present at very high concentrations, and is capable of causing short or long-term harm (Daly and Zannetti, 2007). It is characterised by significant temporal and spatial variability, with high exposure risks even at relatively low pollutant concentration, with estimated 99% of the global population exposed to somewhat elevated levels of air pollution (World Health Organisation (WHO), 2025).

Natural sources of air pollution include geogenic and biogenic sources, i.e. in-situ weathering processes of crustal material, sea salt, biological material in the form of pollen, spores, algae, plant and animal debris, as well as volcanic eruptions and wind erosion. In addition to natural sources, anthropogenic sources can be divided into stationary and mobile, and include combustion sources, such as burning of biomass and fossil fuels, industrial emissions, raw material excavation and ore processing, agricultural activities, waste incineration plants and vehicle emissions (Fenger et al., 1998; Gatari et al., 2006; Kukutschová et al., 2011; Pant and Harrison, 2013; Pénard-Morand and Annesi-Maesano, 2004; Sanderson et al., 2014; Thorpe and Harrison, 2008).

Polluted outdoor air can also significantly influence indoor air quality, particularly in poorly ventilated buildings, where pollutants accumulate and potentially reach higher concentrations than outside, a phenomenon known as “sick building syndrome”. The main sources typically include tobacco smoke, heating, cleaning and renovation activities, bacteria and algae-derived endotoxins and radon emissions (Daly and Zannetti, 2007).

1.1.1 Air pollutants

Air pollutants are categorised into primary and secondary air pollutants. Primary pollutants are those released directly from a source in their original chemical form, while secondary pollutants result from the transformations of primary pollutants through various mechanical, physical, chemical or biological processes (Daly and Zannetti, 2007; Phalen and Phalen, 2013). These processes can include: advection (transport due to mass transfer), dispersion (transport from the source), diffusion (transport controlled by concentration gradients), sedimentation (denser compounds deposit first), filtration (mesh retention), volatilisation (phase partitioning to vapour), dissolution (formation of hydrated compounds), absorption and adsorption(retention on a solid surface), hydrolysis (reaction of water molecules with pollutants), oxidation or reduction (electron loss or

gain), photolysis (light induced chemical bond breaking), photooxidation (light induced oxidation reactions) and biodegradation (microbially-catalysed reactions) (Vallero, 2008).

The most common primary pollutants are carbon compounds (e.g. carbon monoxide (CO), carbon dioxide (CO_2), methane, volatile organic compounds (VOCs)), nitrogen compounds (e.g. nitric oxide (NO), nitrous oxide, ammonia (NH_3)), sulfur compounds (e.g. hydrogen sulfide, sulfur dioxide (SO_2)), halogen compounds (chlorine (Cl^-), fluorine, bromine (Br^-)) and particulate matter (PM) (Daly and Zannetti, 2007).

Secondary compounds include: nitrogen dioxide (NO_2) and nitric acid (HNO_3) formed from NO, ozone (O_3) formed by photochemical reactions of nitrogen oxides (NO_x) and VOCs, sulfuric acid (H_2SO_4) and HNO_3 droplets formed from SO_2 and NO_2, sulfate and nitrate aerosols formed by reactions of H_2SO_4 and HNO_3 droplets with NH_3, and organic aerosols formed from VOCs in gas to particle partitioning reactions (Daly and Zannetti, 2007).

1.1.2 Brief history of air pollution

Indoor and outdoor air pollution were recognised as a threat to human health early in human history (Fenger et al., 1998; Fowler et al., 2020). In ancient times, the first mentions of indoor air pollution were associated with improper cooking and heating with open fires in poorly ventilated dwellings. Early health implications associated with poor air quality were evident in mummified lung tissue showing anthracosis and skeletal indications such as destruction of the palate and wall of the maxillary sinus as evidence of sinusitis resulting from long-term exposure to acrid smoke from domestic fireplaces (Brimblecombe, 1999; Fenger et al., 1998; Mosley, 2014). Outdoor air pollution was a particular issue in cities, which importance was first highlighted by Hippocrates (400 BC) (Fowler et al., 2020; Mosley, 2014). Air pollution was also an everyday problem for the inhabitants of Athens and Rome, the term described by Horace and Seneca as smoke clouds of heavy heaven and infamous air (Fowler et al., 2020; Mosley, 2014; Vallero, 2008).

The radical transition from wood to coal (13^{th} century) and the subsequent development of chimneys and steam engines (16^{th} century) initiated the industrial revolution, the rise of industrial towns and cities, as well as the unprecedented emission increase (Brimblecombe, 1999; Fenger et al., 1998; Fowler et al., 2020; Vallero, 2008).

One of the earliest laws regulating environmental and air pollution was enacted with the English Common Law (17^{th} century), which invoked the right to clean air on private properties (Mosley, 2014). In 1810, Emperor Napoleon imposed regulations on odorous businesses and limited the height of industrial chimneys (Fenger et al., 1998). The 20^{th} century began with a greater acceptance of the adverse effects of air pollution and the introduction of quantitative monitoring methods, including dust counters, lead (Pb) candles and paper filters for smoke monitoring (Brimblecombe, 1999; Fenger et al., 1998). In addition, air quality legislation intensified following the Great London Smog Event (1952), a major pollution disaster responsible for an estimated 12,000 deaths (Fenger et al., 1998; Fowler et al., 2020; Mosley, 2014; Vallero, 2008). This disaster was the catalyst for stricter air pollution control, including the Clean Air Act (1956), which encouraged the transition from coal-fired home heating to central or electric heating and introduced the first comprehensive regulation of residential and industrial smoke emissions (Fowler et al., 2020; Mosley, 2014; Vallero, 2008). After the Second World War, automobiles emerged and air pollution increased, with emitted NO_2 recognised as the main cause of acid rain (Mosley, 2014).

Concurrently, the understanding of primary pollutants (e.g. SO_2, NO_2) and their atmospheric transformations into secondary pollutants became increasingly important

(Brimblecombe, 1999). To mitigate their impacts, the United States Environmental Protection Agency (US EPA) established the National ambient air quality standards under the Clean Air Act in 1970, defining and regulating six criteria pollutants, including PM with additional subcategories classified by size, SO_2, NO_x, CO, O_3 and Pb (Daly and Zannetti, 2007; Vallero, 2008).

In 1972, the United Nations (UN) conference was organised, providing a platform for a global dialogue on environmental issues and leading to the acceptance of the Convention on long-range transboundary pollution to reduce SO_2 emissions (Mosley, 2014). Unfortunately, in 2012, SO_2 levels in Beijing, China reached concentrations comparable to those observed during the Great London Smog event. Moreover, NO_2 concentrations peaked in 2019, but in 2020 a global decline in SO_2, NO_2, VOCs and primary PM concentrations was recorded as a consequence of the COVID-19 pandemic (Fowler et al., 2020).

1.1.3 Effects of air pollution on health, environment and economy

Air pollution is one of the biggest health and environmental risks, particularly in urban and densely populated areas due to the high morbidity and mortality rates caused mainly by six pollutants – PM, SO_2, NO_x, CO, O_3 and Pb (Daly and Zannetti, 2007; The Organisation for Economic Cooperation and Development (OECD) 2016; Vallero 2008).

PM is considered as one of the most prevalent primary airborne pollutants and can cause significant environmental and health risks. The accumulation of PM in the respiratory system is associated with impaired pulmonary and cardiovascular function, including stroke and lung cancer, neuroinflammation, neuron apoptosis, induced oxidative stress and dopaminergic neurotoxicity, deterioration of cognitive functions and altered brain development. High concentrations can also cause haze and reduce visibility (Chen et al., 2008; Cohen et al., 2017; Dominici et al., 2006; Fan et al., 2020; Potter et al., 2021; Russell and Brunekreef, 2009). In addition, increased PM levels also disrupt aquatic and terrestrial ecosystems, cause soil acidification, nutrient depletion, eutrophication, reduce biodiversity, damage crops and forests, as well as contribute to acid rain formation (Daly and Zannetti, 2007; Gozzi et al., 2017; Kuo, 2018; Vallero, 2008).

SO_2 is a colourless compound with a pungent odour, derived from fuels containing sulfur (e.g. oil, coal). Long-term exposure can lead to irritation of lung tissue and damage of foliage, impaired plant growth, formation of acid rain and also reduce visibility (Daly and Zannetti, 2007; Kuo, 2018).

NO_x (NO, NO_2), produced in vehicle exhaust gases, play an important role in the formation of O_3 in the troposphere and acid rain. Large quantities of NO_x in the environment impair visibility, contribute to nutrient pollution in coastal waters and increase the risk of acute and chronic respiratory diseases (Daly and Zannetti, 2007; Kuo, 2018; Vallero, 2008).

CO is an odourless and colourless gas produced by the incomplete combustion of fossil fuels. Long-term inhalation can lead to a reduction in blood oxygen levels, which can result in headaches, dizziness or death (Daly and Zannetti, 2007; Kuo, 2018; Vallero, 2008).

O_3 is a secondary pollutant produced by photochemical reactions of NO_x and VOCs and can cause eye irritation, shortness of breath or asthma. Elevated O_3 concentrations also reduce photosynthesis, slow down plant growth, increase the risk of disease and insect damage, lead to a loss of biodiversity and habitat quality, as well as impair water and nutrient cycling (Daly and Zannetti, 2007; Kuo, 2018; Vallero, 2008).

Elevated concentrations of atmospheric Pb primarily originated from the historical use of leaded gasoline, but have decreased significantly due to its gradual elimination in

recent years. Pb is also produced by solid waste, coal and oil combustion, iron and steel production, Pb smelting and tobacco smoke. It can accumulate in bones and damage kidneys, nervous and immune system, as well as cardiovascular and reproductive system (Daly and Zannetti, 2007; Kuo, 2018; Vallero, 2008).

In addition to the effects on health and the environment, air pollution also causes material damage, affects agriculture, tourism and leisure activities and has an impact on historical and cultural monuments and electronics (Fenger et al., 1998; OECD, 2016).

The negative effects of air pollution on health and environment also lead to high economic costs, with the value of a statistical life (VSL) estimating the economic costs of outdoor air pollution. The VSL in OECD countries was USD 1.7 trillion in 2010, USD 3 trillion in 2015 and is estimated to reach USD 18−25 trillion by 2060 (OECD, 2015; OECD, 2016). The greatest impact of air pollution on the global economy results in premature deaths due to high PM and O_3 concentrations, estimated at 6−9 million deaths by 2060, particularly in densely populated cities (e.g. China and India) and in regions with ageing populations (e.g. China, Eastern Europe). The estimated increase in sickness-related absences, hospital admissions and associated healthcare expenditure, with the total estimated cost rising from USD 21 billion in 2015 to USD 176 billion in 2060. The economic costs of poor air quality is estimated to reach 1% of global gross domestic product by 2060, with the highest losses projected for China (−2.6%), the Caspian region (−3.1%) and Eastern Europe (non-OECD European Union (EU): −2.7%, the rest of Europe: −2.0%), with the main impact of air pollution leading to a reduction in capital accumulation and a slowdown in economic growth. The average global per capita welfare costs due to mortality and morbidity are expected to rise from USD <500 per person in 2015 to around USD 2100−2800 in 2060 (OECD, 2016).

1.1.4 Air pollution prevention

Ground-level O_3, NO_2 and PM, particularly fine particulate matter ($PM_{2.5}$) or smaller, are considered as one of the most detrimental urban air pollutants. Although concentrations have steadily decreased across the EU, there are still significant environmental and health challenges associated with poor air quality in many cities. Between 2000 and 2019, total PM and $PM_{2.5}$ concentrations have decreased at average rates of -4% year^{-1} and -0.2% year^{-1}, respectively, while annual NO_2 and O_3 concentrations have increased by $+0.4\%$ year^{-1} and $+0.8\%$ year^{-1}, respectively (Anenberg et al., 2022; Gozzi et al., 2017; Pascal et al., 2013; Sicard et al., 2023).

In Slovenia, concentrations of PM_{10} and $PM_{2.5}$ decreased by 25% between 2000 and 2019, mainly due to improvements in energy efficiency, modernisation of combustion and technological processes, the substitution of solid fuels with natural gas and renewable energy sources, the implementation of stricter regulatory standards for vehicle and industrial emissions, as well as short- and long-term air quality limit values (Slovenian Environment Agency (ARSO), 2021). Available data indicate that poor air quality is responsible for an estimated 300,000 premature deaths annually in the EU, including approximately 1,200 in Slovenia (ARSO, 2021; European Environment Agency (EEA), 2022).

Air quality is commonly assessed using the air quality index (AQI) developed by the US EPA, a measure of a degree of air pollution relative to its potential to inflict harm to the environment and human health. In general, the AQI is categorised as good (AQI <50), moderate or unhealthy (AQI >100) (Orosa, 2011).

In Slovenia, the Decree on ambient air quality (Official Gazette of the Republic of Slovenia no. 9/11, 8/15, 66/18, 14/22 − ZVO-2) is currently in force, which transposes the Directive 2008/50/EC of the European Parliament and of the Council of 21 May

2008 on ambient air quality and cleaner air for Europe into national legislation. This directive defines and sets criteria, as well as annual and daily limit values for ambient air pollutants, in order to prevent and mitigate adverse effects (Table 1). The current annual limit values are 40 µg m^{-3} for the coarse PM fraction (PM_{10}) and 25 µg m^{-3} for $PM_{2.5}$. A new Directive 2024/2881 of the European Parliament and of the Council of 23 October 2024 on ambient air quality and cleaner air for Europe, adopted in 2024, introduces stricter limit values to be achieved by 2030, with a limit of 20 µg m^{-3} for PM_{10} and 10 µg m^{-3} for $PM_{2.5}$.

In addition to the legally established standards, WHO guidelines indicate that harmful effects can already occur at concentrations as low as 5 µg m^{-3} for PM_{10} and 15 µg m^{-3} for $PM_{2.5}$ (WHO, 2025).

Table 1: Legal air quality standards and WHO guidelines for PM_{10} and $PM_{2.5}$ monitoring.

	Directive 2008/50/EC	Directive 2024/2881	WHO guidelines	Averaging time (AT)
PM_{10} (µg m^{-3})	40	20	15	1 year
	50	*n/a*	45	24 hours
$PM_{2.5}$ (µg m^{-3})	25	10	5	1 year
	n/a	*n/a*	15	24 hours

Glossary: *n/a* = not applicable.

The Decree on ambient air quality (2011) also sets limit values for SO_2, with limits of 350 µg m^{-3} for hourly measurements and 125 µg m^{-3} for daily measurements; a daily limit of 10 mg m^{-3} is set for CO and 0.5 µg m^{-3} for Pb. The annual limit value for CO_2 is 40 µg m^{-3} and 200 µg m^{-3} for hourly measurements. The annual limit value for benzene is 5 µg m^{-3}, while O_3 concentrations have daily limit value set at 120 µg m^{-3} (Decree on ambient air quality, Off. Gaz. of RS no. 9/11, 8/15, 66/18, 14/22 − ZVO-2). Certain air pollutants with well-established epidemiological and toxicological impacts are also regulated by the Decree on arsenic (As), cadmium (Cd), mercury, nickel (Ni) and polycyclic aromatic hydrocarbons (PAHs) in the ambient air (Off. Gaz. of RS no. 56/06, 44/22 − ZVO-2), which implements Directive 2004/107/EC of the European Parliament and of the Council of 15 December 2004 relating to arsenic, cadmium, mercury, nickel and PAHs in ambient air. This legislation establishes annual target values of 1 ng m^{-3} for benzo(a)pyrene (BaP), and 6 ng m^{-3}, 5 ng m^{-3} and 20 ng m^{-3} for As, Cd and Ni, respectively (Off. Gaz. of RS no. 56/06, 44/22 − ZVO-2). In addition, the Decree on the rules of assessment of ambient air quality (Off. Gaz. of RS no. 55/11, 6/15, 5/17, 44/22 − ZVO-2) and the Decree on the classification of areas, agglomerations and sub-areas according to ambient air pollution (Off. Gaz. of RS no. 38/17, 3/20, 152/20, 203/21, 44/22 − ZVO-2, 30/23) provide essential frameworks for evaluating air quality and ensuring a healthy urban environment.

In general, national target levels for reducing outdoor air pollution are defined within each country's obligations and are established within the National emission reduction commitments directive (2016/2884). In Slovenia, these commitments are implemented through the Regulation on national upper limits of ambient air pollutant emissions (Off. Gaz. of RS no. 48/18, 44/22 − ZVO-2, 95/24).

Beyond the regulatory framework and social responsibilities, the mitigation and reduction of air pollutants is also advanced by the European Green Deal, an EU strategy aiming to achieve climate neutrality by 2050 and a pollution-free environment. Key supporting sub-strategies and plans include: i) the zero-pollution action plan for water,

air and soil (2021), which targets a 55% reduction in premature deaths from air pollutants by 2030, relative to 2005, and a 25% reduction in ecosystem biodiversity risks, ii) the Euro 7 regulation under the Sustainable and smart mobility strategy (2020), which introduces stricter emission limits for vehicles, including exhaust and non-exhaust sources (e.g. tyre wear and brake wear), iii) nature-based solutions for cleaner air, outlined in Biodiversity strategy for 2030 (2020) (European Commission, 2025; European Council, 2024; European Parliament, 2024). These measures are also closely aligned with the 17 sustainable development goals (SDGs), a global agenda set by the UN in 2014, in particular with SDG 3 – Good health and well-being, SDG 7 – Affordable and clean energy, SDG 11 – Sustainable cities and communities, SDG 12 – Responsible consumption and production, SDG 13 – Climate action and SDG 15 – Life on land (UN, 2024).

1.2 Particulate Matter

PM is defined as a dispersed, heterogeneous mixture of liquid and solid particles suspended in the air. It consists mainly of organic matter (OM) and elemental carbon (EC), which account for approximately 70% of the total PM mass, but also of secondary inorganic aerosols, including sulfates and nitrogen compounds, as well as crustal material and metals, which contribute up to 15% of the total PM mass (Calvo et al., 2013; Hopke et al., 2020; Kelly and Fussell, 2012; Kim et al., 2013). Particles originate from natural sources, including sea salt, dust, volcanic eruptions, forest fires and microbial activity, as well as anthropogenic activities such as fossil fuel combustion, vehicular emissions, industrial and agricultural processes, construction and demolition work (Gatari et al., 2006; Gozzi et al., 2017; Kukutschová et al., 2011; Pant and Harrison, 2013; Phalen and Phalen, 2013; Potter et al., 2021; Sanderson et al., 2014; Thorpe and Harrison, 2008).

PM can also be categorised into primary and secondary PM, with secondary PM produced primarily by the following mechanisms: condensation or chemical transformation of gases and vapours into particles, chemical reactions of primary PM with gases or vapours producing new particle species, coagulation of different primary PM into larger and more complex particles, acquisition of surface coatings on solid particles that alter their composition and possibly biological activity (Phalen and Phalen, 2013).

The main sources of PM in Europe are secondary inorganic aerosols (32%), traffic (23%), coal (22%), dust (18%), sea salt (13%), biomass burning (12%) and industrial emissions (9%). In Slovenia, domestic heating (66%) and traffic emissions (8%), in particular diesel emissions, are recognised as the main anthropogenic source of PM (ARSO, 2021; Terzič, 2020). Most households (62%) use central heating systems powered by coal or wood biomass, while the most common primary heating fuels are wood logs (30%), natural or propane gas (19%) and renewable sources (14%) (Inglič et al., 2024). In 2021, the average PM_{10} concentration in Slovenia was 20.6 µg m^{-3}, while in the EU it was 18.5 µg m^{-3}, and the average $PM_{2.5}$ concentration in Slovenia was 12.3 µg m^{-3}, while in the EU it was 10.5 µg m^{-3} (ARSO, 2021).

The toxicological and environmental implications of PM are influenced by its size, chemical composition, water affinity and optical properties, such as light scattering and absorption (Chow, 1995). Both, atmospheric and biological behaviour, primarily depend on PM chemical composition and particle size (Fernández-Camacho et al., 2012; Morawska et al., 2008; Raaschou-Nielsen et al., 2013). Therefore, the systematic classification of particles based on their aerodynamic diameter is considered one of the most important parameters (Figure 1). Total suspended particles (TSP) with an

aerodynamic diameter between 50 and 100 µm and coarse particles or PM_{10} (aerodynamic diameter <10 µm) tend to deposit in the upper respiratory tract, in the nasopharynx, while fine particles or $PM_{2.5}$ (aerodynamic diameter <2.5 µm) and ultrafine particles (UFP) or $PM_{0.1}$ with aerodynamic diameter <0.1 µm behave similarly to gas molecules, enabling them to reach the terminal bronchioles and alveoli, cross the pulmonary blood-air barrier and translocate further into cell tissue and possibly cause damage to the nervous system (Gozzi et al., 2017; Potter et al., 2021; Valavanidis et al., 2008; Zioła and Słaby, 2020). In addition, 50% of fine and UFPs remain in the lung parenchyma and adsorb toxic pollutants more efficiently due to their large specific surface area (Lippmann, 1998; MacNee and Donaldson, 2003; Valavanidis et al., 2008). These particles have longer atmospheric residing times, ranging from a few hours to weeks, until they are removed by either wet or dry deposition (US EPA, 2019).

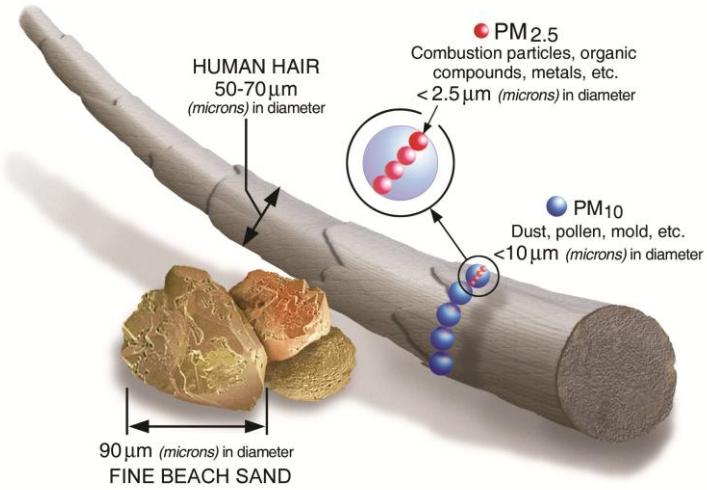


Figure 1: Schematic presentation of size-fractionated PM (Reproduced from US EPA, 2016).

Due to the proven linear relationship between ambient PM concentration and increased health risks, the International Agency for Research on Cancer (IARC) has classified outdoor air pollution with PM as a Group 1 carcinogen (IARC, 2016; WHO, 2015). The accumulation of PM in the respiratory system is associated with the development of chronic respiratory and cardiovascular diseases, including atherosclerosis progression, impaired lung function and increased premature mortality (Guaita et al., 2011; Halonen et al., 2009; Perez et al., 2012; Samoli et al., 2008; Suwa et al., 2002). In addition, increased PM concentrations also disrupt aquatic and terrestrial ecosystems (Gozzi et al., 2017). These adverse effects are commonly attributed to metal(oid)s or PAHs bound to PM, due to their high toxicity, a high bioaccumulation potential and the capacity to induce oxidative stress (EEA, 2012; Gao and Ji, 2018).

1.2.1 Particulate matter-bound metal(oid)s

Metal(oid) pollutants such as As, Cd, Ni and Pb are persistent, non-degradable and recognised as genotoxic carcinogens (Directive 2004/107/EC; EEA, 2013). They accumulate in fatty tissue, potentially impair organ and endocrine functions and induce DNA mutations (Briffa et al., 2020; Sah et al., 2019). Due to their atmospheric stability, certain elemental ratios, including barium (Ba), Cd, copper (Cu), Ni, Pb, vanadium (V)

and zinc (Zn), serve as reliable tracers of emission sources from combustion (gasoline, diesel), non-exhaust traffic emissions (tyre and break wear) and also mineral dust re-suspension (Alves et al., 2017; Fomba et al., 2018; IARC, 2016; Morawska et al., 2008; Pio et al., 2013; Prati et al., 2000; Qin et al., 1997; Thorpe and Harrison, 2008).

1.2.2 Particulate matter-bound polycyclic aromatic hydrocarbons

PAHs are a group of semi-volatile organic pollutants that contain at least two benzene rings fused linearly, angularly or in cluster arrangements and exhibit carcinogenic, mutagenic and immunosuppressive properties (Jakovljević et al., 2020; Ravindra et al., 2008; Zioła and Słaby, 2020). They are formed by incomplete combustion of OM (e.g. coal, natural gas or oil) or pyrolysis at high temperatures and in the absence of oxygen, with the main urban sources associated with municipal and domestic emissions (Kim et al., 2013; Ravindra et al., 2008; Zioła and Słaby, 2020).

In the atmosphere, PAHs partition based on their volatility, with low-molecular weight (LMW) PAHs (2−3 rings) occurring predominantly in the gaseous phase, while high-molecular weight (HMW) PAHs (4 or more benzene rings), which exhibit lower vapour pressures, favour partitioning to PM. The carcinogenicity of PAHs increases with the molecular weight (Bandowe et al., 2014; Ravindra et al., 2008). It is estimated, that more than 95% of all PAHs are bound to PM <3 µm. (Agudelo-Castañeda and Teixeira, 2014; Morawska et al., 2008; Wei et al., 2010).

The US EPA has classified 16 unsubstituted PAHs as priority pollutants, of which benzo(a)anthracene (BaA), BaP, benzo(b)fluoranthene (BbF), benzo(g,h,i)perylene (BghiP), chrysene (Ch) and indeno(1,2,3-cd)pyrene (IP) are of particular concern. Other compounds include naphthalene, acenaphthylene, acenaphthene, fluorine, phenanthrene, anthracene, fluoranthene (Fl), pyrene (Pyr), benzo(k)fluoranthene and dibenzo(a,h)anthracene (US EPA, 2017; WHO, 2010).

PAHs are typically characterised by strong seasonal variations, primarily due to greater atmospheric stability in winter, enhanced partitioning of HMW PAHs into particulate phase due to reduced volatility and more efficient volatilisation of LMW PAHs into gaseous phase combined with intensified photochemical degradation during summer (Ambade et al., 2022; Khan et al., 2018; Liu et al., 2017; Pindado et al., 2009; Song et al., 2019). HMW PAHs are more stable and less reactive compared to LMW PAHs, therefore their diagnostic ratios with similar physiochemical properties derived from a specific formation mechanism, can serve as characteristic markers for the main PAH sources (e.g pyrogenic, petrogenic), as well as for the pollutant transport distances (Alam et al., 2015; Khalili et al., 1995; Ravindra et al., 2008; Tan et al., 2011).

1.3 Aerosol Particulate Monitoring

Particulate aerosol samples in urban areas are typically collected by drawing ambient air through filter materials or by inertial impaction with a pump, followed by subsequent quantification of particle mass and their chemical components by off-site laboratory analysis (Kumar et al., 2021). Size-selective inlets in cascade sampling setups allow fractionation, with the most common cut-off points of 10 µm, 2.5 µm and 1 µm (Chow, 1995; Kuo, 2018).

Traditionally, air pollutant concentrations are measured at stationary monitoring stations with complex equipment that adhere to standardised quality assurance and control protocols (QA/QC), such as the National ambient air quality standards, which were established to protect public health and enforced for CO, NO_2, SO_2, O_3, Pb and suspended particulate matter (PM_{10}, $PM_{2.5}$) (Chow, 1995; Fenger et al., 1998). Appropriate sampling protocols must be representative of the emission sources, area, population exposure or personal exposure samples. Samples for regulatory compliance are usually representative of the area and population exposure (Fenger et al., 1998). Monitoring stations established by environmental and governmental agencies provide information on a wide range of pollutants, measurement reliability and long-term pollutant trends (Jerrett et al., 2005; Kanaroglou et al., 2005; Xie et al., 2017).

In situ monitoring devices can be divided into three categories: i) mass measurement methods, ii) chemical-specific methods and iii) measurements of other aerosol properties. The mass measurement devices include beta attenuation monitor (Wedding and Weigand, 1993), tempered element oscillating microbalance (Meyer et al., 1992; Patashnick and Rupprecht, 1991) and piezoelectric microbalance. Chemical-specific devices include SO_2 and sulfate analysers, chemiluminescent and flame photometric detection (Appel et al., 1990; Schorran et al., 1994), gaseous HNO_3 analysers (Appel et al., 1990), gaseous NH_3 fluorescence analysers (Harrison and Msibi, 1994) and in-situ thermal or optical carbon analysers (Turpin and Huntzicker, 1991). Instruments for measuring other aerosol properties such as nephelometers, aethalometers, condensation nuclei counters and photoacoustic spectrometers continuously monitor characteristics like light scattering, light absorption, nucleation, diffusion rates, electrical mobility and molecular time of flight for various compounds (Chow, 1995).

Conventional monitoring typically relies on high-volume samplers (HVS, 1000 L min^{-1}), as they allow adequate sample deposition on the filter media for detecting compounds at lower limits of detection (LOD), however, portable, low-cost and low-volume samplers (LVS; 20 L min^{-1}) are increasingly being deployed as they are easier to handle, maintain good collection efficiency and are more suitable for quantifying personal emission exposures due to flow rates being more in line with commuter inhalation rates (6 L min^{-1}) (Chow, 1995; Ilenič et al., 2025; Karthikeyan et al., 2006; Kumar et al., 2021; Marina Montes et al., 2023; Salcedo et al., 2014; Samek et al., 2018; Saraga et al., 2021; Szabó et al., 2015).

A comprehensive review of publications published from 2010 onwards on existing sampling protocols and analytical approaches for metal(oid)s and PAHs in size-fractionated PM, with a particular emphasis on their characteristic chemical composition, seasonal variability, global spatial distribution and data on quality assurance, which included 81 studies from 33 different countries (Article 5), found that the majority of reported studies (87% of studies) installed PM samplers at elevated levels (EL; above 2.5 m, e.g. on building roofs), which is not representative of the residing area of commuters. Most studies reported sampling $PM_{2.5}$ (52%), followed by PM_{10} (30%) and particulate matter with aerodynamic diameter smaller than 1 µm (PM_1; 13%). Only 5% of studies

reported sampling of PM smaller than 0.1 µm, despite UFPs being the most prevalent fraction, accounting for approximately 90% of the total PM particles found in the atmosphere, followed by fine particles (9%) and coarse particles, which contribute less than 1% (Figure 2) (Kumar et al., 2010). In general, PAHs are more commonly analysed (56% of the selected studies) in comparison to metal(oid)s (31%), while 14% of the studies reported analysing both pollutants simultaneously, indicating on a significant gap in comprehensive PM chemical characterisation.

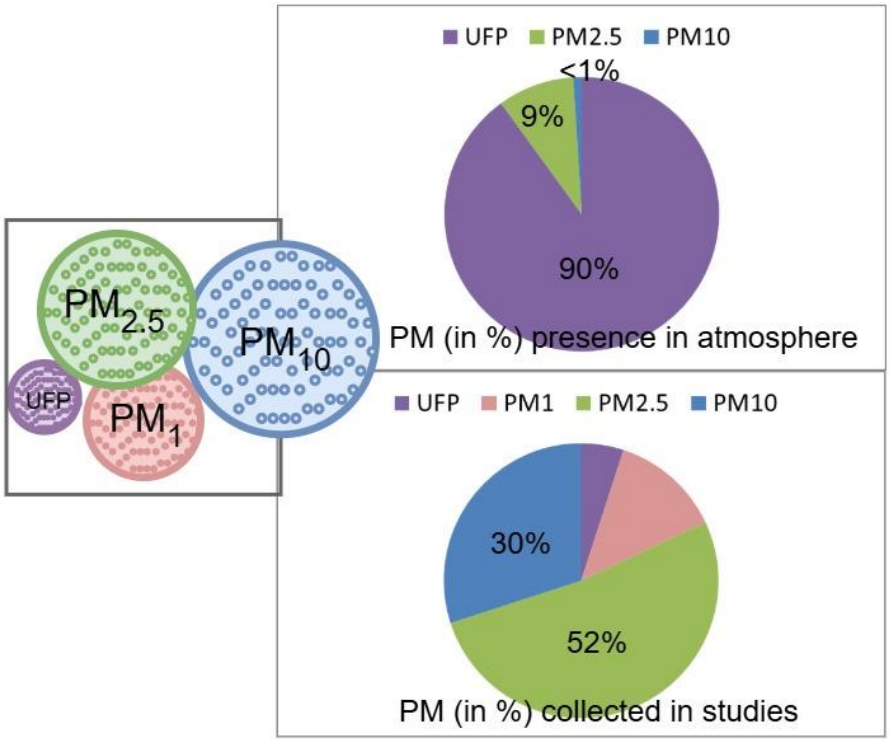


Figure 2: Comparison of PM fractions in the atmosphere and selected studies.

Prior to PM sample collection, it is essential to identify the nature of the pollutants bound to the PM in order to select the appropriate analytical procedure, including the types of filter, pollutant extraction methods, solvents used and analytical techniques to obtain reliable data on the chemical composition of size-fractionated PM samples. The main challenges of analytical procedures include the identification and determination of species in the sample, separation of the species, determination of low concentrations with adequate precision and accuracy, as well as effective elimination of matrix effects (Cornelis et al., 2003). Therefore, ensuring the accuracy of analytical procedures and results by selecting high-resolution and sensitive techniques along with the use of certified reference materials (CRMs) is essential (Celo et al., 2010; Dabek Zlotorzynska, 2010; Hopke et al., 2020; Salcedo et al., 2014). However, only 32% of studies reported their use, most commonly the National Institute of Standards and Technology (NIST) standard reference material (SRM) 1648a. Overall, 82% of studies included QA/QC in their methods.

When selecting suitable filter media for compliance measurements, several filter characteristics are important, including particle sampling efficiency, mechanical, chemical and temperature stability, blank concentrations, flow resistance and loading capacity to obtain adequate PM deposits, as well as cost efficiency and availability. Potential

positive or negative artefacts due to gas adsorption or particle volatilisation may also affect mass balance and chemical composition (Chow, 1995). The most commonly used filters are cellulose filters (fibrous, hydrophobic), glass fiber filters (GFF; fibrous, hydrophobic), mixed cellulose filters (membrane, hydrophilic), polycarbonate filters (PF; membrane, hydrophobic), polyvinyl chloride filters (membrane, hydrophobic), polytetrafluoroethylene filters (PTFE; membrane, hydrophobic) and quartz fiber filters (QFF; fibrous, hydrophobic) (Phalen and Phalen, 2013). The choice of filter depends on the nature of the pollutants (organic, inorganic), which in turn determines also the subsequent analysis. Overall, QFFs were the most commonly used in all selected studies (65%), followed by PTFEs (16%) and GFFs (12%). GFFs are often incorporated in HVS systems due to their high collection efficiency and low airflow resistance. However, due to their poor chemical stability and relatively high content of impurities, their use is limited to areas with higher levels of air pollution (Chow, 1995; Fernández Camacho et al., 2012; Marrero et al., 2005; McDow and Huntzicker, 1990). Compared to QFF and PTFE, GFFs offer the highest mechanical strength and are the most cost-effective, but also require pre-treatment (baking at >500 $^{\circ}$C) prior to sampling to remove adsorbed organic vapours (Chow, 1995). PTFE filters are the most chemically inert, exhibit minimal blank values and low hygroscopicity, but are unsuitable for elemental and organic carbon analysis (EC/OC) due to the high temperatures required for the analysis. EC/OC is best performed on QFF (Chow and Watson, 1998). Based on overall properties, PTFE outperforms GFF and QFF in several other key properties and is also best suited for chromatography, trace element analysis and microscopy (Chow, 1995).

Inductively coupled plasma mass spectrometry (ICP-MS) (68% of studies), X-ray analysis (20%) and atomic absorption spectroscopy (AAS) (11%) were the most commonly used spectroscopic techniques used to determine metal(oid)s in PM size-fractionated samples. The most common sample digestion technique was microwave assisted digestion (MAD; 83% of studies). Total metal concentration was also determined in samples after hot plate (HOP; 21%), ultrasound assisted (UAE; 8%) and mechanical shaking extraction (MSE; 4%). Among the analytical techniques for the determination of PAHs, gas chromatography mass spectrometry (GC-MS) was predominantly used for the separation of PAHs (84%). Other techniques were based on high performance liquid chromatography (HPLC; 16%). When separated by GC, PAHs are detected with higher sensitivity, speed, selectivity and also cost efficiency. The most common extraction method for PAHs was UAE (64%), followed by accelerated solvent extraction (ASE; 23%), Soxhlet extraction (SOE, 21%), MAD (4%) and MSE (4%).

Air quality monitoring stations (AQMS) located at stationary urban sites provide detailed air pollutant data; however, their sparse distribution across cities can result in low spatial resolutions (Kousis et al., 2022; Samad and Vogt, 2020). In Slovenia, national air quality monitoring network includes a total of 23 monitoring stations that monitor the following parameters on an hourly, daily and monthly basis: particulate matter (PM_{10}, $PM_{2.5}$), SO_2, NO_2, CO, O_3 and concurrently carry out analyses of the chemical composition of the collected samples (ARSO, 2023). High spatial variability of emissions, influenced by meteorological and topographical conditions, as well as physiochemical and photochemical processes, emphasises the need for more detailed PM measurements (Kuo, 2018).

Therefore, rapid development and deployment of remote sensing and portable measuring techniques has also been observed in recent years, including real-time, low-cost wireless sensors (LCSs), remote data logging sensors and satellite-based instruments (Fenger et al., 1998; Kumar et al., 2015; Morawska et al., 2018). These sensors offer great health and environmental applications with several inherent advantages, including affordability, portability, improved spatial resolution and the ability to identify emission

hotspots (Chong and Kumar, 2003; Leavey et al., 2015; Rai et al., 2017). Various applications of these sensors have been reported, including environmental awareness activities and citizen science campaigns using different modes of transport (e.g. bicycle, car, bus), municipal and industrial emission monitoring, indoor and outdoor personal exposure assessment and data collection in remote places (Kingham et al., 2013; Williams et al., 2019). However, compared to AQMS, LCS exhibit lower accuracy and sensitivity levels, as well as higher LODs. Therefore, an assessment of their dynamic response is essential before their widespread implementation (Austin et al., 2015; Malings et al., 2020; Williams et al., 2019; Zimmerman, 2022). LCS operating on the principle of light scattering can be influenced by particle composition and density, hygroscopicity, refractive index, relative humidity (RH), pollutant concentration and averaging time (Aleixandre and Gerboles, 2012; Castell et al., 2017; Giordano et al., 2021; Karagulian et al., 2019). It is consequently imperative to compare these sensors with reference instruments, such as AQMS using co-location field assessment methods (Bergmann et al., 2022; Castell et al., 2017; Crilley et al., 2018; deSouza et al., 2023; Ilenič et al., 2024; Karagulian et al., 2019; Kousis et al., 2022; Kumar et al., 2015; Vogt et al., 2021) or under controlled laboratory conditions (Castell et al., 2017; Crilley et al., 2018; Karagulian et al., 2019; Kelly et al., 2017; Kuula et al., 2020). In addition, various methods, such as linear regression models (Barkjohn et al., 2021; Kosmopoulos et al., 2020; Malings et al., 2020), multiple linear regression (Barkjohn et al., 2021; Malings et al., 2020) and mechanistic models based on hygroscopic growth correction (Barkjohn et al., 2021; Crilley et al., 2018; Malings et al., 2020) are also employed. More recently, multimodal data fusion methods combining ground-level monitoring data, satellite remote sensing data and also images from surveillance cameras at local, regional and global scales, have been applied to improve the spatio-temporal accuracy of air quality predictions (Choi and Hummel, 2025; Malings et al., 2024).

1.4 Characterisation Methods

1.4.1 Inductively coupled plasma mass spectrometry

ICP-MS (Figure 3) is a powerful, versatile and highly sensitive technique for the determination of trace and ultratrace elements, characterised by low LODs (<0.01 µg L^{-1} if not influenced by a high ionisation potential (e.g. Br^-, Cl^-) or high background noise due to impurities), a wide linear dynamic range of about nine orders of magnitude and fast, simultaneous quantitative and semi-quantitative multi-elemental analysis (Broekaert, 2005; Cornelis et al., 2003; Thomas, 2008). The main mechanisms by which atomic species are quantified are: sample ionisation, focusing and acceleration of the ions through lenses, separation of the ions by MSD according to their mass-to-charge ratio (m/z) and detection of the ions and measurement of the electrical charge (Nelms, 2005; Rouessac and Rouessac, 2013; Thomas, 2008).

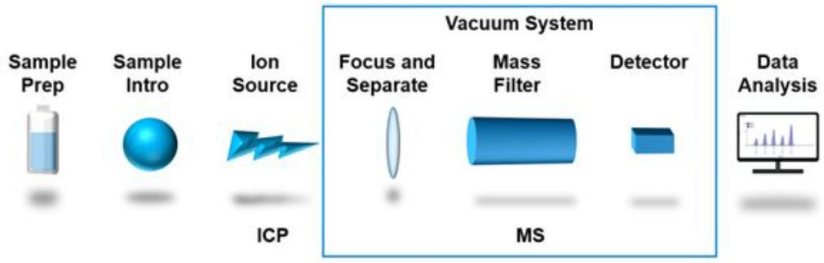


Figure 3: Schematic diagram of ICP-MS setup (Reproduced from Agilent, 2025a).

The non-thermal equilibrium ICP, an ion source that generates monoatomic, positively charged ions and electrons, is generated in an argon (Ar) stream within a quartz torch located in the centre of a cooled Cu coil (Broekaert, 2005; Cornelis et al., 2003; Thomas, 2008). A radio frequency generator (27−40 MHz) provides a high-frequency, high-power electric current that passes through the coil. The magnetic field generated by this current induces collisions between Ar atoms, leading to the production of ions and electrons (Nelms, 2005; Thomas, 2008). The torch consists of three concentric tubes, where Ar plasma gas is introduced through the centre tube, the sample aerosol carried by Ar, is passed through the inner tube, while Ar gas is passed through the outer tube to cool down the instrument (Broekaert, 2005; Thomas, 2008). A pneumatic nebuliser is used to aspirate the liquid sample into the plasma (up to 10,000 K), removing large droplets (>10 µm) by a spray chamber to ensure stable plasma conditions and efficient atomisation and ionisation in the ICP (Cornelis et al., 2003). Small aerosol droplets, corresponding to 1−5% of the sample, enter the plasma torch, where they are dried, decomposed, vaporised, atomised and finally ionised, mainly as positively charged ions (Broekaert, 2005; Cornelis et al., 2003; Thomas, 2008).The resulting ions are extracted into a high vacuum system through a pair of interface cones (sampler and skimmer) (Cornelis et al., 2003; Nelms, 2005). The electrostatic ion lens system focusses the ions into a compact ion beam as they pass through the vacuum system to the MSD. In general, four types of MSD are used: magnetic sector field (high resolution), time-of-flight, multicollector and quadrupole analyser (Broekaert, 2005; Thomas, 2008). The latter, most commonly used, consists of four parallel rods with hyperbolic cross-section in the interior of the assembly transmitting only positive ions with a narrow m/z window to the MSD. The detector is an electron multiplier that enables the amplification of weak ion currents and has the ability to count and detect each individual ion (Cornelis et al., 2003).

Furthermore, spectral and non-spectral interferences, which occur in ICP-MS, should be minimised or avoided for accurate determination of elemental concentrations. Non-spectral interferences are generated by the suppression or amplification of the matrix signal, while spectral interferences are manifested as overlaps of ion signals (Cornelis et al., 2003).

1.4.2 Gas chromatography mass spectrometry

One of the most common analytical separation mechanisms for detecting and quantifying the abundance of compounds in the gas phase, including PAHs, is gas chromatography (GC), which is often coupled with an MSD (Chow and Watson, 1998; Cornelis et al., 2003). The GC separation technique is based on the concentration equilibrium interaction

of the components with the stationary and mobile phase (Cornelis et al., 2003; Littlewood, 2013; McNair et al., 2019; Rouessac and Rouessac, 2013).

It is a time-efficient, versatile and multidimensional technique that provides good sensitivity, selectivity and resolution to determine the components in the samples based on their volatility and mass (Cecinato et al., 2012; Grob and Barry, 2004; Littlewood, 2013; McNair et al., 2019; Pandey et al., 2011; Rouessac and Rouessac, 2013).

Prior to analysis, the sample should be prepared with regards to its matrix and analyte properties. This typically involves extraction of the analyte from the sample matrix, derivatisation and extraction of the derivatised compounds into an organic solvent and subsequent determination of the volatile compounds in the organic phase using GC-MS (Dettmer Wilde and Engewald, 2014). It consists of an injector, a column and a detector (Figure 4).

First, a small amount of the sample is introduced into the injector, either a split-flow injector or a splitless injector, which vaporises the sample and mixes it with the gas stream. Analytes are then transported through the column with a carrier gas (mobile phase), which normally consists of hydrogen, helium or nitrogen. The mobile phase must be free of all traces of hydrocarbons, water vapour and oxygen, as they can interfere with the polar stationary phase and reduce detector sensitivity (Littlewood, 2013; Rouessac and Rouessac, 2013). As analytes move through the column, they partition between the mobile and stationary phases according to their solubility (McNair et al., 2019). The viscosity and flow rate of the carrier gas influence the dispersion of the analytes in the stationary phase and the diffusion process in the mobile phase. The identification is based on the retention times, i.e. the time from sample introduction to detection of the peak maximum (Rouessac and Rouessac, 2013).

The column is a narrow-bore tube that winds around itself and is 1—100 m long, depending on the type and content of the stationary phase. There are two types of columns: packed columns, in which the stationary phase is deposited on a porous media or bound by a chemical reaction, and the more common capillary column, in which the stationary phase is deposited on the inner surface of the column. The column is stored in a thermostatically controlled oven (up to 400 °C). At the end of the column, the mobile phase passes through a detector before being released into the atmosphere (Grob and Barry, 2004; Rouessac and Rouessac, 2013).

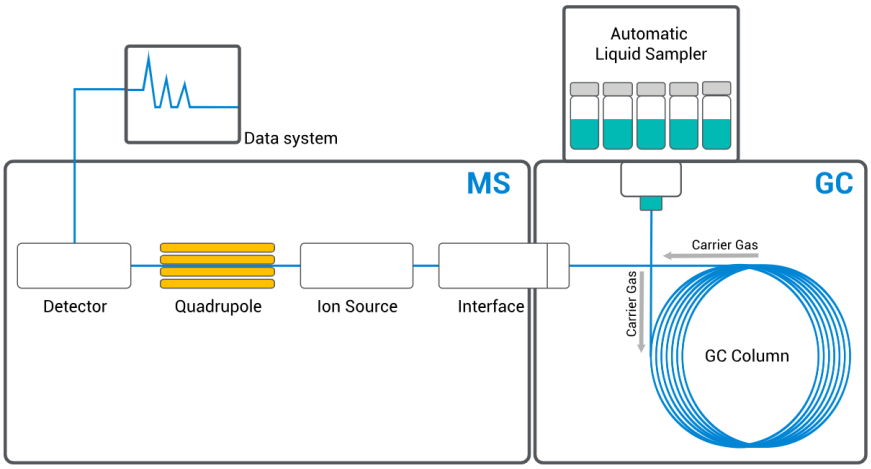


Figure 4: Schematic diagram of GC-MS setup (Reproduced from Agilent, 2025b).

1.4.3 Scanning electron microscopy

Scanning electron microscopy (SEM) is used to analyse the morphological properties of the particles, such as size and shape, as well as the interactions between particles and labile components that have accumulated on the filter medium. When coupled with an energy dispersive X-ray microanalyser (EDX), the chemical composition can also be analysed by detecting characteristic X-rays.

SEM is unable to produce clear images of non-conductive samples; therefore, a prior carbon or gold coating of PM deposited samples is essential to enhance the conductivity and attenuate electron charging. SEM utilises a shaped magnetic field to create an electron-optical lens system, with an accelerated electron serving as an illumination source to generate images of the sample matrix (Yao et al., 2021). The operating principle of the SEM can be divided into six components: electron source, electron optical system for focusing and scanning, specimen chamber, signal detector, evacuation system and display system (Figure 5).

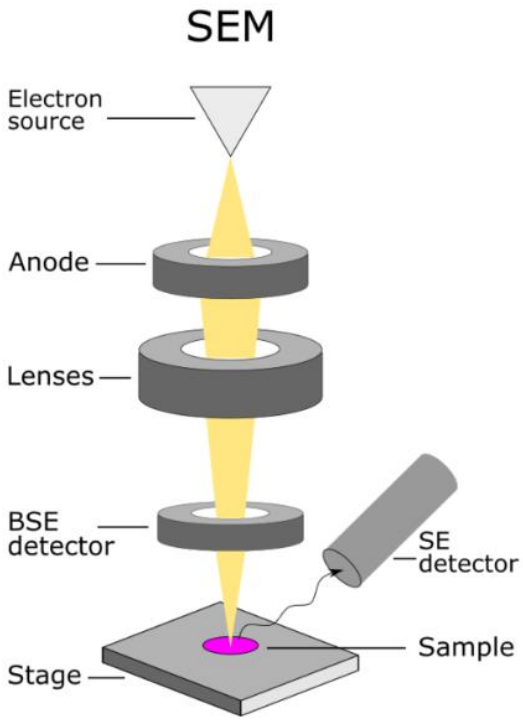


Figure 5: Schematic diagram of SEM setup (Reproduced from AnaPath Research, S.A.U., 2025).

The electron beam of primary free electrons is generated by an electron gun, a V-shaped tungsten filament, which is heated up to 2700 K. The high temperature causes acceleration by an electric field, characterised by thermionic emission, to form a focused electron beam with nanoscale resolution (Lawes, 1987; Yao et al., 2021). The smaller the diameter of the electron beam, the higher the resolution (Yao et al., 2021). After the electron beam strikes the bulk solid material, the electrons are reflected and scattered or absorbed as they undergo a series of elastic or inelastic collisions with the atoms of the material. These collisions generate signals that are recorded in the microscope to create images (Sarkar et al., 2001; Scrivener et al., 2018). The three most important signals

generated are secondary electrons (SE), backscattered electrons (BSE) and characteristic X-rays (Sarkar et al., 2001; Scrivener et al., 2018). BSE are the result of elastic collisions, while SE are produced by inelastic collisions and have a higher resolution levels with a lower interaction volume (Scrivener et al., 2018). SE provide information about the shape of the specimen and are dominated by topographic contrast, while BSE provide information about the composition, as the yield of BSE depends on the atomic number (Okano, 2018; Sarkar et al., 2001). The intensity of the reflected electrons correlates with the atomic number of the substances in the object and the density of the material (Sarkar et al., 2001). SEM is capable of measuring motion with ultra-high precision, with a maximum magnification of more than 400,000x (Yao et al., 2021). The acceleration voltage is typically between 15−20 kV, with a higher voltage providing greater contrast, but possibly also deteriorating image quality (Sarkar et al., 2001).

Chapter 2

Research Aims and Hypothesis

Airborne metal(oid)s and PAHs, particularly those associated with nanoscale PM fractions, pose significant health and environmental risks due to their high toxicity per unit mass, ability to penetrate deep into lung tissue and prolonged atmospheric residing times. Particulate aerosol samples in urban areas are typically collected by AQMS, which rely on high-volume samplers placed at stationary locations and adhere to standardised quality protocols. However, these methods are complex, expensive and limited in spatial coverage, therefore a recent rapid development and deployment of alternative, portable and low-cost sensors has been observed.

Comprehensive chemical characterisation of (ultra)fine PM, combined with quality assurance measures, is essential to ensure high quality data and facilitate cross-study comparability for effective air quality control. This is particularly important for the dynamic exposure assessment of active road users, such as pedestrians and cyclists, for whom data remain limited within the national stationary AQMS networks.

To address these challenges, the doctoral thesis aimed to advance understanding of airborne, size-fractionated PM and its potential harmful implications for public health and the urban environment, through: i) the development and application of an affordable, portable sampling device capable of collecting size-fractionated PM (PM_{10}, $PM_{2.5}$, $PM_{0.1}$ and $PM_{<0.1}$) deployed in urban pedestrian and cycling microenvironments, and ii) the investigation of the potential feasibility of LCS, specifically Sensirion SPS30 for $PM_{2.5}$ monitoring, as well as promoting citizen engagement in the collection of high-resolution air quality data.

The specific goals of the first part were:

- to develop a novel, low-volume cascade sampling device for the collection and size-fractionation of airborne PM, including nanoscale fractions;
- to verify the size of PM collected on filters using SEM analysis;
- to optimise and validate analytical methods for the determination of metal(oid)s and platinum group elements (PGEs) by ICP-MS and for the analysis of PAHs by GC-MS, using NIST SRM 1648a;
- to successfully apply the developed approach and implement systematic one-year monitoring at five different urban environments in Slovenia (Dobrova, Ljubljana, Maribor, Murska Sobota, Piran);
- to assess the seasonal and spatial distribution of pollutants;
- to conduct source apportionment analysis;
- to evaluate the toxic potential and possible health and environmental risk implications associated with pedestrians' and cyclists' inhalation exposure during commuting.

The specific goals of the second part were:

- to assess the dynamic exposure of citizens to $PM_{2.5}$ using LCS mounted on bicycles;
- to evaluate the performance of the LCS in both, controlled laboratory settings and real-world urban environments;
- to assess the seasonal and spatial distribution of $PM_{2.5}$ in Ljubljana and Maribor and identify potential air pollution hotspots;
- to conduct health and environmental risk assessment;
- to raise awareness about the risks associated with air pollution and highlight the importance of individual behavioural patterns in mitigating urban air pollution.

Chapter 3

Scientific Publications

3.1 Article 1: Innovative Sampling Device for Size-Fractionating Airborne Particulate Matter for Improved Air Pollution Control of Metal(oid)s and Polycyclic Aromatic Hydrocarbons

Authors: Anja Ilenič, Radmila Milačič Ščančar, Marija Đurić, Alenka Mauko Pranjić, Janez Ščančar
Published in Royal Society of Chemistry, Analytical Methods (August 2025)
Available at DOI: 10.1039/D5AY00858A

A LVS sampling device was developed for the collection and size-fractionation of airborne PM. The device comprises of a cascade PTFE membrane filter system (PM_{10}, $PM_{2.5}$, $PM_{0.1}$) connected to an ultrapure-water trap, retaining the $PM_{<0.1}$ fraction that passes through the filters. The approach overcomes the limitations of conventional filter-based PM fractionation by enabling efficient collection of (ultra)fine particles, which are of particular concern due to their ability to penetrate deep into the lung tissue and their associated toxicological and health risks. When combined with optimised and validated analytical procedures, this sampling setup provides a reliable analytical tool for detecting metal(oid)s, PGEs and PAHs, including those bound to nanoscaled fractions. Metal(oid)s and PGEs were determined by ICP-MS after MAD using a mixture of acids, while PAHs were extracted with a solvent mixture of Ace (C_3H_6O) and petroleum ether (C_6H_{14}), assisted by MSE and determined by GC-MS. The analytical methods were optimised and validated using the urban PM NIST SRM 1648a, achieving repeatability and accuracy of 6% and 2% for metal(oid)s and PGEs, and 3% and 6% for PAHs, respectively. SEM-EDS imaging was employed to analyse the morphology and particle sizes of fractionated PM, thus also validating the reliability and efficiency of the sampling devices' fractionation ability. Airborne particles were categorised as geogenic, anthropogenic and biogenic, with the most commonly observed morphologies including spherules, floccules, biogenic particles, tabular particles, irregular shaped grains and agglomerate particles. The most common particles were alumosilicates, magnesium silicates and carbonate particles, indicative of soil deposition and re-suspension processes, along with carbon-enriched particles and sulfates, commonly associated with biomass combustion and vehicle emissions. Most particles were non-spherical, thereby providing a larger surface area for potential toxic compound adsorption and enhancement of their interaction with lung

tissue. The applicability of the sampling device was successfully demonstrated through a one-month study conducted at three different locations in Slovenia, which differed in size, population and traffic density. Analysis revealed that metal(oid)s and PGEs were most abundant in the PM_{10}, largely influenced by soil deposition and re-suspension processes, while those trace elements (Ba, Cd, Cu, Ni, Pb, palladium (Pd), platinum (Pt), V, and Zn) originating from traffic-related sources, as well as biomass combustion, were also significantly elevated in the $PM_{<0.1}$. HMW PAHs were distributed between PM_{10} and $PM_{2.5}$ fractions, with 5- (BaP, BbF) and 6-ring (BghiP, IP) PAH compounds associated more significantly with smaller PM fractions. Contaminant levels were generally low, indicating on minimal health risks for daily commuters.

Analytical Methods

ROYAL SOCIETY OF CHEMISTRY

PAPER

View Article Online
View Journal | View Issue

Open Access Article. Published on 29 August 2025. Downloaded on 9/23/2025 2:29:53 PM.
This article is licensed under a Creative Commons Attribution-NonCommercial 3.0 Unported Licence.

Check for updates

Cite this: *Anal. Methods*, 2025, **17**, 7184

An innovative sampling device for size-fractionating airborne particulate matter for improved air pollution control of metal(oid)s and polycyclic aromatic hydrocarbons

Anja Ilenič, [ac] Radmila Milačič Ščančar, [bc] Marija Đurić, [a] Alenka Mauko Pranjić[a] and Janez Ščančar [*bc]

A sampling device was developed for collecting and size-fractionating airborne particulate matter (PM). A low-volume cascade system with polytetrafluoroethylene membrane filters (PM_{10}, $PM_{2.5}$, and $PM_{0.1}$) connected to an ultrapure-water trap was used to retain the $PM_{<0.1}$ fraction that passed through the filters. In the collected samples, metal(oid)s and platinum group elements (PGEs) were determined by inductively coupled plasma mass spectrometry after microwave-assisted digestion using a mixture of acids. Polycyclic aromatic hydrocarbons (PAHs) were extracted with a solvent mixture of acetone and petroleum ether, assisted by mechanical shaking and determined by gas chromatography mass spectrometry. The analytical methods were optimised and validated using the urban PM Standard Reference Material 1648a. Measurement repeatability and accuracy were 6% and 2% for metal(oid)s and PGEs, and 3% and 6% for PAHs, respectively. Field emission scanning electron microscopy analysis confirmed that the sampling device efficiently fractionated airborne PM to nano-sized particles. The sampling device was successfully applied to collect PM, enabling effective air pollution monitoring in urban areas. Analysis revealed that metal(oid)s were most abundant in PM_{10}, while those originating from traffic were also elevated in $PM_{<0.1}$. High-molecular-weight PAHs were distributed between PM_{10} and $PM_{2.5}$ fractions. The sampling device provides valuable insights into the chemical composition of (ultra) fine particles, overcoming the limitations of filter-based PM fractionation and providing improved air pollution control for nanoparticle-bound pollutants.

Received 19th May 2025
Accepted 7th August 2025

DOI: 10.1039/d5ay00858a

rsc.li/methods

Introduction

Urban air pollution is characterised by high levels of airborne particulate matter (PM), a heterogeneous mixture of natural (*e.g.* sea salt, dust, volcanic ash, pollen, fungal spores and forest fires) and anthropogenic (*e.g.* biomass burning, traffic, industry and construction activities) particles.[1–5] The behaviour and toxicity of PM in the atmosphere and within the human respiratory system are primarily influenced by particle size. Coarse particles (aerodynamic diameter >2.5 μm) tend to deposit in the nasopharynx, while fine particles (aerodynamic diameter <2.5 μm) and ultrafine particles (aerodynamic diameter <0.1 μm) can penetrate deep into the terminal bronchioles and alveoli.

Numerous epidemiological and toxicological studies have linked air pollution to adverse health effects and related health risks.[6–8] Even limited exposure can lead to oxidative stress at the air-lung interface, contributing to acute and chronic cardiopulmonary diseases, as well as neurodegenerative and reproductive disorders.[9–14] These effects are more pronounced with fine and ultrafine particles, as 50% of these particles remain in the lung parenchyma.[15] Additionally, fine and ultrafine particles have longer atmospheric residence times, ranging from a few hours to weeks, until they are removed by either wet or dry deposition.[16] Studies have shown that toxicity of PM per mass unit increases as particle size decreases, indicating that fine particles are more toxic than coarser ones.[17,18] This increased toxicity is primarily due to the larger total porous surface area of finer particles, which enables them to more easily adsorb and retain toxic substances.[15]

Understanding the relationship between chemical composition and sizes of particles is crucial, but published data indicate that this remains limited. Most research on airborne pollutants involves the use of high-volume samplers (>100 L min^{-1}) to collect larger sample quantities, enabling the detection of compounds with lower limits of detections (LODs).[19–22] However, increased air flow rates can potentially reduce the adsorption capacity of filters and increase the likelihood of filter clogging,

[a]*Department of Materials, Slovenian National Building and Civil Engineering Institute, Ljubljana, Slovenia. E-mail: janez.scancar@ijs.si*
[b]*Department of Environmental Sciences, Institute Jožef Stefan, Ljubljana, Slovenia*
[c]*Jožef Stefan International Postgraduate School, Ljubljana, Slovenia*

This journal is © The Royal Society of Chemistry 2025

Open Access Article. Published on 29 August 2025. Downloaded on 9/23/2025 2:29:53 PM.
This article is licensed under a Creative Commons Attribution-NonCommercial 3.0 Unported Licence.

making them less suitable for accurately assessing human health risks during daily commuting. People typically inhale 10 to 15 times per minute, equating to about 6 L min^{-1}, making low-volume samplers (10 L min^{-1}) more suitable alternatives for human health risk assessments.[23–28]

Adequate sampling techniques are particularly important for detecting pollutants present at very low concentrations, such as metal(oid)s and polycyclic aromatic hydrocarbons (PAHs), which pose significant health and environmental risks. The United States Environmental Protection Agency (US EPA) has identified 16 priority PAHs for analysis in various environmental samples.[29] Among these, benzo[*a*]pyrene (BaP) is recognised as one of the most potent carcinogens. Other PAHs, such as benzo[*a*]anthracene (BaA), benzo[*b*]fluoranthene (BbF), benzo[k]fluoranthene (BkF), chrysene (Ch) and indeno[1,2,3-*cd*] pyrene (IP) are classified as possibly carcinogenic to humans.[30,31] Among metal(oid)s, arsenic (As), hexavalent chromium (Cr(VI)), cadmium (Cd), nickel (Ni), and lead (Pb) are of particular concern as carcinogenic airborne contaminants.[32] Accurate chemical analysis of these PAH compounds and metal(oid)s is essential across all inhalable PM sizes, including nanoparticles, which are often overlooked.

Previous studies have reported PAHs in size-fractioned PM_{10} and $PM_{2.5}$ (ref. 33–35) and metals in size-fractioned PM_{10} and $PM_{2.5}$.[36–38] However, the simultaneous determination of both types of pollutants in different PM sizes is rarely reported.[39,40] Very few studies performed characterisation of PM of smaller fractions.[41–44] Physio-chemical analyses of samples collected on filters by low-volume cascade samplers present significant challenges, mainly due to the small amount of the PM collected. Therefore, highly sensitive analytical techniques such as inductively coupled plasma mass spectrometry (ICP-MS) and gas chromatography mass spectrometry (GC-MS) are used for chemical analysis of samples. Analytical methods with high selectivity, resolution and sensitivity must be applied to provide data for reliable assessment of health and environmental hazards. However, only a few atmospheric studies report the use of certified reference materials (CRMs). These materials are analysed to check the accuracy of results and validate the analytical procedures.[26,45–47]

Given that pollutants bound to airborne (ultra)fine particles have the most harmful effects on human health, it is essential to improve pollution control measures and enhance risk assessment strategies by taking into account various PM fractions, including the nano-sized PM particles. Therefore, the objectives of our work were (i) to develop a low-volume cascade sampling device for collecting and size-fractionating airborne PM, consisting of polytetrafluoroethylene (PTFE) membrane filters (PM_{10}, $PM_{2.5}$, and $PM_{0.1}$) connected to an ultrapure-water trap designed to retain the $PM_{<0.1}$ fraction; (ii) to verify the size of PM particles collected on filters using field emission scanning electron microscopy (SEM) analysis; (iii) to optimise and validate analytical methods for the determination of metal(oid)s, including platinum group elements (PGEs) using ICP-MS, and PAHs in the collected sample fractions using GC-MS; and (iv) to analyse the concentrations of metal(oid)s and PAHs in collected samples at different urban locations in Slovenia using the developed sampling device, placed within one metre of bicycle lanes, in order to assess the air pollution-related health risks for daily commuters.

Experimental

Instrumentation

Total elemental concentrations were determined by ICP-MS on an Agilent 7900 instrument (Agilent Technologies, Tokyo, Japan). The ICP-MS operating parameters are presented in Table S1 (SI). Data were acquired using Agilent MassHunter 5.1 software and further processed with Microsoft Excel 2019 (Redmond, WA, USA).

PAH determination was carried out by GC-MS, using an Agilent HP6890 GC (Agilent Technologies, Tokyo, Japan) with a 5973 mass selective detector (MSD) and equipped with an Agilent 6890 Series autosampler injector. PAHs were separated on an Agilent capillary column HP-5MS (30 m × 0.25 mm, film thickness 0.25 μm) coated with 5% phenylmethylpolysiloxane. The GC-MS operating parameters are presented in Table S2.

A Milestone ETHOS UP Microwave Digestion System (Sorisole, Italy) was used for sample digestion in the analysis of metal(oid)s and PGEs. For PAH analysis, the samples were mechanically shaken using a Vibromix 40 orbital shaker (Tehtnica, Železniki, Slovenia). The sample extracts were concentrated using a sample concentrator Dri-Block Heater DB100/3 (Techne Inc., Vernon Hills, IL, USA). A Mettler AE 163 analytical balance (Zürich, Switzerland) was used for weighing.

Morphological analysis of airborne PM was conducted using SEM with a Zeiss ULTRA plus scanning electron microscope (Carl Zeiss AG, Oberkochen, Germany) equipped with an energy dispersive X-ray spectrometer (EDS) system manufactured by Oxford Instruments (High Wycombe, UK).

A Vacuubrand (Wertheim, Germany) low-volume diaphragm pump ME 1C (100 mbar, 0.8 m^3 h^{-1}) was used for sampling of real airborne PM, while air flow through the system was measured using a G1.6 gas meter (Dadolab, Cinisello Balsamo, Italy). The air flow rate was controlled using a variable area flow meter DK46/800 (Krohne, Wellingborough, UK). PM was collected using a three-stage cascade NILU polycarbonate filter holder system (Innovation NILU, Kjeller, Norway) equipped with hydrophobic Whatman PTFE membrane filters (pore sizes of 10 μm, 2.5 μm and 0.1 μm and diameters of 47 mm) obtained from Merck (Darmstadt, Germany).

Reagents and materials

An ultrapure water system (PURELAB Flex 3, ELGA, LabWater, UK) was used for the preparation of samples and reagents.

For metal(oid)s analysis, Suprapur nitric acid (67–70% HNO_3) was obtained from Carlo Erba Reagents (Val-de-Reuil, Normandie, France), while Suprapur hydrochloric acid (30% HCl) and Suprapur hydrofluoric acid (40% HF) were purchased from Merck (Darmstadt, Germany). ICP multi-element standard solution XVI (21 elements in diluted nitric acid, 100 mg L^{-1}, part no. 1.09487.0100) was used to prepare calibration curves for the metal(oid)s arsenic (As), cadmium (Cd), chromium (Cr), cobalt (Co), copper (Cu), molybdenum (Mo), nickel (Ni), lead

Open Access Article. Published on 29 August 2025. Downloaded on 9/23/2025 2:29:53 PM. This article is licensed under a Creative Commons Attribution-NonCommercial 3.0 Unported Licence.

(Pb), thallium (Tl), vanadium(v) and zinc (Zn). For barium (Ba), a single standard (1000 ± 2 mg L^{-1} in 2–3% HNO_3, part No. 1.70304.0100) was used. Single standard solutions of palladium (Pd) (1000 ± 2 mg L^{-1} in 0.5 mol L^{-1} HNO_3, part no. 1.14282.0100) and platinum (Pt) (1000 ± 2 mg L^{-1} in 2 mol L^{-1} HCl, part no. 1.102645.0100) were used to prepare the calibration curve for PGEs. Stock standard solutions of germanium (Ge), rhodium (Rh) (1000 ± 2 mg L^{-1} in 2–3% HNO_3, part Nos. 1.70320.0100 and 1.02650.0100, respectively), and iridium (Ir) (1000 ± 2 mg L^{-1} in 7% HCl, part no. 1.70325.0100) were used to prepare internal standards in ICP-MS analysis. All standard solutions were purchased from Merck.

For PAH analysis, acetone (C_3H_6O) and petroleum ether, both purchased from Merck, were used for extraction of the high-molecular weight PAHs benzo[*a*]anthracene (BaA), benzo [*a*]pyrene (BaP), benzo[*b*]fluoranthene (BbF), benzo[ghi]perylene (BghiP), chrysene (Ch), fluoranthene (Fl), indeno[1,2,3-*cd*] pyrene (IP) and pyrene (P). Anhydrous sodium sulphate (Na_2SO_4) from Merck was used for water removal from the organic phase. Strata FL-PR Florisil (activated magnesium silicate, MgO_3Si, 170 μm, 80 Å, 500 mg^3 mL^{-1}; Phenomenex, Inc., Torrance, CA, USA) was used for the cleaning of sample extracts. A standard stock solution PAH-Mix 9 (10 μg mL^{-1}, part no. DRE-XA20950009CY) in cyclohexane, containing 16 analytes, was used to create calibration curves for the determination of PAHs by GC-MS. A deuterated PAH-Mix 9 (10 μg mL^{-1}, part no. DRE-L20950902CY) in cyclohexane, also containing 16 analytes, was used as an internal standard. Both the PAH-Mix standard and internal standard were purchased from LGC (Teddington, UK). Isooctane (2,2,4-trimethylpentane) obtained from Merck was used as a reference standard to calibrate the GC-MS system. The retention times of PAHs in the samples were compared to the retention time of isooctane, aiding in the identification of PAHs during the GC-MS analysis. A typical chromatogram illustrating the separation of the PAH-Mix 9 standard solution (16 PAHs, 500 ng mL^{-1}) and the deuterated PAH-Mix 9 (16 PAHs-D, 500 ng mL^{-1}) used as an internal standard, applying the GC-MS procedure, with PAHs considered for analysis marked in red, is presented in Fig. S1. Retention times of the separated PAHs and deuterated PAH compounds are presented in Table S3. The certified standard reference material SPS-SW1 (reference material for measuring elements in surface waters), obtained from Spectrapure Standards (Oslo, Norway), was used daily during ICP-MS analysis to verify the accuracy of the calibration curves and measurement procedures for metal(oid)s. Standard Reference Material (SRM) 1648a (Urban Particulate Matter) from the National Institute of Standards and Technology (NIST) (Gaithersburg, MD, USA), certified for selected elements and PAHs, was employed to verify the accuracy of metal(oid) determinations in digested PM, as well as PAHs in the extracted PM from both the filters and the aqueous phase. This SRM was also used to optimise and validate the analytical procedures.

Sampling sites and sample collection

Sampling of airborne PM was carried out from December 1, 2023, to December 31, 2023, at three different urban settings in Slovenia: Dobrova (DB: 46.067450, 14.409407), Ljubljana (LJ: 46.033985, 14.518328) and Maribor (MB: 46.548294, 15.649047). Sampling points were positioned at the ground level at an average human height (170 cm), within one metre of bicycle lanes. Samples were collected monthly using an innovative sampling device, consisting of two identical units – one for metal(oid)s and the other for PAHs. The units were installed in a metal cage to protect them from damage caused by precipitation and vandalism, while ensuring uninterrupted access to the surrounding air (Fig. S2).

The sampling unit consisted of a three-stage cascade filter holding system incorporating hydrophobic PTFE membrane filters with pore sizes of 10 μm, 2.5 μm and 0.1 μm (Fig. S3). This cascade filter system was connected to the water trap inside a 2000 mL amber glass Pyrex burette bottle in order to retain the nano-sized particles ($PM_{<0.1}$). The air volume passing through the system was controlled by using a low-volume diaphragm pump connected to a gas meter. Prior to the sample analysis, the stability of the airflow rate of a low-volume diaphragm pump was monitored continuously over one month using a flow meter.

After the sampling, the nano-sized $PM_{<0.1}$ fraction (captured in a water trap) and the PTFE membrane filters were stored at −15 °C until analysis. Each filter and the aqueous phase of the nano-sized $PM_{<0.1}$ fraction represented the total monthly amount of PM. The volume of air pumped through the sampling unit was monitored throughout the entire sampling period, allowing for the reporting of metal(oid) and PAH concentrations in ng m^{-3} of air.

Optimized analytical procedures for the analysis of metal(oid)s and PGEs by ICP-MS

To avoid contamination, all glassware was soaked in 10% HNO_3 for 48 h, rinsed three times with ultra-pure water and dried at 80 °C. Teflon vessels were cleaned with 10% HNO_3 using the same protocol as that for the microwave-assisted digestion of samples. The vessels were then rinsed three times with ultra-pure water and kept at 150 °C for 6 h, in order to remove any residual HNO_3 vapours.

After sampling, filters (PM_{10}, $PM_{2.5}$, and $PM_{0.1}$) were weighed, cut in half with iron scissors, and aliquots of the filters were weighed again to accurately determine the proportion of the whole PM collected in each aliquot. The nano-sized $PM_{<0.1}$ collected in the 1 L water trap was acidified with 1 mL of HNO_3, evaporated to 20 mL in a sand bath at 200 °C, and then divided into two 10 mL aliquots. One half of the filters (PM_{10}, $PM_{2.5}$, and $PM_{0.1}$) and one aliquot of the nano-sized $PM_{<0.1}$ fraction were used for the analysis of metal(oid)s, while the other half was used for the analysis of PGEs.

For the determination of metal(oid)s, 3 mL of HNO_3, 1 mL of HCl and 0.2 mL of HF were used in microwave-assisted digestion, while for the determination of PGEs, *aqua regia* (3 mL of HCl and 1 mL of HNO_3) with the addition of 0.2 mL of HF was used. Samples were subjected to closed-vessel microwave-assisted digestion, using the following temperature programme: ramp to 140 °C for 15 min, hold at 140 °C for 5 min,

 This journal is © The Royal Society of Chemistry 2025

Open Access Article. Published on 29 August 2025. Downloaded on 9/23/2025 2:29:53 PM.
This article is licensed under a Creative Commons Attribution-NonCommercial 3.0 Unported Licence.

ramp to 200 °C for 20 min, hold at 200 °C for 60 min, and cool down for 30 min. The clear digests of the filters and the nano-sized $PM_{<0.1}$ aqueous phase fraction were quantitatively transferred to 30 mL polypropylene graduated tubes and filled to the mark with ultra-pure water. Concentrations of metal(oid)s in digested samples were determined by ICP-MS using external calibration for quantification. The same analytical procedures, with no samples added, were applied to determine procedural blanks. Concentrations of metal(oid)s and PGEs in the procedural blanks were below the LODs, or did not exceed 3% of the measured elemental concentrations.

Optimized analytical procedures for the analysis of PAHs by GC-MS

To avoid contamination, all glassware was rinsed three times with tap water, soaked in 10% nitric acid for 48 h, rinsed three times with tap water and three times with ultra-pure water and heated at 400 °C for at least 4 h. Prior to use, all glassware was rinsed with petroleum ether and acetone and dried at room temperature.

After sampling, PAHs collected on the filters (PM_{10}, $PM_{2.5}$, and $PM_{0.1}$) and the nano-sized $PM_{<0.1}$ fraction retained in the aqueous phase were extracted using organic solvents. The filters were transferred to Erlenmeyer flasks, and a mixture of 15 mL of acetone and petroleum ether (1 : 1, *v*/*v*) and 100 μL of isooctane was added. The samples were then spiked with 50 μL of an internal standard solution (10 μg mL^{-1}) and shaken on a mechanical shaker for 16 h at 180 rpm.

For the nano-sized $PM_{<0.1}$ fraction, a liquid–liquid extraction (LLE) was performed. A mixture of 100 mL of acetone and petroleum ether (1 : 1, *v*/*v*) along with 100 μL of isooctane was added to 1 L of the sample. After spiking with 50 μL of the internal standard solution (10 μg mL^{-1}), the mixture was shaken for 16 h at 180 rpm. The content was quantitatively transferred into a glass separatory funnel to separate the organic phase from the aqueous phase. Traces of water in the organic phase were removed using anhydrous Na_2SO_4, and pre-heated at 550 °C for 6 h.

The organic phase from both the filter extracts and the nano-sized $PM_{<0.1}$ fraction was passed through a 3 mL column filled with Florisil for sample clean-up. The organic phase was concentrated to approximately 1 mL under a nitrogen stream at 40 °C using a sample concentrator. The concentrated samples were then transferred to 2 mL amber vials with a Pasteur pipette and sealed. Finally, 1 μL of the sample was injected onto the column for the determination of PAHs by GC-MS, using external calibration for quantification. The same analytical procedure, with no samples added, was applied to determine procedural blanks. Concentrations of PAHs in the procedural blanks were below the LODs.

A flow chart illustrating the optimised analytical procedures for the determination of metal(oid)s, PGEs and PAHs is presented in Fig. 1.

Morphological analysis

SEM-EDS was used to examine particle sizes and shapes (morphology), the chemical composition of selected elements in PM and the size distribution of particles collected on filters. The analysis was conducted in high-vacuum mode (pressure of 25 Pa) with an accelerating voltage of 8–10 kV. For SEM analysis, PM was collected on PTFE filters (with pore sizes of 10 μm, 2.5 μm and 0.1 μm) over two days, after the experiments for the analysis of metal(oid)s and PAHs. In prior microstructural analysis, samples were coated with a 15 nm layer of carbon or gold to enhance conductivity and mitigate electron charging. A

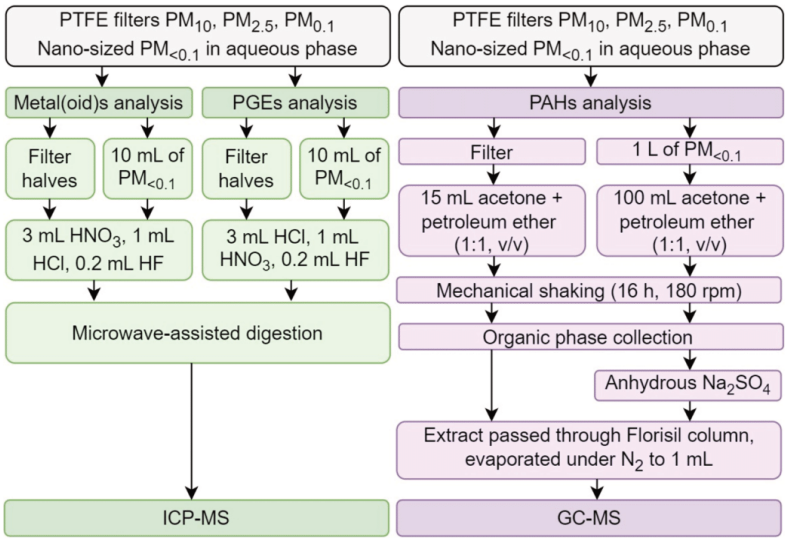


Fig. 1 Flow chart of the optimised analytical procedures for the determination of metal(oid)s, PGEs and PAHs in size-fractionated airborne PM.

Open Access Article. Published on 29 August 2025. Downloaded on 9/23/2025 2:29:53 PM. This article is licensed under a Creative Commons Attribution-NonCommercial 3.0 Unported Licence.

gold coating was chosen as it resulted in lower electron charging and enabled the use of higher magnifications.

Optimization of the analytical procedures

The analytical procedures for the determination of metal(oid)s, PGEs and PAHs were optimised using urban dust SRM 1648a. This SRM was chosen due to its similarity to the sample matrix and its certified values for both analytes – metal(oid)s and PAHs. Aliquots of approximately 40 mg were used for the analysis, as the homogeneity of SRM was confirmed for sample amounts larger than 5 mg in the NIST Certificate of Analysis.[48] For the optimisation of analytical procedures, experiments were carried out in duplicate. The performance of the optimised analytical procedures for the analysis of metal(oid)s, PGEs and PAHs was evaluated by determining the repeatability of measurements, the limits of detection (LODs), limits of quantification (LOQs), and linearity and by performing an accuracy check.

Analytical procedures for the determination of metal(oid)s and PGEs by ICP-MS

To achieve effective decomposition of the sample matrix for metal(oid)s or PGEs, 3 mL of HNO_3 and 1 mL of HCl (for nitric acid digestion) or 3 mL of HCl and 1 mL of HNO_3 (for *aqua regia* digestion) were added to the urban dust SRM, along with varying amounts of HF, using microwave-assisted digestion. The ICP-MS analysis revealed that the addition of HF was crucial for the dissolution of silicates, which can occlude metal(loid)s and PGEs in the PM. The optimal amount of HF added was 0.2 mL. The procedure optimised for the urban dust SRM sample was subsequently applied to the determination of metal(oid)s and PGEs in PM_{10}, $PM_{2.5}$ and $PM_{0.1}$ fractions collected on filters, as well as the $PM_{<0.1}$ fraction retained in the aqueous phase, as described in the section Optimised analytical procedures for the analysis of metal(oid)s and PGEs.

The studied metal(oid)s and PGEs were selected due to their association with traffic emissions from the wear of engine parts, lubricants and additives used in gasoline (Ba, Cr, Cu, Mo, Pb, V, and Zn),[38,49] and emissions from diesel fuels (Ba, Cd, Cr, Mo, Ni, V, and Zn),[49,50] brake pads (Ba, Cu, and Mo) and tyre wear (Ba, Cd, and Zn),[38] as well as their use as catalysts to control car exhaust emissions (Pd and Pt).[51]

Figures of merit for the determination of metal(oid)s and PGEs in urban dust

The repeatability of metal(oid) measurements was tested by performing six analyses of SRM 1648a using nitric acid digestion, while the repeatability of measurement of PGEs was checked by analysing six SRM 1648a samples with *aqua regia* digestion. The results for repeatability, calculated as the relative standard deviation (RSD), are presented in Table 1.

Good repeatability of measurement was obtained for metal(oid)s, with an average of RSD 6% and accuracy of 2%. However, the repeatability for Pt and Pd was lower, with RSDs of 21% and 17%, respectively, due to their low concentrations in the urban dust samples analysed.

The LODs and LOQs for the determination of individual metal(oid) and PGE concentrations in the sample digests were calculated as the concentration that provided signals equal to 3s or 10s of the blank sample, respectively. To calculate the LODs and LOQs, 8 blank samples (acids used for digestion) were analysed by ICP-MS. The LODs and LOQs for metal(oid)s and PGEs, expressed in ng mL^{-1}, and for urban dust samples expressed in mg kg^{-1}, are provided in Table S4. Values expressed in ng m^{-3} are presented in Table S5. Low LODs, ranging from 0.001 to 0.02 ng mL^{-1} were achieved, enabling the quantification of metal(oid)s and PGEs in urban dust and airborne PM using the optimised analytical procedures.

The linearity of measurement for metal(oid)s and PGEs ranged from the LOQ to 1000 ng mL^{-1}, with correlation coefficients (R^2) for the calibration curves better than 0.998.

The accuracy of the optimised analytical procedures was verified by analysing SRM 1648a and comparing the determined concentrations with the certified concentrations. For elements

Table 1 Concentrations of metal(oid)s in SRM 1648a (urban particulate matter) determined after nitric acid microwave-assisted digestion and PGEs after *aqua regia* microwave-assisted digestion by ICP-MS. The results represent the concentrations of six individual samples, along with RSDs between the parallel samples

Element	Concentration (mg kg^{-1})	Concentration (mg kg^{-1})	Concentration (mg kg^{-1})	Concentration (mg kg^{-1})	Concentration (mg kg^{-1})	Concentration (mg kg^{-1})	Average (mg kg^{-1})	RSD (%)
As	127	129	123	120	118	109	119	5.4
Ba	801	812	807	806	805	815	808	0.6
Cd	75.0	72.8	74.5	71.3	73.4	73.6	73.4	1.6
Co	18.7	19.1	18.6	18.4	17.3	19.0	18.5	3.3
Cr	390	400	391	367	384	426	393	4.5
Cu	738	748	748	749	700	658	724	4.7
Mo	22.6	21.1	22.9	21.4	22.9	21.3	22.0	3.5
Ni	85.3	86.4	87.5	85.7	82.3	76.5	84.0	4.4
Pb	6527	6374	6455	6544	6359	6441	6450	1.1
Pd	0.69	0.49	0.52	0.62	0.50	0.41	0.54	17
Pt	0.041	0.027	0.040	0.022	0.030	0.033	0–032	21
Tl	1.87	1.91	1.96	1.81	1.86	1.66	1.85	5.6
V	137	139	153	150	140	131	142	5.3
Zn	5241	5260	4744	4561	4610	4263	4780	7.6

 This journal is © The Royal Society of Chemistry 2025

Open Access Article. Published on 29 August 2025. Downloaded on 9/23/2025 2:29:53 PM.
This article is licensed under a Creative Commons Attribution-NonCommercial 3.0 Unported Licence.

Table 2 Concentrations of metal(oid)s in SRM 1648a (urban particulate matter) determined after nitric acid microwave-assisted digestion and PGEs after *aqua regia* microwave-assisted digestion by ICP-MS. The results from a spike recovery test are provided for elements that are not certified. The results represent the mean concentration obtained from six parallel samples ± standard deviation between the parallel samples

Element	Determined concentration (mg kg^{-1})	Certified concentration (mg kg^{-1})	Added concentration (mg kg^{-1})	Found concentration (mg kg^{-1})	Relative recovery (%)
As	121 ± 2.9	115.5 ± 3.9	—	—	—
Ba	808 ± 2.0	—	472	1321	103
Cd	73.4 ± 0.5	73.7 ± 2.3	—	—	—
Co	18.5 ± 0.3	17.93 ± 0.68	—	—	—
Cr	393 ± 7.9	402 ± 13	—	—	—
Cu	724 ± 15.2	610 ± 70	—	—	—
Mo	22.0 ± 0.3	—	18.9	41.3	101
Ni	84.0 ± 1.6	81.1 ± 6.8	—	—	—
Pb	6450 ± 31.1	6550 ± 330	—	—	—
Pd	0.54 ± 0.04	—	9.5	10.24	98.5
Pt	0.032 ± 0.003	—	14.35	13.83	96.2
Tl	1.85 ± 0.04	—	1.9	3.6	97.3
V	142 ± 3.3	127 ± 11	—	—	—
Zn	4780 ± 162	4800 ± 270	—	—	—

not certified in SRM 1648a, a spike recovery test was applied. The sample was spiked with an appropriate amount of selected elements before microwave-assisted digestion. Nitric acid digestion was used for Ba, Mo and Tl, and *aqua regia* digestion for Pd and Pt. The relative recovery, expressed as a percentage, was calculated as the ratio between the found and expected concentrations (the sum of the element concentration in urban dust and the added concentration) multiplied by 100. The results are presented in Table 2.

It is evident that the determined concentrations are in good agreement with the certified values. The relative recoveries of the spiked elements ranged between 96% and 103%, indicating quantitative determination of Ba, Mo, Pd, Pt and Tl in urban dust samples. Therefore, it can be concluded that the optimised analytical procedures provide accurate results for the analysis of the studied metal(oid)s and PGEs.

Analytical procedures for the determination of PAHs by GC-MS

The procedure was modified based on the extraction methods described in SIST ISO 18287:2019; SIST EN 15549:2008; and SIST EN 15527:2009,[52–54] using acetone and petroleum ether. This modification involved reducing the amount of extracting agent and optimizing the extraction duration and the clean-up step. PAHs in the petroleum ether extract were quantified according to the method described in ISO 28540:2011[55] for PAH determination in water samples by GC-MS.

Initially, extraction was performed using a 100 mL mixture of acetone and petroleum ether (1 : 1, *v*/*v*). However, due to the small quantity of the sample, it was experimentally found that the volume of the extracting agent can be significantly reduced. For a 40 mg urban dust SRM sample, a mixture of 15 mL of acetone and petroleum ether (1 : 1, *v*/*v*), along with 100 μL of isooctane, was added. The samples were spiked with 50 μL of an internal standard solution (10 μg mL^{-1}) and subjected to microwave-assisted extraction (40 °C, 600 W) for 1 h, or shaken on a mechanical shaker for 16 h or 24 h (25 °C, 180 rpm).

The organic phase was passed through a 3 mL column filled with Florisil for sample clean-up and concentrated to approximately 1 mL under a nitrogen stream at 40 °C using a sample concentrator. GC-MS analysis indicated that samples shaken for 16 h achieved better recovery rates than those shaken for 24 h (recoveries greater than 7% and 11%, respectively), while the recovery rate for microwave-assisted extraction was lower (14%). Thus, mechanical shaking for a duration of 16 h was chosen as the optimal extraction procedure, followed by the clean-up step. Additionally, the results indicated that a single cleaning of the organic phase with Florisil yielded better recoveries compared to a double cleaning (recoveries of 7% and 11%, respectively). Consequently, a single cleaning procedure was employed for the petroleum ether extract containing SRM urban dust.

The optimised procedure was then applied to the determination of PAHs in the PM_{10}, $PM_{2.5}$ and $PM_{0.1}$ fractions collected on filters and for the $PM_{<0.1}$ fraction retained in the aqueous phase, as described in the section Optimised analytical procedure for the analysis of PAHs.

In this study, PAHs were investigated due to their common presence as organic contaminants in urban dust and PM, originating from vehicle exhaust, combustion processes and industrial activities.[56,57] The following 8 PAHs were selected for monitoring due to their high toxicity and prevalence in the environment: BaA, BaP, BbF, BghiP, Ch, Fl, IP, and P.[31]

Figures of merit for the determination of PAHs in urban dust

The repeatability of measurement of PAHs was evaluated by performing six analyses of SRM 1648a. The repeatability results, calculated as the RSD, are presented in Table 3.

The results in Table 3 demonstrate good repeatability of measurement, with an average RSD of 3% and accuracy of 6%.

The LODs and LOQs for the determination of concentrations of PAHs in sample extracts were calculated as the concentration that provided a signal equal to 3s or 10s of the blank sample, respectively. To calculate the LODs and LOQs, 8 blank samples (petroleum ether extract) were analysed by GC-MS. The LODs

Open Access Article. Published on 29 August 2025. Downloaded on 9/23/2025 2:29:53 PM. This article is licensed under a Creative Commons Attribution-NonCommercial 3.0 Unported Licence.

Table 3 Concentrations of PAHs in SRM 1648a (urban particulate matter) determined after extraction into petroleum ether by GC-MS. The results represent the concentrations of six individual samples ± the standard deviation of measurement, along with RSDs between the parallel samples

PAH	Concentration (mg kg^{-1})	Concentration (mg kg^{-1})	Concentration (mg kg^{-1})	Concentration (mg kg^{-1})	Concentration (mg kg^{-1})	Concentration (mg kg^{-1})	Average (mg kg^{-1})	RSD (%)
BaA	2.63	2.56	2.52	2.56	2.59	2.59	2.58	1.3
BaP	2.39	2.27	2.30	2.20	2.37	2.32	2.31	2.8
BbF	7.70	8.88	8.48	8.33	7.90	8.04	8.22	4.8
BghiP	4.32	4.03	4.23	4.18	4.17	4.14	4.18	2.1
Ch	6.75	6.70	6.81	6.66	6.85	6.81	6.76	1.0
Fl	7.59	7.65	7.57	7.40	7.52	7.96	7.62	2.3
IP	4.08	4.55	4.15	4.16	3.95	3.78	4.11	5.7
P	6.03	6.00	5.92	5.86	5.98	6.16	5.99	1.6

and LOQs for PAHs, expressed in ng mL^{-1}, and for urban dust samples expressed in mg kg^{-1}, are provided in Table S6, and expressed in ng m^{-3} in Table S7. The LODs for the PAHs measured (4.5 ng mL^{-1}) were adequate for the quantification of PAHs in urban dust and airborne PM using the optimised analytical procedures.

The linearity of measurement for PAHs ranged from the LOQ to 1000 ng mL^{-1}, with correlation coefficients (R^2) for the calibration curves better than 0.997.

The accuracy of the optimised analytical procedures was verified by analysing SRM 1648a and comparing the determined concentrations with the certified values. The results are presented in Table 4.

Data from Table 4 show good agreement between the determined PAH concentrations. Deviations from the certified value did not exceed 10%, and the exception was only BghiP, for which the determined concentration was 16% lower than the certified value. These data confirm that the optimised analytical procedure provides accurate results for the analysis of the studied PAHs.

Flow rates of low-volume pumps during sampling of size-fractionating airborne particulate matter over 28 days

To check the variation in flow rates during the one-month air sampling period, 6 cascade sampling devices with PTFE membrane filters (PM_{10}, $PM_{2.5}$, and $PM_{0.1}$) and an ultrapure-water trap for retaining the $PM_{<0.1}$ fraction were connected to 6 low-volume pumps and placed outside. The flow rate of each pump was measured on days 0, 14, 21 and 28. The data on the measured flow rates are presented in Table S8. As shown, the flow rates for all 6 pumps remained relatively unchanged throughout the course of the experiment (12 L min^{-1}). This preliminary experiment confirmed that the low-volume cascade system enables continuous sampling over a one-month period without causing filter clogging.

Table 4 Concentrations of PAHs in SRM 1648a (urban particulate matter) determined after extraction into petroleum ether by GC-MS. The results represent the mean concentrations obtained from six parallel samples ± standard deviation between the parallel samples

PAH	Determined concentration (mg kg^{-1})	Certified concentration (mg kg^{-1})
BaA	2.58 ± 0.02	2.71 ± 0.15
BaP	2.31 ± 0.03	2.57 ± 0.10
BbF	8.22 ± 0.18	8.89 ± 0.05
BghiP	4.18 ± 0.04	5.00 ± 0.18
Ch	6.76 ± 0.03	6.12 ± 0.06
Fl	7.62 ± 0.08	8.07 ± 0.14
IP	4.11 ± 0.11	4.17 ± 0.17
P	5.99 ± 0.04	5.88 ± 0.07

Evaluation of morphological characteristics and particle size distribution of particulate matter collected on filters

Airborne particles are generally classified into geogenic, anthropogenic and biogenic categories. Geogenic particles, which originate naturally, include quartz, aluminosilicates, calcium-rich particles, chlorides and Fe/Ti oxides. Anthropogenic particles, predominantly carbonaceous and sulphates, are commonly associated with vehicular emissions and biomass burning.[58,59] Biogenic particles are typically characterised as pollen, fungal spores and plant debris, contributing significant portions to airborne PM.[60] The main aim was to determine the morphology and size of fractioned PM on filters using SEM-EDS (Fig. 2), to distinguish its potential sources.

The identified particles were classified into six morphological clusters (Fig. 2): spherules (P1, P7, P12, and P13), floccules (P2), biogenic particles (P3), tabular particles (P5 and P10), irregular shaped grains (P6 and P8) and agglomerate particles (P9 and P11). Most of the identified particles were non-spherical, thereby providing a higher surface area for potential toxic compound adsorption and enhancement of their interaction with lung tissues.[61] The most common particles found in this study include alumosilicates (P1), magnesium silicates (P7), and carbonate particles (P6), along with sulphates (P8 and P10) and carbon-enriched particles (P5) (Table S9).

Anthropogenic particles include spherules, floccules and agglomerates. Spherules are typically smaller, with an average diameter of less than 3 μm,[62–65] and generally exhibit a Si–Al–Fe elemental composition. Floccules consist of small spherical particles (<1 μm) with a loose structure, while agglomerates are characterised by flexuous, fractal edge branches or crinkles randomly distributed on the surface, forming a lump-like morphology. Agglomerate and spherical particles are typically

 This journal is © The Royal Society of Chemistry 2025

Open Access Article. Published on 29 August 2025. Downloaded on 9/23/2025 2:29:53 PM.
This article is licensed under a Creative Commons Attribution-NonCommercial 3.0 Unported Licence.

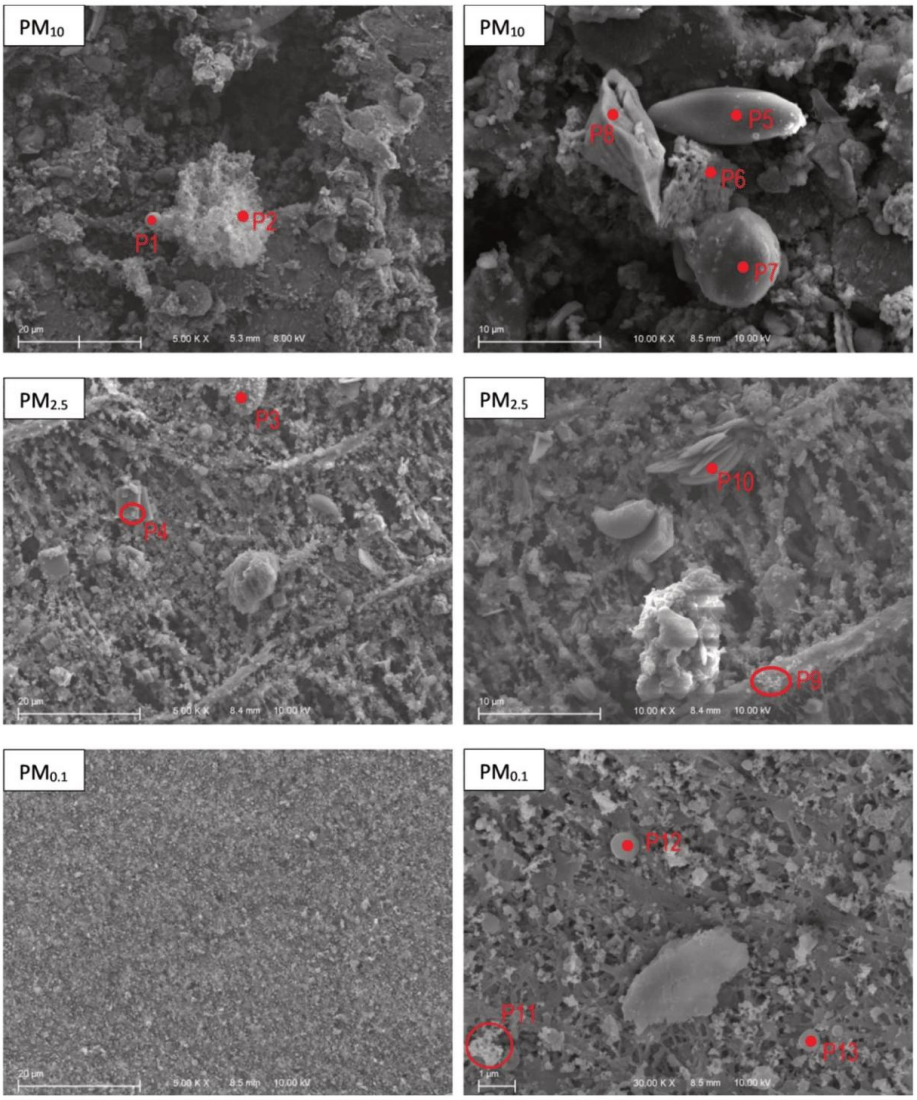


Fig. 2 SEM imaging of PM_{10} (left at 5000× magnification;right at 10 000× magnification), $PM_{2.5}$ (left at 5000× magnification; right at 10 000× magnification) and $PM_{0.1}$ (left at 5000× magnification; right at 30 000× magnification).

derived from coal combustion, while floccules result from vehicle emissions.[65]

Geogenic particles are mostly characterised by irregularly shaped grains, which exhibit smooth, flat surfaces (P5 and P8) or semi-coarse to coarse, holed surfaces (P6), with an average diameter of around 10 μm. These particles result from mechanical abrasion and originate from soil and surface deposits.[65] Tabular particles appear more elongated, either rectangular or elliptical, and are generally emitted through geogenic processes and biological activity.[65]

The SEM-EDS images show that the particles collected on filters align with the pore sizes of the filters used, confirming the reliability of the low-volume cascade PTFE membrane filter system for fractionating PM_{10}, $PM_{2.5}$ and $PM_{0.1}$ particle size fractions.

Analysis of metal(oid)s, PGEs and PAHs in size-fractionated particulate matter in urban settings in Slovenia

To demonstrate the applicability of the developed sampling device, size-fractionated PM was collected during December

Open Access Article. Published on 29 August 2025. Downloaded on 9/23/2025 2:29:53 PM.
This article is licensed under a Creative Commons Attribution-NonCommercial 3.0 Unported Licence.

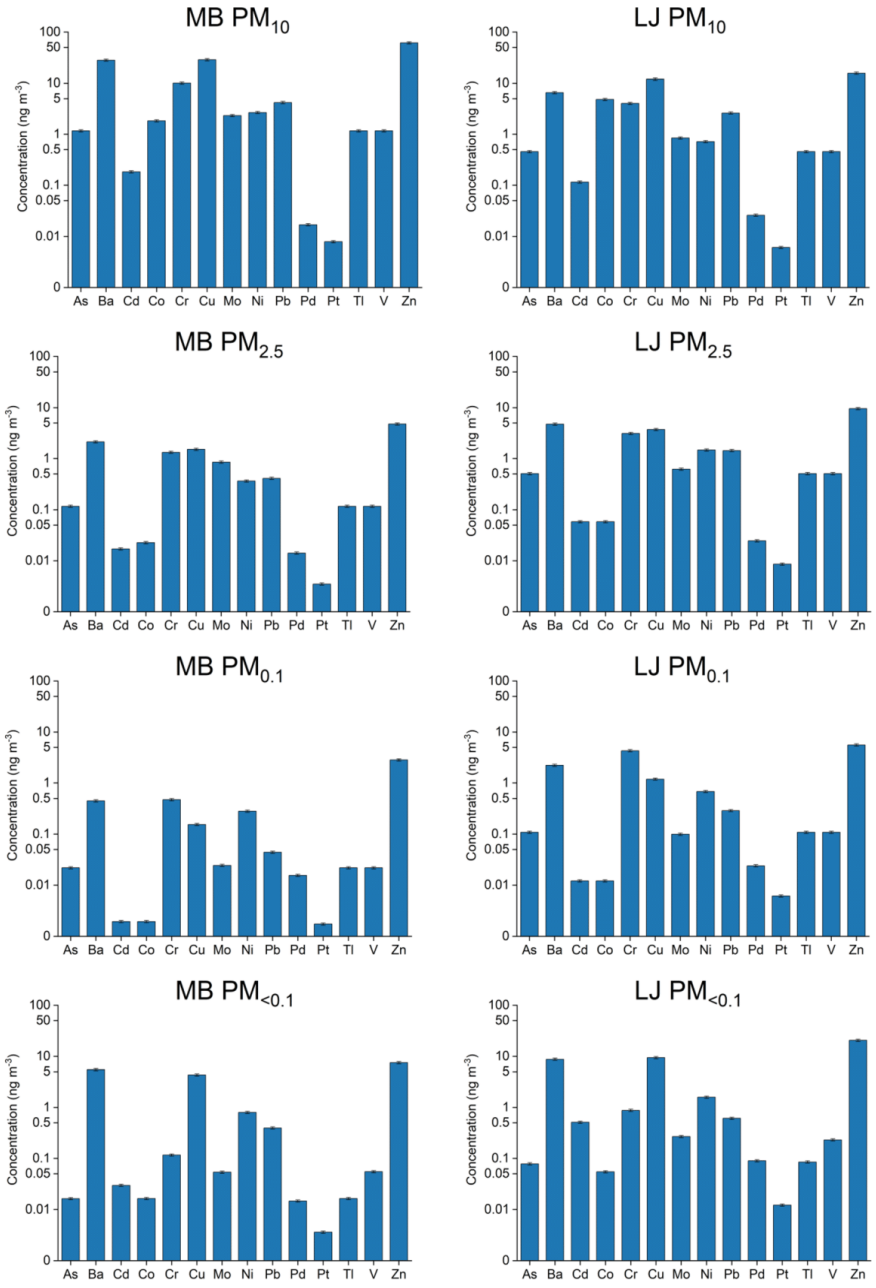


Fig. 3 The distribution of metal(oid)s in size-fractionated airborne PM in Maribor (MB), Ljubljana (LJ) and Dobrova (DB).

 This journal is © The Royal Society of Chemistry 2025

Open Access Article. Published on 29 August 2025. Downloaded on 9/23/2025 2:29:53 PM.
This article is licensed under a Creative Commons Attribution-NonCommercial 3.0 Unported Licence.

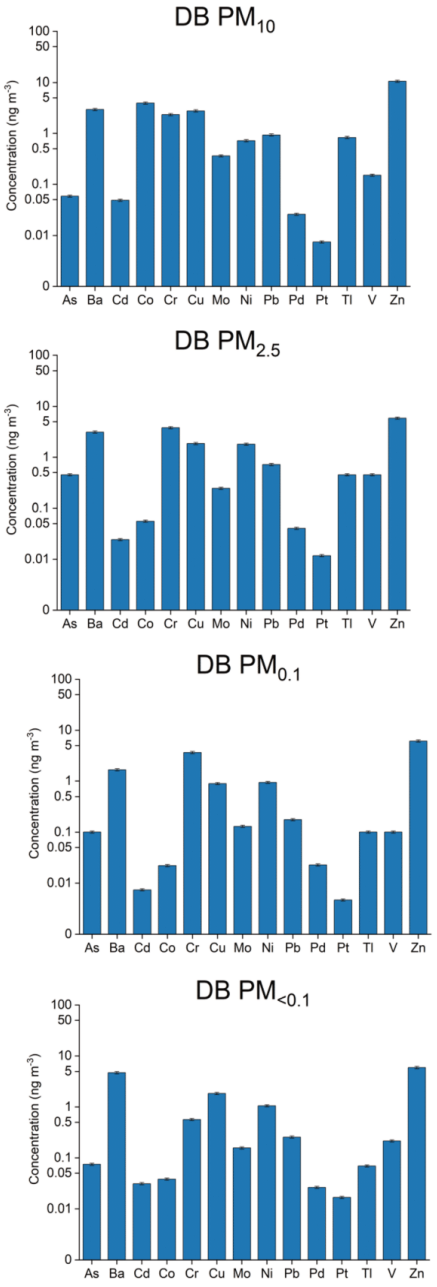


Fig. 3 *(contd.)*

2023 at three different urban settings in Slovenia: Dobrova (DB), Ljubljana (LJ) and Maribor (MB). LJ, the Slovenian capital, and MB, the second-largest city, represent densely populated areas with significant traffic-related emissions. In contrast, DB is a residential area located approximately 10 km from LJ, characterised by more localised sources of air pollution. PM samples were collected within one metre of bicycle lanes. Concentrations of metal(oid)s, PGEs and PAHs in the size-fractionated PM were determined using optimised analytical procedures. The results for metal(oid)s and PGEs are presented in Fig. 3, while the results for PAHs are shown in Fig. 4.

Fig. 3 (continued) shows the distribution of metal(oid)s in size-fractionated airborne PM in Maribor (MB), Ljubljana (LJ) and Dobrova (DB).

As shown in Fig. 3, the highest concentrations of metal(oid)s are primarily found in PM_{10} particles, with lower concentrations observed in $PM_{2.5}$ and $PM_{0.1}$. In the $PM_{<0.1}$ fraction, the concentrations of metal(oid)s (Ba, Cd, Cu, Ni, Pb, Pd, Pt, V and Zn) originating from traffic-related and coal combustion as well biomass sources, increased again to levels similar to those observed in PM_{10}. This indicates that the $PM_{<0.1}$ fraction, which penetrates most deeply into lung tissue and is potentially the most harmful to health, contributes significantly to the overall exposure to metal(oid)s.

The origin of As, Cr, Ni, Pb and V is primarily linked to high-temperature processes and fossil fuel combustion.[37,40,69,70] Ba, Cr, Cu, Mo, Pb, V and Zn are associated with gasoline engines,[38,49] while Ba, Cu and Mo arre related to lubricants and additives used in brake pads. Ba, Cd and Zn are linked to tyre wear[38] and Pd and Pt originate from catalyst emissions in car exhausts.[51]

The data in Fig. 3 further show that the highest concentrations of metal(oid)s were recorded at MB and LJ, as these sites are impacted by relatively dense traffic and are moderately populated, with populations of approximately 100 000 and 350 000, respectively. Lower metal(oid) concentrations were found at DB, which is a less densely populated residential area with less traffic. Additionally, LJ and MB also have a stronger presence of industrial facilities, including energy production plants, chemical manufacturing sites, and metal processing and waste management facilities.

Among metal(oid)s, Ba, Cr, Cu, Ni and Zn were measured in the highest concentrations in all size-fractioned PM, being elements typically associated with vehicular emissions. In MB, the PM_{10} fraction exhibited higher concentrations of As, Ba, Cr, Cu, Ni, Pb, and Zn compared to other fractions and locations, suggesting a more pronounced resuspension process and dust redistribution from both natural and anthropogenic sources.

In the PM_{10} fraction, Zn concentrations reached approximately 70 ng m^{-3} in MB and up to 15 ng m^{-3} in LJ, while Ba concentrations were around 30 ng m^{-3} in MB and 7 ng m^{-3} in LJ. Concentrations were significantly lower than those reported in larger cities, such as Fez in Morocco (with a population of about 1.1 million) or Changsha, China, where concentrations reached up to 250 ng m^{-3} for Zn and 70 ng m^{-3} for Ba.[66,67] The concentrations of Zn and Ba determined in DB in the PM_{10} fraction (Fig. 3) reached up to 10 ng m^{-3} for Zn and 5 ng m^{-3} for Ba, showing slightly lower concentrations than those reported by Jandacka *et al.*[41] for PM_{10} in the smaller city of Žilina, Slovakia (approximately 80 000 inhabitants). Across all observed

Open Access Article. Published on 29 August 2025. Downloaded on 9/23/2025 2:29:53 PM. This article is licensed under a Creative Commons Attribution-NonCommercial 3.0 Unported Licence.

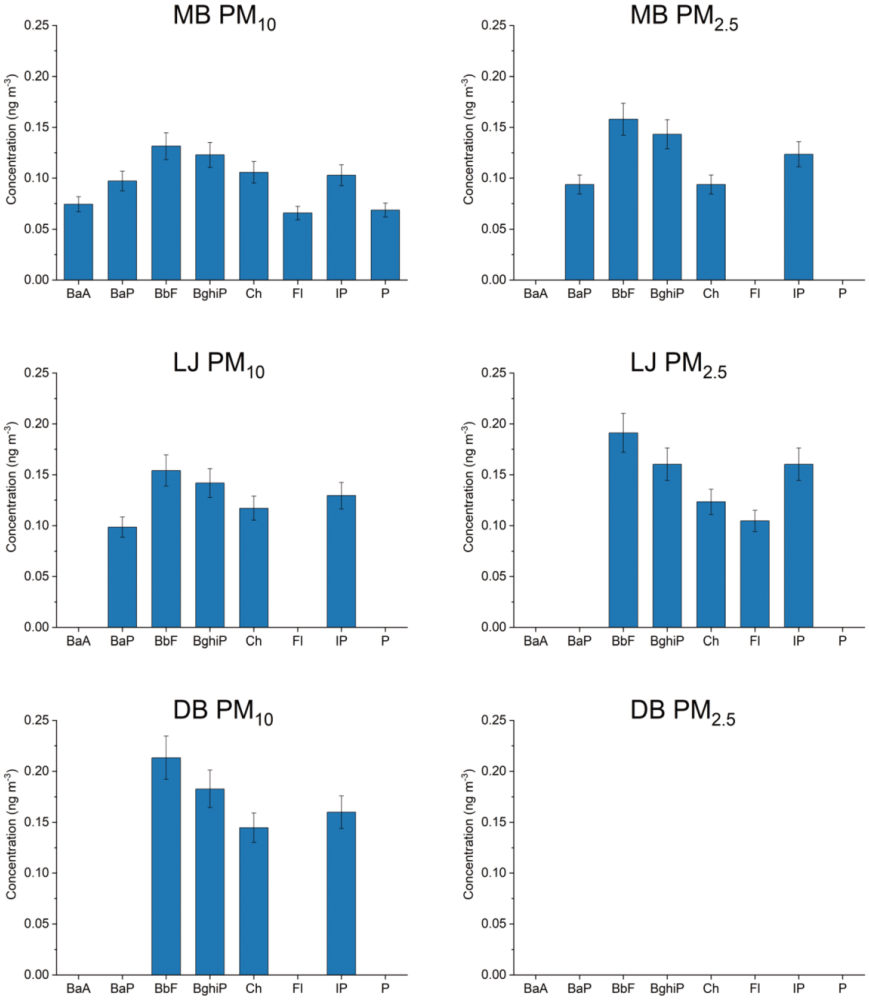


Fig. 4 The distribution of PAHs in size-fractionated airborne PM in Maribor (MB), Ljubljana (LJ) and Dobrova (DB).

PM fractions from this study (2.8–61.5 ng m^{-3} for Zn; 0.45–28.0 ng m^{-3} for Ba), concentrations were similar to those in Turin, Italy, where Zn varied between 5 and 90 ng m^{-3} for 0.54–11 μm PM fractions,[44] and to those reported in the Los Angeles area,[38] where Zn varied between 6 ng m^{-3} and 8.7 ng m^{-3} for PM_{10} and $PM_{2.5}$ respectively, and Ba between 16.5 ng m^{-3} and 14.9 ng m^{-3}. Ba and Zn, most abundant in coarse PM fractions, are typical of tyre and brake wear. Since their emissions are largely unaffected by fuel type or emission standards, this contributes to the observed similarities in their concentrations across different cities.

The highest concentrations of Cu in MB in the PM_{10} fraction (around 30 ng m^{-3}) were similar to those reported in Fez, Morocco,[67] while Ni concentrations in MB (around 2.5 ng m^{-3}) were significantly lower than those reported in Fez (95 ng m^{-3}). At the DB and LJ sampling sites, Cu concentrations in the PM_{10} fraction ranged from 2.8 and 12 ng m^{-3}, which is lower than the levels reported for Žilina (20 ng m^{-3}).[41] Ni concentrations in the PM_{10} fraction ranging from 0.7 to 2.7 ng m^{-3} were similar to those reported for Žilina (0.6 ng m^{-3}).[41] Additionally, Cu (0.15–28.6 ng m^{-3}) and Ni (0.28–2.7 ng m^{-3}) values across all PM fractions were similar to those reported in Leipzig (0.14–50 ng m^{-3} for Cu; 0.02–2.3 ng m^{-3} for Ni)[36] and Los Angeles (7.5 ng m^{-3} for Cu; 0.4–0.5 ng m^{-3} for Ni).[38] In Changsha, China,[66] Cu values across PM > 9 μm and PM < 0.4 μm varied between 10 and 20 ng m^{-3}. In Turin, Italy, Cu and Ni across 0.54–11.0 μm PM fractions varied from 0.5–3.3 ng m^{-3} and 0.5–6.0 ng m^{-3}, respectively.[44] Similarly to Ba and Zn, Cu concentrations are

 This journal is © The Royal Society of Chemistry 2025

Open Access Article. Published on 29 August 2025. Downloaded on 9/23/2025 2:29:53 PM. This article is licensed under a Creative Commons Attribution-NonCommercial 3.0 Unported Licence.

mainly influenced by non-exhaust traffic emissions, resulting in similar Cu emission profiles. In contrast, Ni is more characteristic of gasoline and diesel vehicles.

The levels of Pb in MB in PM_{10} (4 ng m^{-3}) and $PM_{2.5}$ as well as $PM_{<0.1}$ (0.4 ng m^{-3}) were similar to those observed across all PM fractions in Turin, Italy (0.25–4.5 ng m^{-3}).[44] In Los Angeles,[38] average Pb concentrations in $PM_{2.5}$ and PM_{10} varied between 0.7 and 1.9 ng m^{-3}, significantly lower than those found in Fez (around 40 ng m^{-3})[67] and Changsha, China (30−120 ng m^{-3}),[66] but higher than Pb concentrations at other sampling sites in this study (0.9 to 2.6 ng m^{-3}) and in those reported for Žilina (1.7 ng m^{-3}).[41] The concentrations of Cr in the PM_{10} fraction were also the highest in MB (around 10 ng m^{-3}) and in LJ in PM_{10} and $PM_{0.1}$ (around 4 ng m^{-3}). In $PM_{<0.1}$, Cr varied between 0.12 and 0.88 ng m^{-3}. Concentrations were lower than those reported for Fez (35 ng m^{-3})[67] and Changsha (15−20 ng m^{-3}).[66] However, they were similar to those measured in Turin (0.3–2.5 ng m^{-3}) and Los Angeles (0.8–1.4 ng m^{-3}).[38,44] At other sampling sites in this study, Cr in the PM_{10} fraction was considerably lower (between 2.3 and 4 ng m^{-3}) and similar to the concentration level of Cr in Žilina (1.7 ng m^{-3}).[41] Higher concentrations of Pb in MB can be attributed to industrial activities such as metal processing and battery manufacturing, along with exhaust emissions. Similarly elevated concentrations of Cd, Cu and Zn were also attributed to the anthropogenic activities in the local area.[67]

In the PM_{10} fraction, As concentrations in MB were 1.2 ng m^{-3}, while at other sampling sites, the levels reached 0.5 ng m^{-3}, which is similar to the reported As concentration in Žilina.[41] As in $PM_{0.1}$ and $PM_{<0.1}$ across all observed locations varied between 0.02 and 0.11 ng m^{-3}. As in Turin, Italy[44] in the PM fraction 0.54–11 μm varied between 0.04 and 0.16 ng m^{-3}. Cd concentrations at all sampling sites were very low, ranging from 0.05 to 0.2 ng m^{-3}. In Los Angeles,[38] Cd concentrations in $PM_{2.5}$ and PM_{10} varied between 0.013 and 0.047 ng m^{-3}. Co, Mo, V and Tl were also found at low levels, with concentrations not exceeding 2 ng m^{-3}.

As expected, PGEs (Pd and Pt) related to the traffic emissions were present in low concentrations at all sampling sites. Across all size fractions, Pd concentrations were generally higher than those of Pt. Pt concentrations varied between 0.002 and 0.02 ng m^{-3}, while Pd ranged from 0.01 to 0.09 ng m^{-3}. These concentrations are similar to those reported for side streets, non-urban and rural areas with low traffic near Frankfurt, Germany,[43,69] and in aerosols from cities around the world, except for metropolitan areas such as Beijing, where Pt and Pd concentrations were significantly higher (around 0.2 and 0.8 ng m^{-3}, respectively).[51] In Changsha, China,[66] Pd concentrations in PM_{10} and $PM_{2.5}$ averaged around 0.02 ng m^{-3}.

Despite the differences in city size between the urban areas selected in this study and larger cities like Turin or Los Angeles, the similar chemical fingerprinting of size-fractionated PM (PM_{10} and $PM_{2.5}$) suggests comparable pollution level profiles for selected metal(oid)s. This may be attributed to more localised emission sources in Slovenian cities, higher traffic density per unit volume of air, and limited dispersion of air pollutants. Additionally, the timing and location of sampling also plays a significant role in comparability of detected metal(oid)s; for instance, PM sampling in Turin and Fez was conducted on rooftops, reflecting a greater influence of meteorological and regional emission factors rather than direct local exposure to traffic-related emissions.

High-molecular-weight PAHs (BaA, BaP, BbF, BghiP, Ch, Fl, IP and P), typically bound to particles, were found in the highest concentrations in the PM_{10} fraction. They were also present in the $PM_{2.5}$ fraction at the MB and LJ sampling sites, but were not detected in the $PM_{0.1}$ and $PM_{<0.1}$ fractions. BbF, BghiP and IP, 5- and 6-ring PAHs typically associated with traffic-related sources exhibited higher concentrations in the $PM_{2.5}$ fraction. Their concentrations were low, ranging from 0.07 to 0.2 ng m^{-3}. BbF, BghiP and IP values in PM_{10}, $PM_{2.5}$ and PM_1 observed in Zagreb, Croatia (population about one million)[71] were higher, ranging between 0.4 and 3.4 ng m^{-3}. Higher PAH concentrations (with the sum of PAHs in the PM_{10} fraction ranging from 7 to 10 ng m^{-3}) were reported for the large city of Fez.[68] Comparable concentrations of PAHs to those reported in our study were found by Xing *et al.*[72] in Kanazawa, Japan (population of about 450 000). They observed that the sum of 9 PAHs (Fl, P, BaA, Ch, BbF, BkF, BaP BghiP and IP) in the $PM_{2.5}$ fraction ranged from 0.2 ng m^{-3} in summer to 1 ng m^{-3} in winter. A similarly low sum of PAHs (1–2.1 ng m^{-3}) was reported by Jedynska *et al.*[73] in PM_{10} and $PM_{2.5}$ fractions observed in Rome, Copenhagen, London and Oslo. For comparison, in our study conducted in MB in December 2024, the sum of 8 PAHs in PM_{10} was 0.8 ng m^{-3} and in $PM_{2.5}$ was 0.7 ng m^{-3}. In LJ, the sum of 8 PAHs in the PM_{10} fraction was 0.7 ng m^{-3}, while in the $PM_{2.5}$ fraction, it was 0.8 ng m^{-3}. The presence of high-molecular-weight PAHs can be attributed to traffic emissions as well as biomass burning.[33–35]

BaP, characterised as one of the most carcinogenic PAHs, varied between <0.02 ng m^{-3} and 0.1 ng m^{-3}, with the highest concentrations observed in the PM_{10} fraction in MB. The data from the literature show that the concentration of BaP in Porto varied between 0.01 ng m^{-3} and 2.7 ng m^{-3}, with an average value of 0.37 ng m^{-3}; while in Athens it averaged at 0.25 ng m^{-3} and 0.21 ng m^{-3} in Copenhagen.[73] In Zagreb, Croatia,[71] BaP in PM_{10}, $PM_{2.5}$ and PM_1 varied between 0.8 ng m^{-3} and 2 ng m^{-3}.

Certain compounds, such as As, Cd, Ni and BaP, are identified as human genotoxic carcinogens. The European Union Directive (Directive 2004/107/EC 2004)[74] has established threshold levels to mitigate their harmful effects on human health, with annual target values set for PM_{10} at 6 ng m^{-3} for As, 5 ng m^{-3} for Cd, 20 ng m^{-3} for Ni and 1 ng m^{-3} for BaP. In this study, none of the target values were exceeded in any size-fractioned PM samples. Threshold limits for other metal(oid)s, PGEs and PAHs for finer PM fractions have not yet been established.

The results of this study revealed that metal(oid)s, PGEs and PAHs are primarily attributed to anthropogenic activities, particularly traffic emissions and biomass burning. However, their concentrations at the selected sampling sites, located within one metre of bicycle lanes, were low, indicating that the pollution-related health risks for daily commuters are minimal.

Open Access Article. Published on 29 August 2025. Downloaded on 9/23/2025 2:29:53 PM. This article is licensed under a Creative Commons Attribution-NonCommercial 3.0 Unported Licence.

The developed sampling device for size-fractionated PM, in combination with optimised analytical procedures, enables reliable and sensitive analysis of metal(loid)s, PGEs and PAHs at very low concentrations and is also applicable in areas with high levels of air pollution. It makes a significant contribution to improving air pollution control and legislation, identifying the sources of air pollution and assessing the associated health and environmental risks.

Conclusions

In this study, a sampling device was developed, consisting of low-volume cascade PTFE membrane filter system (PM_{10}, $PM_{2.5}$, and $PM_{0.1}$), connected to an ultrapure water trap that retains the nano-sized fraction ($PM_{<0.1}$). When combined with optimised analytical procedures, this setup provides a reliable analytical tool for detecting metal(oid)s, PGEs and PAHs, including those bound to nano-sized fractions, a capability not achievable with previous sampling devices that relied solely on filters for PM fractionation, thus enabling a more accurate residential exposure assessment.

The applicability of the sampling device was demonstrated through a one-month study conducted at three different locations in Slovenia, which differ in size, population and traffic density. The results revealed that the highest concentrations of metal(oid)s and PGEs were predominantly found in the PM_{10} fraction, largely influenced by resuspension processes and dust redistribution. Trace elements linked to traffic related emissions, both exhaust and non-exhaust, as well as coal and biomass combustion (Ba, Cd, Cu, Ni, Pb, Pd, Pt, V, and Zn) were significantly elevated in $PM_{<0.1}$ across all sampling locations, indicating the importance of characterising this size range. High-molecular-weight PAHs were distributed between PM_{10} and $PM_{2.5}$ fractions, with 5-ring (BaP and BbF) and 6-ring (BghiP and IP) PAH compounds, typically associated with traffic emissions, found in higher concentrations in the $PM_{2.5}$ fraction. Contaminant concentrations were low, indicating the minimal pollution-related health risks for daily commuters using bicycle lanes.

This one-month study, incorporating a newly developed sampling device, will be further expanded into a systematic one-year study to analyse size-fractionated PM samples across urban areas in Slovenia.

Author contributions

AI: writing – original draft, methodology, analysis, data curation, conceptualisation. RMŠ: writing – review & editing, supervision, methodology, conceptualisation. MD: analysis, writing – review & editing. AMP: resources, project administration, funding acquisition, review & editing. JŠ: funding acquisition, writing – review & editing, supervision, methodology.

Conflicts of interest

There are no conflicts to declare.

Data availability

The data supporting this article have been included as part of the SI. See DOI: https://doi.org/10.1039/d5ay00858a.

Acknowledgements

The authors acknowledge Mateja Štefančič (PhD) and Mateja Košir (PhD) for morphological analysis. The authors acknowledge financial support from the Slovenian Research and Innovation Agency (ARIS), specifically from the Developmental Funding Pillar (SI: "razvojni steber financiranja, RSF"), and ARIS financial support in programme groups P2-0273 and P1-0143.

References

1 M. J. Gatari, J. Boman, A. Wagner, S. Janhäll and J. Isakson, Assessment of inorganic content of PM2.5 particles sampled in a rural area north-east of Hanoi, Vietnam, *Sci. Total Environ.*, 2006, **368**(2), 675–685.
2 J. Kukutschová, P. Moravec, V. Tomášek, V. Matějka, J. Smolík, J. Schwarz, *et al.* On airborne nano/micro-sized wear particles released from low-metallic automotive brakes, *Environ. Pollut.*, 2011, **159**(4), 998–1006.
3 P. Pant and R. M. Harrison, Estimation of the contribution of road traffic emissions to particulate matter concentrations from field measurements: A review, *Atmos. Environ.*, 2013, **77**, 78–97.
4 P. Sanderson, J. M. Delgado-Saborit and R. M. Harrison, A review of chemical and physical characterisation of atmospheric metallic nanoparticles, *Atmos. Environ.*, 2014, **94**, 353–365.
5 A. Thorpe and R. M. Harrison, Sources and properties of non-exhaust particulate matter from road traffic: A review, *Sci. Total Environ.*, 2008, **400**(1), 270–282.
6 W. Lin, H. Zhang, Y. Lai, S. Zhuang, Q. Wei, S. Fu, *et al.* Source-Specific Ecological Risk of Atmospheric PM2.5-Bound Metals and Implications for Air Pollution Control: A Regional Perspective from China, *Expo Health*, 2024, **16**(3), 745–757.
7 W. H. Shetaya, A. El-Mekawy and S. K. Hassan, Tempo-Spatial Variability and Health Risks of PM2.5 and Associated Metal(loid)s in Greater Cairo, Egypt, *Expo Health*, 2024, **16**(4), 973–988.
8 Y. Wu, N. Zhang, Y. Shi, Z. Chen, H. Zhang, J. Yin, *et al.* PAH Pollution and Risk in Particulate Matter in Chinese Cities, *Exposure Health*, 2024, **16**, 401–415.
9 H. Chen, M. S. Goldberg and P. J. Villeneuve, A systematic review of the relation between long-term exposure to ambient air pollution and chronic diseases, *Rev. Environ. Health*, 2008, **23**(4), 243–297.
10 A. J. Cohen, M. Brauer, R. Burnett, H. R. Anderson, J. Frostad, K. Estep, *et al.* Estimates and 25-year trends of the global burden of disease attributable to ambient air pollution: an analysis of data from the Global Burden of Diseases Study, *Lancet*, 2015, **389**(10082), 1907–1918.

 This journal is © The Royal Society of Chemistry 2025

Open Access Article. Published on 29 August 2025. Downloaded on 9/23/2025 2:29:53 PM.
This article is licensed under a Creative Commons Attribution-NonCommercial 3.0 Unported Licence.

11 F. J. Kelly and J. C. Fussell, Size, source and chemical composition as determinants of toxicity attributable to ambient particulate matter, *Atmos. Environ.*, 2012, **60**, 504–526.
12 H. Kim, W. H. Kim, Y. Y. Kim and H. Y. Park, Air Pollution and Central Nervous System Disease: A Review of the Impact of Fine Particulate Matter on Neurological Disorders, *Public Health Front.*, 2020, **8**, 575330.
13 A. G. Russell and B. Brunekreef, A Focus on Particulate Matter and Health, *Environ. Sci. Technol.*, 2009, **43**(13), 4620–4625.
14 Y. Wang, L. Xiong and M. Tang, Toxicity of inhaled particulate matter on the central nervous system: neuroinflammation, neuropsychological effects and neurodegenerative disease, *J. Appl. Toxicol.*, 2017, **37**(6), 644–667.
15 A. Valavanidis, K. Fiotakis and T. Vlachogianni, Airborne Particulate Matter and Human Health: Toxicological Assessment and Importance of Size and Composition of Particles for Oxidative Damage and Carcinogenic Mechanisms, *J. Environ. Sci. Health, Part C*, 2008, **26**(4), 339–362.
16 US EPA, 2019, *Integrated Science Assessment (ISA) for Particulate Matter (Final Report, Dec 2019)*.
17 M. Lippmann, *The US EPA Standards for Particulate Matter and Ozone*, Royal Society of Chemistry, 1997, pp. 75–99.
18 W. MacNee and K. Donaldson, Mechanism of lung injury caused by PM10 and ultrafine particles with special reference to COPD, *Eur. Respir. J.*, 2003, 47–51.
19 I. Drventić, M. Šala, K. Vidović and A. Kroflič, Direct quantification of PAHs and nitro-PAHs in atmospheric PM by thermal desorption gas chromatography with electron ionization mass spectroscopic detection, *Talanta*, 2023, **251**, 123761.
20 J. Sánchez-Piñero, J. Moreda-Piñeiro, E. Concha-Graña, M. Fernández-Amado, S. Muniategui-Lorenzo and P. López-Mahía, Inhalation bioaccessibility estimation of polycyclic aromatic hydrocarbons from atmospheric particulate matter (PM10): Influence of PM10 composition and health risk assessment, *Chemosphere*, 2021, **263**, 127847.
21 D. Saraga, T. Maggos, C. Degrendele, J. Klánová, M. Horvat, D. Kocman, *et al.* Multi-city comparative PM2.5 source apportionment for fifteen sites in Europe: The ICARUS project, *Sci. Total Environ.*, 2021, **751**, 141855.
22 J. Szabó, A. Nagy and J. Erdős, Ambient concentrations of PM10, PM10-bound polycyclic aromatic hydrocarbons and heavy metals in an urban site of Győr, Hungary, *Air Qual., Atmos. Health*, 2015, **8**, 229–241.
23 S. Karthikeyan, U. M. Joshi and R. Balasubramanian, Microwave assisted sample preparation for determining water-soluble fraction of trace elements in urban airborne particulate matter: evaluation of bioavailability, *Anal. Chim. Acta*, 2006, **576**(1), 23–30.
24 C. Marina-Montes, E. Abás, J. Buil-García and J. Anzano, From multi to single-particle analysis: A seasonal spectroscopic study of airborne particulate matter in Zaragoza, Spain, *Talanta*, 2023, **259**, 124550.
25 R. Milačič, H. Leskovšek, F. Dolinšek and D. Hrček, A complex study of air pollution with cadmium, lead, polycyclic aromatic hydrocarbons, sulfur dioxide, and black smoke in the Zasavje industrialized urban region in Slovenia, *Ann. Chim*, 1995, **85**, 131–148.
26 D. Salcedo, J. P. Bernal, O. Pérez-Arvizu and E. Lounejeva, Assessment of sample preparation methods for the analysis of trace elements in airborne particulate matter, *J. Anal. At. Spectrom.*, 2014, **29**(4), 753–761.
27 L. Samek, Z. Stegowski, K. Styszko, L. Furman and J. Fiedor, Seasonal contribution of assessed sources to submicron and fine particulate matter in a Central European urban area, *Environ. Pollut.*, 2018, **241**, 406–411.
28 N. Zioła and K. Słaby, The Content of Selected Heavy Metals and Polycyclic Aromatic Hydrocarbons (PAHs) in PM10 in Urban-Industrial Area, *Sustainability*, 2020, **13**, 5284.
29 L. H. Keith, The Source of U.S. EPA's Sixteen PAH Priority Pollutants, *Polycyclic Aromat. Compd.*, 2015, **35**(2–4), 147–160.
30 US EPA, 2017, *Polycyclic Aromatic Hydrocarbons (PAHs) - Integrated Risk Information System (IRIS)*.
31 WHO, Some Non-heterocyclic Polycyclic Aromatic Hydrocarbons and Some Related Exposures, *Int. Agency Res. Cancer*, 2010, **92**, 819.
32 International Agency for Research on Cancer. 2016, *Outdoor Air Pollution 109*.
33 W. Insian, N. Yabueng, W. Wiriya and S. Chantara, Size-fractionated PM-bound PAHs in urban and rural atmospheres of northern Thailand for respiratory health risk assessment, *Environ. Pollut.*, 2022, **293**, 118488.
34 R. Shen, Y. Wang, W. Gao, X. Cong, L. Cheng and X. Li, Size-segregated particulate matter bound polycyclic aromatic hydrocarbons (PAHs) over China: Size distribution, characteristics and health risk assessment, *Sci. Total Environ.*, 2019, **685**, 116–123.
35 Q. Yu, X. Ding, Q. He, W. Yang, M. Zhu, S. Li, *et al.* Nationwide increase of polycyclic aromatic hydrocarbons in ultrafine particles during winter over China revealed by size-segregated measurements, *Atmos. Chem. Phys.*, 2020, **20**(23), 14581–14595.
36 K. W. Fomba, D. van Pinxteren, K. Müller, G. Spindler and H. Herrmann, Assessment of trace metal levels in size-resolved particulate matter in the area of Leipzig, *Atmos. Environ.*, 2018, **176**, 60–70.
37 Y. Gao and H. Ji, Microscopic morphology and seasonal variation of health effect arising from heavy metals in PM2.5 and PM10: One-year measurement in a densely populated area of urban Beijing, *Atmos. Res.*, 2018, **212**, 213–226.
38 F. Oroumiyeh, M. Jerrett, I. Del Rosario, J. Lipsitt, J. Liu, S. E. Paulson, *et al.* Elemental composition of fine and coarse particles across the greater Los Angeles area: Spatial variation and contributing sources, *Environ. Pollut.*, 2022, **292**, 118356.
39 V. Evagelopoulos, N. D. Charisiou and S. Zoras, Dataset of Polycyclic aromatic hydrocarbons and trace elements in

Open Access Article. Published on 29 August 2025. Downloaded on 9/23/2025 2:29:53 PM. This article is licensed under a Creative Commons Attribution-NonCommercial 3.0 Unported Licence.

PM2.5 and PM10 atmospheric particles from two locations in North-Western Greece, *Data Brief*, 2022, **42**, 108266.
40 Y. Tian, B. Jia, P. Zhao, D. Song, F. Huang and Y. Feng, Size distribution, meteorological influence and uncertainty for source-specific risks: PM2.5 and PM10-bound PAHs and heavy metals in a Chinese megacity during 2011–2021, *Environ. Pollut.*, 2022, **312**, 120004.
41 D. Jandacka, D. Durcanska and M. Bujdos, The contribution of road traffic to particulate matter and metals in air pollution in the vicinity of an urban road, *Transp. Res. D: Transp. Environ.*, 2017, **50**, 397–408.
42 A. Teffahi, Y. Kerchich, Y. Moussaoui, P. Romagnoli, C. Balducci, C. Malherbe, *et al.* Exposure levels and health risk of PAHs associated with fine and ultrafine aerosols in an urban site in northern Algeria, *Air Qual., Atmos. Health*, 2021, **14**(9), 1375–1391.
43 F. Zereini, H. Alsenz, C. L. S. Wiseman, W. Püttmann, E. Reimer, R. Schleyer, *et al.* Platinum group elements (Pt, Pd, Rh) in airborne particulate matter in rural *vs.* urban areas of Germany: Concentrations and spatial patterns of distribution, *Sci. Total Environ.*, 2012, **416**, 261–268.
44 M. Malandrino, M. Casazza, O. Abollino, C. Minero and V. Maurino, Size resolved metal distribution in the PM matter of the city of Turin (Italy), *Chemosphere*, 2016, **147**, 477–489.
45 V. Celo, E. Dabek, D. Mathieu and I. Okonskaia, Validation of a Simple Microwave-Assisted Acid Digestion Method Using Microvessels for Analysis of Trace Elements in Atmospheric PM2.5 in Monitoring and Fingerprinting Studies, *Open Chem. Biomed. Methods J.*, 2010, **3**, 141–150.
46 E. Dabek-Zlotorzynska, Validation of a Simple Microwave-Assisted Acid Digestion Method Using Microvessels for Analysis of Trace Elements in Atmospheric PM2.5 in Monitoring and Fingerprinting Studies, *Open Chem. Biomed. Methods J.*, 2010, **3**(1), 143–152.
47 P. K. Hopke, Q. Dai, L. Li and Y. Feng, Global review of recent source apportionments for airborne particulate matter, *Sci. Total Environ.*, 2020, **740**, 140091.
48 S. A. Wise and R. L. Watters, 2020, *Standard Reference Material 1648a - Urban Particulate Matter, Certificate Analysis*, Gaithersburg.
49 P. Coufalík, P. Mikuška, T. Matoušek and Z. Večeřa, Determination of the bioaccessible fraction of metals in urban aerosol using simulated lung fluids, *Atmos. Environ.*, 2016, **140**, 469–475.
50 R. Viskup, Comparison of Different Techniques for Measurement of Soot and Particulate Matter Emissions from Diesel Engine Introduction to Diesel Emissions, *IntechOpen*, 2020, 1–19.
51 L. Zhang, Y. Wang, Y. Liu, Z. Li and X. Li, Variation of platinum group elements (PGE) in airborne particulate matter (PM2.5) in the Beijing urban area, China: A case study of the 2014 APEC summit, *Atmos. Environ.*, 2019, **198**, 70–76.
52 SIST ISO 18287:2019, *Soil Quality - Determination of Polycyclic Aromatic Hydrocarbons (PAH) - Gas Chromatographic Method with Mass Spectrometric Detection (GC-MS)*, 2019.
53 SIST EN 15527:2009, *Characterization of Waste - Determination of Polycyclic Aromatic Hydrocarbons (PAH) in Waste Using Gas Chromatography Mass Spectrometry (GC/MS)*, 2009.
54 EN 15549:2008, *Air Quality - Standard Method for the Measurement of the Concentration of Benzo[a]pyrene in Ambient Air*, 2008.
55 ISO 28540:2011, *Water Quality — Determination of 16 Polycyclic Aromatic Hydrocarbons (PAH) in Water — Method Using Gas Chromatography with Mass Spectrometric Detection (GC-MS)*, 2011.
56 K. Ravindra, R. Sokhi and R. Van Grieken, Atmospheric polycyclic aromatic hydrocarbons: Source attribution, emission factors and regulation, *Atmos. Environ.*, 2008, **42**(13), 2895–2921.
57 R. Roy, R. Jan, G. Gunjal, R. Bhor, K. Pai and P. G. Satsangi, Particulate matter bound polycyclic aromatic hydrocarbons: Toxicity and health risk assessment of exposed inhabitants, *Atmos. Environ.*, 2019, **210**, 47–57.
58 F. Usman, B. Zeb, K. Alam, Z. Huang, A. Shah, I. Ahmad, *et al.* In-Depth Analysis of Physicochemical Properties of Particulate Matter (PM10, PM2.5 and PM1) and Its Characterization through FTIR, XRD and SEM–EDX Techniques in the Foothills of the Hindu Kush Region of Northern Pakistan, *Atmosphere*, 2022, **13**(1), 124.
59 B. Zeb, K. Alam, A. Sorooshian, T. Blaschke, I. Ahmad and I. Shahid, On the Morphology and Composition of Particulate Matter in an Urban Environment, *Aerosol Air Qual. Res.*, 2018, **18**(6), 1431–1447.
60 S. Romano, Bioaerosols: Composition, Meteorological Impact, and Transport, *Atmosphere*, 2023, **14**(3), 590.
61 G. Carabali, R. Mamani-Paco, T. Castro, O. Peralta, E. Herrera and B. Trujillo, Optical properties, morphology and elemental composition of atmospheric particles at T1 supersite on MILAGRO campaign, *Atmos. Chem. Phys.*, 2012, **12**(5), 2747–2755.
62 C. A. Breed, J. M. Arocena and D. Sutherland, Possible sources of PM10 in Prince George (Canada) as revealed by morphology and *in situ* chemical composition of particulate, *Atmos. Environ.*, 2002, **36**(10), 1721–1731.
63 L. T. González, F. E. Longoria-Rodríguez, M. Sánchez-Domínguez, C. Leyva-Porras, K. Acuña-Askar, B. I. Kharissov, *et al.* Seasonal variation and chemical composition of particulate matter: A study by XPS, ICP-AES and sequential microanalysis using Raman with SEM/EDS, *J. Environ. Sci.*, 2018, **74**, 32–49.
64 W. Li and L. Shao, Transmission electron microscopy study of aerosol particles from the brown hazes in northern China, *J. Geophys. Res.:Atmos.*, 2009, **114**, D09302.
65 Z. Wang, L. Zhang, Y. Zhang, Z. Zhao and S. Zhang, Morphology of single inhalable particle in the air polluted city of Shijiazhuang, China, *J. Environ. Sci.*, 2008, **20**(4), 429–435.
66 X. Liu, Y. Zhai, Y. Zhu, Y. Liu, H. Chen, P. Li, *et al.* Mass concentration and health risk assessment of heavy metals in size-segregated airborne particulate matter in Changsha, *Sci. Total Environ.*, 2015, **517**, 215–221.

Open Access Article. Published on 29 August 2025. Downloaded on 9/23/2025 2:29:53 PM.
This article is licensed under a Creative Commons Attribution-NonCommercial 3.0 Unported Licence.

67 M. Gaberšek, M. J. Watts and M. Gosar, Attic dust: an archive of historical air contamination of the urban environment and potential hazard to health?, *J. Hazard. Mater.*, 2022, **432**, 128745.
68 N. Deabji, K. W. Fomba, E. J. dos Santos Souza, A. Mellouki and H. Herrmann, Influence of anthropogenic activities on metals, sugars and PAHs in PM10 in the city of Fez, Morocco: Implications on air quality, *Environ. Sci. Pollut. Res.*, 2024, **31**(17), 25238–25257.
69 F. Zereini, F. Alt, J. Messerschmidt, A. von Bohlen, K. Liebl and W. Püttmann, Concentration and distribution of platinum group elements (Pt, Pd, Rh) in airborne particulate matter in Frankfurt am Main, Germany, *Environ. Sci. Technol.*, 2004, **15–38**(6), 1686–1692.
70 E. Sarti, L. Pasti, M. Rossi, M. Ascanelli, A. Pagnoni, M. Trombini, *et al.* The composition of PM1 and PM2.5 samples, metals and their water soluble fractions in the Bologna area (Italy), *Atmos. Pollut. Res.*, 2015, **6**(4), 708–718.
71 I. Jakovljević, G. Pehnec, V. Vađić, M. Čačković, V. Tomašić and J. D. Jelinić, Polycyclic aromatic hydrocarbons in PM10, PM2.5 and PM1 particle fractions in an urban area, *Air Qual., Atmos. Health*, 2018, **11**(7), 843–854.
72 W. Xing, L. Zhang, L. Yang, Q. Zhou, X. Zhang, A. Toriba, *et al.* Characteristics of PM2.5-Bound Polycyclic Aromatic Hydrocarbons and Nitro-Polycyclic Aromatic Hydrocarbons at A Roadside Air Pollution Monitoring Station in Kanazawa, Japan, *Int. J. Environ. Res. Public Health*, 2020, **17**(3), 805.
73 A. Jedynska, G. Hoek, M. Eeftens, J. Cyrys, M. Keuken, C. Ampe, *et al.* Spatial variations of PAH, hopanes/steranes and EC/OC concentrations within and between European study areas, *Atmos. Environ.*, 2014, **87**, 239–248.
74 *Directive 2004/107/EC of the European Parliament and of the Council of 15 December 2004 Relating to Arsenic, Cadmium, Mercury, Nickel and Polycyclic Aromatic Hydrocarbons in Ambient Air*, **https://eur-lex.europa.eu/LexUriServ/LexUriServ.do?uri=OJ:L:2005:023:0003:0016:EN:PDF**.

Supplementary Information Article 1

Supplementary Information (SI) for Analytical Methods.
This journal is © The Royal Society of Chemistry 2025

Supplementary Information:

Innovative sampling device for size-fractionating airborne particulate matter for improved air pollution control of metal(oid)s and polycyclic aromatic hydrocarbons

Anja Ilenič,[ac] Radmila Milačič Ščančar,[bc] Marija Đurić,[a] Alenka Mauko Pranjić[a] and Janez Ščančar*[bc]

[a] *Department of Materials, Slovenian National Building and Civil Engineering Institute, Ljubljana, Slovenia*
[b] *Department of Environmental Sciences, Institute Jožef Stefan, Ljubljana, Slovenia*
[c] *Jožef Stefan International Postgraduate School, Ljubljana, Slovenia*
* *janez.scancar@ijs.si*

Table S1 ICP-MS operating parameters for the analysis of metal(oid)s.

Parameter	Type/Value	Helium mode	No gas mode
Sample introduction			
Nebuliser	Micromist		
Spray chamber	Scott		
Skimmer and sampler	Ni		
Plasma conditions			
Forward power	1550 W		
Plasma gas flow	15.0 L min^{-1}		
Carrier gas flow		1.05 L min^{-1}	1.05 L min^{-1}
He gas flow		4.5 mL min^{-1}	
QP bias		–15.0 V	–3.6 V
Oct bias		–18.0 V	–8.0 V
Cell entrance		–40 V	–40 V
Cell exit		–60 V	–50 V
Deflect		–2.2 V	13.4 V
Plate bias		–60 V	–40 V
Sample uptake rate	0.3 mL min^{-1}		
Data acquisition parameters			
m/z isotopes monitored		^{51}V, ^{52}Cr, ^{59}Co, ^{60}Ni, ^{63}Cu, ^{66}Zn, ^{75}As, ^{95}Mo	^{105}Pd, ^{111}Cd, ^{137}Ba, ^{195}Pt, ^{205}Tl, ^{208}Pb
m/z of isotopes of internal standards		^{72}Ge, ^{103}Rh, ^{193}Ir	^{72}Ge, ^{103}Rh, ^{193}Ir

Table S2 GC-MS operating parameters for the analysis of PAHs.

Parameter	Type/Value				
Sample introduction					
Injection ports	Pulsed splitless mode				
Injection volume	1 µL				
GC parameters					
Carrier gas	He				
Carrier gas flow	1.1 mL min^{-1}				
Carrier gas velocity	38 cm sec^{-1}				
Oven parameters	First ramp: 50 ˚C (hold 1 min) to 120 ˚C at a rate of 30 ˚C min^{-1}; Second ramp: 120 ˚C to 250 ˚C at a rate of 10 ˚C min^{-1}; Third ramp: 250 ˚C to 300 ˚C at a rate 5 ˚C min^{-1}; Hold time 8 min				
MS parameters					
MS Quadrupole temperature	180 ˚C				
MS Source temperature	280 ˚C				
Selected ions for monitoring PAHs and retention times	Target ion (m/z)	Qualifier ion 1 (m/z)	Qualifier ion 2 (m/z)	Qualifier ion 3 (m/z)	Retention time (min)
BaA	228	151	153	76	17.87
BaP	252				21.93
BbF	252	154	152	76	20.99
BghiP	276				26.01
Ch	228				17.97
Fl	202				14.39
IP	138				25.29
P	202	200	203	101	14.89

Table S3 Retention times of separated PAHs and PAHs-D compounds used as internal standards, applying the GC-MS procedure.

PAH and PAH-D compound	Retention time (min)
Nap-D8	5,40
Nap	5,42
Acy-D8	8,06
Acy	8,08
Ace-D10	8,40
Ace	8,46
Fle-D10	9,46
Fle	9,51
Ph-D10	11,57
Ph	11,62
An-D10	11,68
An	11,72
Fl-D10	14,35
Fl	14,39
P-D10	14,85
P	14,89
BaA-D12	17,81
BaA	17,87
Ch-D12	17,91
Ch	17,97
BbF-D12	20,92
BbF	20,99
BkF-D12	21,01
BkF	21,06
BaP-D12	21,86
BaP	21,93
IP-D12	25,24
IP	25,29
DahA-D14	25,34
DahA	25,43
BghiP-D12	25,93
BghiP	26,01

Table S4 LODs and LOQs for the determination of metal(oid)s and PGEs in sample digests and in urban dust samples after microwave-assisted digestion by ICP-MS.

Element	Sample digest		Urban dust sample	
	LOD ($ng\ mL^{-1}$)	LOQ ($ng\ mL^{-1}$)	LOD ($mg\ kg^{-1}$)	LOQ ($mg\ kg^{-1}$)
As	0.003	0.010	0.002	0.007
Ba	0.017	0.057	0.013	0.042
Cd	0.001	0.003	0.001	0.002
Co	0.002	0.007	0.002	0.005
Cr	0.003	0.010	0.002	0.007
Cu	0.023	0.077	0.017	0.057
Mo	0.003	0.010	0.002	0.007
Ni	0.010	0.033	0.008	0.025
Pb	0.023	0.077	0.017	0.057
Pd	0.002	0.007	0.002	0.005
Pt	0.007	0.023	0.005	0.017
Tl	0.007	0.023	0.005	0.017
V	0.001	0.003	0.001	0.002
Zn	0.017	0.057	0.013	0.042

Table S5 LODs and LOQs for the determination of metal(oid)s and PGEs in size-fractionated airborne PM after microwave-assisted digestion by ICP-MS.

Element	Size-fractionated airborne PM	
	LOD ($ng\ m^{-3}$)	LOQ ($ng\ m^{-3}$)
As	0.000016	0.000052
Ba	0.000088	0.000294
Cd	0.000005	0.000017
Co	0.000010	0.000035
Cr	0.000016	0.000052
Cu	0.000119	0.000398
Mo	0.000016	0.000052
Ni	0.000052	0.000173
Pb	0.000119	0.000398
Pd	0.000010	0.000035
Pt	0.000036	0.000121
Tl	0.000036	0.000027
V	0.000005	0.000004
Zn	0.000088	0.000065

Table S6 LODs and LOQs for the determination of PAHs in sample extracts and in urban dust samples after extraction in acetone and petroleum ether by GC-MS.

PAH compound	Sample extract		Urban dust sample	
	LOD ($ng\ mL^{-1}$)	LOQ ($ng\ mL^{-1}$)	LOD ($mg\ kg^{-1}$)	LOQ ($mg\ kg^{-1}$)
BaA	4.50	15	0.090	0.300
BaP	4.50	15	0.090	0.300
BbF	4.50	15	0.090	0.300
BghiP	4.50	15	0.090	0.300
Ch	4.50	15	0.090	0.300
Fl	4.50	15	0.090	0.300
IP	4.50	15	0.090	0.300
P	4.50	15	0.090	0.300

Table S7 LODs and LOQs for the determination of PAHs in size-fractionated airborne PM after extraction in acetone and petroleum ether by GC-MS.

PAH compound	Size-fractionated airborne PM	
	LOD ($ng\ m^{-3}$)	LOQ ($ng\ m^{-3}$)
BaA	0.023	0.076
BaP	0.023	0.076
BbF	0.023	0.076
BghiP	0.023	0.076
Ch	0.023	0.076
Fl	0.023	0.076
IP	0.023	0.076
P	0.023	0.076

Table S8 Flow rates measured for low-volume pumps at the start of the experiment (day 0) and on days 14, 21, and 28 using a sampling device for size-fractionating airborne PM.

	Pump No.					
	1	2	3	4	5	6
Day	(L min^{-1})	(L min^{-1})	(L min^{-1})	(L min^{-1})	(L min^{-1})	(L min^{-1})
0	12±1	12±1	12±1	12±1	12±1	12±1
14	12±1	12±1	12±1	12±1	12±1	12±1
21	12±1	12±1	10±1	12±1	10±1	12±1
28	12±1	12±1	12±1	12±1	12±1	12±1

Table S9 Results of semi-quantitative chemical analysis (EDS) of the most common particles found in this study, collected on various PTFE filter fractions, related to SEM imaging (see Fig. 2).

Particle P1	Element	O	Na	Mg	Al	Si	K	Au
(alumosilicates)	Atomic %	69.12	1.22	1.18	9.50	15.76	1.72	1.50
	Weight %	49.73	1.27	1.29	11.53	19.90	3.03	13.27
Particle P5	Element	C	O					
(carbon-enriched particles)	Atomic %	58.56	41.44					
	Weight %	65.30	34.70					
Particle P6	Element	C	O	Mg	Ca			
(carbonate particles)	Atomic %	19.47	54.66	12.49	13.38			
	Weight %	27.55	58.05	8.73	5.67			
Particle P7	Element	C	O	Mg	Si			
(magnesium silicates)	Atomic %	57.49	27.19	8.39	6.93			
	Weight %	67.63	24.01	4.88	3.48			
Particle P8	Element	O	F	S	Ca			
(sulphates)	Atomic %	48.19	6.08	21.33	24.41			
	Weight %	65.39	6.94	14.44	13.22			
Particle P10	Element	O	S	K	Ca			
(sulphates)	Atomic %	44.42	25.19	10.86	19.53			
	Weight %	64.17	18.16	6.42	11.26			

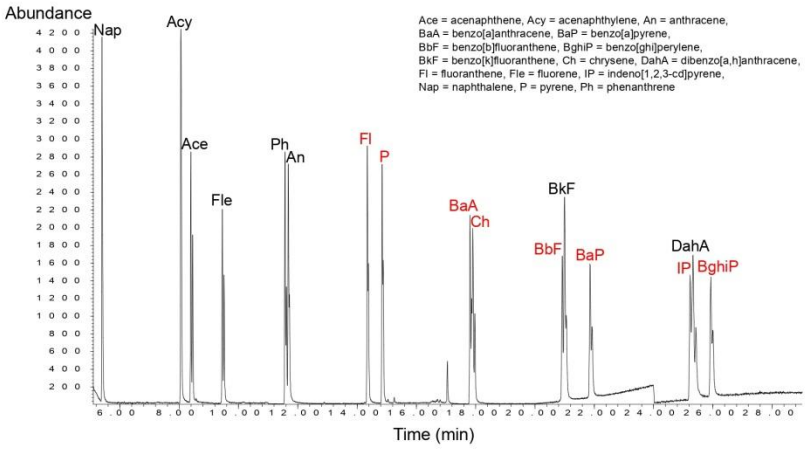


Fig. S1 Typical chromatogram showing the separation of a solution consisting of standard PAH-Mix 9 solution (16 PAHs, 500 ng mL^{-1}) and the deuterated PAH-Mix 9 (16 PAHs-D, 500 ng mL^{-1}) used as an internal standard, applying the GC-MS procedure. The PAHs analysed in the present manuscript are marked in red. The retention times for the separated PAHs analogues are provided in Table S3.



Fig. S2 Sample collection device.

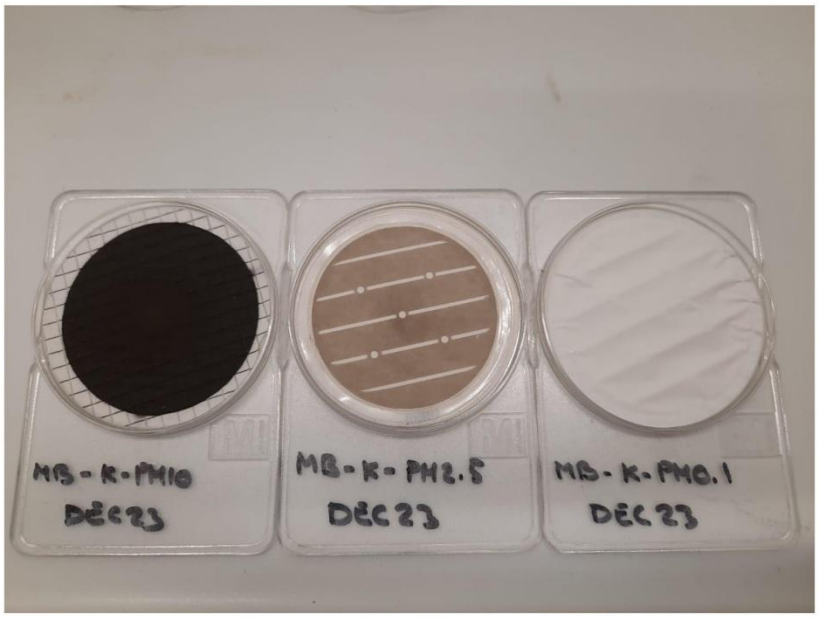


Fig. S3 PM_{10}, $PM_{2.5}$ and $PM_{0.1}$ fractions collected on PTFE filters.

3.2 Article 2: Size-Fractionated Airborne Particulate Matter-Bound Metal(oid)s and Polycyclic Aromatic Hydrocarbons in Urban Pedestrian and Cycling Microenvironments: Seasonal Trends, Source Apportionment and Health Risk Assessment

Authors: Anja Ilenič, Radmila Milačič Ščančar, Alenka Mauko Pranjić, Nina Zupančič, Marija Đurić, Janez Ščančar
Manuscript submitted to Environmental Research, Elsevier, under review

Action	Manuscript Number	Title	Initial Date Submitted	Status Date	Current Status
Action Links	ER-25-21607	Size-fractionated Airborne Particulate Matter-Bound Metal(oid)s and Polycyclic Aromatic Hydrocarbons in Urban Pedestrian and Cycling Microenvironments: Seasonal Trends, Source Apportionment and Health Risk Assessment	Nov 25 2025 7:47AM	Dec 8 2025 3:38AM	Under Review

Size-fractionated airborne particulate matter (PM_{10}, $PM_{2.5}$, $PM_{0.1}$, $PM_{<0.1}$) was collected over a one year (2023−2024) near bicycle lanes at five urban pedestrian and cycling locations in Slovenia (Dobrova (DB), Ljubljana (LJ), Murska Sobota (MS), Maribor (MB), Piran (PR)) to assess potential health risks from residential inhalation exposure to metal(oid)s and PAHs. At all locations, the highest concentrations of metal(oid)s, in descending order, were observed for Zn, Ba, Cu and chromium (Cr), predominantly found in PM_{10}, while Ba, Cd, Cu, Ni, Pb and Zn, elements primarily associated with direct vehicular exhaust and non-exhaust emissions, were also significantly enriched in $PM_{<0.1}$. Among PAHs, BbF, BghiP and IP were the most abundant, with the total sum of PAHs being the highest for PM_{10}, followed by $PM_{0.1}$ and $PM_{2.5}$. The highest concentrations of metal(oid)s and PAHs were observed during the heating period (HP), with an average HP-to-non-heating period (NHP) metal(oid) ratios of 1.8, 2.1, 3.4 and 1.5 for PM_{10}, $PM_{2.5}$, $PM_{0.1}$ and $PM_{<0.1}$, respectively, and the highest differences observed for cobalt (Co), molybdenum (Mo) and thallium (Tl), all typically associated with high-temperature fossil fuel combustion. Metal(oid)s were mostly influenced by PM size, while PAH concentrations were significantly affected by seasonal variations, primarily due to greater atmospheric stability in winter, enhanced partitioning of HMW PAHs into particulate phase due to reduced volatility and more efficient volatilisation of LMW PAHs into gaseous phase combined with intensified photochemical degradation during summer. The highest concentrations, particularly during the HP, were recorded in more densely populated and higher traffic cities of LJ and MB, also resulting from unfavourable meteorological conditions with frequent thermal inversions, low planetary boundary layer (PBL) height and weak vertical mixing of air masses, allowing submicronic particles to remain airborne longer. It was observed that air pollution sources were the least localised in areas with the highest pollution levels. Source apportionment using different statistical analysis, diagnostic ratios and elemental fingerprinting indicated a dominance of pyrogenic sources, including i) vehicle exhausts from diesel engines (BbF, BghiP, IP, Ni, Pb); ii) deposition and re-suspension of mineral dust and non-exhaust sources, such as tyre and brake wear (Ba, cerium (Ce), Cu, lanthanum (La), V, Zn); and iii) combustion of coal and biomass during HP (BaA, BaP, Fl and Pyr, along with As, Co, Cr, Mo and Tl). The carcinogenic risk assessment

observed for pedestrians and cyclist for different demographic groups and exposure scenarios, using lifetime average daily dose (LADD) and hazard quotient (HQ), indicated an overall negligible cancer risk, with the exception of As, Co and Cr, which exhibited a low potential risk through inhalation, particularly for child cyclists. The calculated HQ values remained below the threshold, and the European limit values for As, Cd and BaP in PM_{10} were not exceeded.

Size-fractionated Airborne Particulate Matter-Bound Metal(oid)s and Polycyclic Aromatic Hydrocarbons in Urban Pedestrian and Cycling Microenvironments: Seasonal Trends, Source Apportionment and Health Risk Assessment

Anja Ilenič[1,2], Radmila Milačič Ščančar[2,3], Alenka Mauko Pranjić[1], Nina Zupančič[4,5], Marija Đurić[1], Janez Ščančar[2,3]

[1]Slovenian National Building and Civil Engineering Institute, Department of Materials, Ljubljana 1000, Slovenia

[2]Jožef Stefan International Postgraduate School, Ljubljana 1000, Slovenia

[3]Jožef Stefan Institute, Department of Environmental Sciences, Ljubljana 1000, Slovenia

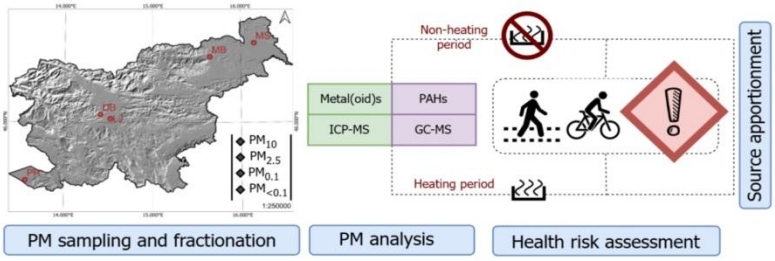
[4]University of Ljubljana, Faculty of Natural Sciences and Engineering, Ljubljana 1000, Slovenia

[5]ZRC SAZU Ivan Rakovec Institute of Paleontology, Ljubljana 1000, Slovenia

Abstract

Size-fractionated airborne particulate matter (PM_{10}, $PM_{2.5}$, $PM_{0.1}$, $PM_{<0.1}$) was collected over one year (2023–2024) at five urban pedestrian and cycling locations in Slovenia to assess potential health risks from residential inhalation exposure to metal(oid)s and polycyclic aromatic hydrocarbons (PAHs). At all locations, the highest concentrations among metal(oid)s, in descending order, were observed for Zn, Ba, Cu and Cr, predominantly in PM_{10}, while Ba, Cd, Cu, Ni, Pb and Zn were also significantly enriched in $PM_{<0.1}$. Among PAHs, BbF, BghiP and IP were most abundant, with the total PAH sum being the highest for PM_{10}, followed by $PM_{0.1}$ and $PM_{2.5}$. The elemental distribution was primarily influenced by PM size, reflecting the enhanced size-selective adsorption potential of smaller PM due to their larger specific surface area. In contrast, PAH levels were significantly affected by seasonal variations, primarily due to increased atmospheric stability and limited vertical air mixing in winter, along with particulate phase partitioning of low-volatile, high-molecular-weight PAHs and intensified photochemical degradation during summer. Peak pollutant concentrations occurred during the heating period, particularly in more densely populated and high-traffic cities. Source apportionment revealed a dominance of pyrogenic sources, including i) vehicular exhaust from diesel engines, ii) mineral dust and non-exhaust emissions and iii) coal and biomass combustion. The calculated carcinogenic health risk was negligible, except for As, Co and Cr, which exhibited a low potential risk through inhalation, particularly for child cyclists. The European limit values for As, Cd and BaP in PM_{10} were not exceeded.

Keywords: Size-fractionation; Particulate matter; Metal(oid)s; Polycyclic aromatic hydrocarbons; Sources; Health risk assessment


MS
MB
CB
PM10
PM2.5
PM0.1
PM<0.1
Non-heating period
Heating period
Metal(oid)s
PAHs
ICP-MS
GC-MS
Source apportionment
PM sampling and fractionation
PM analysis
Health risk assessment

42

43

44

1. Introduction

The health impacts of urban airborne particulate matter (PM) are significantly influenced by its size and chemical composition, with the most detrimental effects associated with particles smaller than 2.5 μm, which predominantly originate from anthropogenic sources (Fernández Camacho et al., 2012; Morawska et al., 2008; Raaschou Nielsen et al., 2013). Exposure to fine and ultrafine particles, which can penetrate deep into the respiratory system, has been linked to numerous adverse health effects, including chronic and acute respiratory and cardiovascular diseases, such as stroke and lung cancer, ultimately leading to reduced life expectancy (Chen et al., 2008; Cohen et al., 2017; Dominici et al., 2006). These health risks are at least partially attributed to the toxic substances bound to PM, such as metal(oid)s and polycyclic aromatic hydrocarbons (PAHs). These highly persistent compounds tend to bioaccumulate and can induce oxidative stress, highlighting the importance of understanding their environmental distribution (EEA, 2012; Gao and Ji, 2018). Certain metal(oid)s are considered useful conservative indicators of particulate emission sources due to their high atmospheric stability (Fomba et al., 2018; Morawska et al., 2008). In urban environments, they are associated with high-temperature combustion processes, motor vehicle emissions, tyre and break wear and road dust, with contributions varying depending on the location and meteorological conditions (Fomba et al., 2018; Gao and Ji, 2018). PAHs are semi-volatile organic compounds with fused ring structures containing at least two benzene rings (Ravindra et al., 2008). They are formed through incomplete combustion processes or the pyrolysis of organic matter such as wood, coal, natural gas or oil (Jakovljević et al., 2018; Ravindra et al., 2008). In the atmosphere, PAHs partition into gaseous and particulate phases based on their volatility, with low-molecular-weight (LMW) PAHs (2−3 rings) in the gas phase and high-molecular-weight (HMW) PAHs (4 or more rings) in the particulate phase (Ravindra et al., 2008). The carcinogenicity of PAHs increases with the molecular weight (Ravindra et al., 2008). Understanding the relationship between the particle chemical composition and size is essential, yet the available data remains limited. Sampling stations are typically installed on buildings' rooftops, and therefore do not accurately reflect the local

environments where commuters (e.g. pedestrians, cyclists) reside (Akhbarizadeh et al., 2021; Chen et al., 2019; Fadel et al., 2021; Fomba et al., 2018; Gao and Ji, 2018). Moreover, most studies have focused on a single pollutant type, either organic or inorganic, in size-fractionated PM_{10} or $PM_{2.5}$ (Fomba et al., 2018; Gao and Ji, 2018; Jedynska et al., 2014); therefore, research on the multi-pollutant chemical composition of nanoparticles (PM_1 or smaller) is limited (Jakovljević et al., 2018; Jandacka et al., 2017; Mbengue et al., 2014). The aim of this study was to advance the understanding of urban airborne size-fractionated PM and its association with the size-specific chemical composition, with particular emphasis on the PM < 0.1 μm. We present the results of one year monitoring analysis of selected metal(oid)s and PAHs bound to PM_{10}, $PM_{2.5}$, $PM_{0.1}$ and $PM_{<0.1}$ collected in urban pedestrian and cyclist microenvironments. The objectives were to i) assess the seasonal and spatial variability of pollutant concentrations, ii) apportion the potential sources and iii) evaluate the toxic potential and possible health risk implications associated with exposure of pedestrians and cyclists via inhalation.

2. Materials and methods

2.1. Sampling sites and sample collection

The airborne size-fractionated PM was collected over a one-year period, from 1 June 2023 to 31 June 2024, at five urban locations in Slovenia, distributed along a traverse from south-west to north-west. The sampling sites included three distinctive urban locations – Maribor (MB: 46.548294, 15.649047), Ljubljana (LJ: 46.033985, 14.518328) and Murska Sobota (MS: 46.661490, 16.151619) – one residential area – Dobrova (DB: 46.067450, 14.409407) – and one reference area, with minimal or negligible pollution, – Piran (PR: 45.517636, 13.568725) (Fig. 1). Dobrova (population: 100) is a roadside settlement situated on the western outskirts of Ljubljana, the capital of Slovenia (population: 293,000). Both sampling sites lie within the Sava River basin, surrounded by the hills of the Dinaric Alps. Maribor,

Slovenia's second largest city (population: 114,000), is located in the Drava River basin. Murska Sobota (population: 19,000) is situated in the Pannonian-flat landscape, while Piran (population: 18,000) is a coastal sampling location.

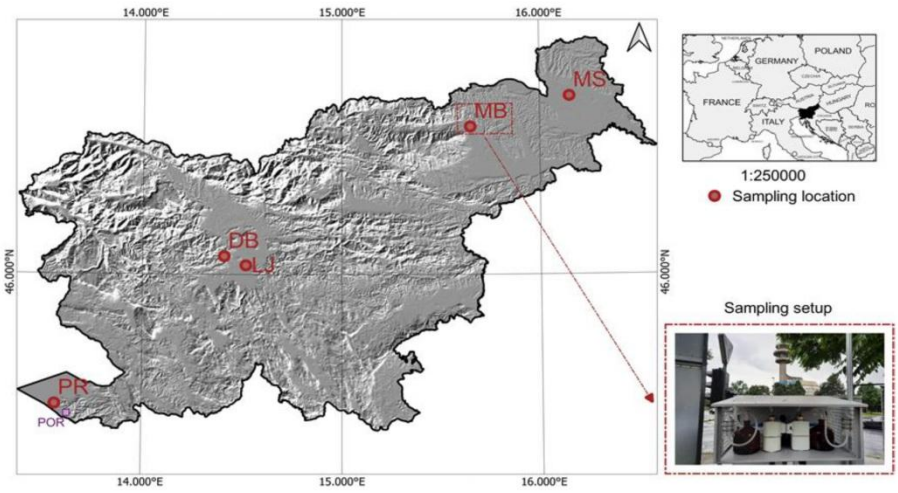


Fig. 1 A map of the study area indicating sampling sites in Maribor (MB), Ljubljana (LJ), Murska Sobota (MS), Dobrova (DB) and Piran (PR). MB, LJ and MS represent urban areas, DB represents a residential area and PR a reference site.

The sampling setups were positioned at ground level, at an average human height (170 cm), and they were located within one metre of bicycle lanes. Monthly samples were collected using a low-volume sampling cascade system, consisting of two identical units, one for the determination of PM-bound metal(oid)s and the other for the determination of PM-bound PAHs. Each unit was equipped with a three-stage cascade polytetrafluoroethylene (PTFE) membrane filter holding system (Innovation NILU, Norway), incorporating hydrophobic filters with pore sizes of 10 μm, 2.5 μm and 0.1 μm (Mitex, Whatman, Omnipore; 47 mm diameter; Merck, KGaA, Darmstadt, Germany). The system was connected to an ultrapure-water trap (18.2 MΩ cm; Direct-Q 5 Ultrapure water system, PURELAB Flex 3, ELGA LabWater, UK)

117 inside a 2000 mL amber glass burette bottle, used for collecting nanosized PM (<0.1 μm).
118 The airflow (approximately 11 L min^{-1}) passing through the system was controlled by a low-
119 volume diaphragm pump (Vacuubrand ME 1C; 100mbar, 0.8 m^3 h^{-1}) connected to a gas
120 meter (Dadolab Class G1.6 Laboratory dry gas meter, Italy). The airflow was monitored
121 monthly throughout the entire sampling period, with an average airflow of 198 m^3 $month^{-1}$,
122 making it possible to report metal(oid) and PAH concentrations in ng m^{-3} of air.
123
124 ***2.2. Analytical methods for characterising PM size-fractionated samples***
125 A total of 480 size-fractionated airborne PM samples (PM_{10}, $PM_{2.5}$, $PM_{0.1}$, $PM_{<0.1}$) were
126 collected and analysed for metal(oid)s and PAHs (Tables S1−S9; Supplementary
127 Information). Each PTFE filter (PM_{10}, $PM_{2.5}$, $PM_{0.1}$), along with $PM_{<0.1}$ retained in the
128 ultrapure aqueous phase, represented the average monthly PM concentrations. Prior to
129 sampling, PTFE filters were pre-desiccated for at least 24 h and weighed (Mettler AE 163
130 analytical balance, Zürich, Switzerland) before and after PM collection to determine the
131 precise proportion of PM. For analysis, two consecutive monthly filters from each location
132 were combined.
133
134 ***2.2.1. Determination of metal(oid)s in airborne size-fractionated PM***
135 Arsenic (As), barium (Ba), cadmium (Cd), cerium (Ce), cobalt (Co), chromium (Cr), copper
136 (Cu), lanthanum (La), molybdenum (Mo), nickel (Ni), lead (Pb), thallium (Tl), vanadium (V)
137 and zinc (Zn) were determined in size-fractionated airborne PM using microwave-assisted
138 acid digestion (Milestone Microwave Digestion System, Sorisole, Italy). A mixture of 3 mL
139 nitric (HNO_3), 1 mL hydrochloric (HCl) and 0.2 mL hydrofluoric (HF) Suprapure acids was
140 used. Prior to the total digestion, $PM_{<0.1}$ samples retained in the ultrapure aqueous phase
141 were evaporated to 20 mL at 200 °C. Samples were subjected to closed-vessel microwave-
142 assisted digestion using the following temperature programme: ramp to 140 °C for 15 min,
143 hold at 140 °C for 5 min, ramp to 200 °C for 20 min, hold at 200 °C for 60 min and cool down

144 for 30 min. The clear digests were diluted to 30 mL with ultrapure water and the total
145 elemental concentrations were determined by inductively coupled plasma mass
146 spectrometry (ICP-MS, Agilent 7900 instrument, Agilent Technologies, Tokyo, Japan), using
147 external calibration for quantification.

148

149 ***2.2.2. Determination of PAHs in airborne size-fractionated PM***

150 The United States Environmental Protection Agency (US EPA) has identified 16
151 unsubstituted PAHs as priority pollutants, among which benzo(a)anthracene (BaA),
152 benzo(a)pyrene (BaP), benzo(b)fluoranthene (BbF), benzo(g,h,i)perylene (BghiP), chrysene
153 (Ch) and indeno(1,2,3-cd)pyrene (IP) are of particular concern due to their carcinogenic,
154 teratogenic and mutagenic properties (US EPA, 2017; WHO, 2010). These compounds,
155 along with fluoranthene (Fl) and pyrene (P) were extracted from size-fractionated airborne
156 PM using an organic solvent mixture of acetone (C_3H_6O) and petroleum ether (C_6H_{14}) (1:1,
157 v:v), along with 2,2,4-Trimethylpentane (C_8H_{18}) used as a retention agent. All samples were
158 spiked with 50 µL of an internal standard (PAH-Mix 9 deuterated 10 µg mL^{-1} in
159 cyclohexane). Extraction was performed by mechanical shaking (Vibromix 40 orbital shaker,
160 Tehtnica, Železniki, Slovenia) at 180 rpm for 16 h. Extracts from $PM_{<0.1}$ retained in the
161 ultrapure aqueous phase were then subjected to liquid-liquid extraction (LLE), followed by
162 the removal of trace water with anhydrous sodium sulphate (Na_2SO_4, 550 °C, 6 h). The
163 organic phase from both the filter extracts and the $PM_{<0.1}$ retained in the ultrapure aqueous
164 phase was filtered through activated magnesium silicate (MgO_3Si; Strata FL-PR Florisil; 170
165 µm, 80 A, 500 mg^3 mL^{-1}; U.S. Silica Company) for sample clean-up and concentrated to
166 approximately 1 mL under a nitrogen stream (N_2, 40 °C) using a sample concentrator (Dri-
167 Block Heater DB100/3, Techne Inc., Vernon Hills, IL, USA). Finally, 1 µL of the concentrated
168 sample was injected onto the column for PAH determination through gas chromatography

169 mass spectrometry (GC-MS, Agilent HP6890; Mass selective detector 5973, Agilent
170 Technologies, Tokyo, Japan), using external calibration for quantification.

171

172 ***2.2.3. Quality assurance and quality control***

173 Prior to the analysis of size-fractionated airborne PM samples, the analytical procedures for
174 determining metal(oid)s and PAHs were optimised using Standard Reference Material
175 (SRM)® 1648a, Urban Particulate Matter, from the National Institute of Standards and
176 Technology (NIST, USA); it was chosen for its matrix similarity and certified values for both
177 analytes (Wise and Watters, 2020). The repeatability of extraction methods for metal(oid)s
178 (Gao and Ji, 2018; Jakovljević et al., 2018; Mbengue et al., 2014) and PAHs (Akhbarizadeh
179 et al., 2021) is rarely reported. Optimisation experiments were conducted in duplicate to
180 evaluate the repeatability of measurements, limits of detection (LODs), limits of quantification
181 (LOQs), linearity and accuracy. Measurement repeatability, calculated as the relative
182 standard deviation (RSD), was evaluated using six analyses of SRM 1648a, while LODs and
183 LOQs were determined from eight blank sample measurements; they were calculated as the
184 concentration corresponding to signals equal to 3*s* or 10*s* of the blank sample. The
185 measurement repeatability and accuracy were 4% and 2% for selected metal(oid)s, and 3%
186 and 6% for selected HMW PAHs. Low LODs were achieved, ranging from 0.001–0.02 ng
187 mL^{-1} for metal(oid)s and 4.5 ng mL^{-1} for PAHs. The linearity of measurement for both
188 metal(oid)s and PAHs ranged from the LOQ to 1000 ng mL^{-1}, with correlation coefficients (r)
189 for the calibration curves better than 0.998 and 0.997 for metal(oid)s and PAHs, respectively.
190 A spike recovery test was applied for elements not certified in SRM 1648a (Ba, Mo, Tl), with
191 the relative recoveries ranging from 92% to 107%.
192 Detailed and optimised analytical procedures along with quality assurance and quality
193 control parameters are provided in Ilenič et al. (2025).

194

2.3. Data analysis

The variability in the measured concentrations between different sampling sites (MB, LJ, MS, DB, PR), sampling seasons – non-heating period (NHP; March−October) and heating period (HP; November−February) – and PM size fractions (PM_{10}, $PM_{2.5}$, $PM_{0.1}$, $PM_{<0.1}$) were statistically analysed using parametric tests, including the t-test and analysis of variance (ANOVA). Pearson's correlation coefficients were applied to assess the relationship between variables, while cluster analysis using Ward's method as an amalgamation rule, 1-Pearson r as a distance measure for variables and the Euclidian distance for observations was used to identify natural groupings of the data. Prior to the analysis, outliers were removed and values below the LOD were replaced with $\frac{LOD}{\sqrt{2}}$ (Croghan and Egeghy, 2003). Data analysis was conducted using TIBCO Statistica software (TIBCO Software Inc., 2017), and the results were plotted using Origin (OriginLab Corporation, 2021). Potential sources were identified through correlation analysis, diagnostic ratios (DRs) and source apportionment using principal component analysis, hierarchical clustering, factor analysis and correlation coefficients. Additionally, health risk assessment for residential exposure via inhalation was conducted.

2.3.1. Diagnostic ratios

DRs are a common conventional qualitative method for identifying potential sources of PAH pollution. The characteristic PAH ratios can be used to differentiate between contributions from various sources and are indicative of pyrogenic and petrogenic origins, as well as petroleum combustion sources (diesel or gasoline), biomass or coal burning and both traffic and non-traffic-related emissions, as these ratios remain constant between different emission sources (Akyüz and Çabuk, 2010; Caricchia et al., 1999; Katsoyiannis et al., 2007; Khalili et al., 1995; Yunker et al., 2002). DRs were assessed for each sampling location and PM size fraction.

221

222 ***2.3.2. Health risk assessment***

223 The residential exposure of adults (female and male; 18−70 years old) and children (6 years
224 old) to airborne PM-bound metal(oid)s and PAHs via inhalation was assessed through the
225 calculation of the average daily dose (ADD, mg kg^{-1} day^{-1}), the incremental lifetime cancer
226 risk (ILCR) and the hazard quotient (HQ). The assessment was conducted for each specific
227 sampling site (MB, LJ, MS, DB, PR), PM size fraction (PM_{10}, $PM_{2.5}$, $PM_{0.1}$, $PM_{<0.1}$), activity
228 type (cycling, walking), demographic group (male, female, child), sampling period (HP, NHP)
229 and exposure scenario (normal, worst). The ADD (Eq. 1) for the respiratory pathway of
230 metal(oid)s and PAHs was determined according to the following equation (US EPA, 2009):

231

232 $$\boldsymbol{ADD} = \frac{\boldsymbol{c_{air}} \times \boldsymbol{IR} \times \boldsymbol{ET} \times \boldsymbol{EF} \times \boldsymbol{ED}}{\boldsymbol{AT} \times \boldsymbol{BW}} \times \mathbf{10^{-3}} \qquad \textbf{Eq. 1}$$

233

234 where c_{air} represents the average measured concentration of the selected metal(oid) or PAH
235 (in ng m^{-3}) bound to size-fractionated PM during a given sampling period at a specific
236 sampling site. *ED* represents the exposure duration, defined as 30 years for adults and 6
237 years for children, while *ET* refers to the average exposure time. In the normal-case
238 scenario, *ET* reflects the average time an individual spends outdoors in Slovenia (1.8 h
239 day^{-1}), whereas the worst-case scenario represents continuous 24 h day^{-1} exposure. *EF* is
240 the exposure frequency (350 days $year^{-1}$), and *AT* is the total average exposure time over a
241 lifetime (*ED* x 365) (SURS, 2025). The inhalation rate (*IR*) varies by activity and
242 demographic group, where its respective values for men, women and children during cycling
243 are 2.5 m^3 h^{-1}, 1.6 m^3 h^{-1} and 3.5 m^3 h^{-1}, respectively, and 0.8 m^3 h^{-1}, 0.5 m^3 h^{-1} and 1 m^3
244 h^{-1}, respectively, during walking (US EPA, 1997). The average body weight (*BW*) is
245 assumed to be 85 kg for male adults, 68 kg for female adults and 32 kg for children (SURS,
246 2025).

The ILCR (Eq. 2) is defined as the incremental probability of an individual developing any form of cancer over their lifetime as a result of exposure to pollutants. The ILCR was determined according to the following:

$$ILCR = ADD \times IUR \quad \text{Eq. 2}$$

IUR is the inhalation unit risk and is set to the following values for different compounds: As – 4.3 x 10^{-3} µg m^{-3}, Cd – 1.8 x 10^{-3} µg m^{-3}, Co – 9 x 10^{-3} µg m^{-3}, Cr(VI) – 1.1 x 10^{-2} µg m^{-3}, Ni – 2.6 x 10^{-4} µg m^{-3}, Pb – 1.2 x 10^{-5} µg m^{-3}, BaA – 6 x 10^{-5} µg m^{-3}, BaP – 6 x 10^{-4} µg m^{-3}, BbF – 6 x 10^{-5} µg m^{-3}, Ch – 6 x 10^{-7} µg m^{-3} and IP – 6 x 10^{-5} µg m^{-3} (US EPA, 2024). An ILCR greater than 10^{-4} indicates a significant potential cancer risk, whereas an ILCR less than 10^{-6} suggests that the cancer risk from carcinogen exposure can be considered negligible. An ILCR value of 10^{-6} corresponds to the probability that 1 in 1,000,000 individuals may develop cancer due to exposure to carcinogenic compounds (US EPA, 2011).

The HQ (Eq. 3) reflects the probability of an individual experiencing an adverse effect and was calculated as follows:

$$HQ = \frac{ADD}{RfC} \quad \text{Eq. 3}$$

where the chronic reference concentration (*RfC*) for metal(oid)s and PAHs is set as follows: As – 1.5 x 10^{-2} µg m^{-2}, Ba – 5 x 10^{-1} µg m^{-3}, Ce – 9 x 10^{-1} µg m^{-3}, Cd – 1 x 10^{-2} µg m^{-3}, Co – 6 x 10^{-3} µg m^{-3}, Cr(VI) – 3 x 10^{-2} µg m^{-3}, Mo – 2 µg m^{-3}, Ni – 1 x 10^{-2} µg m^{-3}, V – 1 x 10^{-1} µg m^{-3} and BaP – 2 x 10^{-3} µg m^{-3}. If the calculated HQ exceeds 1, adverse health effects could potentially be expected (US EPA, 1997).

2.4. Meteorological conditions

The meteorological conditions were derived from monthly data collected between 2010 and 2016 for selected sampling locations (Table 1) (ARSO, 2025). As the locations Dobrova and Piran do not have national meteorological stations, data were sourced from the nearby locations – Ljubljana and Portorož (45.4753, 13.6160; see Fig. 1), respectively. The temperature (T) and relative humidity (RH) remain relatively stable between all locations during both the HP and NHP. Ljubljana experiences the most rainfall compared to the other sampling locations, particularly during the HP. The wind speed (WS) and atmospheric pressure (P) are highest in Piran, the coastal sampling location, where SE winds prevail. In Maribor, P was not determined and is denoted as *nd*.

Table 1 The meteorological conditions at the various locations.

Location	Maribor	Ljubljana	Murska Sobota	Piran
HP				
T (°C)[a]	4.8 ± 3.0	5.1 ± 2.7	3.8 ± 3.3	8.3 ± 2.1
RH (%)[b]	75.8 ± 4.5	79.3 ± 3.9	81.8 ± 4.9	78.0 ± 3.2
TP (mm)[c]	63.5 ± 34.9	122 ± 47	60.1 ± 26.3	89.0 ± 36.8
P (hPa)[d]	*nd*	981 ± 4	993 ± 4	1015 ± 5
WS (m s^{-1})[e]	2.0 ± 0.2	1.1 ± 0.1	1.7 ± 0.3	2.6 ± 0.3
WD[f]	NW, SE	NE, N	N, E	SE
NHP				
T (°C)	16.4 ± 4.4	17.3 ± 4.7	16.9 ± 4.5	18.9 ± 4.7
RH (%)	74.0 ± 3.9	72.5 ± 5.5	74.6 ± 4.4	71.3 ± 3.7
TP (mm)	121 ± 67	181 ± 87	86.0 ± 47.9	121 ± 76
P (hPa)	*nd*	980 ± 3	993 ± 2	1014 ± 2
WS (m s^{-1})	2.2 ± 0.1	1.4 ± 0.4	1.9 ± 0.3	2.9 ± 0.3
WD	NW	NE	N, E	SE

[a] Temperature (T)
[b] Relative humidity (RH)
[c] Total precipitation (TP)
[d] Atmospheric pressure (P)
[e] Wind speed (WS)
[f] Wind direction (WD) – NW (north-west), NE (north-east), N (north), E (east), SE (south-east)
nd = not determined

297 ## 3. Results and discussion

298 ### *3.1. Composition and distribution of metal(oid)s in airborne size-fractionated PM*

299 A total of 14 metal(oid)s were identified, including As, Ba, Ce, Cd, Co, Cr, Cu, La, Mo, Ni,
300 Pb, Tl, V and Zn. Across all locations, the trend of decreasing average values was: Zn > Ba
301 > Cu > Cr > Pb > Ni > Co > Mo > V > Ce > As > La > Cd > Tl. While most of the identified
302 elements were concentrated during the HP, Ce, La, Ni and V showed increased
303 concentrations during the NHP, typical of mineral dust resuspension and (non)exhaust
304 emissions on dry surfaces during summer (Fomba et al., 2018; Mbengue et al., 2014). A
305 similar trend was observed in Poland, where non-exhaust sources dominated in the NHP
306 (Jandacka et al., 2017). As shown in Fig. 2, the largest contents of metal(oid)s were primarily
307 concentrated in PM_{10}, with lower concentrations observed in $PM_{2.5}$ and $PM_{0.1}$. In the $PM_{<0.1}$
308 fraction, Ba, Cd, Cu, Ni, Pb and Zn are primarily associated with vehicular exhaust and non-
309 exhaust emissions (Valavanidis et al., 2008), reaching levels similar to those observed in
310 PM_{10}. This indicates that the $PM_{<0.1}$ fraction, which can penetrate the deepest into lung
311 tissue and poses potentially the highest health risks, plays a substantial role in overall
312 metal(oid) exposure. Concentrations were higher during the HP than during the NHP, with
313 average HP-to-NHP ratios of 1.8, 2.1, 3.4 and 1.5 for PM_{10}, $PM_{2.5}$, $PM_{0.1}$ and $PM_{<0.1}$,
314 respectively. The highest differences were observed for Co (ratio of 5.4), Mo (ratio of 3.1)
315 and Tl (ratio of 6.5), with high correlations between Co and Mo, particularly in small PM
316 fractions ($r = 0.9$), all typically associated with high-temperature fossil fuel combustion
317 processes (Negral et al., 2020). Similar trends were observed in Poland and Germany,
318 where HP levels were 2−3 times higher, mainly due to coal heating and poor dispersion
319 conditions (Fomba et al., 2018). Generally, statistically significant differences ($p < 0.05$) were
320 observed for all elements between different sampling locations, PM size fractions and
321 seasons, with the PM size predominantly contributing most to the overall variability.

322 Among the studied locations, the highest levels of metal(oid)s were observed in MB,
323 followed by LJ, MS, DB and PR (Fig. 2).

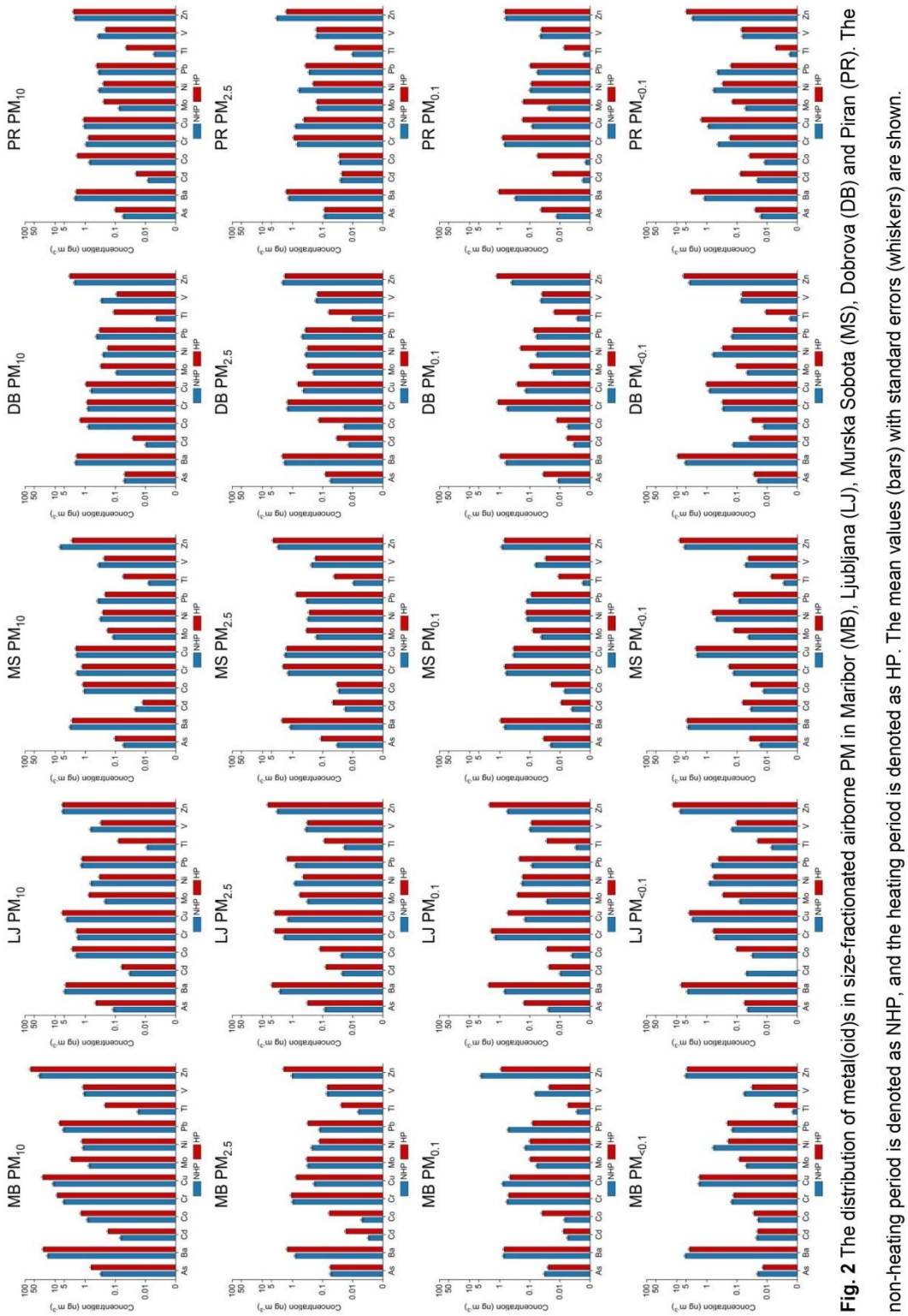


Fig. 2 The distribution of metal(oid)s in size-fractionated airborne PM in Maribor (MB), Ljubljana (LJ), Murska Sobota (MS), Dobrova (DB) and Piran (PR). The non-heating period is denoted as NHP, and the heating period is denoted as HP. The mean values (bars) with standard errors (whiskers) are shown.

326 Concentrations ranges of metal(oid)s were compared to other urban areas across the world
327 (Table 2). It was observed, that the metal(oid) concentrations in this study were significantly
328 lower than those reported for larger cities, such as Fez, Morocco (population: 1.1 million),
329 but similar to Žilina, Slovakia (population: 0.6 million), Leipzig, Germany (population: 0.6
330 million), reflecting similarities in population density, dominant influence of traffic-related
331 emission in Slovenian cities. Across them, similar order of metal(oid) abundances was
332 observed: Zn > Cu > Pb > Ba > Cr (Table 2).
333

334 **Table 2** Metal(oid)s and PAHs concentration ranges across different urban locations.

Loc.	Ele.	Metal(oid)s concentration range in ng m^{-3}						Ref.
		PM_{11}–$PM_{0.54}$	PM_{10}	$PM_{2.5}$	PM_1	$PM_{0.1}$	$PM_{<0.1}$	
Fez, Morocco	As	/	0.03	/	/	/	/	(Deabji et al., 2024)
	Ba		28					
	Co		31					
	Cr		35					
	Cu		27					
	Pb		36					
	Zn		156					
Turin, Italy	As	0.04–0.16	/	/	/	/	/	(Malandrino et al., 2016)
	Cd	0–6						
	Co	0.005–0.07						
	Cr	0.25–2.5						
	Cu	0.75–4.5						
	Pb	0.5–4.2						
	Zn	1–90						
Los Angeles, USA	Ba	/	26.2	25.7	/	/	/	(Oroumiyeh et al., 2022)
	Co		0.11	0.09				
	Cr		1.1	2.0				
	Cu		12.1	12.8				
	Pb		0.9	2.2				
	Zn		9.2	11.5				
Žilina, Slovakia	As	/	0.4	0.7	2.2	/	/	(Jandacka et al., 2017)
	Ba		14.1	2.1	1.9			
	Cd		0.0	0.1	0.5			
	Cr		1.7	0.9	1.2			
	Cu		19.5	5.8	10.5			
	Pb		1.7	3.8	13.7			
	Zn		14.2	22.1	72.5			
Leipzig, Germany	As	/	0–7.7	/	/	/	/	(Fomba et al., 2018)
	Ba		0–20					
	Co		0–1.2					
	Cr		0–5.9					
	Cu		0.14–50					
	Pb		0.02–48					
	Zn		1.1–171					
Manlleu, Spain	As	/	0.9	/	/	/	/	(Canals-Angerri et al., 2024)
	Ba		17					
	Cd		0.7					
	Co		0.1					
	Cr		6.1					
	Cu		73					
	Pb		24					
	Zn		124					
Rome, Italy	As	/	/	0.36–0.60	/	/	/	(Mazziotti Tagliani et al., 2017)
	Cd			0.09–0.37				
	Cr			2.43–4.40				
	Cu			9.02–18.6				
	Pb			4.08–13.0				
	Zn			12.1–29.3				

Loc.	PAH	PAHs concentration range in ng m^{-3}					Ref.
		PM_{10}	$PM_{2.5}$	PM_1	$PM_{0.1}$	$PM_{<0.1}$	
Nanjing, China	BaP	/	0.5	/	/	/	(Q. Chen et al., 2019)
	BbF		2.5				
	BghiP		0.7				
	Chr		1.5				
	IP		0.6				
Delhi, India	BaP	7	10	/	/	/	(Hazarika & Srivastava, 2017)
	BbF	3	4				
	BghiP	2	4				
	Chr	4	6				
	IP	2	3				
Zagreb, Croatia	BaP	*nd*–29.27	*nd*–27.2	*nd*–10.3	/	/	(Jakovljević et al., 2018)
	BbF	*nd*–16.56	*nd*–10.9	*nd*–10.7			
	Chr	*nd*–13.78	*nd*–11.1	*nd*–11			
	BghiP	*nd*–38.78	*nd*–37.7	*nd*–19.2			
	IP	2.45–119	0.53–11.5	0.42–84			
Naples, Italy	BaP	0.065–0.872	/	/	/	/	(Di Vaio et al., 2016)
	Chr	0.003–0.805					
	IP	0.001–0.516					
Ankara, Turkey	BaP	/	2.46	/	/	/	(Koçak et al., 2025)
	BbF		5.34				
	BghiP		1.48				
	Chr		3.07				
	IP		4.65				
Manlleu, Spain	BaP	1.5	/	/	/	/	(Canals-Angerri et al., 2024)
Giza, Egypt	BaP	/	0.55–78.75	/	/	/	(Farah et al., 2024)
	BbF		*nd*–54.89				
	BghiP		1.61–192.57				
	Chr		0.68–45.99				
	IP		0.12–118.23				

Loc.	Ele.	Ref.						
Katowice, Poland	As	/	/	1.38–3.68	/	/	/	(Rogula-Kozlowska et al., 2014)
	Cd			0.49–2.92				
	Pb			22.92–83.46				
Thessaloniki, Greece	Cr	/	/	*nd*–0.261	/	/	/	(Tolis et al., 2015)
	Cu			0.009–2.218				
	Pb			0.011–0.201				
	Zn			*nd*–4.126				
This study	As	/	0.02–0.71	0.01–0.44	/	0.003–0.26	0.01–0.10	/
	Ba		0.84–26.0	0.35–6.68		0.15–3.18	1.15–12.99	
	Cd		0.004–0.20	0.002–0.10		0.001–0.05	0.01–0.10	
	Co		0.37–4.33	0.003–0.24		0.001–0.16	0.01–0.17	
	Cr		0.46–8.89	0.22–5.75		0.24–3.54	0.09–1.33	
	Cu		0.35–29.1	0.11–5.02		0.05–2.94	0.42–6.88	
	Pb		0.14–10.1	0.09–1.65		0.02–1.98	0.06–2.01	
	Zn		0.53–69.2	0.53–7.14		0.19–14.4	0.84–15.5	/

Loc.	Ele.	Ref.						
Katowice, Poland	BaP	/	0.79–35.93	/	/	/	/	(Rogula-Kozlowska et al., 2014)
Thessaloniki, Greece	BaP	/	*nd*–2.14	/	/	/	/	(Tolis et al., 2015)
	BbF		0.05–5.52					
	BghiP		*nd*–2.66					
	Chr		*nd*–3.62,					
	IP		*nd*–3.92					
This study	BaP	<0.02–0.11	<0.02–0.05	/	<0.02–0.11	*nd*		
	BbF	<0.02–0.18	<0.02–0.11		<0.02–0.20			
	BghiP	<0.02–0.17	<0.02–0.10		<0.02–0.16			
	Chr	<0.02–0.12	<0.02–0.06		<0.02–0.18			
	IP	<0.02–0.14	<0.02–0.08		<0.02–0.13			

Loc. = location, Ele. = element, Ref. = reference, *nd* = not determined, / = not reported

337 Similar trends across different cities confirm similar chemical fingerprinting results of size-
338 fractionated PM, attributed to more localised emission sources in Slovenian cities, a higher
339 traffic density per unit volume of air and the limited dispersion of air pollutants. Among the
340 analysed elements, As, Cd and Ni have established annual threshold levels, with annual
341 target values set for PM_{10} at 6 ng m^{-3}, 5 ng m^{-3} and 20 ng m^{-3}, respectively (Directive
342 2004/107/EC). In this study, none of the target values were exceeded in any of the size-
343 fractionated PM samples.
344
345 ***3.2. Composition and distribution of PAHs in airborne size-fractionated PM***
346 A total of eight HMW PAHs were identified, including BaA (4-ring), BaP (5-ring), BbF (5-ring),
347 BghiP (6-ring), Ch (4-ring), Fl (4-ring), IP (6-ring) and P (4-ring). The highest concentrations
348 of PAHs, in descending order, were observed for BbF, BghiP and IP, followed by Ch, BaP,
349 Fl, P and BaA. As shown in Fig. 3, the PAH concentrations were relatively low, ranging from
350 0.03–0.15 ng m^{-3}.
351
352

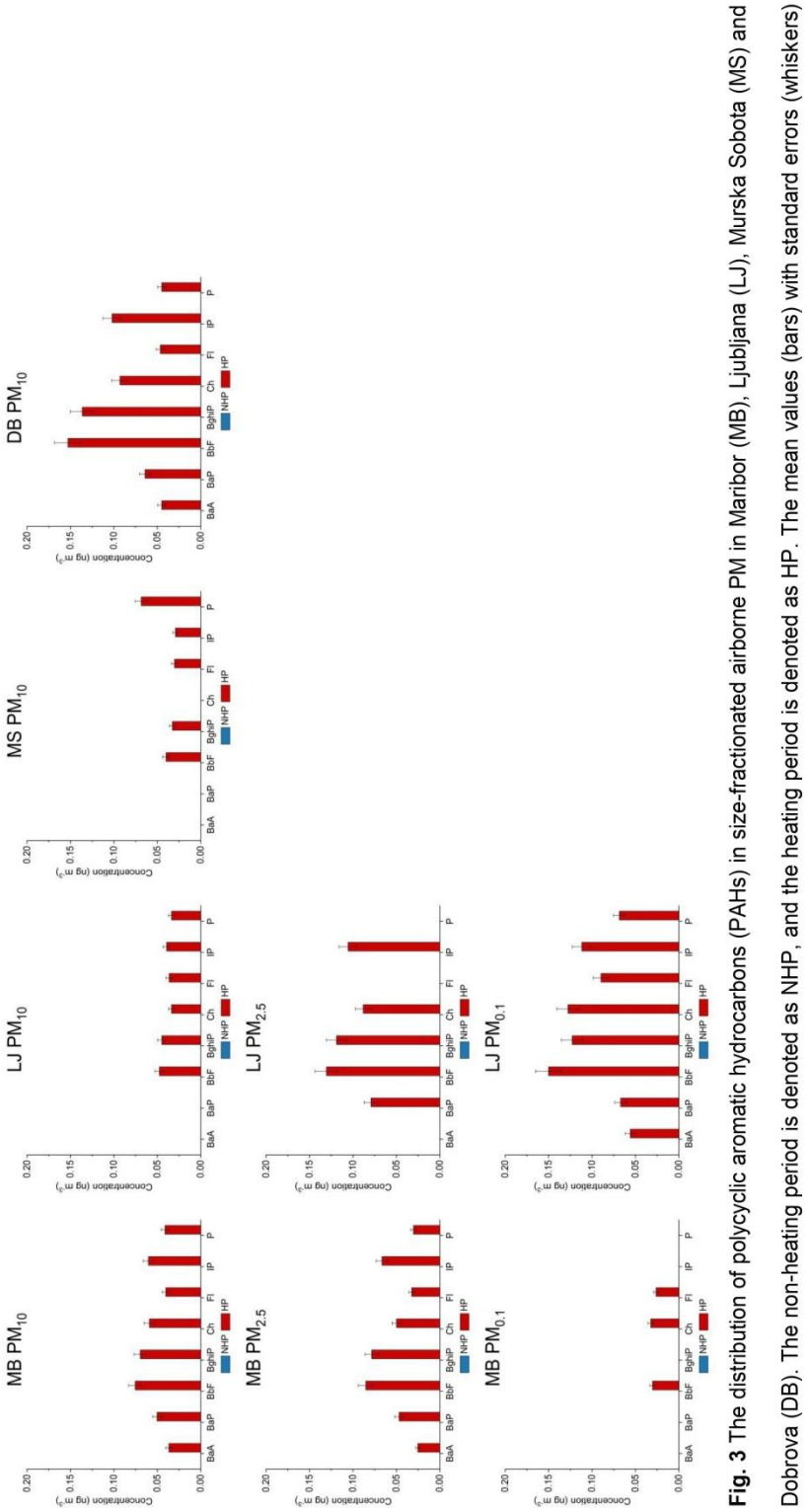


Fig. 3 The distribution of polycyclic aromatic hydrocarbons (PAHs) in size-fractionated airborne PM in Maribor (MB), Ljubljana (LJ), Murska Sobota (MS) and Dobrova (DB). The non-heating period is denoted as NHP, and the heating period is denoted as HP. The mean values (bars) with standard errors (whiskers) are shown.

359 The highest concentrations of HMW PAHs were associated with PM_{10}, $PM_{2.5}$ and $PM_{0.1}$, with
360 total PAH sums of 3.4 ng m^{-3}, 1.1 ng m^{-3} and 1.6 ng m^{-3}, respectively. This may be due to
361 the higher surface area and fresh combustion origins of $PM_{0.1}$. The spatial distribution of
362 PAH concentrations exhibited a consistent trend across all locations, with the highest
363 concentrations observed in LJ (sum of PAHs equal to 2.9 ng m^{-3}), followed by MB (sum of
364 PAHs equal to 1.7 ng m^{-3}), DB (sum of PAHs equal to 1.3 ng m^{-3}) and MS (sum of PAHs
365 equal to 0.2 ng m^{-3}). No PAHs were detected in PR or during the NHP at all locations.
366 Generally, no statistically significant differences ($p < 0.05$) in HMW PAH concentrations were
367 observed between different locations and PM size fractions. Seasonal variations contributed
368 significantly to the overall variability. Similar distribution patterns were observed in Zagreb,
369 Croatia (population 0.8 million) (Table 2)., where the following PAHs were observed in PM_{10}
370 – BghiP, BaP, Chr, BbF and IP, in $PM_{2.5}$ – BghiP, BaP, IP, BbF and Chr; and in PM_1 –
371 BghiP, BbF, Chr, IP and BaP, with the highest total PAH concentrations also observed
372 during the HP (Jakovljević et al., 2018). Similarly low sums of PAHs (1−2.1 ng m^{-3}) in PM_{10}
373 and $PM_{2.5}$ were observed in Rome, Italy, Copenhagen, Denmark, London, United Kingdom,
374 and Oslo, Norway (Jedynska et al., 2014). 5- and 6-ring PAHs prevailed across all studied
375 locations, similar to Naples, Italy (Di Vaio et al., 2016). PAHs with 4-, 5- and 6-rings exhibit
376 lower vapour pressures, which favour their partitioning in PM (Bandowe et al., 2014). The
377 presence of HMW PAHs can be attributed to traffic emissions, as well as biomass burning
378 (Shen et al., 2019). Among the analysed compounds, BaP is recognised as the most
379 genotoxic carcinogen for humans, with an established annual threshold level for PM_{10} set at
380 1 ng m^{-3} (Directive 2004/107/EC). In this study, BaP did not exceed the regulatory target at
381 any location across all size-fractionated PM samples. The highest BaP concentrations, equal
382 to 0.11 ng m^{-3}, were measured in LJ and DB. Regarding other European cities, the highest
383 BaP values were recorded in Athens, Greece, and Copenhagen, Denmark, with values of
384 0.25 ng m^{-3} and 0.21 ng m^{-3}, respectively (Jedynska et al., 2014). In Zagreb, Croatia, BaP
385 values exceeded the regulatory threshold level of 1 ng m^{-3} (Jakovljević et al., 2018). BaP
386 values in Porto, Portugal, varied between 0.01 ng m^{-3} and 2.7 ng m^{-3}, with an average value

387 0.37 ng m^{-3}; meanwhile, the average BaP values were 0.25 ng m^{-3} in Athens and 0.21 ng m^{-3} in Copenhagen (Jedynska et al., 2014).

389

390 ***3.3. Influence of meteorological conditions on PM air pollution levels***

391 Precipitation is considered one of the major meteorological factors influencing PM
392 concentrations, primarily through wet deposition, which facilitates the removal of particles
393 from the entire atmospheric column (US EPA, 2019). In Slovenia, precipitation increases
394 from the coastal region (Piran) towards Ljubljana (NE), followed by a decrease towards the
395 NE (Zupančič, 2017). Another factor hindering effective air pollutant dispersion is a low wind
396 speed (approximately 2 m s^{-1}, with the lowest values observed in LJ and MB). Elevated
397 pollutant concentrations in LJ and MB during the HP, result from unfavourable
398 meteorological conditions, including a low WS, high RH and low T. Both locations are
399 surrounded by hills and are susceptible to frequent thermal inversions due to the presence of
400 a low planetary boundary layer level, a stable high-pressure system and the weak vertical
401 mixing of air masses in the winter months (Jiang et al., 2019; Schauer et al., 2003). The
402 presence of the surrounding wetlands in LJ can decrease the overall air pollution levels. Air
403 masses originating from high-PM areas can increase air pollution levels in low-PM areas
404 (Jiang et al., 2019), likely contributing to the higher metal(oid) and PAH concentrations in DB
405 due to pollutant transport from LJ, facilitated by NE winds (Table 1). Higher T during the
406 NHP enhances HMW PAH photodegradation, reducing PAH concentrations in summer (Di
407 Vaio et al., 2016; Elzein et al., 2020). Additionally, dry surfaces and low wind speeds
408 promote non-exhaust tracer resuspension, allowing submicronic particles to remain airborne
409 longer (Fomba et al., 2018). Although precipitation alleviates airborne pollutant levels, its
410 impact appears limited. LJ, despite receiving the highest rainfall (115 mm in the NHP, 208
411 mm in the HP), still experiences the most elevated pollution levels in comparison to the other
412 studied cities. High ozone concentrations, especially in summer, can also significantly affect
413 PAH levels and their degradation (Elzein et al., 2020). The average monthly ambient ozone

414 levels during the NHP were approximately twice as high as those in the HP, with the highest
415 concentrations recorded at the coastal sampling site PR during the NHP, reaching 202 µg
416 m^{-3} in June. Exceedances of the 120 µg m^{-3} target for 8-hour observations were recorded at
417 all locations (ARSO, 2025; Directive 2008/50/EC).
418

419 ***3.4. Source apportionment***

420 In this study, PCA, hierarchical clustering, factor analysis, ANOVA and Pearson correlation
421 coefficient, along with DRs were employed for the source apportionment of selected
422 metal(oid)s and HMW PAHs. The PCA explained 79.5% quality of representative and along
423 with hierarchical clustering along with factor analysis differentiating strongly between
424 metal(oid)s and PAHs. HMW PAHs are, in comparison to LMW PAHs, more stable and less
425 reactive to ozone oxidation and photodegradation processes; therefore, they serve as a
426 reliable indicator of urban emission sources (Alam et al., 2013). While differences in PAH
427 reactivity, volatility and solubility may introduce biases, DRs with similar physiochemical
428 properties, derived from a specific formation mechanism, can serve as characteristic
429 markers of major PAH sources (Khalili et al., 1995; Ravindra et al., 2008). Table 3 shows the
430 DRs of the selected PAHs related to their respective sources. Certain isomeric PAH ratios in
431 MS and PR were not determined (denoted as *nd*) due to the PAH concentrations falling
432 below the LOD. The calculated DRs indicate a dominance of pyrogenic sources, connected
433 to exhaust and non-exhaust traffic emissions, primarily associated with the incomplete
434 combustion of fossil fuels such as coal, oil and natural gas. In MB and LJ, vehicular
435 emissions – particularly from diesel engines, which represent 51% of the vehicles in Slovenia
436 – appear to have a stronger influence compared to DB, where PAH diagnostic ratios indicate
437 non-traffic-related emission sources (Terzič, 2020). Diesel engines also emit significantly
438 higher levels of PM compared to gasoline engines (Ono Ogasawara and Smith, 2004).
439

440 **Table 3** PAH diagnostic ratios in size-fractionated PM at the various sampling locations with
441 typical characteristic values.

PAH ratio	DB	LJ	MB	MS	PR	Source	Reference
Fl/(Fl+P)	0.51	0.57	0.51	*nd*	*nd*	Petrogenic: <0.4 Fossil fuel combustion: 0.4−0.5 Grass, wood, coal combustion: >0.5	(Yunker et al., 2002)
BaA/(BaA+Ch)	0.33	0.30	0.36	*nd*	*nd*	Coal combustion: 0.2−0.35 Vehicular emissions: >0.35 Petrogenic: <0.2 Combustion: >0.35	(Akyüz and Çabuk, 2010; Yunker et al., 2002)
IP/(IP+BghiP)	0.43	0.47	0.46	0.47	*nd*	Petrogenic: <0.2 Petroleum combustion: 0.2−0.5 Grass, wood, coal combustion: >0.5	(Yunker et al., 2002)
BaP/BghiP	0.47	0.61	0.66	*nd*	*nd*	Non-traffic emissions: <0.6 Traffic emissions: >0.6	(Katsoyiannis et al., 2007)
IP/BghiP	0.75	0.89	0.86	0.89	*nd*	Gasoline: <0.4 Diesel: ~1	(Caricchia et al., 1999)
BaP/(BaP+Ch)	0.41	0.41	0.47	*nd*	*nd*	Gasoline: ~0.73 Diesel: ~0.5	(Khalili et al., 1995)

442 *nd* = not determined

443

444 The presence of HMW PAHs is generally attributed to traffic emissions and biomass burning
445 (Jedynska et al., 2014). Consistent with findings from previous studies, the DR exhibited
446 minimal variations between different PM size fractions (Akyüz and Çabuk, 2010).
447 Additionally, the PAH ratio (3- and 4-ring PAHs)/(5- and 6-ring PAHs) serves as an indicator
448 of the pollutant transport distance, with higher values suggesting longer-range transport (Tan
449 et al., 2011). In this study, the highest ratio was observed in MB (1.0), followed by LJ (0.6),
450 DB (0.5) and MS (0.3), indicating that air pollution sources in MS are predominantly more
451 localised.

452 Additionally, elemental ratios are also used as fingerprints of specific anthropogenic
453 emission sources. The V/Ni ratio, typically reported in the range of 0.5−1.9, is indicative of
454 gasoline and diesel vehicle combustion sources (Qin et al., 1997). In this study, the V/Ni
455 ratios (r = 0.9) were below 2.0, ranging from 0.1 to1.2. The average values were 0.9 for
456 PM_{10}, 0.6 for $PM_{2.5}$, 0.4 for $PM_{0.1}$ and 0.2 for $PM_{<0.1}$. Zn/Pb ratios (r = 0.9) exhibited higher

457 values compared to those associated with traffic-related sources (<1) reported by Prati et al.
458 (2000). In this study, Zn/Pb ranged from 3.6 to 65.4, with average values of 6.7 for PM_{10}, 5.2
459 for $PM_{2.5}$, 9.1 for $PM_{0.1}$ and 27.5 for $PM_{<0.1}$. Cu, along with Ba and Zn, is a well-established
460 marker of non-exhaust emissions, particularly from tyre and brake wear (Thorpe and
461 Harrison, 2008). These elements showed a strong linear relationship across all size-
462 fractionated PM. The Ba/Cu ratio (r = 0.9) varied between 0.6 and 9.2, with the highest
463 values observed for $PM_{0.1}$ (3.5) and $PM_{<0.1}$ (3.6). A similar pattern was observed for the
464 Zn/Cu ratio (r = 1.0), which varied between 0.7 and 6.9. The average values were 1.8 for
465 PM_{10}, 2.9 for $PM_{2.5}$, 3.8 for $PM_{0.1}$ and 3.2 for $PM_{<0.1}$. These ratios were higher than those in
466 the literature, suggesting a predominant contribution of Ba and Zn in fine PM fractions (Alves
467 et al., 2017; Pio et al., 2013). The La/Ce ratio (r = 1.0) in this study ranged from 0.485 to
468 0.496 across different PM fractions, aligning with the typical crustal material value of 0.492.
469 A decreasing trend of La/Ce was observed with decreasing particle size (0.27−0.15),
470 indicative of a crustal origin of these metal(oid)s, likely through soil resuspension (Pio et al.,
471 2013). The Pb/Cd ratio showed a wide range (1.1−95.2) and remained relatively constant
472 across sampling sites, with the exception of MB, where a higher average value was
473 recorded, indicating the localised enrichment of Pb sources connected to industrial activities
474 (Gaberšek et al., 2022). The Zn/Pb ratios (r = 0.9), varying from 3.6−65.4, were substantially
475 elevated for $PM_{<0.1}$, further supporting a stronger influence of Zn sources in ultrafine
476 particles. The elemental ratios remained constant between the NHP and HP, except for
477 Pb/Cd. During the NHP, the average Pb/Cd ratio was 31.6, significantly higher than the
478 values of 13.5 observed in the HP, suggesting enhanced contributions from traffic emission
479 sources and resuspended dust outside the heating season.

480 A coefficient of variation (CV = 100 x standard deviation/mean) greater than 20% indicates a
481 heterogeneous distribution in the environment (Wilson et al., 2005). In this study, Ba, Cd,
482 Cu, Ni, Pb and Zn exhibited heterogeneous distributions across all locations, with the highest
483 CV observed in MB (145%), followed by DB (78%), MS (75%), LJ (73%) and PR (72%).

484 Among the particle size fractions, the CV associated with PM_{10} was the highest, followed by
485 $PM_{0.1}$, $PM_{<0.1}$ and $PM_{2.5}$.
486 In LJ and MB, key industries include energy production (power and heating plants), chemical
487 manufacturing, metal processing and waste management. In MS and PR, key industries
488 include tourism, food production (particularly meat processing) and metal manufacturing,
489 with PR having significant contributions from logistics and port operations. Across Slovenia,
490 the primary contributors to PM_{10} and $PM_{2.5}$ are fuel use in households and the service sector
491 and industrial processes, followed by traffic emissions, agriculture and heat production
492 (Logar, 2023). In 2023, the majority of households (62%) had central heating (coal and wood
493 biomass), and the most common primary heating sources were wood logs (30%), natural or
494 propane gas (19%) and renewable sources (14%) (Inglič et al., 2024). In this study, the
495 highest concentrations of 5- and 6-ring PAHs, including BbF, BghiP and IP, were detected
496 across all locations. Typically, 3- and 4-ring PAHs are primarily emitted from coal
497 combustion (Harrison et al., 1996), and 4-, 5- and 6-ring PAHs are linked to vehicle
498 emissions (Ravindra et al., 2008); 5- and 6-ring PAHs are indicative of petroleum and oil
499 combustion (Harrison et al., 1996; Ravindra et al., 2008). BaA, Ch, Fl and P are commonly
500 used as tracers of coal combustion and biomass burning (Akhbarizadeh et al., 2021; Chen et
501 al., 2019), while BaP, IP and BghiP are vehicle exhaust markers (Chen et al., 2019). The
502 highest correlation between PAHs and metal(oid)s was found for As ($r = 0.8$), especially at
503 smaller PM sizes, indicating a similar origin, further also strongly connected with Co, Cr, Mo
504 and Tl. Among the metal(oid)s, the highest concentrations, given in descending order, were
505 observed for Zn, Ba, Cu, Cr and Pb, while Ba, Cu, Cr and Zn are commonly associated with
506 brake and wear tracers, predominantly found in coarser PM (Fomba et al., 2018; Jandacka
507 et al., 2017; Li et al., 2019; Pant and Harrison, 2013; Thorpe and Harrison, 2008). In
508 contrast, tailpipe tracers (e.g. Ni, Pb) are more prevalent in finer PM fractions (Fernández
509 Camacho et al., 2012; Fomba et al., 2018; Li et al., 2019; Mbengue et al., 2014). It has also
510 been reported that Co, Cd, Ni, Pb and Zn are linked to tyre wear, but Zn, Cr, Cu, Fe, Ba, Sb

511 and Sn are more frequently connected with brake abrasion from road traffic (Thorpe and
512 Harrison, 2008).
513
514 ***3.5. Potential health risk implications***

515 Potential health risks associated with As, Cd, Co, Cr, Mo, Pb, V, BaA, BaP, BbF, Ch and IP
516 (Tables S10−S13, Supplementary Information) were evaluated for both, typical exposure
517 conditions (1.8 h day^{-1}, representing the average outdoor time in Slovenia) (SURS, 2025)
518 and the worst-case scenario (24 h day^{-1} exposure), across the NHP and HP and different
519 size-fractionated PM. In this study, no ILCR or HQ values for the specific groups exceeded
520 the recommended threshold levels (US EPA, 1997; US EPA, 2011). However, some ILCR
521 values for As, Co and Cr were above 10^{-6}, suggesting a minimal potential carcinogenic risk
522 through inhalation exposure (US EPA, 2011). The highest exposure risk was observed for Cr
523 in PM_{10} during cycling by children in the HP under 24 h day^{-1} exposure (6.6 x 10^{-5}), while an
524 ILCR of 4.9 x 10^{-5} was observed under 1.8 h day^{-1} exposure. Elevated ILCR values for
525 children were also noted for the ILCR values calculated for $PM_{2.5}$ (4.5 x 10^{-5}), $PM_{0.1}$ (2.3 x
526 10^{-5}) and $PM_{<0.1}$ (6.2 x 10^{-5}) during cycling in the HP under 24 h day^{-1} exposure. Under
527 normal exposure conditions (1.8 h day^{-1}), Cr ILCR values exceeded the 1 x 10^{-6} threshold in
528 $PM_{2.5}$ (3.3 x 10^{-6}) and $PM_{0.1}$ (1.7 x 10^{-6}). For adults, Cr-related ILCR values also exceeded
529 the threshold in both exposure scenarios during cycling. Co-related ILCR values were of
530 concern particularly under 24 h day^{-1} exposure in PM_{10} (2.0 x 10^{-6} – 3.3 x 10^{-5}), as well as in
531 the normal-case scenario for children cycling (2 x 10^{-6}). As-related ILCR values were
532 similarly elevated for children during cycling activities under 24 h day^{-1} exposure in PM_{10} (2 x
533 10^{-6}) and $PM_{2.5}$ (1 x 10^{-6}).

534 Overall, under both normal and high-exposure scenarios, the most concerning metal(oid)s in
535 PM_{10} were Cr, Co and As, with ILCR values of 2 x 10^{-6} and 2 x 10^{-5}, 8 x 10^{-7} and 1 x 10^{-5},
536 and 5 x 10^{-8} and 6 x 10^{-7}, respectively. Among the PAHs, BaP (1 x 10^{-9} and 1 x 10^{-8},
537 respectively), BbF (2 x 10^{-10} and 2 x 10^{-9}, respectively) and P (8 x 10^{-11} and 1 x 10^{-9},

538 respectively) were associated with the highest ILCR values. In $PM_{2.5}$, the highest ILCR
539 values were calculated for Pb (1×10^{-6} and 1×10^{-5}, respectively), Cd (2×10^{-8} and 3×10^{-7},
540 respectively) and Cr (2×10^{-8} and 2×10^{-5}, respectively), as well as for P (5×10^{-9} and $7 \times$
541 10^{-8}, respectively) and BaA (4×10^{-10} and 5×10^{-9}, respectively). In $PM_{0.1}$, the highest ILCR
542 values were calculated for Ce (5×10^{-7} and 7×10^{-6}, respectively), Ni (1×10^{-8} and 1×10^{-7},
543 respectively) and Pb (9×10^{-9} and 1×10^{-7}, respectively). Among PAHs, P (9×10^{-10} and $1 \times$
544 10^{-8}, respectively), BaP (1×10^{-10} and 1×10^{-9}, respectively) and Ch (8×10^{-11} and 1×10^{-9},
545 respectively) exhibited the highest ILCR values. In $PM_{<0.1}$, the highest ILCR values were
546 calculated for As (2×10^{-7} and 2×10^{-6}, respectively), V (8×10^{-9} and 1×10^{-7}, respectively)
547 and Ce (7×10^{-9} and 9×10^{-8}, respectively).

548 ILCR values were consistently higher during the HP compared to the NHP, ranging from $2 \times$
549 10^{-13} to 4×10^{-6} for the NHP, and from 1×10^{-13} to 5×10^{-6} for the HP. The highest average
550 ILCR values were observed in MB and LJ, with values of 1×10^{-6} and 8×10^{-7}, respectively.
551 Additionally, higher ILCR values were also observed during cycling activities (1×10^{-6})
552 compared to walking (3×10^{-7}); this is primarily attributed to the increased respiratory rates
553 and greater volume of inhaled air associated with demanding physical activities. On average,
554 cyclists experience three-times-higher levels of exposure to air pollution than pedestrians
555 when subjected to the same exposure duration (Hofman et al., 2018; Ilenič et al., 2024; Int
556 Panis et al., 2010).

557 Additionally, the calculated HQ did not exceed the threshold level of 1, signifying minimal
558 exposure risks for the observed compounds (US EPA, 1997). Similar to the ILCR values, HQ
559 values were generally higher during the HP, with the highest levels observed in MB, followed
560 by LJ, DB, MS and PR. Under the worst-case conditions, carcinogenic risk factors were
561 markedly elevated, reflecting the same trend observed for ILCR values.

562 Based on both the calculated ILCR and HQ values, Cr exhibited the highest potential
563 carcinogenic risk among the assessed metal(oid)s, while BaP posed the greatest risk among
564 PAHs (Fig. 4, Fig. 5).

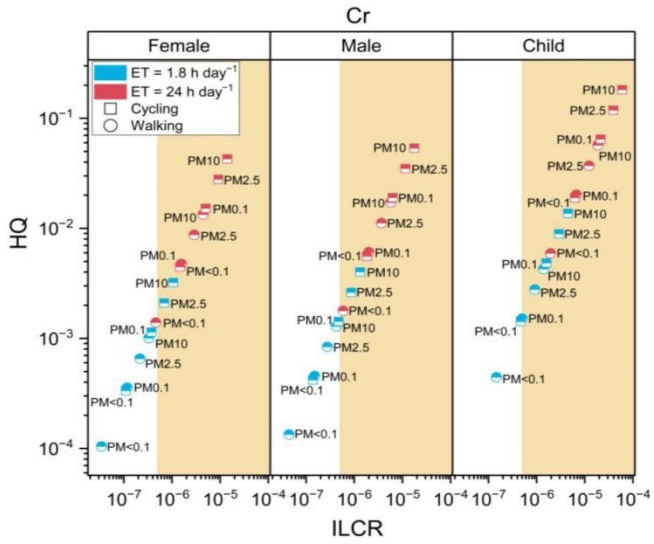


Fig. 4 The incremental lifetime cancer risk (ILCR) and hazard quotient (HQ) values associated with the inhalation of chromium (Cr).

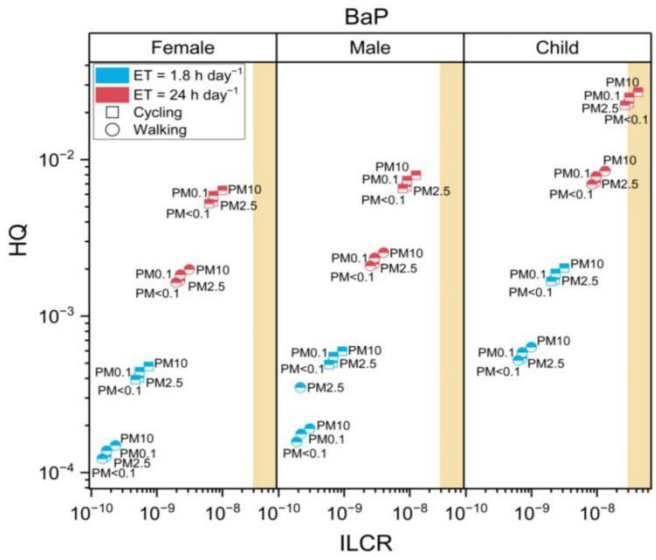


Fig. 5 The incremental lifetime cancer risk (ILCR) and hazard quotient (HQ) values associated with the inhalation of benzo(a)pyrene (BaP).

572 For comparison, the ILCR values reported in Seoul, South Korea, were relatively low,
573 ranging from 5.6 x 10^{-6} to 7.5 x 10^{-6} (Choi et al., 2022). In Naples, Italy, PAH-related ILCR
574 values for PM_{10} were negligible. The BaA-related ILCR was 2.1 x 10^{-7} for adults and 5.8 x
575 10^{-8} for children, respectively. The Chr-related ILCR was 2.7 x 10^{-10} for adults and 7.7 x
576 10^{-10} for children, while the BaP-related ILCR values were 4.8 x 10^{-7} for adults and 1.4 x
577 10^{-6} for children. The IP-related ILCR values were 1.6 x 10^{-8} for adults and 4.6 x 10^{-7} for
578 children (Di Vaio et al., 2016). In Zhengzhou and Beijing, China, elevated ILCR values and
579 high concentrations of BaA, BaP, BbF, Pb, As, Cr, Cd and Ni were observed, particularly
580 during the NHP (Gao and Ji, 2018; Jiang et al., 2019).
581

582 **4. Conclusions**

583 The data of size-fractionated airborne PM-bound metal(oid)s and PAHs in PM_{10}, $PM_{2.5}$, $PM_{0.1}$
584 and $PM_{<0.1}$ collected over a one-year period at five different pedestrian and cycling urban
585 microenvironments in Slovenia, revealed that the highest concentrations of metal(oid)s
586 among different locations were observed for Zn (6.98 ± 2.24 ng m^{-3}), Ba (4.46 ± 0.89 ng
587 m^{-3}), Cu (2.81 ± 0.90 ng m^{-3}) and Cr (1.52 ± 0.31 ng m^{-3}) in the HP, while Ce (0.15 ± 0.04
588 ng m^{-3}), La (0.07 ± 0.02 ng m^{-3}), V (0.25 ± 0.04 ng m^{-3}) and Ni (0.47 ± 0.05 ng m^{-3})
589 dominated in the NHP. Metal(oid) levels were highest in PM_{10}, followed by $PM_{2.5}$ and $PM_{0.1}$,
590 with Ba, Cd, Cu, Ni, Pb and Zn significantly enriched in $PM_{<0.1}$, indicating a strong
591 contribution from vehicular sources. Among PAHs, BbF (0.05 ± 0.01 ng m^{-3}), BghiP (0.04 ±
592 0.01 ng m^{-3}) and IP (0.04 ± 0.01 ng m^{-3}) exhibited the highest concentrations, predominantly
593 found in PM_{10}, $PM_{2.5}$ and $PM_{0.1}$, with total PAH sums of 3.4 ng m^{-3}, 1.1 ng m^{-3} and 1.6 ng
594 m^{-3}, respectively. The elemental distribution was mainly influenced by the PM size, while
595 PAH levels were significantly affected by seasonal variations.
596 The highest concentrations, particularly in the HP, were recorded in more densely populated
597 cities of Ljubljana and Maribor, resulting from unfavourable meteorological conditions, with

598 frequent thermal inversions, a low planetary boundary layer height and the weak vertical
599 mixing of air masses, allowing submicronic particles to remain airborne longer.

600 Source apportionment using PCA, DRs and elemental fingerprinting indicated a dominance
601 of pyrogenic sources, with elevated contributions from i) vehicular exhaust emissions,
602 primarily associated with diesel engines, and characterised by BbF, BghiP, Ch, IP, Ni and
603 Pb; ii) mineral dust resuspension and non-exhaust emission sources, such as tyre and brake
604 wear, marked by Ce, La, V, Ba, Cu and Zn; and iii) coal and biomass combustion during the
605 HP, indicated by BaA, BaP, Fl and P, along with As, Co, Cr, Mo and Tl.

606 The carcinogenic risk assessment, observed for pedestrians and cyclist among different
607 demographic groups, indicated an overall negligible cancer risk, except for As (2×10^{-7}), Co
608 (1×10^{-6}) and Cr (6×10^{-6}), which exhibited low potential risks through inhalation. The
609 highest exposure levels were identified for children engaged in cycling activities in the HP.
610 The calculated HQ values were below the threshold of 1, and the annual European threshold
611 limit values for As, Cd and BaP in PM_{10} were not exceeded, suggesting minimal exposure-
612 related health risks in the study area.

613

614 **Declaration of competing interest**

615 The authors declare that they have no known competing financial interests or personal
616 relationships that could have appeared to influence the work reported in this paper.

617

618 **Acknowledgements**

619 Anja Ilenič acknowledges Jožef Stefan International Postgraduate School as the institution
620 where her PhD studies are carried out. This research was funded by the Slovenian
621 Research Agency, financial support programme groups P2-0273, P1-0143 and P1-0008,
622 and research project J7-60124.

623 In addition, authors would like to thank the Municipality of Maribor, Municipality of Murska
624 Sobota, Municipality of Dobrova - Polhov Gradec, National Institute of Biology (NIB) – Marine

625 Biology Station Piran, as well as the Pavlič family (Ana, Maša, Dana, Bojan) for their
626 valuable cooperation and assistance in installing the sampling devices.
627

628 **5. References**

629 ARSO, Slovenian Environment Agency, 2025. https://meteo.arso.gov.si/ (accessed 15
630 January 2025).
631 Akhbarizadeh R, Dobaradaran S, Amouei Torkmahalleh M, Saeedi R, Aibaghi R, Faraji
632 Ghasemi F. 2021. Suspended fine particulate matter (PM2.5), microplastics (MPs), and
633 polycyclic aromatic hydrocarbons (PAHs) in air: their possible relationships and health
634 implications. Environ. Res. 192, 110339. https://doi.org/10.1016/j.envres.2020.110339.
635 Akyüz M, Çabuk H. 2010. Gas–particle partitioning and seasonal variation of polycyclic
636 aromatic hydrocarbons in the atmosphere of Zonguldak, Turkey. Sci. Total Environ. 408,
637 5550–8. https://doi.org/10.1016/j.scitotenv.2010.07.063.
638 Alam MS, Delgado Saborit JM, Stark C, Harrison RM. 2013. Using atmospheric
639 measurements of PAH and quinone compounds at roadside and urban background sites to
640 assess sources and reactivity. Atmos. Environ. 77, 24–35.
641 https://doi.org/10.1016/j.atmosenv.2013.04.068.
642 Alves CA, Vicente AM, Custódio D, Cerqueira M, Nunes T, Pio C, Lucarelli F, Calzolai G,
643 Nava S, Diapouli E, Eleftheriadis K, Querol X, Musa Bandowe BA. 2017. Polycyclic aromatic
644 hydrocarbons and their derivatives (nitro-PAHs, oxygenated PAHs, and azaarenes) in PM2.5
645 from Southern European cities. Sci. Total Environ. 595, 494–504.
646 https://doi.org/10.1016/j.scitotenv.2017.03.256.
647 Bandowe BAM, Meusel H, Huang RJ, Ho K, Cao J, Hoffmann T, Wilcke W. 2014. $PM_{2.5}$-
648 bound oxygenated PAHs, nitro-PAHs and parent-PAHs from the atmosphere of a Chinese
649 megacity: seasonal variation, sources and cancer risk assessment. Sci. Total Environ. 473–
650 474, 77–87. https://doi.org/10.1016/j.scitotenv.2013.11.108.
651 Canals-Angerri A, Via M, Lara R, Alastuey A, Minguillón MC, Pandolfi M. 2024. Causes of
652 the unremitting high ambient levels of PM10 in a suburban background site in NE Spain.
653 Environ Pollut. 363, 125113. https://doi.org/10.1016/j.envpol.2024.125113.
654 Caricchia AM, Chiavarini S, Pezza M. 1999. Polycyclic aromatic hydrocarbons in the urban

655 atmospheric particulate matter in the city of Naples (Italy). Atmos. Environ. 33, 3731–8.
656 https://doi.org/10.1016/S1352-2310(99)00199-5.
657 Chen H, Goldberg MS, Villeneuve PJ. 2008. A systematic review of the relation between
658 long-term exposure to ambient air pollution and chronic diseases. REVEH. 23, 243–97.
659 https://doi.org/10.1515/reveh.2008.23.4.243.
660 Chen Q, Chen Y, Luo XS, Hong Y, Hong Z, Zhao Z, Chen J. 2019. Seasonal characteristics
661 and health risks of PM2.5-bound organic pollutants in industrial and urban areas of a China
662 megacity. JEM. 245, 273–81. https://doi.org/10.1016/j.jenvman.2019.05.061.
663 Choi E, Yi SM, Lee YS, Jo H, Baek SO, Heo JB. 2022. Sources of airborne particulate
664 matter-bound metals and spatial-seasonal variability of health risk potentials in four large
665 cities, South Korea. ESPR. 29, 28359–74. https://doi.org/10.1007/s11356-021-18445-8.
666 Cohen AJ, Brauer M, Burnett R, Anderson HR, Frostad J, Estep K, Balakrishnan K,
667 Brunekreef B, Dandona L, Dandona R, Feigin V, Freedman G, Hubbell B, Jobling A, Kan H,
668 Knibbs L, Liu Y, Martin R, Morawska L, Forouzanfar MH. 2017. Estimates and 25-year
669 trends of the global burden of disease attributable to ambient air pollution: an analysis of
670 data from the Global Burden of Diseases Study 2015. Lancet. 389, 1907–18.
671 https://doi.org/10.1016/S0140-6736(17)30505-6.
672 Croghan W, Egeghy P. 2009. Methods of dealing with values below the limit of detection
673 using SAS.
674 Deabji N, Fomba KW, dos Santos Souza EJ, Mellouki A, Herrmann H. 2024. Influence of
675 anthropogenic activities on metals, sugars and PAHs in PM10 in the city of Fez, Morocco:
676 implications on air quality. ESPR. 31, 25238–57. https://doi.org/10.1007/s11356-024-32740-
677 0.
678 Di Vaio P, Cocozziello B, Corvino A, Fiorino F, Frecentese F, Magli E, Onorati G, Saccone I,
679 Santagada V, Settimo G, Severino B, Perissutti E. 2016. Level, potential sources of
680 polycyclic aromatic hydrocarbons (PAHs) in particulate matter (PM10) in Naples. Atmos.
681 Environ. 129, 186–96. https://doi.org/10.1016/j.atmosenv.2016.01.020.
682 Directive 2004/107/EC of the European Parliament and of the Council of 15 December 2004

683 relating to arsenic, cadmium, mercury, nickel and polycyclic aromatic hydrocarbons in
684 ambient air, http://data.europa.eu/eli/dir/2004/107/oj/eng (accessed 14 July 2024).
685 Directive 2008/50/EC of the European Parliament and of the Council of 21 May 2008 on
686 ambient air quality and cleaner air for Europe, http://data.europa.eu/eli/dir/2008/50/oj
687 (accessed 8 January 2024).
688 Dominici F, Peng RD, Bell ML, Pham L, McDermott A, Zeger SL, Samet JM. 2006. Fine
689 particulate air pollution and hospital admission for cardiovascular and respiratory diseases.
690 JAMA. 295, 1127–34. https://doi.org/10.1001/jama.295.10.1127.
691 EEA, European Environment Agency. 2012. Air quality in Europe—2012 report (EEA Report
692 No 4/2012). https://www.eea.europa.eu/en/analysis/publications/air-quality-in-europe-2012
693 (accessed 2 February 2025).
694 Elzein A, Stewart GJ, Swift SJ, Nelson BS, Crilley LR, Alam MS, Reyes Villegas E, Gadi R,
695 Harrison RM, Hamilton JF, Lewis AC. 2020. A comparison of $PM_{2.5}$-bound polycyclic
696 aromatic hydrocarbons in summer Beijing (China) and Delhi (India). ACP. 20, 14303–19.
697 https://doi.org/10.5194/acp-20-14303-2020.
698 Fadel M, Ledoux F, Farhat M, Kfoury A, Courcot D, Afif C. 2021. PM2.5 characterization of
699 primary and secondary organic aerosols in two urban-industrial areas in the East
700 Mediterranean. J. Environ. Sci. 101, 98–116. https://doi.org/10.1016/j.jes.2020.07.030.
701 Fernández Camacho R, Rodríguez S, de la Rosa J, Sánchez de la Campa AM, Alastuey A,
702 Querol X, González Castanedo Y, Garcia Orellana I, Nava S. 2012. Ultrafine particle and
703 fine trace metal (As, Cd, Cu, Pb and Zn) pollution episodes induced by industrial emissions
704 in Huelva, SW Spain. Atmos. Environ. 61, 507–17.
705 https://doi.org/10.1016/j.atmosenv.2012.08.003.
706 Fomba KW, van Pinxteren D, Müller K, Spindler G, Herrmann H. 2018. Assessment of trace
707 metal levels in size-resolved particulate matter in the area of Leipzig. Atmos. Environ. 176,
708 60–70. https://doi.org/10.1016/j.atmosenv.2017.12.024.
709 Gaberšek M, Watts MJ, Gosar M. 2022. Attic dust: an archive of historical air contamination
710 of the urban environment and potential hazard to health? J. Hazard. Mater. 432, 128745.

711 https://doi.org/10.1016/j.jhazmat.2022.128745.
712 Gao Y, Ji H. 2018. Microscopic morphology and seasonal variation of health effect arising
713 from heavy metals in PM2.5 and PM10: one-year measurement in a densely populated area
714 of urban Beijing. Atmos. Res. 212, 213–26. https://doi.org/10.1016/j.atmosres.2018.04.027.
715 Harrison RM, Smith DJT, Luhana L. 1996. Source apportionment of atmospheric polycyclic
716 aromatic hydrocarbons collected from an urban location in Birmingham, U.K. Environ. Sci.
717 Technol. 30, 825–32. https://doi.org/10.1021/es950252d.
718 Hazarika N, Srivastava A. 2017. Estimation of risk factor of elements and PAHs in size-
719 differentiated particles in the National Capital Region of India. Air Qual Atmos Health. 10,
720 469–82. 10.1007/s11869-016-0438-8.
721 Hofman J, Samson R, Joosen S, Blust R, Lenaerts S. 2018. Cyclist exposure to black
722 carbon, ultrafine particles and heavy metals: an experimental study along two commuting
723 routes near Antwerp, Belgium. Environ. Res. 164, 530–8.
724 https://doi.org/10.1016/j.envres.2018.03.004.
725 Ilenič A, Milačič Ščančar R, Đurić M, Mauko Pranjić A, Ščančar J. 2025. An innovative
726 sampling device for size-fractionating airborne particulate matter for improved air pollution
727 control of metal(oid)s and polycyclic aromatic hydrocarbons, Anal Methods. 17, 7184−7199.
728 https://doi.org/10.1039/D5AY00858A.
729 Ilenič A, Pranjić AM, Zupančič N, Milačič R, Ščančar J. 2024. Fine particulate matter (PM2.5)
730 exposure assessment among active daily commuters to induce behaviour change to reduce
731 air pollution. Sci. Total Environ. 912, 169117.
732 https://doi.org/10.1016/j.scitotenv.2023.169117.
733 Inglič RT, Pirnat U, Stare M. 2023. Household energy efficiency, Statistical Office, Republic
734 of Slovenia, https://www.stat.si/StatWeb/en/News/Index/12783?utm_source=chatgpt.com;
735 2024 (accessed 14 February 2025).
736 Int Panis L, de Geus B, Vandenbulcke G, Willems H, Degraeuwe B, Bleux N, Mishra V,
737 Thomas I, Meeusen R. 2010. Exposure to particulate matter in traffic: a comparison of

738 cyclists and car passengers. Atmos. Environ. 44, 2263–70.
739 https://doi.org/10.1016/j.atmosenv.2010.04.028.
740 Jakovljević I, Pehnec G, Vađić V, Čačković M, Tomašić V, Jelinić JD. 2018. Polycyclic
741 aromatic hydrocarbons in PM10, PM2.5 and PM1 particle fractions in an urban area. Air
742 Qual. Atmos. Hlth. 11, 843–54. https://doi.org/10.1007/s11869-018-0603-3.
743 Jandacka D, Durcanska D, Bujdos M. 2017. The contribution of road traffic to particulate
744 matter and metals in air pollution in the vicinity of an urban road. Transp. Res. D: Transp.
745 Environ. 50, 397–408. https://doi.org/10.1016/j.trd.2016.11.024.
746 Jedynska A, Hoek G, Eeftens M, Cyrys J, Keuken M, Ampe C, Beelen R, Cesaroni G,
747 Forastiere F, Cirach M, de Hoogh K, De Nazelle A, Madsen C, Declercq C, Eriksen KT,
748 Katsouyanni K, Akhlaghi HM, Lanki T, Meliefste K, Kooter IM. 2014. Spatial variations of
749 PAH, hopanes/steranes and EC/OC concentrations within and between European study
750 areas. Atmos. Environ. 87, 239–48. https://doi.org/10.1016/j.atmosenv.2014.01.026.
751 Jiang N, Li L, Wang S, Li Q, Dong Z, Duan S, Zhang R, Li S. 2019. Variation tendency of
752 pollution characterization, sources, and health risks of PM2.5-bound polycyclic aromatic
753 hydrocarbons in an emerging megacity in China: based on three-year data. Atmos. Res.
754 217, 81–92. https://doi.org/10.1016/j.atmosres.2018.10.023.
755 Katsoyiannis A, Terzi E, Cai QY. 2007. On the use of PAH molecular diagnostic ratios in
756 sewage sludge for the understanding of the PAH sources. Is this use appropriate?
757 Chemosphere. 69, 1337–9. https://doi.org/10.1016/j.chemosphere.2007.05.084.
758 Khalili NR, Scheff PA, Holsen TM. 1995. PAH source fingerprints for coke ovens, diesel and
759 gasoline engines, highway tunnels, and wood combustion emissions. Atmosp. Environ. 29.
760 https://doi.org/10.1016/1352-2310(94)00275-P.
761 Koçak E, Aslan S, İmamoğlu İ, Tuncel G. 2025. Multi-group organic pollutants in urban and
762 suburban atmospheric particulate matter (PM2.5): Temporal variation, meteorological
763 impact, and sources. Air Qual Atmos Health. 18, 1359–76. https://doi.org/10.1007/s11869-
764 025-01716-5.
765 Li X, Jiang L, Bai Y, Yang Y, Liu S, Chen X, Xu J, Liu Y, Wang Y, Guo X, Wang Y, Wang G.

766 2019. Wintertime aerosol chemistry in Beijing during haze period: significant contribution
767 from secondary formation and biomass burning emission. Atmos. Res. 218, 25–33.
768 https://doi.org/10.1016/j.atmosres.2018.10.010.
769 Logar M. 2023. Izpusti delcev v zrak | Okoljski kazalci,
770 https://kazalci.arso.gov.si/sl/content/izpusti-delcev-v-zrak-8?tid=2 (accessed 14 February
771 2025).
772 Malandrino M, Casazza M, Abollino O, Minero C, Maurino V. 2015. Size resolved metal
773 distribution in the PM matter of the city of Turin (Italy). Chemosphere.147, 477–89.
774 https://doi.org/10.1016/j.chemosphere.2015.12.089.
775 Mazziotti Tagliani S, Carnevale M, Armiento G, Montereali MR, Nardi E, Inglessis M. 2017.
776 Content, mineral allocation and leaching behavior of heavy metals in urban PM2.5, Atmos
777 Environ. 153, 47–60. https://doi.org/10.1016/j.atmosenv.2017.01.009.
778 Mbengue S, Alleman LY, Flament P. 2014. Size-distributed metallic elements in submicronic
779 and ultrafine atmospheric particles from urban and industrial areas in northern France.
780 Atmos. Res. 135–136, 35–47. https://doi.org/10.1016/j.atmosres.2013.08.010.
781 Morawska L, Ristovski Z, Jayaratne ER, Keogh DU, Ling X. 2008. Ambient nano and
782 ultrafine particles from motor vehicle emissions: characteristics, ambient processing and
783 implications on human exposure. Atmos. Environ. 42, 8113–38.
784 https://doi.org/10.1016/j.atmosenv.2008.07.050.
785 Negral L, Suárez Peña B, Zapico E, Fernández Nava Y, Megido L, Moreno J, Marañón E,
786 Castrillón L. 2020. Anthropogenic and meteorological influences on PM10 metal/semi-metal
787 concentrations: implications for human health. Chemosphere. 243, 125347.
788 https://doi.org/10.1016/j.chemosphere.2019.125347.
789 Ono Ogasawara M, Smith TJ. 2004. Diesel exhaust particles in the work environment and
790 their analysis. Ind. Health. 42, 389–99. https://doi.org/10.2486/indhealth.42.389.
791 OriginLab Corporation. 2021. Origin [Computer software].
792 Oroumiyeh F, Jerrett M, Del Rosario I, Lipsitt J, Liu J, Paulson SE, Ritz B, Schauer JJ,
793 Shafer MM, Shen J, Weichenthal S, Banerjee S, Zhu Y. 2022. Elemental composition of fine

794 and coarse particles across the greater Los Angeles area: spatial variation and contributing
795 sources. Environ. Pollut. 292, 118356. https://doi.org/10.1016/j.envpol.2021.118356.
796 Pant P, Harrison RM. 2013. Estimation of the contribution of road traffic emissions to
797 particulate matter concentrations from field measurements: a review. Atmos. Environ. 77,
798 78–97. https://doi.org/10.1016/j.atmosenv.2013.04.028.
799 Pio C, Mirante F, Oliveira C, Matos M, Caseiro A, Oliveira C, Querol X, Alves C, Martins N,
800 Cerqueira M, Camões F, Silva H, Plana F. 2013. Size-segregated chemical composition of
801 aerosol emissions in an urban road tunnel in Portugal. Atmos. Environ. 71, 15–25.
802 https://doi.org/10.1016/j.atmosenv.2013.01.037.
803 Prati P, Zucchiatti A, Lucarelli F, Mandò PA. 2000. Source apportionment near a steel plant
804 in Genoa (Italy) by continuous aerosol sampling and PIXE analysis. Atmos. Environ. 34,
805 3149–57. https://doi.org/10.1016/S1352-2310(99)00421-5.
806 Qin Y, Chan CK, Chan LY. 1997. Characteristics of chemical compositions of atmospheric
807 aerosols in Hong Kong: spatial and seasonal distributions. Sci. Total Environ. 206, 25–37.
808 https://doi.org/10.1016/S0048-9697(97)00214-3.
809 Raaschou Nielsen O, Andersen ZJ, Beelen R, Samoli E, Stafoggia M, Weinmayr G,
810 Hoffmann B, Fischer P, Nieuwenhuijsen MJ, Brunekreef B, Xun WW, Katsouyanni K,
811 Dimakopoulou K, Sommar J, Forsberg B, Modig L, Oudin A, Oftedal B, Schwarze PE, Hoek
812 G. 2013. Air pollution and lung cancer incidence in 17 European cohorts: prospective
813 analyses from the European Study of Cohorts for Air Pollution Effects (ESCAPE). The
814 Lancet. Oncology. 14, 813–22. https://doi.org/10.1016/S1470-2045(13)70279-1.
815 Ravindra K, Sokhi R, Van Grieken R. 2008. Atmospheric polycyclic aromatic hydrocarbons:
816 source attribution, emission factors and regulation. Atmos. Environ. 42, 2895–921.
817 https://doi.org/10.1016/j.atmosenv.2007.12.010.
818 SURS, Statistical Office of the Republic of Slovenia. 2025. Prebivalstvo,
819 https://www.stat.si/StatWeb/Field/Index/17 (accessed 15 August 2024).
820 Schauer C, Niessner R, Pöschl U. 2003. Polycyclic aromatic hydrocarbons in urban air
821 particulate matter: Decadal and seasonal trends, chemical degradation, and sampling

822 artifacts. Environ. Sci. Technol. 37, 2861–8. https://doi.org/10.1021/es034059s.
823 Shen R, Wang Y, Gao W, Cong X, Cheng L, Li X. 2019. Size-segregated particulate matter
824 bound polycyclic aromatic hydrocarbons (PAHs) over China: size distribution, characteristics
825 and health risk assessment. Sci. Total Environ. 685, 116–23.
826 https://doi.org/10.1016/j.scitotenv.2019.05.436.
827 Tan J, Guo S, Ma Y, Duan J, Cheng Y, He K, Yang F. 2011. Characteristics of particulate
828 PAHs during a typical haze episode in Guangzhou, China. Atmos. Res. 102, 91–8.
829 https://doi.org/10.1016/j.atmosres.2011.06.012.
830 Terzič M. 2020. Avtomobili v EU. https://www.dnevnik.si/nedeljski/prosti-cas/svet-
831 vozil/avtomobili-v-eu-2224578/ (accessed 11 August 2024).
832 Thorpe A, Harrison RM. 2008. Sources and properties of non-exhaust particulate matter
833 from road traffic: a review. Sci. Total Environ. 400, 270–82.
834 https://doi.org/10.1016/j.scitotenv.2008.06.007.
835 TIBCO, TIBCO Software Inc. 2017. Statistica [Data analysis software system], version 13,
836 http://statistica.io (accessed 6 January 2024).
837 Tolis EI, Saraga DE, Lytra MK, Papathanasiou AC, Bougaidis PN, Prekas-Patronakis OE.
838 2015. Concentration and chemical composition of PM2.5 for a one-year period at
839 Thessaloniki, Greece: A comparison between city and port area. Atmos Environ. 113, 197–
840 207. https://doi.org/10.1016/j.atmosenv.2015.05.014.
841 US EPA, United States Environmental Protection Agency. 1997. Exposure factors handbook
842 https://cfpub.epa.gov/ncea/risk/recordisplay.cfm?deid=12464 (accessed 15 August 2024).
843 US EPA, United States Environmental Protection Agency. 2009. Risk assessment guidance
844 for superfund volume I: human health evaluation manual (Part F, Supplemental guidance for
845 inhalation risk assessment). Office of Superfund Remediation and Technology Innovation.
846 US EPA, United States Environmental Protection Agency. 2011. Exposure factors handbook
847 https://www.epa.gov/expobox/exposure-factors-handbook-2011-edition (accessed 28 August
848 2024).
849 US EPA, United States Environmental Protection Agency. 2017. Polycyclic aromatic

850 hydrocarbons (PAHs)—Integrated risk information system (IRIS). https://www.epa.gov/iris
851 (accessed 15 October 2024).
852 US EPA, United States Environmental Protection Agency. 2019. Integrated science
853 assessment (ISA) for particulate matter.
854 https://cfpub.epa.gov/ncea/isa/recordisplay.cfm?deid=347534 (accessed 17 June 2024).
855 US EPA, United States Environmental Protection Agency. 2024. Regional screening level
856 (RSL) resident ambient air table as of November 2024. https://www.epa.gov/risk/regional-
857 screening-levels-rsls-generic-tables (accessed 10 February 2025).
858 Valavanidis A, Fiotakis K, Vlachogianni T. 2008. Airborne particulate matter and human
859 health: toxicological assessment and importance of size and composition of particles for
860 oxidative damage and carcinogenic mechanisms. J. Environ. Sci. Health C. 26, 339–62.
861 https://doi.org/10.1080/10590500802494538.
862 WHO, World Health Organisation. 2010. Some non-heterocyclic polycyclic aromatic
863 hydrocarbons and some related exposures (Vol. 92). International Agency for Research on
864 Cancer.
865 Wilson JG, Kingham S, Pearce J, Sturman AP. 2005. A review of intraurban variations in
866 particulate air pollution: implications for epidemiological research. Atmos. Environ. 39, 6444–
867 62. https://doi.org/10.1016/j.atmosenv.2005.07.030.
868 Wise SA, Watters RL. 2020. Standard Reference Material 1648a—Urban particulate matter,
869 certificate analysis.
870 Yunker MB, Macdonald RW, Vingarzan R, Mitchell RH, Goyette D, Sylvestre S. 2002. PAHs
871 in the Fraser River basin: a critical appraisal of PAH ratios as indicators of PAH source and
872 composition. Org. Geochem. 33, 489–515. https://doi.org/10.1016/S0146-6380(02)00002-5.
873 Zupančič N. 2017. Influence of climate factors on soil heavy metal content in Slovenia. JSS.
874 17, 1073–83. https://doi.org/10.1007/s11368-016-1614-z.
875
876

Supplementary Information Article 2

Supplementary information

Size-fractionated Airborne Particulate Matter-Bound Metal(oid)s and Polycyclic Aromatic Hydrocarbons in Urban Pedestrian and Cycling Microenvironments: Seasonal Trends, Source Apportionment and Health Risk Assessment

Anja Ilenič[1,2], Radmila Milačič Ščančar[2,3], Alenka Mauko Pranjić[1], Nina Zupančič[4,5], Marija Đurić[1], Janez Ščančar[2,3]

[1]Slovenian National Building and Civil Engineering Institute, Department of Materials, Ljubljana 1000, Slovenia

[2]Jožef Stefan International Postgraduate School, Ljubljana 1000, Slovenia

[3]Jožef Stefan Institute, Department of Environmental Sciences, Ljubljana 1000, Slovenia

[4]University of Ljubljana, Faculty of Natural Sciences and Engineering, Ljubljana 1000, Slovenia

[5]ZRC SAZU Ivan Rakovec Institute of Paleontology, Ljubljana 1000, Slovenia

16 **Table S1:** Mean concentrations of metal(oid)s in size-fractionated particulate matter in Maribor.

	As	Ba	Cd	Ce	Co	Cr	Cu	La	Mo	Ni	Pb	Tl	V	Zn
July – August														
PM_{10}	0.291	16.6	0.055	1.11	0.777	4.82	16.4	0.530	0.930	1.36	3.47	0.011	1.19	31.7
$PM_{2.5}$	0.024	0.496	0.003	0.038	0.005	1.17	0.401	0.018	0.182	0.184	0.206	0.005	0.070	2.0
$PM_{0.1}$	0.010	0.308	0.001	0.003	0.001	0.486	0.064	0.002	0.013	0.063	0.041	0.000	0.033	0.546
$PM_{<0.1}$	0.023	<0.017	0.031	0.008	0.018	0.110	1.91	0.006	0.038	0.419	0.077	0.001	0.068	4.00
September – October														
PM_{10}	0.513	26.0	0.104	1.89	0.738	8.80	27.7	0.865	1.88	2.75	8.21	0.020	1.77	51.4
$PM_{2.5}$	0.014	0.506	0.002	0.030	0.005	1.11	0.126	0.015	0.034	0.262	0.102	0.007	0.057	0.919
$PM_{0.1}$	0.008	0.469	0.001	0.005	0.002	0.424	0.120	0.002	0.011	0.257	0.046	0.002	0.029	1.64
$PM_{<0.1}$	0.018	<0.017	0.026	0.011	0.016	0.099	2.09	0.008	0.081	0.638	0.094	0.002	0.032	2.95
November – December														
PM_{10}	0.660	24.3	0.152	0.861	1.14	8.89	29.1	0.401	2.12	2.50	6.18	0.426	1.13	69.2
$PM_{2.5}$	0.048	1.22	0.007	0.074	0.010	1.11	0.739	0.037	0.311	0.248	0.193	0.043	0.059	2.08
$PM_{0.1}$	0.013	0.456	0.001	0.008	0.002	0.552	0.845	0.004	0.025	0.192	0.084	0.008	0.018	1.58
$PM_{<0.1}$	0.011	4.05	0.017	0.015	0.009	0.086	2.14	0.010	0.034	0.373	0.193	0.010	0.038	3.65
January – February														
PM_{10}	0.625	25.7	0.199	0.785	1.64	8.39	23.0	0.330	3.84	0.063	8.20	0.010	1.22	62.8
$PM_{2.5}$	0.062	1.77	0.027	0.059	0.109	1.08	0.754	0.024	0.348	0.007	0.419	0.004	0.079	1.84
$PM_{0.1}$	0.036	0.980	0.014	0.017	0.076	0.453	0.066	0.005	0.170	0.003	0.079	0.003	0.028	0.197
$PM_{<0.1}$	0.016	3.61	0.023	0.026	0.045	0.172	1.39	0.010	0.133	0.012	0.219	0.001	0.025	5.35
March – April														
PM_{10}	0.242	21.9	0.114	1.50	1.04	4.97	14.6	0.685	0.892	1.49	10.1	0.029	1.44	28.2
$PM_{2.5}$	0.005	0.435	0.004	0.037	0.005	0.442	0.109	0.019	0.808	0.118	0.095	0.007	0.049	0.533
$PM_{0.1}$	0.003	0.208	0.001	0.013	0.003	0.237	0.053	0.007	0.007	0.017	0.023	0.001	0.016	0.253
$PM_{<0.1}$	0.006	3.02	0.016	0.026	0.014	0.086	1.53	0.013	0.021	0.380	0.180	0.001	0.038	7.09
May – June														
PM_{10}	0.168	6.68	0.032	0.308	1.58	2.64	8.65	0.150	0.428	0.724	2.56	0.010	0.660	23.2
$PM_{2.5}$	0.172	1.80	0.003	0.196	0.005	1.27	0.126	0.096	0.226	0.352	0.104	0.006	0.108	0.647
$PM_{0.1}$	0.109	2.02	0.019	0.071	0.022	1.16	2.94	0.032	0.204	0.238	1.98	0.008	0.187	14.4
$PM_{<0.1}$	0.036	7.56	0.016	0.177	0.031	0.310	1.79	0.088	0.055	1.01	0.228	0.001	0.093	6.34

17

18

Table S2: Mean concentrations of metal(oid)s in size-fractionated particulate matter in Ljubljana.

	As	Ba	Cd	Ce	Co	Cr	Cu	La	Mo	Ni	Pb	Tl	V	Zn
July – August														
PM_{10}	0.103	2.93	0.018	0.264	0.671	1.13	2.50	0.138	0.146	0.533	0.819	0.005	0.795	3.90
$PM_{2.5}$	0.064	0.818	0.015	0.064	0.024	0.655	0.829	0.033	0.103	0.504	0.543	0.008	0.565	3.78
$PM_{0.1}$	0.013	0.195	0.002	0.002	0.001	0.545	0.062	0.001	0.004	0.035	0.030	0.001	0.072	0.370
$PM_{<0.1}$	0.023	5.06	0.010	0.011	0.016	0.161	2.10	0.006	0.039	0.680	0.249	0.001	0.097	3.71
September – October														
PM_{10}	0.123	5.91	0.038	0.272	0.980	1.66	5.92	0.145	0.265	0.596	1.71	0.010	0.532	6.43
$PM_{2.5}$	0.091	1.95	0.031	0.099	0.019	2.28	2.67	0.049	0.145	0.376	1.19	0.016	0.229	3.13
$PM_{0.1}$	0.020	0.390	0.029	0.007	0.003	0.848	0.164	0.003	0.019	0.101	0.105	0.005	0.061	0.417
$PM_{<0.1}$	0.016	1.76	0.087	0.011	0.012	0.145	1.25	0.006	0.045	1.07	0.102	0.004	0.036	2.58
November – December														
PM_{10}	0.181	5.37	0.072	0.143	3.05	2.44	9.32	0.073	0.505	0.654	1.99	0.128	0.299	10.4
$PM_{2.5}$	0.184	2.95	0.051	0.201	0.031	2.03	4.70	0.105	0.382	0.838	1.39	0.143	0.270	7.14
$PM_{0.1}$	0.046	1.50	0.007	0.045	0.008	2.28	0.668	0.025	0.209	0.334	0.182	0.032	0.067	3.40
$PM_{<0.1}$	0.051	6.71	0.330	0.052	0.040	0.760	4.87	0.031	0.149	1.16	0.390	0.038	0.127	15.0
January – February														
PM_{10}	0.710	3.52	0.050	0.219	2.36	1.47	2.21	0.091	1.01	0.016	0.558	0.029	0.302	0.947
$PM_{2.5}$	0.442	6.68	0.104	0.270	0.214	5.75	3.05	0.113	0.760	0.038	1.65	0.032	0.366	6.04
$PM_{0.1}$	0.264	3.18	0.039	0.100	0.046	1.49	0.397	0.034	0.306	0.010	0.260	0.022	0.109	0.946
$PM_{<0.1}$	0.062	7.42	0.306	0.073	0.169	0.452	2.83	0.026	0.431	0.026	0.433	0.003	0.078	11.9
March – April														
PM_{10}	0.076	5.48	0.048	0.369	4.33	1.97	3.88	0.191	0.225	0.466	1.48	0.010	0.459	6.11
$PM_{2.5}$	0.040	2.02	0.027	0.163	0.021	2.350	1.24	0.083	0.828	0.748	0.792	0.023	0.210	3.13
$PM_{0.1}$	0.011	0.871	0.003	0.043	0.005	0.806	0.177	0.024	0.026	0.037	0.081	0.003	0.064	0.907
$PM_{<0.1}$	0.034	2.85	0.274	0.074	0.022	0.460	2.062	0.029	0.091	0.784	0.386	0.016	0.119	9.15
May – June														
PM_{10}	0.167	5.28	0.029	0.318	6.11	2.35	4.68	0.170	0.248	0.994	1.44	0.011	0.877	6.18
$PM_{2.5}$	0.144	5.79	0.016	0.210	0.032	2.31	1.02	0.106	0.186	1.75	0.677	0.028	0.440	2.83
$PM_{0.1}$	0.053	1.31	0.005	0.029	0.007	3.54	0.179	0.017	0.059	0.555	0.126	0.004	0.202	0.499
$PM_{<0.1}$	0.104	8.07	<0.001	*<0.002*	0.076	1.33	6.88	<0.001	0.149	<0.010	2.01	0.007	0.341	<0.017

Table S3: Mean concentrations of metal(oid)s in size-fractionated particulate matter in Murska Sobota.

	As	Ba	Cd	Ce	Co	Cr	Cu	La	Mo	Ni	Pb	Tl	V	Zn
July – August														
PM_{10}	0.315	<0.003	0.054	0.626	0.934	4.43	13.9	0.301	0.642	1.20	2.83	0.011	1.52	<0.017
$PM_{2.5}$	0.018	0.348	0.002	0.029	0.003	0.224	0.212	0.014	0.194	0.119	0.106	0.004	0.051	1.19
$PM_{0.1}$	0.011	0.182	0.002	0.002	0.001	0.453	0.071	0.001	0.039	0.083	0.055	0.000	0.029	0.457
$PM_{<0.1}$	0.012	8.18	0.048	0.007	0.011	0.106	3.56	0.004	0.019	0.435	0.062	0.001	0.055	4.67
September – October														
PM_{10}	0.031	1.43	0.004	0.119	0.570	0.934	0.850	0.057	0.089	0.281	0.229	0.006	0.238	2.28
$PM_{2.5}$	0.039	1.27	0.006	0.073	0.015	1.76	0.757	0.035	0.064	0.280	0.295	0.010	0.142	2.66
$PM_{0.1}$	0.015	0.693	0.002	0.013	0.011	0.844	0.372	0.006	0.028	0.143	0.095	0.003	0.087	1.38
$PM_{<0.1}$	0.026	5.63	0.044	0.011	0.017	0.105	2.23	0.008	0.080	0.325	0.062	0.007	0.043	5.71
November – December														
PM_{10}	0.118	2.47	0.005	0.107	1.38	1.12	2.30	0.055	0.093	0.514	0.137	0.103	0.194	2.30
$PM_{2.5}$	0.090	1.91	0.020	0.084	0.018	1.58	1.41	0.042	0.135	0.550	0.450	0.075	0.130	3.51
$PM_{0.1}$	0.026	1.01	0.004	0.016	0.004	0.939	0.560	0.008	0.044	0.263	0.095	0.019	0.035	1.21
$PM_{<0.1}$	0.034	6.89	0.061	0.024	0.028	0.286	3.59	0.015	0.124	<0.010	0.154	0.013	0.061	11.0
January – February														
PM_{10}	0.088	2.99	0.019	0.089	0.993	1.42	1.81	0.041	0.270	0.007	0.301	0.004	0.274	2.47
$PM_{2.5}$	0.136	2.51	0.072	0.095	0.048	2.53	1.73	0.043	0.552	0.009	1.06	0.006	0.220	5.39
$PM_{0.1}$	0.043	0.86	0.014	0.017	0.035	0.400	0.126	0.006	0.114	0.002	0.085	0.003	0.025	0.188
$PM_{<0.1}$	0.042	2.22	0.067	0.016	0.042	0.086	1.03	0.006	0.129	0.014	0.105	0.001	0.023	5.05
March – April														
PM_{10}	0.039	4.03	0.016	0.232	0.943	0.935	1.88	0.113	0.081	0.269	0.479	0.005	0.369	2.61
$PM_{2.5}$	0.039	2.25	0.025	0.140	0.026	1.33	1.16	0.068	0.108	0.250	0.631	0.011	0.178	2.17
$PM_{0.1}$	0.003	0.266	0.001	0.009	0.002	0.274	0.081	0.004	0.010	0.041	0.036	0.001	0.022	0.368
$PM_{<0.1}$	0.009	1.15	0.014	0.015	0.010	0.094	1.10	0.008	0.043	0.365	0.060	0.002	0.040	3.42
May – June														
PM_{10}	0.091	4.14	0.014	0.159	1.97	1.39	3.15	0.079	0.191	0.410	0.442	0.010	0.489	5.75
$PM_{2.5}$	0.035	0.873	0.039	0.052	0.074	2.35	5.02	0.026	0.281	0.587	1.28	0.013	0.569	6.19
$PM_{0.1}$	0.053	1.63	0.010	0.035	0.014	0.880	0.876	0.017	0.089	0.237	0.318	0.003	0.122	1.21
$PM_{<0.1}$	0.021	2.20	<0.001	0.234	0.015	0.224	1.80	0.118	0.026	0.881	0.159	0.002	0.074	8.60

Table S4: Mean concentrations of metal(oid)s in size-fractionated particulate matter in Dobrova.

	As	Ba	Cd	Ce	Co	Cr	Cu	La	Mo	Ni	Pb	Tl	V	Zn
July – August														
PM_{10}	0.078	3.29	0.015	0.164	0.367	1.04	4.04	0.085	0.145	0.279	0.852	0.003	0.336	3.80
$PM_{2.5}$	0.080	1.20	0.022	0.058	0.016	0.547	2.99	0.028	0.111	0.215	0.899	0.006	0.162	3.13
$PM_{0.1}$	0.009	0.147	0.001	0.002	0.001	0.417	0.107	0.001	0.013	0.026	0.052	0.001	0.033	0.279
$PM_{0.1}$	0.015	6.89	0.223	0.007	0.009	0.172	1.23	0.004	0.018	0.419	0.192	0.001	0.065	2.39
September – October														
PM_{10}	0.055	2.32	0.009	0.158	1.23	0.978	0.969	0.082	0.080	0.453	0.379	0.007	0.356	2.97
$PM_{2.5}$	0.045	1.04	0.009	0.079	0.013	2.07	0.423	0.042	0.053	0.362	0.310	0.015	0.141	1.41
$PM_{0.1}$	0.014	0.449	0.002	0.009	0.003	0.726	0.113	0.005	0.016	0.102	0.086	0.003	0.062	0.597
$PM_{0.1}$	0.023	1.53	0.011	0.013	0.008	0.138	0.423	0.007	0.040	0.542	0.059	0.003	0.043	0.837
November – December														
PM_{10}	0.040	1.92	0.019	0.055	1.50	1.11	1.46	0.028	0.234	0.351	0.435	0.219	0.108	6.02
$PM_{2.5}$	0.135	1.82	0.013	0.159	0.021	1.45	0.898	0.087	0.128	0.613	0.391	0.119	0.211	2.92
$PM_{0.1}$	0.038	0.893	0.004	0.020	0.008	1.76	0.439	0.011	0.066	0.394	0.098	0.028	0.050	2.27
$PM_{0.1}$	0.042	5.86	0.023	0.038	0.023	0.431	1.56	0.024	0.125	0.593	0.199	0.021	0.114	9.11
January – February														
PM_{10}	0.057	1.91	0.032	0.045	1.43	0.627	0.415	0.018	0.369	0.004	0.232	0.004	0.070	0.530
$PM_{2.5}$	0.080	2.49	0.054	0.057	0.245	1.45	0.422	0.024	0.509	0.010	0.346	0.004	0.086	0.650
$PM_{0.1}$	0.033	1.04	0.008	0.025	0.018	0.540	0.084	0.008	0.132	0.005	0.048	0.003	0.028	0.222
$PM_{0.1}$	0.012	13.0	0.054	0.022	0.040	0.168	0.490	0.008	0.085	0.006	0.072	0.001	0.022	2.69
March – April														
PM_{10}	0.029	2.04	0.010	0.173	0.946	0.814	0.618	0.091	0.105	0.220	0.327	0.004	0.273	1.68
$PM_{2.5}$	0.024	1.03	0.013	0.086	0.021	1.29	0.341	0.044	0.515	0.199	0.373	0.012	0.127	1.40
$PM_{0.1}$	0.003	0.259	0.001	0.012	0.003	0.349	0.064	0.006	0.017	0.034	0.033	0.001	0.024	0.362
$PM_{0.1}$	0.011	6.11	0.161	0.020	0.010	0.106	0.625	0.009	0.033	0.250	0.060	0.002	0.053	6.38
May – June														
PM_{10}	0.041	0.840	0.005	0.111	0.642	0.491	0.349	0.058	0.045	0.079	0.147	0.003	0.213	0.715
$PM_{2.5}$	0.069	4.10	0.009	0.081	0.026	1.98	0.542	0.041	0.128	0.694	0.339	0.008	0.236	2.65
$PM_{0.1}$	0.019	1.64	0.009	0.010	0.015	0.789	0.270	0.005	0.022	0.074	0.066	0.006	0.052	0.354
$PM_{0.1}$	0.033	6.24	0.144	0.340	0.025	0.763	1.08	0.171	0.092	1.28	0.279	0.002	0.135	5.58

Table S5: Mean concentrations of metal(oid)s in size-fractionated particulate matter in Piran.

	As	Ba	Cd	Ce	Co	Cr	Cu	La	Mo	Ni	Pb	Tl	V	Zn
July – August														
PM_{10}	0.052	1.93	0.007	0.208	0.730	0.875	0.833	0.102	0.072	0.305	0.249	0.003	0.335	1.97
$PM_{2.5}$	0.050	0.855	0.008	0.045	0.014	0.513	0.602	0.022	0.068	0.370	0.282	0.007	0.159	2.32
$PM_{0.1}$	0.011	0.246	0.002	0.003	0.001	0.682	0.065	0.001	0.028	0.062	0.049	0.000	0.040	0.522
$PM_{<0.1}$	0.027	<0.017	0.011	0.013	0.013	0.704	0.882	0.008	0.047	1.04	0.796	0.002	0.093	4.20
September – October														
PM_{10}	0.059	2.50	0.010	0.223	0.720	1.00	1.33	0.115	0.078	0.398	0.471	0.007	0.406	2.45
$PM_{2.5}$	0.127	1.82	0.043	0.133	0.040	0.872	0.986	0.076	0.230	0.861	1.142	0.013	0.556	4.39
$PM_{0.1}$	0.014	0.360	0.002	0.007	0.002	0.697	0.101	0.004	0.021	0.133	0.063	0.003	0.049	0.748
$PM_{<0.1}$	0.006	1.21	0.031	0.012	0.011	0.146	0.927	0.006	0.057	0.594	0.096	0.002	0.038	1.84
November – December														
PM_{10}	0.130	2.22	0.019	0.059	1.28	0.935	2.02	0.040	0.119	0.502	0.560	0.115	0.200	3.95
$PM_{2.5}$	0.130	1.44	0.037	0.095	0.018	0.637	0.876	0.057	0.165	0.454	0.654	0.098	0.212	3.30
$PM_{0.1}$	0.018	0.476	0.003	0.018	0.002	0.655	0.252	0.010	0.036	0.194	0.057	0.013	0.023	0.918
$PM_{<0.1}$	0.023	3.18	0.084	0.021	0.016	0.179	1.88	0.013	0.079	0.440	0.177	0.012	0.073	4.45
January – February														
PM_{10}	0.151	2.68	0.035	0.092	2.94	0.953	0.865	0.039	0.533	0.018	0.442	0.010	0.280	1.21
$PM_{2.5}$	0.120	2.639	0.028	0.118	0.059	2.61	0.234	0.050	0.271	0.014	0.340	0.011	0.198	0.527
$PM_{0.1}$	0.101	2.348	0.048	0.050	0.160	1.293	0.165	0.017	0.441	0.015	0.184	0.008	0.067	0.511
$PM_{<0.1}$	0.036	14.3	0.052	0.039	0.087	0.229	1.62	0.013	0.204	0.010	0.223	0.002	0.056	5.69
March – April														
PM_{10}	0.019	1.06	0.007	0.032	1.31	0.456	0.474	0.016	0.074	0.219	0.246	0.005	0.155	2.20
$PM_{2.5}$	0.008	0.695	0.003	0.048	0.006	1.18	0.140	0.027	0.029	0.142	0.094	0.006	0.065	0.932
$PM_{0.1}$	0.005	0.381	0.002	0.046	0.003	0.480	0.098	0.018	0.019	0.058	0.048	0.001	0.031	0.568
$PM_{<0.1}$	0.014	3.52	0.095	0.021	0.011	0.105	1.06	0.011	<0.003	0.438	0.074	0.002	0.079	4.20

Table S6: Mean concentrations of PAHs in size-fractionated particulate matter in Maribor.

	BaA	BaP	BbF	BghiP	Ch	Fl	IP	P
July – August								
PM_{10}	<0.02	<0.02	<0.02	<0.02	<0.02	<0.02	<0.02	<0.02
$PM_{2.5}$	<0.02	<0.02	<0.02	<0.02	<0.02	<0.02	<0.02	<0.02
$PM_{0.1}$	<0.02	<0.02	<0.02	<0.02	<0.02	<0.02	<0.02	<0.02
$PM_{<0.1}$	<0.02	<0.02	<0.02	<0.02	<0.02	<0.02	<0.02	<0.02
September – October								
PM_{10}	<0.02	<0.02	<0.02	<0.02	<0.02	<0.02	<0.02	<0.02
$PM_{2.5}$	<0.02	<0.02	<0.02	<0.02	<0.02	<0.02	<0.02	<0.02
$PM_{0.1}$	<0.02	<0.02	<0.02	<0.02	<0.02	<0.02	<0.02	<0.02
$PM_{<0.1}$	<0.02	<0.02	<0.02	<0.02	<0.02	<0.02	<0.02	<0.02
November – December								
PM_{10}	0.05	0.07	0.09	0.08	0.07	0.05	0.07	0.05
$PM_{2.5}$	<0.02	0.04	0.06	0.06	0.04	<0.02	0.05	<0.02
$PM_{0.1}$	<0.02	<0.02	<0.02	<0.02	<0.02	<0.02	<0.02	<0.02
$PM_{<0.1}$	<0.02	<0.02	<0.02	<0.02	<0.02	<0.02	<0.02	<0.02
January – February								
PM_{10}	<0.02	0.03	0.06	0.06	0.05	0.03	0.05	0.03
$PM_{2.5}$	0.03	0.05	0.11	0.10	0.06	0.05	0.08	0.04
$PM_{0.1}$	<0.02	<0.02	0.04	<0.02	0.05	0.03	<0.02	<0.02
$PM_{<0.1}$	<0.02	<0.02	<0.02	<0.02	<0.02	<0.02	<0.02	<0.02
March – April								
PM_{10}	<0.02	<0.02	<0.02	<0.02	<0.02	<0.02	<0.02	<0.02
$PM_{2.5}$	<0.02	<0.02	<0.02	<0.02	<0.02	<0.02	<0.02	<0.02
$PM_{0.1}$	<0.02	<0.02	<0.02	<0.02	<0.02	<0.02	<0.02	<0.02
$PM_{<0.1}$	<0.02	<0.02	<0.02	<0.02	<0.02	<0.02	<0.02	<0.02
May – June								
PM_{10}	<0.02	<0.02	<0.02	<0.02	<0.02	<0.02	<0.02	<0.02
$PM_{2.5}$	<0.02	<0.02	<0.02	<0.02	<0.02	<0.02	<0.02	<0.02
$PM_{0.1}$	<0.02	<0.02	<0.02	<0.02	<0.02	<0.02	<0.02	<0.02
$PM_{<0.1}$	<0.02	<0.02	<0.02	<0.02	<0.02	<0.02	<0.02	<0.02

34 **Table S7:** Mean concentrations of PAHs in size-fractionated particulate matter in Ljubljana.

	BaA	BaP	BbF	BghiP	Ch	Fl	IP	P
July – August								
PM_{10}	<0.02	<0.02	<0.02	<0.02	<0.02	<0.02	<0.02	<0.02
$PM_{2.5}$	<0.02	<0.02	<0.02	<0.02	<0.02	<0.02	<0.02	<0.02
$PM_{0.1}$	<0.02	<0.02	<0.02	<0.02	<0.02	<0.02	<0.02	<0.02
$PM_{<0.1}$	<0.02	<0.02	<0.02	<0.02	<0.02	<0.02	<0.02	<0.02
September – October								
PM_{10}	<0.02	<0.02	<0.02	<0.02	<0.02	<0.02	<0.02	<0.02
$PM_{2.5}$	<0.02	<0.02	<0.02	<0.02	<0.02	<0.02	<0.02	<0.02
$PM_{0.1}$	<0.02	<0.02	<0.02	<0.02	<0.02	<0.02	<0.02	<0.02
$PM_{<0.1}$	<0.02	<0.02	<0.02	<0.02	<0.02	<0.02	<0.02	<0.02
November – December								
PM_{10}	<0.02	0.10	0.16	0.15	0.11	<0.02	0.13	<0.02
$PM_{2.5}$	<0.02	<0.02	<0.02	<0.02	<0.02	<0.02	<0.02	<0.02
$PM_{0.1}$	<0.02	<0.02	0.11	0.09	0.07	0.06	0.09	<0.02
$PM_{<0.1}$	<0.02	<0.02	<0.02	<0.02	<0.02	<0.02	<0.02	<0.02
January – February								
PM_{10}	<0.02	0.06	0.10	0.09	0.06	<0.02	0.08	<0.02
$PM_{2.5}$	<0.02	<0.02	0.08	0.07	0.05	0.05	0.06	0.05
$PM_{0.1}$	0.09	0.11	0.20	0.16	0.18	0.12	0.13	0.12
$PM_{<0.1}$	<0.02	<0.02	<0.02	<0.02	<0.02	<0.02	<0.02	<0.02
March – April								
PM_{10}	<0.02	<0.02	<0.02	<0.02	<0.02	<0.02	<0.02	<0.02
$PM_{2.5}$	<0.02	<0.02	<0.02	<0.02	<0.02	<0.02	<0.02	<0.02
$PM_{0.1}$	<0.02	<0.02	<0.02	<0.02	<0.02	<0.02	<0.02	<0.02
$PM_{<0.1}$	<0.02	<0.02	<0.02	<0.02	<0.02	<0.02	<0.02	<0.02
May – June								
PM_{10}	<0.02	<0.02	<0.02	<0.02	<0.02	<0.02	<0.02	<0.02
$PM_{2.5}$	<0.02	<0.02	<0.02	<0.02	<0.02	<0.02	<0.02	<0.02
$PM_{0.1}$	<0.02	<0.02	<0.02	<0.02	<0.02	<0.02	<0.02	<0.02
$PM_{<0.1}$	<0.02	<0.02	<0.02	<0.02	<0.02	<0.02	<0.02	<0.02

35

36

Table S8: Mean concentrations of PAHs in size-fractionated particulate matter in Murska Sobota.

	BaA	BaP	BbF	BghiP	Ch	Fl	IP	P
July – August								
PM_{10}	<0.02	<0.02	<0.02	<0.02	<0.02	<0.02	<0.02	<0.02
$PM_{2.5}$	<0.02	<0.02	<0.02	<0.02	<0.02	<0.02	<0.02	<0.02
$PM_{0.1}$	<0.02	<0.02	<0.02	<0.02	<0.02	<0.02	<0.02	<0.02
$PM_{ <0.1}$	<0.02	<0.02	<0.02	<0.02	<0.02	<0.02	<0.02	<0.02
September – October								
PM_{10}	<0.02	<0.02	<0.02	<0.02	<0.02	<0.02	<0.02	<0.02
$PM_{2.5}$	<0.02	<0.02	<0.02	<0.02	<0.02	<0.02	<0.02	<0.02
$PM_{0.1}$	<0.02	<0.02	<0.02	<0.02	<0.02	<0.02	<0.02	<0.02
$PM_{ <0.1}$	<0.02	<0.02	<0.02	<0.02	<0.02	<0.02	<0.02	<0.02
November – December								
PM_{10}	<0.02	<0.02	<0.02	<0.02	<0.02	<0.02	<0.02	<0.02
$PM_{2.5}$	<0.02	<0.02	<0.02	<0.02	<0.02	<0.02	<0.02	<0.02
$PM_{0.1}$	<0.02	<0.02	<0.02	<0.02	<0.02	<0.02	<0.02	<0.02
$PM_{ <0.1}$	<0.02	<0.02	<0.02	<0.02	<0.02	<0.02	<0.02	<0.02
January – February								
PM_{10}	<0.02	<0.02	<0.02	<0.02	<0.02	<0.02	<0.02	<0.02
$PM_{2.5}$	<0.02	<0.02	0.06	0.05	<0.02	0.04	0.04	<0.02
$PM_{0.1}$	<0.02	<0.02	<0.02	<0.02	<0.02	<0.02	<0.02	<0.02
$PM_{ <0.1}$	<0.02	<0.02	<0.02	<0.02	<0.02	<0.02	<0.02	<0.02
March – April								
PM_{10}	<0.02	<0.02	<0.02	<0.02	<0.02	<0.02	<0.02	<0.02
$PM_{2.5}$	<0.02	<0.02	<0.02	<0.02	<0.02	<0.02	<0.02	<0.02
$PM_{0.1}$	<0.02	<0.02	<0.02	<0.02	<0.02	<0.02	<0.02	<0.02
$PM_{ <0.1}$	<0.02	<0.02	<0.02	<0.02	<0.02	<0.02	<0.02	<0.02
May – June								
PM_{10}	<0.02	<0.02	<0.02	<0.02	<0.02	<0.02	<0.02	<0.02
$PM_{2.5}$	<0.02	<0.02	<0.02	<0.02	<0.02	<0.02	<0.02	<0.02
$PM_{0.1}$	<0.02	<0.02	<0.02	<0.02	<0.02	<0.02	<0.02	<0.02
$PM_{ <0.1}$	<0.02	<0.02	<0.02	<0.02	<0.02	<0.02	<0.02	<0.02

40 **Table S9:** Mean concentrations of PAHs in size-fractionated particulate matter in Dobrova.

	BaA	BaP	BbF	BghiP	Ch	Fl	IP	P
July – August								
PM_{10}	<0.02	<0.02	<0.02	<0.02	<0.02	<0.02	<0.02	<0.02
$PM_{2.5}$	<0.02	<0.02	<0.02	<0.02	<0.02	<0.02	<0.02	<0.02
$PM_{0.1}$	<0.02	<0.02	<0.02	<0.02	<0.02	<0.02	<0.02	<0.02
$PM_{<0.1}$	<0.02	<0.02	<0.02	<0.02	<0.02	<0.02	<0.02	<0.02
September – October								
PM_{10}	<0.02	<0.02	<0.02	<0.02	<0.02	<0.02	<0.02	<0.02
$PM_{2.5}$	<0.02	<0.02	<0.02	<0.02	<0.02	<0.02	<0.02	<0.02
$PM_{0.1}$	<0.02	<0.02	<0.02	<0.02	<0.02	<0.02	<0.02	<0.02
$PM_{<0.1}$	<0.02	<0.02	<0.02	<0.02	<0.02	<0.02	<0.02	<0.02
November – December								
PM_{10}	<0.02	<0.02	0.121	0.107	0.062	<0.02	0.067	<0.02
$PM_{2.5}$	<0.02	<0.02	<0.02	<0.02	<0.02	<0.02	<0.02	<0.02
$PM_{0.1}$	<0.02	<0.02	<0.02	<0.02	<0.02	<0.02	<0.02	<0.02
$PM_{<0.1}$	<0.02	<0.02	<0.02	<0.02	<0.02	<0.02	<0.02	<0.02
January – February								
PM_{10}	0.070	0.108	0.185	0.166	0.124	0.073	0.137	0.070
$PM_{2.5}$	<0.02	<0.02	<0.02	<0.02	<0.02	<0.02	<0.02	<0.02
$PM_{0.1}$	<0.02	<0.02	<0.02	<0.02	<0.02	<0.02	<0.02	<0.02
$PM_{<0.1}$	<0.02	<0.02	<0.02	<0.02	<0.02	<0.02	<0.02	<0.02
March – April								
PM_{10}	<0.02	<0.02	<0.02	<0.02	<0.02	<0.02	<0.02	<0.02
$PM_{2.5}$	<0.02	<0.02	<0.02	<0.02	<0.02	<0.02	<0.02	<0.02
$PM_{0.1}$	<0.02	<0.02	<0.02	<0.02	<0.02	<0.02	<0.02	<0.02
$PM_{<0.1}$	<0.02	<0.02	<0.02	<0.02	<0.02	<0.02	<0.02	<0.02
May – June								
PM_{10}	<0.02	<0.02	<0.02	<0.02	<0.02	<0.02	<0.02	<0.02
$PM_{2.5}$	<0.02	<0.02	<0.02	<0.02	<0.02	<0.02	<0.02	<0.02
$PM_{0.1}$	<0.02	<0.02	<0.02	<0.02	<0.02	<0.02	<0.02	<0.02
$PM_{<0.1}$	<0.02	<0.02	<0.02	<0.02	<0.02	<0.02	<0.02	<0.02

41

42

43 **Table S10:** The incremental lifetime cancer risk (ILCR) values for the normal case scenario.

	NHP						HP					
	Cycling			Walking			Cycling			Walking		
	Female	Male	Child	Female	Male	Child	Female	Male	Child	Female	Male	Child
PM_{10}												
As	2E-08	3E-08	1E-07	7E-09	9E-09	3E-08	4E-08	5E-08	2E-07	1E-08	2E-08	6E-08
Cd	2E-09	3E-09	9E-09	7E-10	9E-10	3E-09	4E-09	5E-09	2E-08	1E-09	2E-09	5E-09
Co	5E-07	6E-07	2E-06	2E-07	2E-07	6E-07	6E-07	7E-07	2E-06	2E-07	2E-07	8E-07
Cr	1E-06	1E-06	4E-06	3E-07	4E-07	1E-06	1E-06	1E-06	5E-06	4E-07	5E-07	2E-06
Ni	7E-09	9E-09	3E-08	2E-09	3E-09	9E-09	5E-09	6E-09	2E-08	1E-09	2E-09	6E-09
Pb	9E-10	1E-09	4E-09	3E-10	4E-10	1E-09	9E-10	1E-09	4E-09	3E-10	4E-10	1E-09
BaA	*nd*	*nd*	*nd*	*nd*	*nd*	*nd*	7E-11	8E-11	3E-10	2E-11	3E-11	9E-11
BaP	*nd*	*nd*	*nd*	*nd*	*nd*	*nd*	1E-09	1E-09	4E-09	3E-10	4E-10	1E-09
BbF	*nd*	*nd*	*nd*	*nd*	*nd*	*nd*	2E-10	2E-10	7E-10	5E-11	7E-11	2E-10
Ch	*nd*	*nd*	*nd*	*nd*	*nd*	*nd*	1E-12	2E-12	5E-12	4E-13	5E-13	2E-12
P	*nd*	*nd*	*nd*	*nd*	*nd*	*nd*	7E-11	9E-11	3E-10	2E-11	3E-11	9E-11
$PM_{2.5}$												
As	1E-08	1E-08	4E-08	3E-09	4E-09	1E-08	2E-08	3E-08	9E-08	7E-09	9E-09	3E-08
Cd	9E-10	1E-09	4E-09	3E-10	4E-10	1E-09	3E-09	3E-09	1E-08	8E-10	1E-09	4E-09
Co	7E-09	8E-09	3E-08	2E-09	3E-09	9E-09	3E-08	3E-08	1E-07	8E-09	1E-08	3E-08
Cr	6E-07	7E-07	3E-06	2E-07	2E-07	8E-07	8E-07	1E-06	3E-06	2E-07	3E-07	1E-06
Ni	4E-09	6E-09	2E-08	1E-09	2E-09	6E-09	3E-09	3E-09	1E-08	8E-10	1E-09	3E-09
Pb	2E-10	3E-10	9E-10	7E-11	9E-11	3E-10	3E-10	4E-10	1E-09	9E-11	1E-10	4E-10
BaA	*nd*	*nd*	*nd*	*nd*	*nd*	*nd*	5E-11	6E-11	2E-10	2E-11	2E-11	6E-11
BaP	*nd*	*nd*	*nd*	*nd*	*nd*	*nd*	6E-10	7E-10	2E-09	2E-10	2E-10	8E-10
BbF	*nd*	*nd*	*nd*	*nd*	*nd*	*nd*	1E-10	1E-10	4E-10	3E-11	4E-11	1E-10
Ch	*nd*	*nd*	*nd*	*nd*	*nd*	*nd*	6E-13	8E-13	3E-12	2E-13	3E-13	9E-13
P	*nd*	*nd*	*nd*	*nd*	*nd*	*nd*	6E-11	7E-11	2E-10	2E-11	2E-11	7E-11
$PM_{0.1}$												
As	3E-09	4E-09	1E-08	1E-09	1E-09	5E-09	9E-09	1E-08	4E-08	3E-09	4E-09	1E-08
Cd	4E-10	4E-10	2E-09	1E-10	1E-10	5E-10	9E-10	1E-09	4E-09	3E-10	4E-10	1E-09
Co	2E-09	2E-09	8E-09	6E-10	7E-10	2E-09	1E-08	2E-08	5E-08	4E-09	5E-09	2E-08
Cr	3E-07	4E-07	1E-06	1E-07	1E-07	5E-07	4E-07	5E-07	2E-06	1E-07	2E-07	5E-07
Ni	1E-09	2E-09	5E-09	4E-10	5E-10	2E-09	1E-09	2E-09	6E-09	4E-10	5E-10	2E-09
Pb	8E-11	1E-10	3E-10	3E-11	3E-11	1E-10	5E-11	6E-11	2E-10	2E-11	2E-11	7E-11
BaA	*nd*	*nd*	*nd*	*nd*	*nd*	*nd*	6E-11	7E-11	2E-10	2E-11	2E-11	8E-11
BaP	*nd*	*nd*	*nd*	*nd*	*nd*	*nd*	6E-10	8E-10	3E-09	2E-10	2E-10	8E-10
BbF	*nd*	*nd*	*nd*	*nd*	*nd*	*nd*	9E-11	1E-10	4E-10	3E-11	4E-11	1E-10
Ch	*nd*	*nd*	*nd*	*nd*	*nd*	*nd*	9E-13	1E-12	4E-12	3E-13	3E-13	1E-12
P	*nd*	*nd*	*nd*	*nd*	*nd*	*nd*	6E-11	8E-11	3E-10	2E-11	2E-11	8E-11
$PM_{>0.1}$												
As	4E-09	5E-09	2E-08	1E-09	2E-09	5E-09	5E-09	6E-09	2E-08	2E-09	2E-09	7E-09
Cd	5E-09	6E-09	2E-08	2E-09	2E-09	7E-09	6E-09	7E-09	3E-08	2E-09	2E-09	8E-09
Co	6E-09	8E-09	3E-08	2E-09	3E-09	9E-09	2E-08	2E-08	7E-08	5E-09	6E-09	2E-08
Cr	1E-07	1E-07	5E-07	3E-08	4E-08	1E-07	1E-07	1E-07	5E-07	3E-08	4E-08	1E-07
Ni	7E-09	8E-09	3E-08	2E-09	3E-09	9E-09	2E-09	3E-09	1E-08	7E-10	1E-09	3E-09
Pb	1E-10	1E-10	5E-10	4E-11	5E-11	2E-10	9E-11	1E-10	4E-10	3E-11	4E-11	1E-10
BaA	*nd*	*nd*	*nd*	*nd*	*nd*	*nd*	5E-11	6E-11	2E-10	1E-11	2E-11	6E-11
BaP	*nd*	*nd*	*nd*	*nd*	*nd*	*nd*	5E-10	6E-10	2E-09	1E-10	2E-10	6E-10
BbF	*nd*	*nd*	*nd*	*nd*	*nd*	*nd*	5E-11	6E-11	2E-10	1E-11	2E-11	6E-11

44	Ch	*nd*	*nd*	*nd*	*nd*	*nd*	*nd*	*nd*	5E-13	6E-13	2E-12	1E-13	2E-13	6E-13	
	P	*nd*	*nd*	*nd*	*nd*	*nd*	*nd*	*nd*	5E-11	6E-11	2E-10	1E-11	2E-11	6E-11	
	nd = not determined														
45															
46															

47 **Table S11:** The incremental lifetime cancer risk (ILCR) values for the worst case scenario.

	NHP						HP					
	Cycling			Walking			Cycling			Walking		
	Female	Male	Child	Female	Male	Child	Female	Male	Child	Female	Male	Child
PM_{10}												
As	3E-07	4E-07	1E-06	9E-08	1E-07	4E-07	6E-07	7E-07	2E-06	2E-07	2E-07	8E-07
Cd	3E-08	4E-08	1E-07	9E-09	1E-08	4E-08	5E-08	7E-08	2E-07	2E-08	2E-08	7E-08
Co	7E-06	8E-06	3E-05	2E-06	3E-06	9E-06	8E-06	1E-05	3E-05	2E-06	3E-06	1E-05
Cr	1E-05	2E-05	5E-05	4E-06	5E-06	2E-05	2E-05	2E-05	7E-05	5E-06	6E-06	2E-05
Ni	9E-08	1E-07	4E-07	3E-08	4E-08	1E-07	6E-08	8E-08	3E-07	2E-08	2E-08	8E-08
Pb	1E-08	1E-08	5E-08	4E-09	5E-09	2E-08	1E-08	1E-08	5E-08	4E-09	5E-09	2E-08
BaA	*nd*	*nd*	*nd*	*nd*	*nd*	*nd*	9E-10	1E-09	4E-09	3E-10	4E-10	1E-09
BaP	*nd*	*nd*	*nd*	*nd*	*nd*	*nd*	1E-08	2E-08	6E-08	4E-09	5E-09	2E-08
BbF	*nd*	*nd*	*nd*	*nd*	*nd*	*nd*	2E-09	3E-09	1E-08	7E-10	9E-10	3E-09
Ch	*nd*	*nd*	*nd*	*nd*	*nd*	*nd*	2E-11	2E-11	7E-11	5E-12	7E-12	2E-11
P	*nd*	*nd*	*nd*	*nd*	*nd*	*nd*	9E-10	1E-09	4E-09	3E-10	4E-10	1E-09
$PM_{2.5}$												
As	1E-07	2E-07	5E-07	4E-08	5E-08	2E-07	3E-07	4E-07	1E-06	9E-08	1E-07	4E-07
Cd	1E-08	2E-08	5E-08	4E-09	5E-09	2E-08	4E-08	4E-08	1E-07	1E-08	1E-08	5E-08
Co	9E-08	1E-07	4E-07	3E-08	4E-08	1E-07	3E-07	4E-07	1E-06	1E-07	1E-07	4E-07
Cr	8E-06	1E-05	3E-05	2E-06	3E-06	1E-05	1E-05	1E-05	4E-05	3E-06	4E-06	1E-05
Ni	6E-08	7E-08	3E-07	2E-08	2E-08	8E-08	4E-08	4E-08	1E-07	1E-08	1E-08	5E-08
Pb	3E-09	4E-09	1E-08	9E-10	1E-09	4E-09	4E-09	5E-09	2E-08	1E-09	2E-09	5E-09
BaA	*nd*	*nd*	*nd*	*nd*	*nd*	*nd*	6E-10	8E-10	3E-09	2E-10	3E-10	9E-10
BaP	*nd*	*nd*	*nd*	*nd*	*nd*	*nd*	8E-09	1E-08	3E-08	2E-09	3E-09	1E-08
BbF	*nd*	*nd*	*nd*	*nd*	*nd*	*nd*	1E-09	2E-09	5E-09	4E-10	5E-10	2E-09
Ch	*nd*	*nd*	*nd*	*nd*	*nd*	*nd*	9E-12	1E-11	4E-11	3E-12	3E-12	1E-11
P	*nd*	*nd*	*nd*	*nd*	*nd*	*nd*	7E-10	9E-10	3E-09	2E-10	3E-10	1E-09
$PM_{0.1}$												
As	5E-08	6E-08	2E-07	1E-08	2E-08	6E-08	1E-07	1E-07	5E-07	4E-08	5E-08	2E-07
Cd	5E-09	6E-09	2E-08	1E-09	2E-09	6E-09	1E-08	2E-08	5E-08	4E-09	5E-09	2E-08
Co	2E-08	3E-08	1E-07	8E-09	1E-08	3E-08	2E-07	2E-07	7E-07	5E-08	7E-08	2E-07
Cr	5E-06	6E-06	2E-05	1E-06	2E-06	6E-06	5E-06	7E-06	2E-05	2E-06	2E-06	7E-06
Ni	2E-08	2E-08	7E-08	5E-09	6E-09	2E-08	2E-08	2E-08	8E-08	6E-09	7E-09	2E-08
Pb	1E-09	1E-09	5E-09	3E-10	4E-10	1E-09	7E-10	8E-10	3E-09	2E-10	3E-10	9E-10
BaA	*nd*	*nd*	*nd*	*nd*	*nd*	*nd*	8E-10	1E-09	3E-09	2E-10	3E-10	1E-09
BaP	*nd*	*nd*	*nd*	*nd*	*nd*	*nd*	8E-09	1E-08	3E-08	3E-09	3E-09	1E-08
BbF	*nd*	*nd*	*nd*	*nd*	*nd*	*nd*	1E-09	2E-09	5E-09	4E-10	5E-10	2E-09
Ch	*nd*	*nd*	*nd*	*nd*	*nd*	*nd*	1E-11	1E-11	5E-11	4E-12	5E-12	2E-11
P	*nd*	*nd*	*nd*	*nd*	*nd*	*nd*	8E-10	1E-09	3E-09	3E-10	3E-10	1E-09
$PM_{<0.1}$												
As	5E-08	7E-08	2E-07	2E-08	2E-08	7E-08	7E-08	9E-08	3E-07	2E-08	3E-08	9E-08
Cd	7E-08	8E-08	3E-07	2E-08	3E-08	9E-08	8E-08	1E-07	3E-07	2E-08	3E-08	1E-07
Co	9E-08	1E-07	4E-07	3E-08	3E-08	1E-07	2E-07	3E-07	9E-07	7E-08	8E-08	3E-07
Cr	1E-06	2E-06	6E-06	5E-07	6E-07	2E-06	1E-06	2E-06	6E-06	5E-07	6E-07	2E-06
Ni	9E-08	1E-07	4E-07	3E-08	4E-08	1E-07	3E-08	4E-08	1E-07	1E-08	1E-08	4E-08
Pb	2E-09	2E-09	6E-09	5E-10	6E-10	2E-09	1E-09	2E-09	5E-09	4E-10	5E-10	2E-09
BaA	*nd*	*nd*	*nd*	*nd*	*nd*	*nd*	6E-10	8E-10	3E-09	2E-10	2E-10	8E-10
BaP	*nd*	*nd*	*nd*	*nd*	*nd*	*nd*	6E-09	8E-09	3E-08	2E-09	2E-09	8E-09
BbF	*nd*	*nd*	*nd*	*nd*	*nd*	*nd*	6E-10	8E-10	3E-09	2E-10	2E-10	8E-10

Ch	*nd*	*nd*	*nd*	*nd*	*nd*	*nd*	6E-12	8E-12	3E-11	2E-12	2E-12	8E-12
P	*nd*	*nd*	*nd*	*nd*	*nd*	*nd*	6E-10	8E-10	3E-09	2E-10	2E-10	8E-10

nd = not determined

Table S12: The hazard quotient (HQ) values for the normal case scenario.

	NHP						HP					
	Cycling			Walking			Cycling			Walking		
	Female	Male	Child	Female	Male	Child	Female	Male	Child	Female	Male	Child
PM_{10}												
As	3E-04	4E-04	1E-03	1E-04	1E-04	5E-04	7E-04	8E-04	3E-03	2E-04	3E-04	9E-04
Ba	5E-04	6E-04	2E-03	2E-04	2E-04	6E-04	6E-04	7E-04	2E-03	2E-04	2E-04	8E-04
Ce	3E-04	3E-04	1E-03	8E-05	1E-04	4E-04	3E-04	4E-04	1E-03	1E-04	1E-04	4E-04
Cd	1E-04	2E-04	5E-04	4E-05	5E-05	2E-04	2E-04	3E-04	1E-03	7E-05	9E-05	3E-04
Co	9E-03	1E-02	4E-02	3E-03	4E-03	1E-02	1E-02	1E-02	5E-02	3E-03	4E-03	1E-02
Cr	3E-03	4E-03	1E-02	9E-04	1E-03	4E-03	4E-03	4E-03	1E-02	1E-03	1E-03	5E-03
Mo	7E-06	8E-06	3E-05	2E-06	3E-06	9E-06	2E-05	2E-05	7E-05	5E-06	7E-06	2E-05
Ni	3E-03	3E-03	1E-02	8E-04	1E-03	4E-03	2E-03	2E-03	8E-03	6E-04	7E-04	2E-03
V	3E-04	3E-04	1E-03	8E-05	1E-04	3E-04	2E-04	2E-04	7E-04	5E-05	6E-05	2E-04
BaP	*nd*	*nd*	*nd*	*nd*	*nd*	*nd*	5E-04	7E-04	2E-03	2E-04	2E-04	7E-04
$PM_{2.5}$												
As	1E-04	2E-04	6E-04	5E-05	6E-05	2E-04	3E-04	4E-04	1E-03	1E-04	1E-04	4E-04
Ba	1E-04	1E-04	5E-04	4E-05	5E-05	2E-04	2E-04	2E-04	8E-04	6E-05	7E-05	2E-04
Ce	7E-05	8E-05	3E-04	2E-05	3E-05	9E-05	1E-04	1E-04	4E-04	3E-05	4E-05	1E-04
Cd	5E-05	7E-05	2E-04	2E-05	2E-05	7E-05	1E-04	2E-04	6E-04	5E-05	6E-05	2E-04
Co	1E-04	2E-04	5E-04	4E-05	5E-05	2E-04	5E-04	6E-04	2E-03	1E-04	2E-04	6E-04
Cr	2E-03	2E-03	8E-03	6E-04	7E-04	2E-03	2E-03	3E-03	1E-02	7E-04	1E-03	3E-03
Mo	4E-06	5E-06	2E-05	1E-06	2E-06	6E-06	6E-06	8E-06	3E-05	2E-06	3E-06	9E-06
Ni	2E-03	2E-03	7E-03	5E-04	7E-04	2E-03	1E-03	1E-03	4E-03	3E-04	4E-04	1E-03
V	8E-05	1E-04	3E-04	3E-05	3E-05	1E-04	7E-05	8E-05	3E-04	2E-05	3E-05	9E-05
BaP	*nd*	*nd*	*nd*	*nd*	*nd*	*nd*	4E-04	5E-04	2E-03	1E-04	2E-04	5E-04
$PM_{0.1}$												
As	5E-05	7E-05	2E-04	2E-05	2E-05	7E-05	1E-04	2E-04	6E-04	4E-05	6E-05	2E-04
Ba	5E-05	6E-05	2E-04	2E-05	2E-05	7E-05	9E-05	1E-04	4E-04	3E-05	4E-05	1E-04
Ce	3E-05	4E-05	1E-04	9E-06	1E-05	4E-05	5E-05	6E-05	2E-04	2E-05	2E-05	7E-05
Cd	2E-05	2E-05	8E-05	6E-06	8E-06	3E-05	5E-05	6E-05	2E-04	2E-05	2E-05	7E-05
Co	3E-05	4E-05	1E-04	1E-05	1E-05	5E-05	2E-04	3E-04	1E-03	7E-05	9E-05	3E-04
Cr	1E-03	1E-03	4E-03	3E-04	4E-04	1E-03	1E-03	2E-03	5E-03	4E-04	5E-04	2E-03
Mo	7E-07	8E-07	3E-06	2E-07	3E-07	9E-07	3E-06	3E-06	1E-05	9E-07	1E-06	4E-06
Ni	5E-04	6E-04	2E-03	1E-04	2E-04	6E-04	5E-04	7E-04	2E-03	2E-04	2E-04	7E-04
V	3E-05	3E-05	1E-04	8E-06	1E-05	3E-05	2E-05	2E-05	7E-05	5E-06	6E-06	2E-05
BaP	*nd*	*nd*	*nd*	*nd*	*nd*	*nd*	5E-04	6E-04	2E-03	1E-04	2E-04	6E-04
$PM_{<0.1}$												
As	6E-05	8E-05	3E-04	2E-05	3E-05	8E-05	8E-05	1E-04	3E-04	2E-05	3E-05	1E-04
Ba	4E-04	4E-04	1E-03	1E-04	1E-04	5E-04	5E-04	6E-04	2E-03	2E-04	2E-04	7E-04
Ce	2E-04	2E-04	8E-04	6E-05	8E-05	3E-04	3E-04	4E-04	1E-03	9E-05	1E-04	4E-04
Cd	3E-04	4E-04	1E-03	9E-05	1E-04	4E-04	3E-04	4E-04	1E-03	1E-04	1E-04	4E-04
Co	1E-04	1E-04	5E-04	4E-05	5E-05	2E-04	3E-04	4E-04	1E-03	9E-05	1E-04	4E-04
Cr	3E-04	4E-04	1E-03	1E-04	1E-04	4E-04	3E-04	4E-04	1E-03	1E-04	1E-04	4E-04
Mo	1E-06	1E-06	5E-06	3E-07	4E-07	1E-06	3E-06	3E-06	1E-05	8E-07	1E-06	4E-06
Ni	3E-03	3E-03	1E-02	8E-04	1E-03	3E-03	9E-04	1E-03	4E-03	3E-04	4E-04	1E-03
V	3E-05	4E-05	1E-04	1E-05	1E-05	4E-05	2E-05	3E-05	9E-05	7E-06	9E-06	3E-05
BaP	*nd*	*nd*	*nd*	*nd*	*nd*	*nd*	4E-04	5E-04	2E-03	1E-04	2E-04	5E-04

nd = not determined

53 **Table S13:** The hazard quotient (HQ) values for the worst case scenario.

	NHP						HP					
	Cycling			Walking			Cycling			Walking		
	Female	Male	Child	Female	Male	Child	Female	Male	Child	Female	Male	Child
PM_{10}												
As	5E-03	6E-03	2E-02	1E-03	2E-03	6E-03	9E-03	1E-02	4E-02	3E-03	4E-03	1E-02
Ba	6E-03	8E-03	3E-02	2E-03	3E-03	9E-03	8E-03	9E-03	3E-02	2E-03	3E-03	1E-02
Ce	4E-03	5E-03	2E-02	1E-03	1E-03	5E-03	4E-03	5E-03	2E-02	1E-03	2E-03	6E-03
Cd	2E-03	2E-03	7E-03	5E-04	6E-04	2E-03	3E-03	4E-03	1E-02	1E-03	1E-03	4E-03
Co	1E-01	2E-01	5E-01	4E-02	5E-02	2E-01	1E-01	2E-01	6E-01	4E-02	6E-02	2E-01
Cr	4E-02	5E-02	2E-01	1E-02	2E-02	5E-02	5E-02	6E-02	2E-01	1E-02	2E-02	6E-02
Mo	9E-05	1E-04	4E-04	3E-05	4E-05	1E-04	2E-04	3E-04	1E-03	7E-05	9E-05	3E-04
Ni	4E-02	5E-02	2E-01	1E-02	1E-02	5E-02	2E-02	3E-02	1E-01	7E-03	1E-02	3E-02
V	3E-03	4E-03	1E-02	1E-03	1E-03	5E-03	2E-03	3E-03	9E-03	7E-04	8E-04	3E-03
BaP	*nd*	*nd*	*nd*	*nd*	*nd*	*nd*	7E-03	9E-03	3E-02	2E-03	3E-03	1E-02
$PM_{2.5}$												
As	2E-03	2E-03	8E-03	6E-04	8E-04	3E-03	4E-03	5E-03	2E-02	1E-03	2E-03	6E-03
Ba	2E-03	2E-03	7E-03	5E-04	6E-04	2E-03	2E-03	3E-03	1E-02	8E-04	1E-03	3E-03
Ce	9E-04	1E-03	4E-03	3E-04	4E-04	1E-03	1E-03	2E-03	6E-03	4E-04	5E-04	2E-03
Cd	7E-04	9E-04	3E-03	2E-04	3E-04	9E-04	2E-03	2E-03	8E-03	6E-04	8E-04	3E-03
Co	2E-03	2E-03	7E-03	5E-04	7E-04	2E-03	6E-03	8E-03	3E-02	2E-03	2E-03	8E-03
Cr	2E-02	3E-02	1E-01	8E-03	1E-02	3E-02	3E-02	4E-02	1E-01	1E-02	1E-02	4E-02
Mo	6E-05	7E-05	2E-04	2E-05	2E-05	8E-05	9E-05	1E-04	4E-04	3E-05	3E-05	1E-04
Ni	2E-02	3E-02	1E-01	7E-03	9E-03	3E-02	1E-02	2E-02	6E-02	4E-03	5E-03	2E-02
V	1E-03	1E-03	5E-03	3E-04	4E-04	1E-03	9E-04	1E-03	4E-03	3E-04	4E-04	1E-03
BaP	*nd*	*nd*	*nd*	*nd*	*nd*	*nd*	5E-03	7E-03	2E-02	2E-03	2E-03	7E-03
$PM_{0.1}$												
As	7E-04	9E-04	3E-03	2E-04	3E-04	1E-03	2E-03	2E-03	8E-03	6E-04	7E-04	2E-03
Ba	7E-04	8E-04	3E-03	2E-04	3E-04	9E-04	1E-03	2E-03	5E-03	4E-04	5E-04	2E-03
Ce	4E-04	5E-04	2E-03	1E-04	2E-04	5E-04	7E-04	8E-04	3E-03	2E-04	3E-04	9E-04
Cd	3E-04	3E-04	1E-03	8E-05	1E-04	4E-04	7E-04	9E-04	3E-03	2E-04	3E-04	9E-04
Co	5E-04	6E-04	2E-03	1E-04	2E-04	6E-04	3E-03	4E-03	1E-02	1E-03	1E-03	4E-03
Cr	1E-02	2E-02	6E-02	4E-03	6E-03	2E-02	2E-02	2E-02	7E-02	5E-03	7E-03	2E-02
Mo	9E-06	1E-05	4E-05	3E-06	4E-06	1E-05	4E-05	5E-05	2E-04	1E-05	1E-05	5E-05
Ni	6E-03	8E-03	3E-02	2E-03	2E-03	8E-03	7E-03	9E-03	3E-02	2E-03	3E-03	9E-03
V	3E-04	4E-04	1E-03	1E-04	1E-04	5E-04	2E-04	3E-04	9E-04	7E-05	8E-05	3E-04
BaP	*nd*	*nd*	*nd*	*nd*	*nd*	*nd*	6E-03	8E-03	3E-02	2E-03	3E-03	8E-03
$PM_{<0.1}$												
As	8E-04	1E-03	4E-03	3E-04	3E-04	1E-03	1E-03	1E-03	4E-03	3E-04	4E-04	1E-03
Ba	5E-03	6E-03	2E-02	1E-03	2E-03	6E-03	7E-03	8E-03	3E-02	2E-03	3E-03	9E-03
Ce	3E-03	3E-03	1E-02	8E-04	1E-03	3E-03	4E-03	5E-03	2E-02	1E-03	2E-03	5E-03
Cd	4E-03	5E-03	2E-02	1E-03	2E-03	5E-03	4E-03	5E-03	2E-02	1E-03	2E-03	6E-03
Co	2E-03	2E-03	7E-03	5E-04	6E-04	2E-03	4E-03	5E-03	2E-02	1E-03	2E-03	5E-03
Cr	5E-03	6E-03	2E-02	1E-03	2E-03	6E-03	4E-03	6E-03	2E-02	1E-03	2E-03	6E-03
Mo	1E-05	2E-05	6E-05	5E-06	6E-06	2E-05	4E-05	4E-05	1E-04	1E-05	1E-05	5E-05
Ni	3E-02	4E-02	1E-01	1E-02	1E-02	5E-02	1E-02	2E-02	5E-02	4E-03	5E-03	2E-02
V	4E-04	6E-04	2E-03	1E-04	2E-04	6E-04	3E-04	4E-04	1E-03	9E-05	1E-04	4E-04
BaP	*nd*	*nd*	*nd*	*nd*	*nd*	*nd*	5E-03	6E-03	2E-02	2E-03	2E-03	7E-03

54 *nd* = not determined

3.3 Article 3: Can Low-Cost Sensors (LCS) Enhance Air Quality Monitoring for Personal Pollution Exposure Assessment?

Authors: Anja Ilenič, Alenka Mauko Pranjić, Janez Ščančar, Radmila Milačič Ščančar, Prashant Kumar
Published in IOP Publishing, Environmental Research Communications (September 2025)
Available at DOI: 10.1088/2515-7620/ae02ef

In urban environments, stationary AQMS continuously monitor PM levels in accordance with standardised QA/QC procedures. However, these stations are usually sparely distributed and do not comprehensively capture urban air quality status, particularly the dynamic personal exposure of commuters. Thus, in recent years, rapid development and deployment of LCS has been observed, offering several advantages, including affordability, portability, improved spatial resolution and the ability to identify urban emission hot spots. Nevertheless, in comparison to AQMS, LCS exhibit lower levels of accuracy, sensitivity and LODs, therefore it is imperative to evaluate these sensors, using laboratory or co-location field assessment methods against reference instruments. This study assessed the performance of Sensirion SPS30 sensor and its limitations under varying environmental conditions, including different RH, T and $PM_{2.5}$ concentrations, and explored the potential applicability of LCS for widespread community deployment. The results showed that the sensor met micro-environmental monitoring standards (accuracy <25%) and US EPA performance criteria (R^2 >0.7, RMSE ≤7 µg m^{-3}) only at RH <60% and in low-pollution environments, emphasising the need for RH dependent data correction in real-world applications. Under controlled laboratory conditions, R^2 ranged from 0.81−0.99 and RMSE from 0.81−61.72 µg m^{-3}, at an average concentration of 21.5 µg m^{-3}. In contrast, co-location assessment at an average concentration of 9 µg m^{-3} resulted in R^2 = 0.5 and RMSE = 6.82 µg m^{-3}. A strong RH dependence was reflected in the underestimation or overestimation of $PM_{2.5}$ readings under laboratory and field conditions, respectively. These discrepancies were attributed to variations in particle composition and concentration. In ambient air, more hygroscopic and volatile particles tend to absorb water and grow at elevated RH levels, thereby enhancing light scattering and leading to higher $PM_{2.5}$ readings. In contrast, controlled laboratory settings limit particle growth and reduce refractive index, which in turn reduces scattering efficiency per unit mass. Despite the inconsistencies, LCS can effectively detect spatio-temporal patterns and identify urban air pollution hotspots. However, RH dependent correction remains essential for reliable interpretation of $PM_{2.5}$ measurements. LCS SPS30 were deployed by citizens during a campaign in autumn 2023 in Maribor, Slovenia. The results showed that the lowest concentrations were recorded at 15:00 (2.9 µg m^{-3}), while the highest occurred during the morning RHT (4.8 µg m^{-3}), likely attributed to the influence of the PBL on atmospheric particulate dispersion. The spatial analysis showed that hotspots were clustered near intersections, where vehicle waiting time is the longest. In conclusion, LCS help raise public awareness of air pollution challenges; however their absolute $PM_{2.5}$ measurements should be interpreted with caution.

ENVIRONMENTAL RESEARCH
COMMUNICATIONS

INCLUSIVE PUBLISHING TRUSTED SCIENCE

Part of the ENVIRONMENTAL RESEARCH SERIES

PURPOSE-LED PUBLISHING™

PAPER • OPEN ACCESS

Can low-cost sensors (LCS) enhance air quality monitoring for personal pollution exposure assessment?

To cite this article: Anja Ilenič *et al* 2025 *Environ. Res. Commun.* **7** 095007

View the article online for updates and enhancements.

You may also like

- Analyzing Türkiye's ecological footprint: the impact of air transportation, renewable energy, and R&D using a non-linear ARDL approach
Gökhan Konat, Veli Yilanci, Havanur Ergün Tatar et al.
- Woody perennials as bio-monitors of air pollution around brick kilns in peri-urban ecosystem using pollution tolerance indices
Ali Ahmad, Sohaib Muhammad, Fahad Shafiq et al.
- Global gridded population projection via spatial econometric model considering rank-size rule
Masashi Tomari, Hajime Seya, Daisuke Murakami et al.



This content was downloaded from IP address 156.17.177.72 on 27/10/2025 at 14:09

IOP Publishing Environ. Res. Commun. 7 (2025) 095007 https://doi.org/10.1088/2515-7620/ae02ef

Environmental Research Communications



OPEN ACCESS

RECEIVED
1 April 2025

REVISED
22 August 2025

ACCEPTED FOR PUBLICATION
3 September 2025

PUBLISHED
11 September 2025

Original content from this work may be used under the terms of the Creative Commons Attribution 4.0 licence.

Any further distribution of this work must maintain attribution to the author(s) and the title of the work, journal citation and DOI.



PAPER

Can low-cost sensors (LCS) enhance air quality monitoring for personal pollution exposure assessment?

Anja Ilenič[1,2,*], Alenka Mauko Pranjić[1], Janez Ščančar[2,3], Radmila Milačič Ščančar[2,3] and Prashant Kumar[4,5]

[1] Department of Materials, Slovenian National Building and Civil Engineering Institute, Ljubljana, Slovenia
[2] Jožef Stefan International Postgraduate School, Ljubljana, Slovenia
[3] Department of Environmental Sciences, Institute Jožef Stefan, Ljubljana, Slovenia
[4] Global Centre for Clean Air Research (GCARE), School of Engineering, Civil and Environmental Engineering, Faculty of Engineering and Physical Sciences, University of Surrey, Guildford GU2 7XH, Surrey, United Kingdom
[5] Institute for Sustainability, University of Surrey, Guildford GU2 7XH, Surrey, United Kingdom
* Author to whom any correspondence should be addressed.

E-mail: anja.ilenic@zag.si

Keywords: particulate matter, low-cost sensor, sensirion SPS30, citizen science, laboratory assessment, co-location assessment

Supplementary material for this article is available online

Abstract

Laboratory and field assessments of low-cost sensors (LCS) are essential for ensuring the accuracy of $PM_{2.5}$ measurements collected by citizens in air quality campaigns. Evaluation of Sensirion SPS30 (LCS SPS30) in controlled laboratory setting showed a coefficient of determination (R^2) ranging from 0.81–0.99 and a root mean square error (RMSE) from 0.81–61.72 μg m^{-3}, at average concentration of 21.5 μg m^{-3}. In contrast, co-location assessment at an average concentration of 9 μg m^{-3} resulted in R^2 of 0.5 and a RMSE of 6.82 μg m^{-3}. The results demonstrated that the sensor met micro-environmental monitoring standards (accuracy < 25%) and United States Environmental Protection Agency's performance criteria (RMSE ⩽ 7 μg m^{-3}, $R^2 > 0.7$) only at relative humidity (RH) levels below 60%, emphasising its strong sensitivity to RH and the need for RH-dependent data corrections. The observed underestimation or overestimation of $PM_{2.5}$ readings was primarily attributed to variations in particle composition and concentration. Despite accuracy variations, LCSs can effectively capture spatiotemporal urban air quality patterns and identify pollution hotspots in community monitoring, particularly in low-pollution environments. In a citizen-led $PM_{2.5}$ monitoring campaign in Maribor, Slovenia, the lowest concentrations were recorded at 15:00 (2.9 μg m^{-3}), while the highest occurred during the morning rush-hour (4.8 μg m^{-3}), likely attributed to the planetary boundary layer's impact on atmospheric particulate dispersion. Spatial analysis revealed that hotspots clustered near intersections, where vehicle waiting time is the longest.

1. Introduction

The health and environmental hazards associated with airborne fine particulate matter ($PM_{2.5}$, aerodynamic diameter ⩽ 2.5 μm) are prevalent in many European cities, surpassing the air quality threshold levels established by the European Ambient Air Quality Directive (AQD) [1], and the interim targets defined in the World Health Organization's (WHO) air quality guidelines [2]. Exposure to even minimal $PM_{2.5}$ concentrations can increase health risks, including chronic and acute respiratory as well as cardiovascular diseases, such as stroke and lung cancer, leading to a reduced life expectancy. Therefore, systematic monitoring of these atmospheric pollutants is essential [3–6].

In urban environments, air quality monitoring stations (AQMS) continuously monitor $PM_{2.5}$ levels, adhering to standardised quality assurance and control protocols. However, the data acquired is limited and sparsely distributed across cities [7, 8]. Thus, in recent years, rapid development and deployment of light-scattering low-cost sensors (LCS) for air quality monitoring has been observed [9]. These sensors offer great

© 2025 The Author(s). Published by IOP Publishing Ltd

health and environmental applications with several inherent advantages, including affordability, portability, improved spatial resolution and the ability to identify emission hot spots [10–12]. Various applications of these sensors have been reported, including environmental awareness activities and citizen science campaigns, monitoring both community and industrial emissions, assessment of personal indoor and outdoor exposure and data collection in remote places [13]. However, in comparison to AQMS, LCS exhibit lower levels of accuracy, sensitivity and limits of detection (LOD). Consequently, an evaluation of their dynamic response is essential before considering widespread implementation as a supplementary source of air quality data alongside AQMS [13–16]. LCS, utilising light scattering operating principle, are strongly affected by factors such as particle composition and density, hygroscopicity, refraction index, relative humidity (RH), pollutant concentration level and averaging time [17–20]. Consequently, it is imperative to evaluate these sensors using co-location field assessment methods against reference instruments such as AQMS [7, 18, 20–26] or in controlled laboratory settings [18, 20, 22, 27, 28]. Additionally, various methods, such as linear regression models [15, 29, 30], multiple linear regression [15, 29] and mechanistic models based on hygroscopic growth correction [15, 22, 29] are also employed. More recently, multimodal data fusion methods have been applied, combining ground monitoring data, satellite remote sensing data and also surveillance camera images at local, regional and global scales to enhance the spatiotemporal accuracy of air quality predictions [31, 32]. Accurately calibrated LCS offer real-time measurements at lower costs, enabling broader spatial coverage in densely populated urban areas. Unfortunately, there is still a significant gap in regulatory frameworks, accreditation, certification protocols and harmonised assessment protocols, both in laboratory and field settings, hindering the widespread implementation of these sensors [14]. A recent publication by the United States Environmental Protection Agency (US EPA) has outlined recommended target values for the performance metrics of such sensors, which marks the beginning of efforts to address the challenges of standardisation and comparability of these sensors [33].

The assessment of LCS is therefore essential for ensuring accurate data acquisition, necessary for $PM_{2.5}$ personal exposure in citizen science campaigns. In this study, the performance of the Sensirion SPS30 (LCS SPS30) was assessed under both, controlled laboratory conditions and real-world urban environment. The research was focused on identifying the sensor's limitations under varying environmental conditions, including RH, temperature and $PM_{2.5}$ concentrations. Additionally, the study examined the comparability of LCS measurements with reference instruments and explored the potential applicability of LCS for widespread community deployment in air quality monitoring networks.

2. Methods

LCS SPS30 (CanAirIO Sensirion SPS30), real-time optical particle counter, was evaluated under laboratory-controlled conditions using the reference instrument Grimm 11d and in field settings through a co-location evaluation. The LCS SPS30 continuously measures $PM_{2.5}$ concentrations using the laser scattering technique, with results reported in $\mu g\ m^{-3}$. LCS SPS30 was introduced in 2018 and was initially calibrated by the manufacturer during the laboratory testing. They reported $PM_{2.5}$ measurement range of 0–1000 $\mu g\ m^{-3}$, concentration resolution equal to 1 $\mu g\ m^{-3}$ and particle diameter resolution equal to 0.3 μm. $PM_{2.5}$ mass concentration was calibrated to TSI Dust-TrakTM DRX 8533 Ambient Mode and $PM_{2.5}$ number concentration was calibrated to TSI OPS 3330 [34].

2.1. Laboratory assessment of LCS SPS30

The performance assessment of the LCS SPS30 under laboratory-controlled conditions (figure 1) was carried out using an environmental-pollution chamber (Envilution™) with a capacity of 125 L [35]. The chamber facilitates systematic control of specific environmental parameters, such as particulate matter emissions, RH and temperature (T) over a predetermined time period. The Envilution™ chamber features a nebulizer (utilising 0.5% Potassium Chloride [KCl] as a particulate matter emissions source), a humidifier/dehumidifier system; flow controllers for accurate pollutant emission quantification; a heat pump for T regulation and sensors to monitor the T, RH and pressure. Additionally, the chamber includes an adjustable platform for LCS evaluation, a reference instrument (Grimm 11d) for monitoring PM levels and integrated software for controlling diverse environmental conditions and recording data from reference instruments. Grimm 11d measures PM while accounting for RH. The Grimm 11d (Dust Decoder—portable aerosol spectrometer) operates on the principle of light scattering detection using a diode laser to analyse individual particles. It measures particle sizes ranging from 0.253 to 35.15 μm and dust mass concentrations from 0 $\mu g\ m^{-3}$ to 100 $mg\ m^{-3}$, with a volume flow rate of 1.2 $L\ min^{-1}$. It employs humidity compensation algorithms, heated inlets, or drying systems to reduce RH effects, ensuring accurate readings. Additionally, real-time RH monitoring and post-processing software further corrects the data. Digital Temperature and Humidity Sensor



Figure 1. Laboratory assessment of LCS SPS30.

AM2320 was additionally used to control the atmospheric conditions within the chamber. To avoid unintended reactions during assessment tests, all chamber components are made of, or coated with, polytetrafluoroethylene materials [35]. The LCS SPS30 operates within a T range of −40 to +80 °C and can accommodate RH up to 99%. In contrast, the reference instrument, Grimm 11d, functions optimally between +4 and +40 °C, with RH levels below 95%. To evaluate the comparability between both instruments, scenario's parameters corresponded to the field test under Slovenian temperate continental climate conditions, where three different scenarios were simulated. Scenario 1 maintained T between 6 and 8 °C and RH from 50 to 60%. Scenario 2 encompassed T ranging from 15 to 18 °C with RH levels ranging from 60 to 80%. In Scenario 3, T was between 18 and 22 °C with RH levels of 70 to 80%. The $PM_{2.5}$ concentrations ranged from 0 to 367 μg m^{-3}. To minimise the risk of condensation events and potential overestimation of particle mass concentrations [15, 22, 35–38] deliberate measures were taken to avoid extremely high RH levels and elevated T. No correction factors were applied on laboratory data assessment.

2.2. Air quality monitoring campaign with field co-location assessment of LCS SPS30

The $PM_{2.5}$ air quality monitoring campaign, focusing on the impact of traffic congestions on $PM_{2.5}$ concentrations in urban areas, was conducted in Maribor, Slovenia. Maribor is the second-largest city in Slovenia with 94,370 inhabitants (in 2024). The city has a humid continental climate and lies in close proximity to the Drava River. A citizen-led $PM_{2.5}$ exposure campaign was conducted between 9 and 13 October 2023, where volunteers conducted 72 bicycle trips (n = 38,803 data points) during four specific time intervals to gather $PM_{2.5}$ data: (i) 7:00–8:00, (ii) 12:00, (iii) 15:00 and (iv) 18:00–19:00. The LCS SPS30 sensors were mounted perpendicularly to the cyclists' travelling direction in order to minimise the wind effect and consequently the overestimation of the $PM_{2.5}$ concentrations (figure 2). However, since this approach was not validated, wind-induced biases during sampling might have occurred. The 10.5 km-long cycling route remained constant and was pre-determined utilising the Google Traffic feature on Google Maps. It included areas in Maribor with the highest traffic density and formed a closed loop, comprising diverse road types such as high-speed roads and 30 km h^{-1} speed roads. It passed by key locations like the main city hospital, main square and train station.

The initial co-location field assessment yielded 2,536 data points collected during four pre-determined time intervals (7:00–8:00, 12:00, 15:00, 18:00–19:00), over five consecutive days (9−13 October 2023). The assessment took place at the Slovenian Environment Agency AQMS (Maribor—Titova location; 46.558861, 15.651306) (figure 2). Continuous monitoring of $PM_{2.5}$ and PM_{10} levels at AQMS is performed using HORIBA model APDA-371 (measurement resolution of 0.1 μg m^{-3}; LOD < 4.8 μg m^{-3}; flow rate of 16.7 L min^{-1}), which automatically records hourly concentrations of airborne particulates. The instrument utilises ^{14}C (radioactivity: < 2.22 × 106 Beq, 60 ± 15 μCi, half-life of 5730 years) as a beta source using a photomultiplier tube with an organic plastic scintillator as a detector. Additionally, AQMS measurements include hourly and monthly monitoring of carbon monoxide, ozone, nitrogen dioxide and benzene.

During each cycling trip, a volunteer stopped at the AQMS to collect $PM_{2.5}$. The total co-location durations were 42 min 19 s (9 October), 54 min 28 s (10 October), 55 min 26 s (11 October), 58 min 18 s (12 October) and



Figure 2. Co-location field assessment of LCS SPS30.

37 min 35 s (13 October). The data were averaged by time interval and day, and subsequently compared with AQMS hourly data. AQMS reported valid $PM_{2.5}$ values on 9 October (15:00, 18:00–19:00), 10 October (15:00, 18:00–19:00), 11 October (7:00–8:00, 12:00, 15:00, 18:00–19:00), 13 October (12:00, 15:00, 18:00–19:00), yielding 1,543 usable data points.

2.3. Air quality monitoring campaign with field co-location assessment of LCS SPS30

LCS exhibit high sensitivity to RH levels, with numerous studies reporting that RH > 85% often results in LCS overestimation of $PM_{2.5}$ concentration. This overestimation occurs due to enhanced aerosol hygroscopic growth from water vapour condensation on atmospheric particles [15, 22, 35–38]. Consequently, many studies recommend incorporating the RH into calibration equation [22, 39, 40]. Therefore, a following RH dependent correction was applied on field data, including co-location assessment:

$$C = 1 + \frac{\overline{1.65}}{-1 + \frac{1}{a_w}} \tag{1}$$

$$PM_{Corrected} = \frac{PM_{raw} \times \delta}{C} \tag{2}$$

The κ value was applied based on Köhler theory [41], where it represents the degree of particle hygroscopicity depending on particle composition. For simplification, 1.65 g cm^{-3} was used as a bulk dry particle density [22]. Previous studies observed that the dry particle mass of $PM_{2.5}$ ranged from 0.38 to 0.44 [22], with an expected range for Europe of 0.36 ± 0.16 [42], therefore, an average value of 0.41 was used as the κ constant. Water activity (a_w) was defined as RH/100, using an average relative humidity (74%) during the monitoring campaign. δ is defined as a percentage discrepancy between LCS and AQMS, and was equal to 0.37. Temperature fluctuations have negligible to no impact on LCS PM sensors [36]. The LCS SPS30 is set to record data at 5-s intervals, whereas Grimm 11d operates at 1 min intervals. Therefore, for analysis purposes, the laboratory assessment data were averaged based on 1 and 5 min averaging times, while field co-location assessment data on hourly averages. Data were statistically evaluated by analysis of variance (ANOVA), using TIBCO Statistica software [43]. Furthermore, the spatial distribution of $PM_{2.5}$ concentration was examined using QGIS software [44].

Table 1. Average (mean ± standard error) values of selected parameters within during laboratory assessment of LCS.

	LCS SPS30	Grimm 11d
$PM_{2.5}$ [μg m^{-3}]		
Avg.	21.5 ± 2.1	32 ± 4.8
R^2	0.83	
Slope	Grimm 11d = −8.8 + 1.9 * LCS SPS30	
RH [%]		
Avg.	61.2 ± 1.0	67.5 ± 0.8
R^2	0.92	
Slope	Grimm 11d = 17.4 + 0.8 * LCS SPS30	
T [°C]		
Avg.	12.1 ± 0.4	15.7 ± 0.5
R^2	0.98	
Slope	Grimm 11d = 2.7 + 1.1 * LCS SPS30	

3. Results and discussion

LCSs are being increasingly employed in environmental pollution campaigns to evaluate air quality in urban areas. However, they are highly susceptible to systematic biases, time-dependent drifts and aging. Therefore, it is crucial to assess them prior to the widespread use [13–16]. The AQD [1] established data quality objectives, specifying that measurement uncertainty, including coefficient of determination (R^2) and the regression slope, should primarily be used to evaluate the air quality data from monitoring methods. Nevertheless, these metrics are rarely incorporated in citizen science initiatives utilising LCSs [20]. Co-location field assessment is often used to evaluate performance of LCSs [7, 18, 20–22, 24–26], however, due to meteorological and environmental variations across the reported studies, direct comparison of LCS to reference instruments is challenging. Consequently, it is advisable to perform laboratory evaluation, which provides higher levels of reproducibility [13]. Laboratory comparability assessment ensures standardised and controlled testing conditions, enabling the simulation of environmental conditions relevant to specific environment, such as the Slovenian climate. Additionally, such assessment allows for the evaluation of unit-to-unit variability and the independent verification of the manufacturer's calibration results. Additionally, statistical indicators such as the root mean square error (RMSE), standard deviation (SD) and the intercept of the linear regression between LCS and AQMS data are commonly used. While RMSE and R^2 are considered as the most explicative measures [13, 20], factors such as averaging time and the choice of the reference instrument can also significantly affect the evaluation [19]. The US EPA publication 'Performance Testing Protocols, Metrics and Target values for Fine Particulate Matter Air Sensors' recommends specific target values for assessing the suitability of LCSs for micro-environmental air pollution monitoring campaigns. According to the publication, R^2 should remain above 0.7 and the RMSE below 7 μg m^{-3} for LCSs to be considered eligible for air pollution monitoring campaigns [33].

3.1. Laboratory assessment results and comparative analysis of LCS SPS30 and reference instrument Grimm 11d

The performance of the LCS SPS30 was evaluated simultaneously with two different LCS SPS30 under different environmental conditions in relation to reference instrument Grimm 11d, corresponding to the Slovenian moderate continental climate (Tables S1–S3). The Pearson's correlation coefficients between two sensors varied 0.995–0.998. The same sensors were used in all laboratory-based scenarios. The average accuracy error was 9%, 21% and 33% for Scenario 1 Scenario 2 and Scenario 3, respectively, with R^2 values varying from 0.81–0.99. Scenario 1, with RH below 60%, was the only environmental condition in which the LCS SPS30 met the criteria for micro-environmental monitoring.

The average values presented in table 1 were used to facilitate the comparison between LCS SPS 30 and reference instrument Grimm 11d, allowing for the assessment of discrepancies across individual parameters (PM concentration, RH and T). Averaging minimises the influence of random short-term variability, thereby improving the correlation metrics. However, primarily suited for illustrating long-term trends, which are particularly relevant for personal exposure evaluation of individuals in urban environments. The average accuracy was 20.9% for $PM_{2.5}$ measurements, 8.9% for RH and 28.6% for T, with accuracy declining as RH increased.

In addition, the absolute difference between LCS SPS30 and Grimm 11d was 8% for $PM_{2.5}$ concentrations up to 50 μg m^{-3}, 32% for concentrations between 50 in 100 μg m^{-3} and 142% for very high concentrations

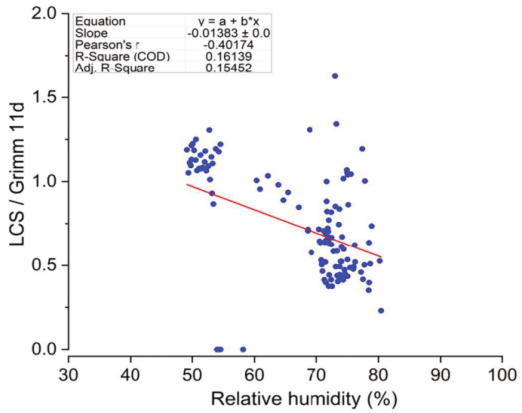


Figure 3. Susceptibility of laboratory-assessed $PM_{2.5}$ concentrations (LCS/AQMS) relative to RH variations.

above 100 μg m^{-3}. These results suggest that LCS SPS3 is not recommended for precise quantification in highly polluted environments, likely due to photodetector oversaturation causing a non-linear response. However, the sensor can still serve as a useful indicator of hazardous conditions, providing practical value for protecting exposed populations.

LCS SPS30 demonstrated an enhanced performance at longer averaging times, as evidenced by progressively higher R^2 values and lower RMSE at a 5 min averaging time compared to 1 min averaging times in all selected scenarios. Similar observations were found in the study, where both instrument and sampling uncertainty with respect to the reference method decreased with increased averaging time [45]. Longer averaging intervals (e.g., 1 h, 8 h, and 24 h) are primarily used for comparisons of LCS data to air quality standard criteria; however, shorter timeframes of 1 min can be indicative for short-term emission spikes related to specific local air pollution events [13].

3.2. Field co-location assessment results and comparative analysis of LCS SPS30 and reference instrument HORIBA model APDA-371

In total, 1543 data points within pre-determined timeframes during 5 consecutive days (9—13 October 2023) were used to assess the co-location field evaluation correspondence between LCS SPS30 and Slovenian Environment Agency AQMS Maribor—Titova HORIBA model APDA-371 (Table S4). The same sensors used in the laboratory assessment were also employed in the field co-location tests. The co-location assessment was carried out in stable atmospheric conditions without rain and at low wind speeds (<5 km h^{-1}), at the fixed placement and negligible external influences. During each cycling lap, cyclists stopped at the AQMS to perform co-location assessment. As Slovenian Environment Agency only reports hourly $PM_{2.5}$ values, LCS SPS30 values were averaged for comparison. Due to AQMS missing data for specific time intervals, some co-located LCS data were excluded from further analysis. Ratio between LCS SPS30 and AQMS varied between 0.4 and 0.8, with an average 0.6.

3.3. RH influence on $PM_{2.5}$ concentrations

The sensitivity of both laboratory- and field-based assessment protocols for $PM_{2.5}$ assessment depends on RH variations. In the controlled laboratory environment, $PM_{2.5}$ concentrations exhibited downward trend relative to RH (figure 3), indicating an underestimation of particle concentrations.

In contrast, field measurements revealed an overestimation of $PM_{2.5}$ concentrations, attributed to enhanced aerosol hygroscopic growth caused by water vapour condensation on particles. The correlation between non-corrected LCS SPS30 values and the reference instrument was 0.70, which slightly improved to 0.71 following RH corrections (equations (1), (2)). Field co-located $PM_{2.5}$ concentrations relative to RH variations exhibited an upward trend (figure 4). The ratio between AQMS and LCS $PM_{2.5}$ data was 0.56 and 0.7 for corrected and not-corrected data. Applying the RH-correction (equations (1), (2)) on the field data resulted in average deviation of 24%. Across the entire sampling period, the mean $PM_{2.5}$ concentration was 9.6 μg m^{-3}

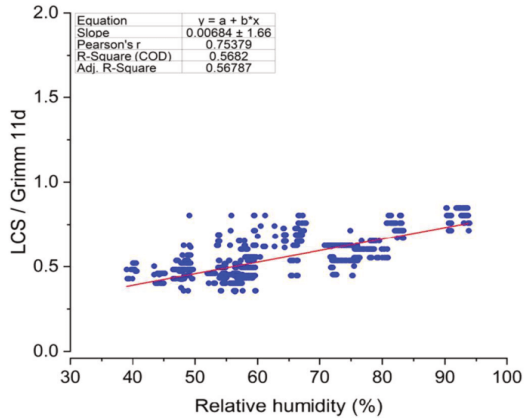


Figure 4. Susceptibility of co-located $PM_{2.5}$ concentrations (LCS/AQMS) relative to RH variations.

(range: 2−126 μg m^{-3}) for the non-corrected data and 7.7 μg m^{-3} (range 1.6−101 μg m^{-3}) for the RH-corrected data.

The discrepancy between laboratory and field co-location assessment can be explained by the differences in particle composition and environmental conditions. In the laboratory environment, solid or partially hydrated KCl particles were used, while ambient particles consist of complex mixture of volatile and hygroscopic particles whose number and composition vary more substantially. These particles absorb water and grow in size under elevated RH, leading to increased light scattering and higher $PM_{2.5}$ concentrations. In the controlled setting, particle growth is more constrained and the refractive index of the KCl particles decreases, reducing the scattering efficiency per unit mass.

3.4. Comparability of laboratory and field assessment results and micro-environmental monitoring metrics

Laboratory comparability yielded moderate to strong correlation ($0.81 < R^2 < 0.99$) between the LCS SPS30 and the Grimm 11, which was also observed by Agrawal [46], who reported R^2 values equal to 0.9. It was observed that when RH increased, it resulted in decrease of R^2. RMSE values varied between 0.81 and 61.72 μg m^{-3}, with an average RMSE of 39 μg m^{-3} at an average $PM_{2.5}$ concentration of 21.5 μg m^{-3} (LCS SPS30). The highest accuracy (8.6%), R^2 value (0.99) and lowest RMSE (0.81 μg m^{-3}) were observed under environmental conditions with a T range of 6 °C−8 °C and RH between 50% and 60%. Similar observations were also reported by [28], who reported that LCS SPS30 did not adhere to the manufacturer's specified detection ranges. They observed very low cross-unit variability, approximately 1.3% for $PM_{2.5}$, and a reported R^2 value of 0.83 [28].

In comparison, the field co-location assessment results yielded R^2 value equal to 0.50, while the RMSE was 6.82 μg m^{-3}, at an average $PM_{2.5}$ concentration 9 μg m^{-3}. Vogt *et al* [26] reported R^2 and RMSE values equal to 0.72 and 0.1–4.17 μg m^{-3}, respectively. Results obtained in this study are lower in comparison to previously reported, where RMSE was equal to 6.7 μg m^{-3} and 3.8 μg m^{-3} for non-corrected and corrected $PM_{2.5}$ values, respectively [47]. Additionally, R^2 is below the average R^2 value of 0.8 reported in various LCS performance evaluation studies [20].

The recommended error threshold for accuracy in micro-environmental monitoring is 25%, as proposed by Schauer [48], and this criteria was met under both laboratory and field conditions. However, additional comparability analyses of identical sensors, based on other micro-environmental monitoring criteria defined by US EPA (R^2, RMSE) [33], indicated that the LCS SPS30 did not meet the performance thresholds, except under conditions where relative humidity (RH) was below 60%. Generally, the co-location field assessment yielded lower R^2 and RMSE in comparison to laboratory test.

Additionally, data was subset into the low concentration range of $PM_{2.5}$ from 0−29.8 μg m^{-3}, which was the maximum value observed during co-location assessment. Across all laboratory and field scenarios, low correlation values ($R^2 < 0.04$) were observed. The highest comparability was found between laboratory and

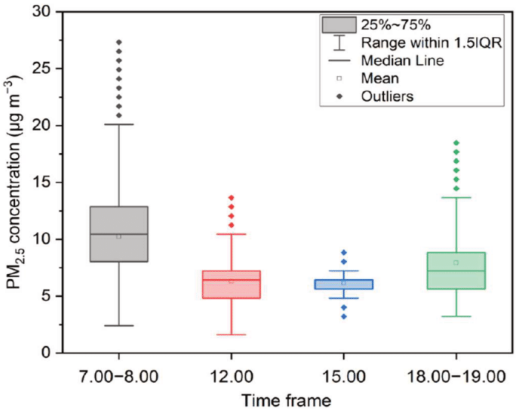


Figure 5. Temporal pattern of $PM_{2.5}$ concentrations across time intervals in Maribor, Slovenia.

Table 2. Performance overview and optimal operating conditions of the LCS SPS30.

LCS SPS30 performance overview:			
	Laboratory settings	Co-location settings	Performance criteria
Accuracy [%]	9–33	37	< 25
R^2	0.81–0.99	0.5	> 0.7
RMSE [µg m^{-3}]	0.81–61.72	6.82	$\leqslant 7$
LCS SPS30 optimal conditions:			
T [°C]	6–8		
RH [%]	50–60		
$PM_{2.5}$ [µg m^{-3}]	<50		

field values, observed under environmental conditions with T ranging from 18 to 22 °C and RH between 70% and 80%, where conditions were most similar.

Based on the laboratory and field co-location assessments, we conclude that the LCS SPS30 provides the most reliable $PM_{2.5}$ measurement under conditions of RH $< 60\%$ and in low-pollution environments ($PM_{2.5} < 50$ µg m^{-3}] [table 2].

3.5. Citizen-led $PM_{2.5}$ monitoring campaign

During a one-week $PM_{2.5}$ monitoring campaign, a total of 72 bicycle trips were conducted in Maribor, Slovenia, resulting in 38,803 data points. After eliminating co-location data and errors, 35,642 remained (92%). All data were corrected following equations (1) and (2), using RH dependent correction. The comparative ANOVA indicated statistically significant differences at the 95% probability level between time intervals. The lowest average $PM_{2.5}$ concentrations were recorded at around 15:00 (2.9 µg m^{-3}), while the highest were observed during the morning rush hour between 7:00 and 8:00 (4.8 µg m^{-3}) (figure 5). A similar pattern was observed in Ljubljana, Slovenia, during a citizen science campaign that utilised LCS SPS30 sensors from September to December 2022 [24]. This trend can be attributed to the presence of the planetary boundary layer (PBL). The PBL, besides other factors such as meteorology, topography, demography, transportation, fuel quality, energy usage, and levels of industrialisation and urbanisation, plays an essential role in daily fluctuations of $PM_{2.5}$ concentrations. The PBL hinders the vertical mixing of air masses, limiting the dilution and dispersion of pollutants. Consequently, PBL thickness at lower T and higher RH, trapping pollutants in close proximity to the surface [49, 50]. The primary local source of $PM_{2.5}$ in Slovenia are the individual wood-burning fireplaces (74%) and traffic emissions (5%) [51].

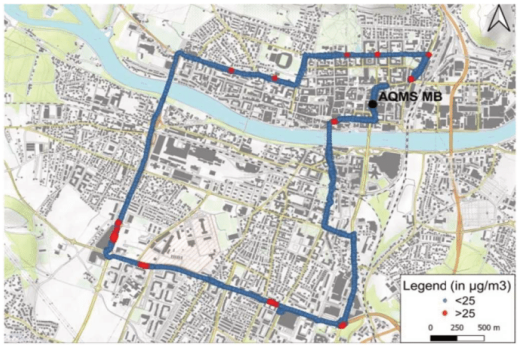


Figure 6. Spatial distribution of $PM_{2.5}$ in Maribor, Slovenia.

Furthermore, the urban layout and proximity to pollution sources can significantly influence air pollution levels, as revealed through the spatial analysis of $PM_{2.5}$. Air pollution hot spots, represented by darker red colour (figure 6), were predominantly concentrated around major intersections near highway entry points, shopping malls and bus station. These areas experience heavier traffic and prolonged vehicle idling, particularly during peak commute hours. Cyclists face higher risks of exposure at congested intersections, underpasses, and roundabouts relative to well-ventilated open bike lanes and street intersections [8, 52, 53].

The corrected $PM_{2.5}$ values were subsequently compared to the threshold value (25 µg m^{-3}) outlined in the AQD [1] which serves as a regulatory framework for managing ambient air quality across Europe Union. AQD only sets annual threshold targets, therefore lacks effective criteria for evaluating short-term $PM_{2.5}$ pollution. Analysis of the $PM_{2.5}$ data collected by LCS SPS30 revealed that the threshold value was surpassed in 0.15% of all cases. In a similar study conducted in Ljubljana, Slovenia [24], 21.2% of all data surpassed this limit, indicating on a better air quality status in Maribor.

4. Conclusions

LCSs offer valuable insights into commuter's personal air pollution exposure but are sensitive to humidity, affecting $PM_{2.5}$ accuracy. Without standardised calibration methods, data comparison across different LCSs and monitoring campaigns is difficult. This study assessed the performance of the Sensirion SPS30 under controlled laboratory and real-world urban conditions to evaluate its potential for widespread community deployment.

The results showed that the sensor met micro-environmental monitoring standards and US EPA performance criteria (R^2, RMSE) only at RH levels below 60% and in low-pollution environments. A strong humidity dependence was observed in both laboratory and field conditions, with the LCS SPS30 exhibiting underestimation or overestimation of $PM_{2.5}$ readings, respectively. These discrepancies are mainly attributed to differences in particle composition and concentration. In ambient air, more hygroscopic and volatile particles absorb water and grow at higher RH levels, increasing light scattering and $PM_{2.5}$ reading. In contrast, controlled settings limit particle growth and reduce refracting index lowering scattering efficiency per unit mass.

Despite inconsistencies in sensor accuracy, LCSs can effectively capture spatiotemporal variations in urban air quality and identify pollution hotspots in community-based monitoring campaign. However, RH dependent correction remains essential for reliable interpretation of $PM_{2.5}$ measurements. In this study, LCS SPS30 were deployed by citizens during an air quality campaign in Maribor, Slovenia. Results indicated that $PM_{2.5}$ hotspots were clustered near intersections, where vehicle waiting times were longest. Elevated $PM_{2.5}$ concentrations were observed during the morning rush hour, corresponding to peak traffic density and the lowest levels of planetary boundary layer, limiting effective pollutant dispersion.

LCS SP30 sensors can serve as valuable supplementary tools for increasing public awareness or air pollution challenges; however their absolute $PM_{2.5}$ measurements should be interpreted with caution. Future work should focus on evaluating the long-term stability of these sensors under both laboratory and field conditions, assessing their performance in highly polluted environments and developing standardised assessment

protocols. Such efforts will improve cross-study comparability and support the use of LCSs as reliable and cost-effective tool exposure assessment.

Acknowledgments

Anja Ilenič acknowledges Jožef Stefan International Postgraduate School as the institution where her PhD studies are carried out. The authors would like to thank Ana Paula Mendes Emygdio (PhD) from the Global Centre for Clean Air Research (GCARE) at the University of Surrey (United Kingdom) for assistance with the laboratory-based calibration experiments, and to Maribor Cycling Association (Slovenia), including all the volunteers involved in the $PM_{2.5}$ measurements for their contributions to this study. The authors acknowledge the financial support from the Slovenian Research Agency (developmental funding pillar, DFP (SI: 'razvojni steber financiranja, RSF') and financial support programme groups P2-0273 and P1-0143. Prashant Kumar acknowledges the support received through the EPSRC funded COTRACE project (EP/W001411/1) which is now running as a SAMHE programme.

Data availability statement

All data that support the findings of this study are included within the article (and any supplementary files).

References

[1] Directive 2008/50/EC 2008 Directive 2008/50/EC of the European Parliament and of the Council of 21 May 2008 on Ambient Air Quality and Cleaner Air for Europe
[2] EEA 2022 European Environmental Agency (EEA) 2022 'Europe's air quality status 2022: Briefing no. 04/2022. [Internet]. European Environmental Agency; 2022. Available from: https://eea.europa.eu/publications/status-of-air-quality-in-Europe-2022
[3] Chen H, Goldberg M S and Villeneuve P J 2008 A systematic review of the relation between long-term exposure to ambient air pollution and chronic diseases *Rev. Environ. Health* **23** 243–97
[4] Cohen A J *et al* 2017 Estimates and 25-year trends of the global burden of disease attributable to ambient air pollution: an analysis of data from the Global Burden of Diseases Study 2015 *Lancet* **389** 1907–18
[5] Dominici F *et al* 2006 Fine particulate air pollution and hospital admission for cardiovascular and respiratory diseases *JAMA* **295** 1127–34
[6] Russell A G and Brunekreef B A 2009 Focus on particulate matter and health *Environ. Sci. Technol.* **43** 4620–5
[7] Kousis I, Manni M and Pisello A L 2022 Environmental mobile monitoring of urban microclimates: a review *Renew. Sustain. Energy Rev.* **169** 112847
[8] Samad A and Vogt U 2020 Investigation of urban air quality by performing mobile measurements using a bicycle (MOBAIR) *Urban Climate* **33** 100650
[9] Morawska L *et al* 2018 Applications of low-cost sensing technologies for air quality monitoring and exposure assessment: how far have they gone? *Environ. Int.* **116** 286–99
[10] Chong C Y and Kumar S P 2003 Sensor networks: evolution, opportunities, and challenges *Proc. of the IEEE*
[11] Leavey A *et al* 2015 Air quality metrics and wireless technology to maximize the energy efficiency of HVAC in a working auditorium *Build. Environ.* **85** 287–97
[12] Rai A C *et al* 2017 End-user perspective of low-cost sensors for outdoor air pollution monitoring *Sci. Total Environ.* **607–608** 691–705
[13] Williams R *et al* 2019 Deliberating performance targets workshop: potential paths for emerging PM2.5 and O3 air sensor progress *Atmospheric Environment: X* **2** 100031
[14] Austin E, Novosselov I, Seto E and Yost M G 2015 Laboratory evaluation of the Shinyei PPD42NS low-cost particulate matter sensor *PLoS One* **10** e0137789
[15] Malings C *et al* 2020 Fine particle mass monitoring with low-cost sensors: corrections and long-term performance evaluation *Aerosol Sci. Technol.* **54** 160–74
[16] Zimmerman N 2022 Tutorial: guidelines for implementing low-cost sensor networks for aerosol monitoring *J. Aerosol Sci.* **159** 105872
[17] Aleixandre M and Gerboles M 2012 Review of small commercial sensors for indicative monitoring of ambient gas *Chemical Engineering Transactions* **30** 169–74
[18] Castell N *et al* 2017 Can commercial low-cost sensor platforms contribute to air quality monitoring and exposure estimates? *Environ. Int.* **99** 293–302
[19] Giordano M R *et al* 2021 From low-cost sensors to high-quality data: a summary of challenges and best practices for effectively calibrating low-cost particulate matter mass sensors *J. Aerosol Sci.* **158** 105833
[20] Karagulian F *et al* 2019 Review of the performance of low-cost sensors for air quality monitoring *Atmosphere* **9** 506
[21] Bergmann M L *et al* 2022 Ultrafine particle exposure for bicycle commutes in rush and non-rush hour traffic: a repeated measures study in Copenhagen, Denmark *Environ. Pollut.* **294** 118631
[22] Crilley L R *et al* 2018 Evaluation of a low-cost optical particle counter (Alphasense OPC-N2) for ambient air monitoring *Atmos. Meas. Tech.* **11** 709–20
[23] deSouza P *et al* 2023 Evaluating the performance of low-cost PM2.5 sensors in mobile settings *Environ. Sci. Technol.* **57** 15401–11
[24] Ilenič A, Pranjić A M, Zupančič N, Milačič R and Ščančar J 2024 Fine particulate matter (PM2.5) exposure assessment among active daily commuters to induce behaviour change to reduce air pollution *Sci. Total Environ.* **912** 169117
[25] Kumar P *et al* 2015 The rise of low-cost sensing for managing air pollution in cities *Environ. Int.* **75** 199–205
[26] Vogt M, Schneider P, Castell N and Hamer P 2021 Assessment of low-cost particulate matter sensor systems against optical and gravimetric methods in a field Co-Location in Norway *Atmosphere* **12** 961
[27] Kelly K E *et al* 2017 Ambient and laboratory evaluation of a low-cost particulate matter sensor *Environ. Pollut.* **221** 491–500

[28] Kuula J *et al* 2020 Laboratory evaluation of particle-size selectivity of optical low-cost particulate matter sensors *Atmos. Meas. Tech.* **13** 2413–23
[29] Barkjohn K K, Gantt B and Clements A L 2021 Development and application of a United States-wide correction for $PM_{2.5}$ data collected with the PurpleAir sensor *Atmos. Meas. Tech.* **14** 4617–37
[30] Kosmopoulos G, Salamalikis V, Pandis S N, Yannopoulos P, Bloutsos A A and Kazantzidis A 2020 Low-cost sensors for measuring airborne particulate matter: field evaluation and calibration at a South-Eastern European site *Sci. Total Environ.* **748** 141396
[31] Malings C, Knowland E, Pavlovic N, Coughlin J G, King D, Keller C, Cohn S and Martin R V 2024 Air quality estimation and forecasting via data fusion with uncertainty quantification: theoretical framework and preliminary results *JGR Machine Learning and Computation* **1** 1–23
[32] Choi B and Hummel M A 2025 Spatiotemporal air quality prediction using stochastic advection–diffusion model for multimodal data fusion *Environ. Res. Lett.* **20** 014065
[33] Duvall R *et al* 2021 *Performance Testing Protocols, Metrics, and Target Values for Fine Particulate Matter Air Sensors: Use in Ambient, Outdoor, Fixed Site, Non-Regulatory Supplemental and Informational Monitoring Applications [Internet]* (U.S. EPA Office of Research and Development) Available from: https://cfpub.epa.gov/si/si_public_record_Report.cfm?dirEntryId=350785&Lab=CEMM
[34] Alfano B *et al* 2020 A review of low-cost particulate matter sensors from the developers' perspectives *Sensors* **23** 6819
[35] Omidvarborna H, Kumar P and Tiwari A 2020 'Envilution^{TM}' chamber for performance evaluation of low-cost sensors *Atmos. Environ.* **223** 117264
[36] Liu H Y, Schneider P, Haugen R and Vogt M 2019 Performance assessment of a low-cost PM2.5 sensor for a near four-month period in Oslo, Norway *Atmosphere* **2** 41
[37] Sohn J H, Atzeni M, Zeller L and Pioggia G 2008 Characterisation of humidity dependence of a metal oxide semiconductor sensor array using partial least squares *Sensors Actuators B* **131** 230–5
[38] Wang Y, Li J, Jing H, Zhang Q, Jiang J and Biswas P 2015 Laboratory evaluation and calibration of three low-cost particle sensors for particulate matter measurement *Aerosol Sci. Technol.* **49** 1063–77
[39] Badura M, Batog P, Drzeniecka-Osiadacz A and Modzel P 2019 Regression methods in the calibration of low-cost sensors for ambient particulate matter measurements *SN Appl Sci* **1** 622
[40] Hua J *et al* 2021 Improved PM2.5 concentration estimates from low-cost sensors using calibration models categorized by relative humidity *Aerosol Sci. Technol.* **55** 600–13
[41] Petters M D and Kreidenweis S M 2007 A single parameter representation of hygroscopic growth and cloud condensation nucleus activity *Atmos. Chem. Phys.* **7** 1961–71
[42] Pringle K J, Tost H, Pozzer A, Pöschl U and Lelieveld J 2010 Global distribution of the effective aerosol hygroscopicity parameter for CCN activation *Atmos. Chem. Phys.* **10** 5241–55
[43] TIBCO 2017 Statistica TIBCO Software Inc.
[44] QGIS (2024) *QGIS Geographic Information System* http://qgis.orgQGIS Geographic Information System
[45] Rose Eilenberg S, Subramanian R, Malings C, Hauryliuk A, Presto A A and Robinson A L 2020 Using a network of lower-cost monitors to identify the influence of modifiable factors driving spatial patterns in fine particulate matter concentrations in an urban environment *J. Expo. Sci. Environ. Epidemio.* **6** 949–61
[46] Agrawal D, Saini A K, Rai A C and Kala P 2024 In chamber calibration and performance evaluation of air quality low-cost sensors *Atmospheric Pollution Research* **15** 102299
[47] Bulot F M J *et al* 2023 Characterisation and calibration of low-cost PM sensors at high temporal resolution to reference-grade performance *Heliyon* **9** e15943
[48] Schauer J 2018 Deployment of low-cost PM sensors: aligning sensor performance and data quality needs *Deliberating Performance Targets for Air Quality Sensors Workshop (Research Triangle Park, NC, June 25-27, 2018)* Available from: https://epa.gov/sites/production/files/2018-08/documents/session_04_c_schauer.pdf
[49] Miao Y *et al* 2019 Interaction between planetary boundary layer and PM2.5 pollution in megacities in China: a review *Curr. Pollution. Rep.* **5** 261–71
[50] Pan L, Xu J, Tie X, Mao X, Gao W and Chang L 2019 Long-term measurements of planetary boundary layer height and interactions with PM2.5 in Shanghai, China *Atmospheric Pollution Research* **10** 989–96
[51] Slovenian Environment Agency (ARSO) 2021 *Air Quality in Slovenia in 2021* https://arso.gov.si/zrak/kakovostzraka/poročila in publikacije/Letno_porocilo_2021_Final.pdf
[52] Hofman J, Samson R, Joosen S, Blust R and Lenaerts S 2018 Cyclist exposure to black carbon, ultrafine particles and heavy metals: an experimental study along two commuting routes near Antwerp, Belgium *Environ. Res.* **164** 530–8
[53] Qiu Z, Wang W, Zheng J and Lv H 2019 Exposure assessment of cyclists to UFP and PM on urban routes in Xi'an, China *Environ. Pollut.* **250** 241–50

Supplementary Information Article 3

Table S1: Raw data laboratory assessment under Scenario 1

Scenario 1	$PM_{2.5}$ (µg m^{-3})			RH (%)			T (°C)		
	Grimm1 1d	SPS30 −1	SPS30 −2	Grimm1 1d	SPS30 −1	SPS30 −2	Grimm1 1d	SPS30 −1	SPS30 −2
09/08/2023 12:07:27	0.2	0.0	0.0	58.2	38.9	40.9	7.3	6.8	10.2
09/08/2023 12:08:27	0.2	0.0	0.0	54.5	37.6	40.1	7.3	6.2	9.5
09/08/2023 12:09:27	0.2	0.0	0.0	54.3	38.4	41.2	7.3	5.6	8.9
09/08/2023 12:10:27	0.2	0.0	0.0	54.5	39.5	42.3	7.2	5.1	8.4
09/08/2023 12:11:27	0.2	0.0	0.0	54.5	40.3	43.2	7.2	4.6	7.8
09/08/2023 12:12:27	0.1	0.0	0.0	54.2	40.9	43.8	7.1	4.2	7.5
09/08/2023 12:13:27	0.1	0.0	0.0	54.0	41.4	44.4	7.1	3.9	7.0
09/08/2023 12:14:27	0.7	3.4	3.2	53.7	41.9	44.9	7.1	3.6	6.7
09/08/2023 12:15:27	17.6	15.2	15.3	53.4	42.2	45.3	7.0	3.3	6.5
09/08/2023 12:16:27	22.9	21.3	21.3	53.2	42.5	45.6	6.9	3.1	6.2
09/08/2023 12:17:27	21.7	21.0	22.9	52.9	42.7	45.9	6.9	2.8	5.9
09/08/2023 12:18:27	18.7	19.3	21.6	52.6	42.9	46.1	6.8	2.6	5.8
09/08/2023 12:19:27	17.3	17.0	19.8	52.3	43.0	46.3	6.8	2.4	5.5
09/08/2023 12:20:27	15.0	15.4	18.1	52.0	43.0	46.3	6.8	2.3	5.3
09/08/2023 12:21:27	13.3	13.6	15.3	51.7	43.0	46.4	6.7	2.1	5.2
09/08/2023 12:22:27	12.2	12.5	13.8	51.4	43.0	46.4	6.7	2.0	5.0
09/08/2023 12:23:27	10.9	10.9	12.6	51.1	43.0	46.5	6.6	1.9	4.9
09/08/2023 12:24:27	9.7	9.9	10.8	50.8	42.9	46.4	6.6	1.8	4.8
09/08/2023 12:25:27	9.2	9.8	11.0	50.6	42.8	46.4	6.6	1.6	4.7
09/08/2023 12:26:27	9.0	10.6	10.8	50.3	42.7	46.4	6.5	1.5	4.5
09/08/2023 12:27:27	8.2	8.9	11.2	50.1	42.7	46.3	6.4	1.4	4.4
09/08/2023 12:28:27	7.7	8.2	9.3	49.9	42.7	46.4	6.4	1.3	4.4
09/08/2023 12:29:27	6.9	7.9	7.4	49.6	42.8	46.4	6.5	1.3	4.3

09/08/2023 12:30:27	6.1	6.3	8.3	49.1	42.8	46.5	6.6	1.3	4.3
09/08/2023 12:32:27	5.1	5.2	6.0	49.8	43.3	47.2	6.7	1.2	4.2
09/08/2023 12:33:27	4.8	5.0	6.0	53.1	45.9	49.9	6.7	1.2	4.2
09/08/2023 12:34:27	4.3	4.7	5.8	54.5	47.5	51.1	6.6	1.2	4.2
09/08/2023 12:35:27	4.0	4.3	5.2	54.3	47.3	50.8	6.6	1.2	4.1
09/08/2023 12:36:27	3.7	4.0	4.8	53.8	46.8	50.4	6.5	1.1	4.1
09/08/2023 12:37:27	3.5	3.8	4.0	53.3	46.4	50.0	6.5	1.1	4.1
09/08/2023 12:38:27	3.0	4.0	3.8	52.7	46.0	49.7	6.5	1.0	4.1
09/08/2023 12:39:27	3.0	4.0	3.1	52.1	45.7	49.4	6.5	1.0	4.0
09/08/2023 12:40:27	2.7	3.3	3.0	51.3	45.4	49.1	6.6	1.0	4.1
09/08/2023 12:41:27	2.5	3.3	2.9	50.6	45.0	48.7	6.6	1.0	4.0
09/08/2023 12:42:27	2.3	2.6	3.0	49.9	44.6	48.3	6.7	1.1	4.0
09/08/2023 12:43:27	2.1	2.2	2.3	49.4	44.1	47.9	6.8	1.1	4.0

$PM_{2.5}$ = particulate matter smaller than 2.5 µm in µg m^{-3}
RH = relative humidity in %
T = temperature in °C

Table S2: Raw data laboratory assessment under Scenario 2

Scenario 2	$PM_{2.5}$ (µg m^{-3})			RH (%)			T (°C)		
	Grimm1 1d	SPS30 −1	SPS30 −2	Grimm1 1d	SPS30 −1	SPS30 −2	Grimm1 1d	SPS30 −1	SPS30 −2
09/08/2023 14:23:27	5.8	8.8	6.4	68.9	64.0	61.7	16.1	14.2	14.2
09/08/2023 14:24:27	26.9	16.4	14.6	69.2	64.8	62.2	16.0	14.2	14.2
09/08/2023 14:25:27	34.5	29.3	20.0	68.6	64.6	62.2	16.2	14.2	14.3
09/08/2023 14:26:27	41.0	29.1	23.8	70.6	64.9	62.3	16.3	14.2	14.4
09/08/2023 14:27:27	41.8	28.6	24.7	71.4	65.8	62.8	16.5	14.4	14.5
09/08/2023 14:28:27	38.8	25.8	24.6	71.5	66.3	63.1	16.5	14.5	14.7
09/08/2023 14:29:27	32.7	22.8	23.2	71.9	66.9	63.6	16.6	14.6	14.8
09/08/2023 14:30:27	25.0	17.3	18.6	70.5	67.8	64.4	17.1	14.8	15.0
09/08/2023 14:31:27	15.6	13.6	14.2	64.6	67.6	63.6	18.2	15.1	15.5
09/08/2023 14:32:27	13.7	13.4	12.8	60.9	65.3	61.0	18.9	15.5	15.8
09/08/2023 14:40:27	6.0	6.3	5.8	60.3	56.7	55.1	17.6	15.6	15.4
09/08/2023 14:41:27	5.4	5.7	5.5	62.1	57.7	56.3	17.3	15.5	15.2
09/08/2023 14:42:27	5.1	5.0	5.0	63.8	58.7	57.5	17.0	15.3	15.0
09/08/2023 14:43:27	5.3	4.9	5.0	65.4	59.8	58.6	16.7	15.1	14.8
09/08/2023 14:44:27	5.9	5.0	5.0	67.1	61.0	60.0	16.5	14.9	14.5
09/08/2023 14:45:27	6.6	5.3	4.1	68.6	62.1	61.3	16.2	14.7	14.3
09/08/2023 14:46:27	11.8	26.9	25.3	70.3	63.4	62.8	16.0	14.4	14.0
09/08/2023 14:47:27	93.6	69.6	62.7	71.2	64.5	64.1	15.7	14.3	13.8
09/08/2023 14:48:27	100.9	72.8	66.3	71.6	64.8	64.6	15.5	14.0	13.6
09/08/2023 14:49:27	86.6	65.6	59.5	71.9	65.1	65.1	15.3	13.8	13.3
09/08/2023 14:50:27	76.9	61.2	57.3	72.0	65.2	65.4	15.1	13.5	13.1
09/08/2023 14:55:27	21.3	22.4	20.3	77.9	83.8	85.5	17.1	13.6	13.6
09/08/2023 14:56:27	18.6	20.1	18.8	75.6	83.3	84.2	17.7	14.0	14.1
09/08/2023	17.0	18.3	17.5	75.0	82.2	83.0	17.9	14.3	14.4

14:57:27									
09/08/2023 14:58:27	15.9	16.8	16.3	75.1	80.8	81.7	17.9	14.5	14.6
09/08/2023 14:59:27	15.4	17.5	15.4	74.9	79.0	80.1	17.7	14.6	14.6
09/08/2023 15:00:27	21.1	22.8	20.2	74.4	76.8	78.4	17.6	14.7	14.6
09/08/2023 15:01:27	26.9	/	22.5	73.7	/	76.7	17.3	/	14.6
09/08/2023 15:02:27	26.3	/	22.4	73.1	/	75.3	17.0	/	14.4
09/08/2023 15:03:27	24.6	/	20.1	72.4	/	74.1	16.8	/	14.3

$PM_{2.5}$ = particulate matter smaller than 2.5 µm in µg m^{-3}
RH = relative humidity in %
T = temperature in °C

Table S3: Raw data laboratory assessment under Scenario 3

Scenario 3	$PM_{2.5}$ (µg m^{-3})			RH (%)			T (°C)		
	Grimm1 1d	SPS30 −1	SPS30 −2	Grimm1 1d	SPS30 −1	SPS30 −2	Grimm1 1d	SPS30 −1	SPS30 −2
10/08/2023 10:20:54	1.8	1.2	32.0	70.9	62.4	57.5	19.3	15.0	15.6
10/08/2023 10:21:54	27.3	29.5	43.8	73.2	63.9	58.6	19.1	14.8	15.7
10/08/2023 10:22:54	79.8	43.0	40.5	74.1	64.7	59.2	19.1	14.8	15.8
10/08/2023 10:23:54	79.3	43.8	39.3	74.0	65.1	59.9	19.2	14.9	16.0
10/08/2023 10:24:54	74.9	41.1	32.8	73.8	65.8	61.2	19.5	15.0	16.2
10/08/2023 10:25:54	70.1	39.8	21.3	75.1	66.5	63.5	19.7	15.2	16.5
10/08/2023 10:26:54	65.8	37.1	17.8	77.5	67.5	65.3	19.8	15.3	16.9
10/08/2023 10:27:54	58.3	31.6	14.8	78.5	68.4	65.6	19.9	15.5	17.3
10/08/2023 10:28:54	27.0	19.6	14.0	76.2	71.4	65.0	20.9	15.9	17.4
10/08/2023 10:29:54	23.0	18.8	15.5	73.7	71.9	64.1	21.7	16.3	17.4
10/08/2023 10:32:54	17.9	13.5	10.5	74.2	70.1	60.2	21.9	16.8	16.8
10/08/2023 10:33:54	20.4	16.6	7.8	74.4	69.3	58.7	21.6	16.8	16.5
10/08/2023 10:34:54	25.9	17.1	6.3	74.6	68.5	57.6	21.4	16.7	16.3
10/08/2023 10:35:54	24.4	14.9	5.3	74.3	67.6	57.2	21.0	16.5	15.9
10/08/2023 10:36:54	21.5	13.3	4.0	73.5	66.4	57.0	20.8	16.3	15.5
10/08/2023 10:37:54	18.1	11.3	3.8	72.4	65.0	57.0	20.4	16.1	15.2
10/08/2023 10:38:54	15.0	10.6	5.0	71.5	63.9	60.0	20.1	15.9	14.9
10/08/2023 10:39:54	13.4	9.0	5.3	70.8	63.0	69.6	19.8	15.6	14.9
10/08/2023 10:40:54	11.8	8.2	3.8	70.9	62.7	72.0	19.6	15.4	15.3
10/08/2023 10:41:54	10.3	7.5	3.3	70.9	62.6	71.4	19.3	15.1	15.7
10/08/2023 10:42:54	9.3	7.3	2.5	71.0	62.5	68.5	19.0	14.8	16.0
10/08/2023 10:43:54	8.5	5.9	2.0	71.0	62.4	65.5	18.8	14.6	16.1
10/08/2023 10:44:54	7.6	5.7	54.3	71.1	62.4	62.9	18.5	14.3	16.0
10/08/2023 10:45:54	7.0	5.3	218.3	74.3	64.0	60.3	18.3	14.1	15.5

10/08/2023 10:49:54	4.1	3.5	128.5	79.3	78.3	61.2	20.5	14.9	14.5
10/08/2023 10:50:54	3.4	2.8	114.8	75.7	75.5	66.7	20.9	15.2	14.6
10/08/2023 10:51:54	2.8	2.7	54.0	73.8	72.7	65.3	21.0	15.4	15.4
10/08/2023 10:52:54	2.5	2.0	41.5	72.5	70.3	62.9	20.9	15.5	15.8
10/08/2023 10:53:54	2.3	2.3	37.8	71.3	68.0	62.3	20.7	15.5	15.9
10/08/2023 10:54:54	2.4	2.5	49.0	70.4	66.2	62.3	20.4	15.4	15.9
10/08/2023 10:55:54	2.7	2.3	49.3	71.2	65.6	62.3	20.1	15.3	15.8
10/08/2023 10:56:54	2.8	2.0	43.8	72.6	66.2	62.0	19.8	15.1	15.6
10/08/2023 10:57:54	51.7	131.2	37.0	73.0	66.2	61.2	19.5	14.9	15.4
10/08/2023 10:58:54	366.6	240.8	34.8	72.6	65.4	61.2	19.2	14.7	15.3
10/08/2023 10:59:54	329.5	215.3	32.0	72.0	64.6	61.8	19.0	14.5	15.3
10/08/2023 11:00:54	270.3	184.3	30.8	71.6	63.9	62.6	18.7	14.3	15.6
10/08/2023 11:01:54	227.8	159.5	29.3	71.3	63.5	64.0	18.5	14.0	15.7
10/08/2023 11:02:54	193.2	145.4	25.8	72.1	63.8	65.6	18.2	13.8	15.9
10/08/2023 11:03:54	173.5	134.8	14.5	74.5	65.5	69.2	18.1	13.7	16.3

$PM_{2.5}$ = particulate matter smaller than 2.5 µm in µg m^{-3}
RH = relative humidity in %
T = temperature in °C

Table S4: Data from field co-location assessment

Date	Time interval	Number of points	$PM_{2.5}$ (µg m^{-3})	RH (%)	T (°C)	Co-location time (min)
9.10.2023	7:00–8:00	39	4.2	69.8	5.7	00:03:10
9.10.2023	7:00–8:00	38	4.4	76.3	8.3	00:03:05
9.10.2023	7:00–8:00	38	4.4	80.8	8.1	00:03:05
9.10.2023	≈15:00	44	5.5	58.9	16.6	00:03:35
9.10.2023	≈12:00	57	3.6	53.7	12.6	00:04:40
9.10.2023	18:00–19:00	14	6.4	58.9	13.5	00:04:09
9.10.2023	≈15:00	45	5.9	55.4	14.4	00:03:40
9.10.2023	≈15:00	12	6.6	48.7	15.9	00:03:30
9.10.2023	18:00–19:00	54	6.3	74.5	14.7	00:04:25
9.10.2023	18:00–19:00	55	6.6	73.5	14.7	00:04:30
9.10.2023	18:00–19:00	55	6.0	66.0	12.5	00:04:30
10.10.2023	7:00–8:00	13	10.7	68.6	9.4	00:03:50
10.10.2023	7:00–8:00	46	6.1	53.7	15.9	00:03:45
10.10.2023	7:00–8:00	48	10.6	91.0	10.6	00:03:55
10.10.2023	7:00–8:00	47	10.3	90.4	10.8	00:03:50
10.10.2023	7:00–8:00	47	9.8	77.9	8.4	00:03:50
10.10.2023	≈12:00	47	6.0	52.9	19.0	00:03:50
10.10.2023	≈12:00	45	6.5	55.1	18.5	00:03:40
10.10.2023	≈12:00	12	5.9	46.3	17.8	00:03:31
10.10.2023	≈12:00	44	7.7	58.2	18.0	00:03:35
10.10.2023	≈15:00	43	9.5	59.2	18.0	00:03:30
10.10.2023	≈15:00	42	7.4	54.4	15.9	00:03:25
10.10.2023	18:00–19:00	44	8.7	72.0	15.2	00:03:35
10.10.2023	18:00–19:00	43	8.3		15.1	00:03:30
10.10.2023	18:00–19:00	41	8.1	65.2	12.8	00:03:20
10.10.2023	18:00–19:00	11	8.2	64.3	14.8	00:03:12
11.10.2023	7:00–8:00	62	17.5	90.8	9.6	00:05:05
11.10.2023	7:00–8:00	13	17.1	67.1	8.4	00:03:51
11.10.2023	7:00–8:00	68	16.5	82.4	6.5	00:05:35

11.10.2023	7:00–8:00	67	18.3	93.1	9.2	00:05:30
11.10.2023	7:00–8:00	35	8.5	56.3	20.2	00:02:50
11.10.2023	≈12:00	33	8.7	57.0	19.8	00:02:40
11.10.2023	≈12:00	9	8.4	44.1	20.3	00:02:33
11.10.2023	≈15:00	44	7.8	52.6	19.4	00:03:35
11.10.2023	≈15:00	45	8.1	56.5	21.5	00:03:40
11.10.2023	≈15:00	43	7.8	54.6	21.8	00:03:29
11.10.2023	≈15:00	11	7.9	44.8	21.6	00:03:12
11.10.2023	18:00–19:00	42	9.0	72.4	13.8	00:03:25
11.10.2023	18:00–19:00	11	12.3	57.7	16.8	00:03:11
11.10.2023	18:00–19:00	42	11.6	76.0	17.5	00:03:25
11.10.2023	18:00–19:00	42	11.9	78.7	17.1	00:03:25
12.10.2023	7:00−8:00	67	28.0	79.5	7.9	00:05:30
12.10.2023	7:00−8:00	68	28.0	88.9	10.8	00:05:09
12.10.2023	7:00−8:00	18	26.3	65.5	9.7	00:05:26
12.10.2023	7:00−8:00	67	29.8	91.3	10.5	00:05:30
12.10.2023	≈12:00	47	7.0	48.9	17.9	00:03:50
12.10.2023	≈12:00	12	7.3	38.8	21.9	00:03:30
12.10.2023	≈12:00	47	8.4	50.1	21.4	00:03:50
12.10.2023	≈12:00	47	7.6	48.0	22.1	00:03:50
12.10.2023	≈12:00	34	7.4	45.0	20.3	00:02:45
12.10.2023	≈15:00	9	7.4	37.3	23.2	00:02:33
12.10.2023	≈15:00	35	7.3	44.7	23.1	00:02:50
12.10.2023	≈15:00	34	7.3	46.9	22.8	00:02:45
12.10.2023	18:00–19:00	45	11.4	69.8	17.0	00:03:40
12.10.2023	18:00–19:00	12	11.3	55.0	16.2	00:03:30

12.10.2023	18:00–19:00	45	12.0	69.1	16.9	00:03:40
13.10.2023	7:00–8:00	36	19.9	86.8	10.6	00:02:55
13.10.2023	7:00–8:00	34	18.9	79.8	7.1	00:02:45
13.10.2023	7:00–8:00	10	18.3	64.8	9.2	00:02:53
13.10.2023	≈12:00	33	8.7	48.4	17.8	00:02:40
13.10.2023	≈12:00	8	8.6	39.7	20.7	00:02:14
13.10.2023	≈12:00	33	8.5	46.9	20.9	00:02:40
13.10.2023	≈15:00	12	10.3	40.5	22.5	00:03:31
13.10.2023	≈15:00	49	11.3	49.0	22.9	00:04:00
13.10.2023	≈15:00	47	9.9	47.9	23.0	00:03:50
13.10.2023	18:00–19:00	43	17.9	66.6	17.8	00:03:30
13.10.2023	18:00–19:00	42	17.4	64.4	18.0	00:03:25
13.10.2023	18:00–19:00	11	17.3	53.8	16.9	00:03:12

$PM_{2.5}$ = particulate matter smaller than 2.5 µm in µg m^{-3}
RH = relative humidity in %
T = temperature in °C

3.4 Article 4: Fine Particulate Matter ($PM_{2.5}$) Exposure Assessment Among Active Daily Commuters to Induce Behaviour Change to Reduce Air Pollution

Authors: Anja Ilenič, Alenka Mauko Pranjić, Nina Zupančič, Radmila Milačič, Janez Ščančar
Published in Elsevier, Science of The Total Environment (February 2024)
Available at DOI: 10.1016/j.scitotenv.2023.169117

$PM_{2.5}$ exposure assessment in urban microenvironments is essential for protecting the health of more vulnerable road users, such as cyclists and pedestrians. However, such assessments are usually carried out at fixed AQMS that do not representatively capture the dynamic exposure of commuters. Therefore, citizen-led campaigns using LCS can supplement official AQMS by providing high-resolution spatio-temporal air quality data, enhancing evidence-based policy and facilitating the effective regulatory frameworks realignments to reduce urban air pollution. This study was conducted in Ljubljana, Slovenia, between September and December 2022, to assess $PM_{2.5}$ exposure among daily commuters and evaluate the associated potential health risks. In total, 19 cyclists completed 312 bicycle trips using the LCS Sensirion SPS30. The LCS quality assurance results, verified by co-location field assessment by ARSO AQMS, yielded comparable results, with an average difference of 21%, attributed to RH-induced nucleation effects. During the campaign, 46,945 measurement points were recorded, with average $PM_{2.5}$ concentrations varying between 5−32 µg m^{-3}. Colder months exhibited higher $PM_{2.5}$ concentrations due to frequent thermal inversions and weak wind circulation, which hindered vertical air mixing and thus adequate pollutant dispersion. In addition, $PM_{2.5}$ concentrations in all sampling periods were lowest in the afternoon (12.09 µg m^{-3}) and highest at night (61 µg m^{-3}), when the thinning PBL promotes pollutant accumulation near the surface, thus significantly affecting diurnal and seasonal patterns. The spatial analysis identified several air pollution hotspots within the city, closely associated with high traffic density and proximity to major local $PM_{2.5}$ sources, such as busy roads, construction sites, bus and train station, industrial areas and the highway. The measured $PM_{2.5}$ values exceeded both the AQD and WHO limit values. Cyclists were roughly three times more exposed than pedestrians over an equivalent average commute, mainly as a result to increased breathing frequency and greater volume of inhaled air. The HQ value did not exceed 1, indicating a minimal potential risk from $PM_{2.5}$ exposure in Ljubljana, Slovenia. Moreover, 94% of participants reported willingness to change their travel behaviour to minimise exposure if the infrastructure – such as open cycling lanes, ventilated road junction and paths separated from roads by vegetation – allowed it.

Science of the Total Environment 912 (2024) 169117

Contents lists available at ScienceDirect

Science of the Total Environment

journal homepage: www.elsevier.com/locate/scitotenv

Fine particulate matter ($PM_{2.5}$) exposure assessment among active daily commuters to induce behaviour change to reduce air pollution

Anja Ilenič [a,b], Alenka Mauko Pranjić [a,*], Nina Zupančič [c,d], Radmila Milačič [b,e], Janez Ščančar [b,e]

[a] Slovenian National Building and Civil Engineering Institute (ZAG), Dimičeva ulica 12, 1000 Ljubljana, Slovenia
[b] Jožef Stefan International Postgraduate School, Jamova cesta 39, 1000 Ljubljana, Slovenia
[c] University of Ljubljana, Faculty of Natural Sciences and Engineering, Aškerčeva 12, 1000 Ljubljana, Slovenia
[d] ZRC SAZU Ivan Rakovec Institute of Paleontology, Novi trg 2, 1000 Ljubljana, Slovenia
[e] Institute Jožef Stefan, Jamova cesta 39, 1000 Ljubljana, Slovenia

HIGHLIGHTS

- $PM_{2.5}$ poses significant health risks at limited exposure during commuting.
- Air quality monitoring stations and citizens' initiatives data integration enhances air pollution assessment.
- Air quality monitoring stations co-location validation of low-cost sensors results yielded comparable outcomes.
- $PM_{2.5}$ increased in cold months due to thermal inversions hindering pollutant dispersion.
- Cyclist had three times higher $PM_{2.5}$ exposure than pedestrians.

GRAPHICAL ABSTRACT



ARTICLE INFO

Editor: Pavlos Kassomenos

Keywords:
Air pollution monitoring
$PM_{2.5}$ exposure
Citizen science
Bicycle-mounted low-cost sensors

ABSTRACT

Fine particulate matter ($PM_{2.5}$), a detrimental urban air pollutant primarily emitted by traffic and biomass burning, poses disproportionately significant health risks at relatively limited exposure during commuting. Previous studies have mainly focused on fixed locations when assessing $PM_{2.5}$ exposure, while neglecting pedestrians and cyclists, who often experience higher pollution levels. In response, this research aimed to independently validate the effectiveness of bicycle-mounted low-cost sensors (LCS) adopted by citizens, evaluate temporal and spatial $PM_{2.5}$ exposure, and assess associated health risks in Ljubljana, Slovenia. The LCS quality assurance results, verified by co-location field tests by air quality monitoring stations (AQMS), showed comparable outcomes with an average percentage difference of 21.29 %, attributed to humidity-induced nucleation effects. The colder months exhibited the highest air pollution levels ($\mu = 32.31\ \mu g/m^3$) due to frequent thermal inversions and weak wind circulation, hindering vertical air mixing and the adequate dispersion of pollutants. Additionally, $PM_{2.5}$ levels in all sampling periods were lowest in the afternoon ($\mu = 12.09\ \mu g/m^3$) and highest during the night ($\mu = 61.00\ \mu g/m^3$) when the planetary boundary layer thins, leading to the trapping of pollutants near the surface, thus significantly affecting diurnal and seasonal patterns. Analysis of exposure factors revealed that cyclists were approximately three times more exposed than pedestrians. However, the toxicological risk assessment indicated a minimal potential risk of $PM_{2.5}$ exposure. The collaborative integration of data from

* Corresponding author.
E-mail address: alenka.mauko@zag.si (A.M. Pranjić).

https://doi.org/10.1016/j.scitotenv.2023.169117
Received 10 August 2023; Received in revised form 14 November 2023; Accepted 3 December 2023
Available online 7 December 2023
0048-9697/© 2023 The Authors. Published by Elsevier B.V. This is an open access article under the CC BY-NC-ND license (http://creativecommons.org/licenses/by-nc-nd/4.0/).

official AQMS and LCS can enhance evidence-based policy-making processes and facilitates the realignment of effective regulatory frameworks to reduce urban air pollution.

1. Introduction

Urban air pollution is a significant public health and environmental issue in the European Union (EU) due to its high temporal and spatial variability and its close association with citizens' daily activities, behaviours and practices (Rodrigues et al., 2021). Despite making progress towards cleaner air, many European cities still experience acute episodes of air pollution, with some areas frequently exceeding the air quality levels permitted by the European legal standards defined within the European Ambient Air Quality Directive (AQD) 2008/50/EC (Directive 2008/50/EC, n.d.) and the interim targets of the World Health Organization's (WHO) Air Quality Guidelines (AQG) (European Environmental Agency (EEA), 2022). Fine particulate matter ($PM_{2.5}$, aerodynamic diameter < 2.5 μm) is a particularly harmful and detrimental air pollutant that poses significant health risks – including chronic and acute respiratory and cardiovascular diseases, such as stroke and lung cancer – and can ultimately lead to reduced life expectancy at very low concentrations (Chen et al., 2008; Cohen et al., 2017; Dominici et al., 2006; Russell and Bert, 2009). According to estimates, exposure to $PM_{2.5}$ increases the risk of non-accidental mortality by 6 % per 10 μg/m^3, independently of age, gender and geographic location. Specifically, exposure to $PM_{2.5}$ increases the risk of mortality by 15–21 % per 10 μg/m^3 and 12–14 % per 10 μg/m^3 from lung cancer and cardiovascular diseases, respectively (Chen et al., 2008). In 2021, 30 European countries reported $PM_{2.5}$ concentrations above the WHO's annual and daily guidelines (European Environmental Agency (EEA), 2022). Compared to other EU countries, Slovenia has a moderate level of air pollution, with an estimated 1238 premature deaths per year being attributed to particulate matter emissions (PM_{10} and $PM_{2.5}$) (Slovenian Environmental Agency, ARSO, 2023; European Environmental Agency (EEA), 2023).

Urban environments act as the source of the majority of anthropogenic particles, which primarily come from vehicle exhausts, road dust resuspension and wear of vehicular components (e.g. tyres, brakes) as well as fossil fuel combustion (Dahl et al., 2006; Kittelson, 1998; Kwak et al., 2013; Ramos et al., 2015). Even though most individuals spend relatively little time commuting, travel exposure to $PM_{2.5}$ concentrations still accounts for a disproportionately large amount of their overall exposure to air pollution (Gulliver and Briggs, 2004; Guzman et al., 2023). Prior research has predominantly focused on assessing individuals' exposure to air pollutants at stationary locations such as homes and workplaces, while rarely investigating the exposure of pedestrians and cyclists. Active commuters frequently encounter elevated levels of air pollution compared to motorised transport users (Boogaard et al., 2009; de Nazelle et al., 2012; Samad and Vogt, 2020). Accurate dynamic exposure assessments and subsequent hazard mitigation measures are, despite their critical importance, often overlooked in environmental studies.

In urban areas, assessments and analyses of air quality primarily rely on stationary monitoring devices and a limited number of air quality monitoring stations (AQMS) that are sparsely located and adhere to standardised quality assurance and control protocols. Although traditional methods of retrieving air pollution data offer high temporal resolution information at specific micro-locations, they fail to provide a comprehensive view of the overall situation and have limited ability to capture the spatial distribution of measured parameters due to significant variations of pollutants in urban areas (Kousis et al., 2022; Samad and Vogt, 2020). Therefore, there is a need for radical changes in air quality monitoring approaches that consider citizens' daily activities and behavioural patterns, which can enable a realignment of policy processes and resilience planning at different levels of aggregation to minimise urban air contaminants (Kousis et al., 2022; Rodrigues et al., 2021). Low-cost sensors (LCS) are rapidly being adopted by citizens and public authorities for air pollution monitoring, in order to provide a detailed evaluation of each city's intra-urban characteristics. However, LCS are sensitive to many factors including atmospheric and environmental conditions such as relative humidity, pollutant concentration levels, chemical interferences and different particle diameters, hygroscopicity, refraction index, composition and averaging time (Aleixandre and Gerboles, 2012; Castell et al., 2017; Giordano et al., 2021; Karagulian et al., 2019; Zhu et al., 2011). Therefore, their instability and potential performance variations in different locations need to be assessed and associated uncertainties must be considered before large-scale deployment. Thus, many environmental campaigns test the data acquired by LCS through co-location processes with reference to AQMS (Bergmann et al., 2022; Castell et al., 2017; Karagulian et al., 2019; Kousis et al., 2022; Kumar et al., 2015; Lewis and Edwards, 2016) to further quantify the exposure of daily commuters (Bergmann et al., 2021; Boogaard et al., 2009; Cole-Hunter et al., 2012; Huang et al., 2012; Int Panis et al., 2010; Kaur et al., 2007; Ljubljana.info, 2021; de Nazelle et al., 2012; Qiu et al., 2019; Salma et al., 2002; Samad and Vogt, 2020; Yang et al., 2021; Zuurbier et al., 2010). In so doing, it is possible to provide greater spatial coverage and authorities and policy makers can anticipate corresponding actions to better mitigate air pollution risks. The affordability and large-scale deployment of such citizen science campaigns, defined as scientific research conducted with participation from the general public, may introduce an extensive and cost-effective monitoring approach, consequently affecting the social behaviour to reduce air pollutant levels.

This study aimed to independently validate the effectiveness of bicycle-mounted LCS as a complementary tool to AQMS in reducing air pollution in urban microenvironments in Ljubljana, Slovenia. The focus was to analyse temporal and spatial $PM_{2.5}$ exposure and evaluate the associated health risks for daily commuters. To the best of the authors' knowledge, this study represented the first long-term air pollution monitoring project involving citizens and LCS in Slovenia. Therefore, the results of this study have the potential to make a valuable scholarly contribution, establishing a strong basis for future research and regulatory alterations aimed at reducing air pollution in Slovenia. Furthermore, the study can serve as a model for similar research in other areas, while also promoting citizens' awareness and empowerment to tackle pollution in urban areas.

2. Material and methods

2.1. Study area

Ljubljana, (Fig. 1) the capital of Slovenia with a population of 293,218, is located within the Sava River basin and is surrounded by the hills of the Dinaric Alps. With its substantial presence of labour-intensive industries (Ljubljana.info, 2021), high urban population density of 920.2 inhabitants per square kilometre, and heavy traffic due to 156,900 daily work migrants (Ljubljana.info, 2021; Ljubljana.si, 2023), Ljubljana stands out as the largest and most developed city in Slovenia. As a result, the city experiences regular thermal inversions and weak wind circulation, which hinders adequate vertical mixing of air masses for pollutant dispersion and thus favours the accumulation of air pollutants. Hourly and monthly measurements of selected air pollutants such as coarse particulate matter (PM_{10}, aerodynamic diameter < 10 μm), fine particulate matter ($PM_{2.5}$, aerodynamic diameter < 2.5 μm), carbon monoxide (CO), ozone (O_3), nitrogen dioxide (NO_2) and benzene are conducted at two Slovenian Environment Agency (ARSO) AQMS: Ljubljana–Bežigrad (46.06601, 14.51249) and Ljubljana–Celovška

(46.07279, 14.48686). According to ARSO (2021), the primary local sources of $PM_{2.5}$ in the region are household fireplaces that use wood biomass (74 %) and traffic emissions (5 %).

2.2. Case study sampling protocol

The $PM_{2.5}$ monitoring campaign applying bicycle-mounted LCS was conducted between September and December 2022. CanAirIO (dimensions: 57 × 24 × 101 mm; weight: 95 g), an open-source, open-design and open-access mobile device that incorporates a real-time optical counter (OPC) Sensirion SPS30 (hereafter referred to as LCS SPS30), was used for this purpose. This mobile system is able to measure $PM_{2.5}$ continuously (programmable intervals of 5 s) and mark global positioning system (GPS) data using Bluetooth Low Energy. $PM_{2.5}$ sensor was mounted perpendicularly to the cyclists' travelling direction in order to minimise the wind effect and consequently the overestimation of the $PM_{2.5}$ concentrations. A built-in fan draws air into the chamber; particles pass through the laser beam and cause the incident light to scatter. The scattered light is then detected by a photodiode and converted to a mass/number concentration expressed in $\mu g/m^3$. In addition to $PM_{2.5}$ concentrations, LCS SPS30 provides information about the ambient temperature (Temp in °C) and relative humidity (RH in %). The sampling protocol for the case study aimed to capture the $PM_{2.5}$ concentrations' variability, accounting for seasonal, diurnal and spatial differences as well as the influence of traffic density.

The study was divided into four sampling periods, during which 19 volunteers (31 % female) rode bicycles to obtain $PM_{2.5}$ concentrations. A total of 312 bicycle trips were made during the following periods: September (12–24 September 2022; $n = 80$ bicycle trips), October (3–16 October 2022; $n = 122$ bicycle trips), November (31 October–13 November 2022; $n = 72$ bicycle trips) and December (5–18 December 2022; $n = 38$ bicycle trips). Each participant completed preliminary instructed co-location calibration of the mobile sensor with one of the two ARSO AQMS (Fig. 1) as well as answered a participatory questionnaire to assess their perceived behaviour regarding air pollution in order to re-evaluate active mobility patterns and strategic designs of urban areas. The collected data were categorised into eight distinct time periods, specifically: 6:00–9:00, 9:00–12:00, 12:00–15:00, 15:00–18:00, 18:00–21:00, 21:00–00:00, 00:00–03:00 and 03:00–06:00. This classification aimed to examine the impacts' of time of day and traffic density. Rush hours were further divided into morning rush hour time (morning-RHT; 6:00–9:00) and afternoon rush hour time (afternoon-RHT; 15:00–18:00). Previous studies have shown that humidity above 85 % is likely to result in an increase in the nucleation rate of $PM_{2.5}$ (Crilley et al., 2018; Liu et al., 2019; Malings et al., 2020). However, in this particular study, the average humidity remained below this threshold, as 11 % of the total RH data were measured above RH = 85 %. Additionally, the temperature has minimal to no effect on LCS PM sensors, as reported by Liu et al. (2019). The data were statistically evaluated by analysis of variance (ANOVA) to establish the differences between sampling periods using TIBCO Statistica software (TIBCO, 2017). Furthermore, spatial distributions of $PM_{2.5}$ concentrations were examined using QGIS software.

2.3. Sensor quality assurance

LCS SPS30 (measurement range: 0–1000 $\mu g/m^3$, concentration resolution: 1 $\mu g/m^3$, particle diameter resolution: 0.3 μm) was introduced in 2018 and was initially calibrated by the manufacturer during laboratory testing, by $PM_{2.5}$ mass concentration calibrated to TSI DustTrakTM DRX 8533 Ambient Mode and $PM_{2.5}$ number concentration calibrated to TSI OPS 3330 (Alfano et al., 2020). The particle size selectivity of LCS SPS30, along with its coefficient of determination for the $PM_{2.5}$ measurement ($R^2 = 0.83$), was compared to a mid-cost aerosol size spectrometer Grimm 1.108, in 2020. The results indicated that LCS SPS30 could provide independent responses for five size bins, while the Grimm 1.108 spectrometer was capable of characterising responses for up to 15 different size bins (Kuula et al., 2020).

In Slovenia, continuous monitoring of PM_{10} and $PM_{2.5}$ is performed with the HORIBA model APDA-371 (measurement resolution: 0.1 $\mu g/m^3$; LOD < 4.8 $\mu g/m^3$; flow rate: 16.7 L/min), which automatically measures and records airborne particulate concentration levels hourly, and utilises ^{14}C (radioactivity: < 2.22 × 106 Beq, 60 μCi ± 15 μCi, half-life 5730 years) as a beta source using a photomultiplier tube with an organic plastic scintillator as a detector. A total of 456 and 574 measurements were recorded at AQMS Ljubljana−Bežigrad and AQMS Ljubljana−Celovška, respectively, over the course of 19 different sampling days, ensuring multiple cross-daily device co-location validation. To ensure that the results would be sufficiently accurate, any data with intervals of <3 min were not considered in the subsequent analysis. The results were based on the aggregation of the average data collected during the same time period using both the mobile LCS SPS30 and stationary APDA-371 devices. The AQD (Directive 2008/50/EC, n.d.) specifies Data Quality Objectives (DQO) with which monitoring methods must comply and stipulates that measurement uncertainty with principle metrics such as the coefficient of determination (R^2) and the slope of the regression curve should be principally used to evaluate the data quality objective of air pollution measurement methods. However,

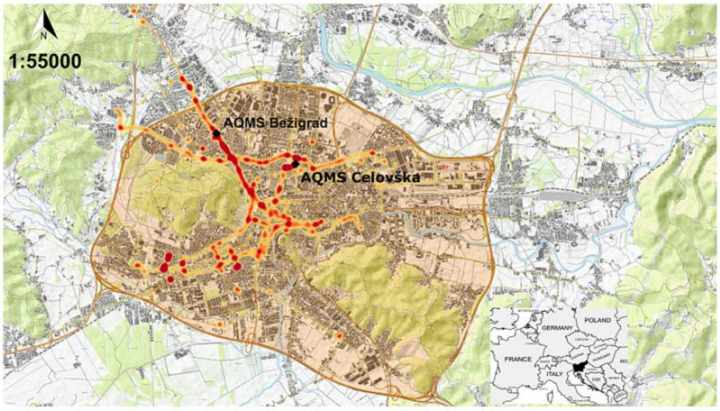


Fig. 1. Spatial distribution of PM2.5 in Ljubljana with two AQMS operated by Slovenian Environmental Agency.

metrics are rarely included in studies that use LCS as a part of citizen science campaigns (Karagulian et al., 2019). The interpolation of the results showed good reliability, as evaluated by the metrics of adjusted R^2 value (0.89; $p > 0.05$) between LCS SPS30 and AQMS APDA-371 (Fig. 2). Karagulian et al. (2019) have reported average calibration R^2 values in different LCS performance evaluation studies equal to 0.8, although they did not assess LCS SPS30. Overall, given these findings, the data from the present study could be considered reliable and therefore no further data iterations were conducted.

2.4. Human health risk assessment

In order to assess the exposure of daily commuters, two parameters were calculated: lifetime average daily dose (*LADD*; μg/kg-day) and toxicological risk (*RQ*) (U.S. Environmental Protection Agency, 1997). *LADD* (Eq. (1)) represents the amount of $PM_{2.5}$ suspected of having adverse health effects that a person is exposed to over a long period of time. It is estimated using the following equation:

$$\mathbf{LADD} = \frac{\mathbf{c_{air}} \times \mathbf{IR} \times \mathbf{ED_{1/2}} \times \mathbf{EF}}{\mathbf{BW} \times \mathbf{AT}} \quad (1)$$

where c_{air} is the concentration of the pollutant in the air (mg/m^3) during a given sampling period, *IR* is the individual's inhalation rate (m^3/h) during a specific activity, *ED* is the duration of exposure (years) for that activity, *EF* is the exposure frequency (365 days/years), *BW* is the individual's body weight (kg) and *AT* is the total averaging lifetime (days). *IR* depends on several factors such as the subject's size, physiology, behaviour, metabolic rate and activity levels, and differs among categories, namely cycling and walking. *IR* was developed by the United States Environmental Protection Agency (U.S. EPA) Office of Environmental Criteria and Assessment and is categorised by light (walking) and moderate (cycling) activity. Its respective values for light and moderate activity for adult men and adult women are 0.8 m^3/h and 2.5 m^3/h, and 0.5 m^3/h and 1.6 m^3/h, respectively (U.S. Environmental Protection Agency, 1997). The average commuting time for Slovenian citizens is 52 min/day (ED_1), while the average time spent undertaking outdoor activities is 106.2 min/day (ED_2) (Statistical Office of the Republic of Slovenia (SURS), 2023a). The life expectancy for adult men and women in Slovenia is 78 and 84 years, respectively (Statistical Office of the Republic of Slovenia (SURS), 2023b). In Slovenia the average *BW* is 85 kg for men and 68 kg for (Statistical Office of the Republic of Slovenia (SURS), n.d.).

Individuals' *RQ* (U.S. EPA 1997) (Eq. (2)) is estimated using the following equation:

$$\mathbf{RQ} = \frac{\mathbf{LADD}}{\mathbf{RfD}} \quad (2)$$

where the R*f*D (reference dose) (U.S. EPA 1997) (Eq. (3)) is expressed as the function of *IR* and *BW*. $PM_{2.5}$ at 15 μg/m^3 was used as a reference concentration (*RfC*), as stated in the WHO AQG, a set of evidence-based recommendations for limit values affecting human health at low levels (EEA 2022):

$$\mathbf{RfD} = \frac{\mathbf{RfC} \times \mathbf{IR}}{\mathbf{BW}} \quad (3)$$

2.5. Participatory questionnaire

A participatory questionnaire was used to assess the social and socio-economic impacts of air pollution and evaluate how it is perceived by daily cyclists. Participants were presented with two documents: a questionnaire and key facts about air pollution. The participatory questionnaire consisted of 15 questions aimed at gathering information on two primary aspects: (1) the participants' understanding of air pollution and (2) their cycling habits in relation to the existing infrastructure.

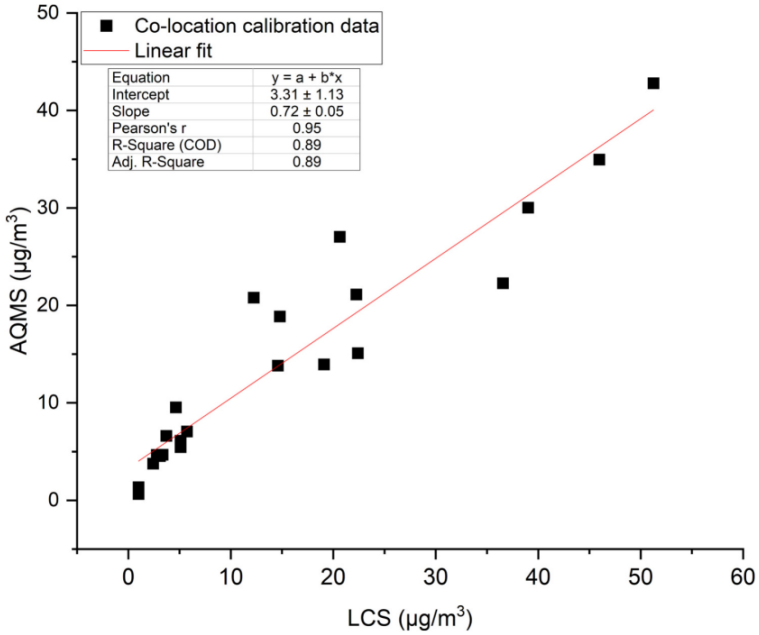


Fig. 2. Regression chart for PM2.5 acquired by LCS SPS30 and AQMS APDA-371.

3. Results and discussion

3.1. LCS and AQMS comparability

In total, co-location calibration yielded 1024 recorded measuring points within the timeframe of 1 h 35 min 35 s. These measurements were carried out on both weekdays and weekends. Notably, the co-location calibration was intentionally omitted during the summer period, potentially introducing a constraint in terms of sensor quality control under these seasonal conditions. The $PM_{2.5}$ data acquired were analysed based on different time periods as follows: at 6:00–9:00, the mean values were 12.86 μg/m^3 for LCS and 15.18 μg/m^3 for AQMS; at 9:00–12:00, the mean values were 6.98 μg/m^3 for LCS and 9.31 μg/m^3 for AQMS; at 12:00–15:00, the mean values were 12.55 μg/m^3 for LCS and 13.35 μg/m^3 for AQMS; at 15:00–18.00, the mean values were 16.02 μg/m^3 for LCS and 12.20 μg/m^3 for AQMS; at 18:00–21:00, the mean values were 30.71 μg/m^3 for LCS and 22.56 μg/m^3 for AQMS; and at 3:00–6:00, the mean values were 22.24 μg/m^3 for LCS and 21.13 μg/m^3 for AQMS (Fig. 3). No co-location validation measurements were conducted between 21:00–00:00 and 00:00–3:00. On average, the percentage difference in $PM_{2.5}$ concentrations measured by LCS SPS30 and AQMS Ljubljana−Bežigrad was 22.78 %, while for AQMS Ljubljana−Celovška, it was 19.80 %. This difference can be mainly attributed to the nucleation effect caused by humidity levels as well as the possibility of pollutants being suppressed near the ground, especially during colder months due to more frequent thermal inversions, leading to inconsistent $PM_{2.5}$ concentrations in the air at different heights (Chen et al., 2020). The co-location validation data produced favourable results in terms of comparability. Subsequently, the discussion focuses solely on the data obtained from the LCS.

3.2. Temporal and spatial variability of $PM_{2.5}$ concentrations

The $PM_{2.5}$ monitoring campaign yielded a total of 52,173 measuring point data, of which 46,945 (89.98 %) remained across four sampling periods once errors had been removed (GPS, false data, co-location data, Fig. 4).

The comparative ANOVA showed statistically significant differences at the 95 % probability level between sampling periods, with the lowest average $PM_{2.5}$ concentrations being observed in September and the highest in December (Fig. 5, Table S1). Lower temperatures result in decreased wind speed and precipitation, with precipitation being the key factor influencing the heightened air pollution levels observed in October. In Ljubljana, increased pollution concentrations during colder months, when meteorological conditions promote surface-level pollutant accumulation (Chen et al., 2020), are mainly attributed to unfavourable micro-conditions caused by the city's location in a valley surrounded by mountains, frequent thermal inversions and weak vertical mixing of air masses. These factors hinder the efficient dispersion of pollutants.

Furthermore, the ANOVA revealed statistically significant differences at the 95 % probability level between different time periods. Across all sampling periods, $PM_{2.5}$ concentrations were highest during the night (21:00–00:00), averaging at 61.00 μg/m^3, and lowest during the afternoon (12:00–15:00), averaging at 12.09 μg/m^3 (Fig. 6), attributed to the effects of the planetary boundary layer (PBL), which modulates the local air pollution level near the surface (Pan et al., 2019). The PBL, along with various factors like meteorology, topography, demography, transportation, fuel quality, energy usage and levels of industrialisation and urbanisation, plays a vital role in the vertical mixing, dilution and dispersion of near-surface pollutants, thus significantly affecting the diurnal and seasonal patterns of $PM_{2.5}$ concentrations (Miao et al., 2019; Su et al., 2018). A higher PBL usually corresponds to stronger turbulence and potentially lower air pollution (Miao et al., 2019; Pan et al., 2019). At night, the PBL thins, trapping pollutants near the surface. As temperatures rise and relative humidity drops, the PBL thickens, reaching its peak in the afternoon, gradually reducing $PM_{2.5}$ levels (Miao et al., 2019). The primary local sources of $PM_{2.5}$ in the area are wood-burning fireplaces (74 %) and traffic emissions (5 %) (ARSO, 2021). The prevalence of diesel engines in Slovenia, accounting for 51 % of the fleet, compared to 48 % gasoline engines (Terzic, 2020), may also contribute to the higher average $PM_{2.5}$ levels due to the tendency of diesel engines to produce more PM (Ono-Ogasawara and Smith, 2004). Morning-RHT (6:00–9:00) and afternoon-RHT

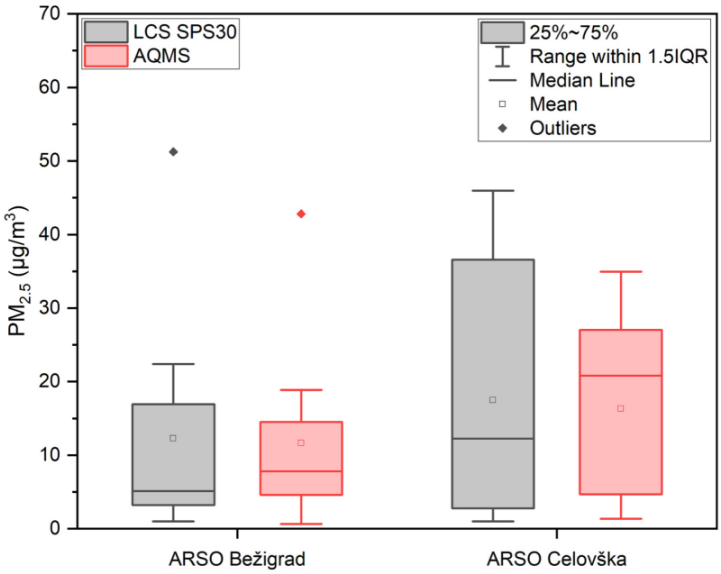


Fig. 3. Comparability of PM2.5 data points obtained by co-location validation measurements.

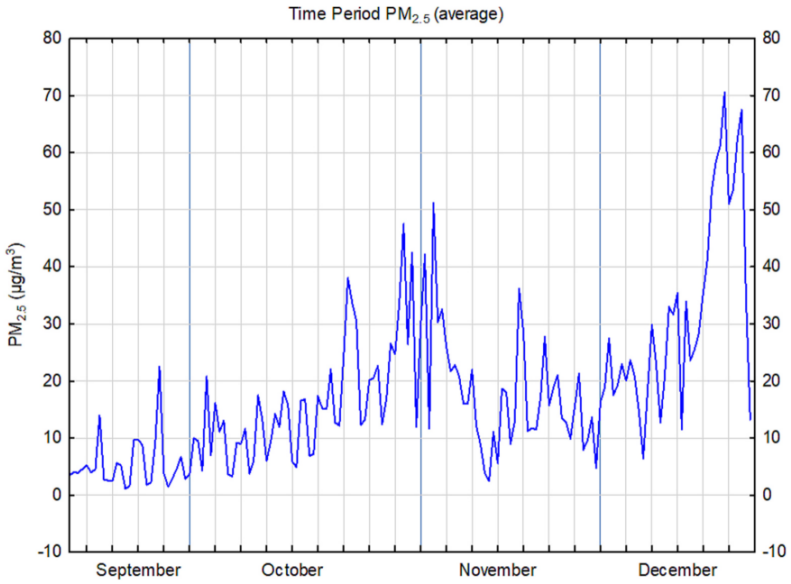


Fig. 4. Timeseries of PM2.5 values.

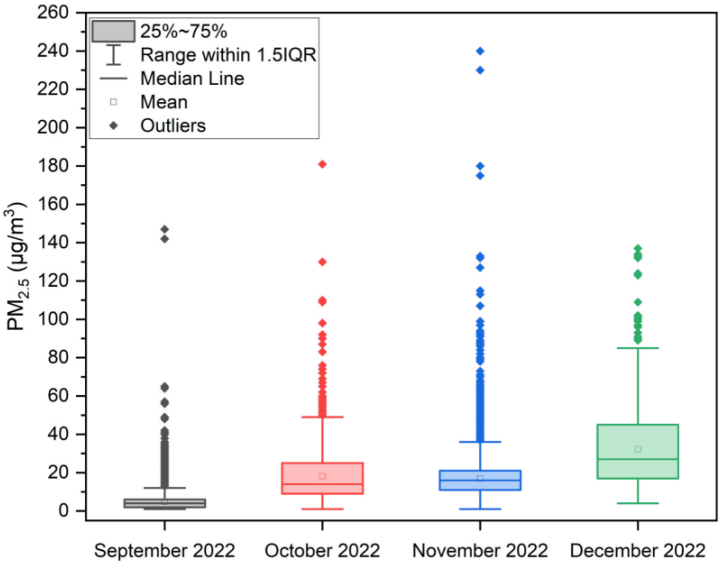


Fig. 5. PM2.5 distribution across sampling periods.

(15:00–18:00) showed varying impacts on $PM_{2.5}$ concentrations, with the latter proving the more problematic, showing an average concentration of 17.34 µg/m^3 across all sampling periods. Atmospheric pollution levels in urban areas vary spatially and temporally due to factors like traffic volume, urban layout and proximity to pollution sources. It was observed that daily and monthly variances contribute significantly more to the overall variance than differences observed within different parts of the day. Temporal variations include day-to-day fluctuations influenced by weather conditions and urban changes as well as within-day fluctuations caused by traffic dynamics and microscale variability (Hofman et al., 2018).

In addition, the spatial distribution of $PM_{2.5}$ concentrations analysed by QGIS software revealed a higher number of air pollution hotspots in December compared to in September. The spatial pattern was correlated

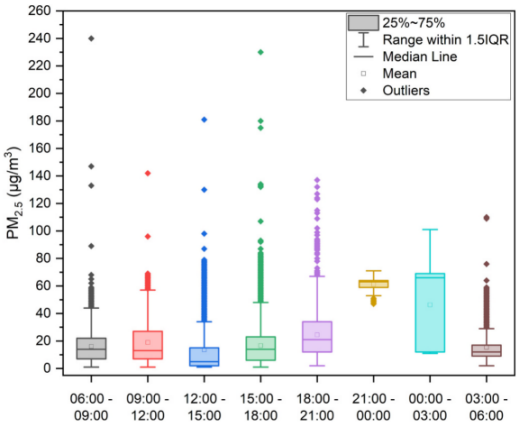


Fig. 6. Hourly distribution of PM2.5.

with the distribution of average traffic density in Ljubljana as well as proximity to major local sources of $PM_{2.5}$, such as busy roads (Celovška Street and Dunajska Street), construction sites (Poljanska Street), bus and train stations (Slovenska Street, Trg Osvobodilne fronte), industrial zones (Celovška Street) and the motorway ring road junction (Podutiška Street). Two significant $PM_{2.5}$ pollution sources were identified, where concentrations exceeded 100 µg/m^3: (1) the junction of a railway track and a busy road with high-density traffic during rush hours (Bleiweisova Street); and (2) the combination of a busy road with high traffic density during rush hours and an industrial zone (Celovška Street by Stegne) (Fig. 1).

The $PM_{2.5}$ values were then compared to the limit values defined in the AQD (Directive 2008/50/EC, n.d.) and the WHO AQG daily interim targets (EEA 2022) (Table S2). These limits define objectives to minimise the adverse impacts of air pollution on human health and the environment. The AQD establishes a standard for managing ambient air quality in Europe, while the WHO's interim targets are steps towards achieving guideline levels. Four daily interim target levels (75 µg/m^3, 50 µg/m^3, 37.5 µg/m^3, 25 µg/m^3) and an AQG level (15 µg/m^3) indicate different air quality levels, where the AQG level (15 µg/m^3) indicates good air quality with regard to fine particulate matter, interim target 4 (25 µg/m^3) indicates fair air quality, interim target 3 (37.5 µg/m^3) indicates moderate air quality, interim target 2 (50 µg/m^3) indicates poor air quality and interim target 1 (75 µg/m^3) indicates poor air quality. The $PM_{2.5}$ data measured by LCS SPS30 exceeded the annual WHO AQG level in 45.21 % of all cases. Additionally, 11.69 % exceeded the WHO's daily interim target 3 (37.5 µg/m^3) and 0.61 % exceeded interim target 1 (75 µg/m^3). AQD provides only an annual threshold target set at 25 µg/m^3, whereas lacks criteria for evaluating short-term $PM_{2.5}$ pollution levels effectively.

3.3. Personal travel $PM_{2.5}$ exposure

Previous air pollution research in Ljubljana involving citizen science activities (Benčina and Gorenc, 2021; Novak et al., 2020; Novak et al., 2020; Robinson and Kontić, 2016; Robinson et al., 2021; Robinson et al., 2021) has remained limited, the focus being mainly on static monitoring devices or a limited time frame to assess air pollutants such as particulate matter (PM_{10}, $PM_{2.5}$), black carbon (BC), nitrogen oxides (NO_x), carbon monoxide (CO), ozone (O_3), carbon dioxide (CO_2) and volatile organic compounds (VOC). Therefore, the results presented in this paper, which incorporate dynamic, mobile and low-cost sensing techniques, represent a significant contribution to the field of air pollution research in Ljubljana. Within the ICARUS Horizon 2020 project, portable low-cost PM measuring units were deployed in February and May 2019. The main objective was to collect data on external environmental exposure as well as to evaluate the influence of individual behaviour on personal exposure to air pollution and to determine the PM intake dose (Novak et al., 2020; Robinson et al., 2021). In addition, a smaller scale static monitoring campaign was conducted in Ljubljana in 2016, where 25 small air quality sensor units (AQMesh) were used to determine various air quality parameters (NO_x, O_3, CO, PM, temperature, relative humidity, noise and pressure). The one-week study conducted, indicated on poor air quality in the vicinity of heavily trafficked roads, such as Tržaška Street, Dunajska Street and Celovška Street, close to the main bus and train station. These findings of $PM_{2.5}$ hotspots identification are consistent with the results of present study (Robinson and Kontić, 2016). Additionally, a three-week NO_2 measuring campaign conducted in Ljubljana in 2021, which included six volunteers, identified 137 locations where NO_2 levels were elevated and exceeded the harmful level of 20 µg/m^3 on high-traffic roads such as Tržaška Street, Dunajska Street, Zaloška Street, Celovška Street and Roška Street (Benčina and Gorenc, 2021).

Urban microenvironments can pose significant air pollutant exposure risk to many people, particularly daily active commuters such as cyclists and pedestrians. Therefore, it is important to assess exposure risks in order to ensure the safety and well-being of individuals. Most studies assess the potential health risks of aerosol inhalation rates based on the average concentrations obtained from AQMS or other fixed monitoring stations, rather than personal exposure to ambient $PM_{2.5}$ concentrations, resulting in an underestimation of the cumulative total exposure during commutes. Consequently, it is crucial to consider hourly activity levels in relation to specific inhalation activities in order to accurately assess the health impact on commuters in urban microenvironments. Although commuting may only account for a small proportion of a person's daily activity, it can still contribute significantly to their total daily exposure to and inhalation doses of air pollutants (Gulliver and Briggs, 2004; Guzman et al., 2023; de Nazelle et al., 2017). Based on the evaluated personal exposure to $PM_{2.5}$, it was observed, that commuting exposure exceeded the 24-h guideline values. According to the exposure factors calculated (Table S3), pedestrians commuting in September were found to experience the lowest exposure to $PM_{2.5}$, while cyclists commuting in December experienced the highest exposure.

3.4. Toxicological risk assessment

The toxicological risk calculated did not exceed 1 for any type of commuter (ranging from 0.011 to 0.071, as shown in Table S4), indicating minimal potential risk of $PM_{2.5}$ exposure in Ljubljana. However, it should also be noted that even short durations of commuting can pose a significant threat to health due to the high levels of air pollution in traffic and repeated exposure during daily commutes, particularly during rush hours (Cole-Hunter et al., 2012; Kaur et al., 2007).

The average difference ratio between the pedestrians and the cyclists involved in this study was 3.2, while the difference between adult men and adult women daily commuters was 1.3. Other studies have also reported significant differences in exposure between different modes of transport. For instance, de Nazelle et al. (2012) and Bergmann et al. (2021) reported an average difference ratio of 2–3 between cycling and car transport, while Int Panis et al. (2010) found that cycling commuters' exposure to traffic exhausts was 4.3 times higher than that of car passengers. Qiu et al. (2019) also reported a 1.3 ratio difference between adult women and adult men cyclists, mainly attributed to differences in breathing frequency and volume of inhaled/exhaled air, as men (59.1 L/min) inhale about 17 % more air than women (46.2 L/min) (Hofman et al., 2018). Present research found that average travel exposure to $PM_{2.5}$ varied from 1.66 µg/m^3 to 78.71 µg/m^3, depending on the exposure duration, with an average value of 11.52 µg/m^3 for the average commuting time of Slovenian citizens (52 min/day) and 23.72 µg/m^3 for

the average time spent outdoors (106.2 min/day). These values did not exceed the WHO's air quality guidelines. Average travel exposure was highest in the evening and night for all sampling periods, ranging from 4.81 μg/m^3 to 78.71 μg/m^3. Compared to the results of other studies conducted in the EU, present research founds that cyclists in Ljubljana were found to be exposed to lower $PM_{2.5}$ values. For example, a study in three Belgian towns (Brussels, Louvain la Nueve and Mol) in June 2009 found higher average $PM_{2.5}$ values of 27.2 μg/m^3 for cyclists (Int Panis et al., 2010), while cyclists in 11 Dutch cities between August and October 2006 were found to be exposed to average $PM_{2.5}$ values of 44.5 μg/m^3 (Boogaard et al., 2009). Similarly, cyclists in Arnhem in the Netherlands between June 2007 and June 2008 were exposed to an average $PM_{2.5}$ value of 68.7 μg/m^3 (Zuurbier et al., 2010), while those in Barcelona in May and June 2009 were exposed to an average of 35 μg/m^3 (de Nazelle et al., 2012). The current study also found that personal exposure to $PM_{2.5}$ was lower than the dynamic mobile measurements yielded in Stuttgart in Germany between February and July 2018, which ranged between 15.1 μg/m^3 and 40 μg/m^3 during rush hour and between 10.1 μg/m^3 and 15 μg/m^3 at other times (Samad and Vogt, 2020). Among the main reasons why cyclists are exposed to relatively high levels of air pollutants are their elevated inhalation rates and increased physical exertion compared to sedentary modes of transport, such as driving and taking the bus or train. Indeed, several studies (Bigazzi and Figliozzi, 2014; Int Panis et al., 2010; de Nazelle et al., 2017; Salma et al., 2002) have indicated that the mode of commuting can have a significant impact on personal exposure $PM_{2.5}$ concentrations in traffic environments (Huang et al., 2012). Additionally, the higher deposition rate observed during maximum exertion levels is partly due to the switch from nose-only breathing to combined nose-and-mouth breathing (Salma et al., 2002).

3.5. Perceived impact of air pollution

Cycling, an active mode of transport, is an effective means of reducing traffic congestion and related air pollution, while also promoting better health (Qiu et al., 2019). However, the benefits of cycling can be negated by air pollution, which emphasises the need for personal evaluations of $PM_{2.5}$ exposure in order to determine safe urban microenvironments with limited air pollution exposure. In Slovenia, where 80.5 % of adolescent individuals are active and thus very likely to commute via active modes of transport (World Health Organization (WHO), 2023), $PM_{2.5}$ monitoring results showed elevated levels of $PM_{2.5}$ pollution in Ljubljana and the existence of air pollution hotspots near local pollution sources. The volunteers who participated in the monitoring study rode a bicycle four times a week or more during both summer (76 %) and winter (70 %). The majority of participants (56 %) rated the air quality in Ljubljana as poor and also incorrectly identified the major sources of air pollution, indicating the importance of such campaigns in raising awareness about air pollution challenges. Indeed, the respondents tended to believe that traffic (65 %) represents the primary source of air pollution in Ljubljana, followed by small individual fireplaces (9 %), construction sites (9 %), industrial and agricultural emissions (9 %) and cigarette smoke (9 %). It is particularly concerning that the majority of volunteers (81 %) had not received any information about air pollution in previous years. Of utmost importance, nearly all of the participants (94 %) expressed their willingness to modify their travel patterns to minimise air pollution and avoid congested roads if infrastructure allowed it. Previous studies have also reported cyclist would adapt to more effective and less congested routes to lower their exposure to pollutants (Cole-Hunter et al., 2015), and would deviate from their most direct route by up to 10 % (Broach et al., 2012). Cyclists experience lower levels of pollution when using open bike lanes and street intersections with superior ventilation as well as when cycling infrastructure is separated from the main road, resulting in decreased exposure to pollutants (Cole-Hunter et al., 2013; Hofman et al., 2018; Qiu et al., 2019; Samad et al., 2021). Heavy traffic intersections, underpasses, roundabouts and bus stops where vehicles start and accelerate frequently tend to manifest the highest concentrations, exposing cyclists to even greater risk due to long wait times (Qiu et al., 2019). Additionally, vegetation acts as a buffer between cyclists and vehicles, providing further protection against exposure (MacNaughton et al., 2014).

4. Conclusions

Assessing exposure risk to air pollutants in urban microenvironments is crucial to ensure the safety of groups that are vulnerable to traffic, such as cyclists and pedestrians. Accurate evaluations of air pollution exposure risks are important for hazard mitigation and potentially for making alterations to regulatory management and infrastructure to minimise and reduce $PM_{2.5}$ health risks. Dynamic monitoring campaigns accompanied by citizens' initiatives deploying low-cost sensors can supplement official AQMS and provide high temporal and spatial distribution air pollution data to enable more efficient regulatory frameworks. While monitoring campaigns using validated LCS are effective tools for self-regulated and self-assessed personal air pollution exposure and hotspot identification, in the future, standardised evaluation methods and mobile monitoring protocols to support policy makers and decision makers should be addressed before large-scale deployment. In addition, citizens' daily activities and behaviour patterns should be included in air quality monitoring approaches to significantly reduce air pollution levels in urban microenvironments. Based on the data obtained through monitoring, citizens have the capacity to make more health-conscious choices by selecting routes located at a greater distance from high-traffic roads and outside the timeframes of higher $PM_{2.5}$ levels, thereby reducing their exposure to $PM_{2.5}$. Furthermore, such data can serve as an instrument in enhancing urban planning processes, with a specific focus on mitigating the exposure of active daily commuters (cyclists and pedestrians), through the strategic development of cycling infrastructure that is physically separated from roadways and interspersed with green spaces. Additionally, due to the prevalent utilisation of wood as a fuel source, resulting in elevated concentrations of $PM_{2.5}$ in Ljubljana, it is imperative to organise periodic public awareness campaigns aimed at promoting proper maintenance for fireplaces, as well as the adoption of high-quality and dry wood as fuel, with regular quality standards and requirement verifications.

Supplementary data to this article can be found online at https://doi.org/10.1016/j.scitotenv.2023.169117.

CRediT authorship contribution statement

Anja Ilenič: Conceptualization, Methodology, Data curation, Visualization, Writing – original draft. **Alenka Mauko Pranjić:** Conceptualization, Writing – review & editing, Supervision. **Nina Zupančič:** Data curation, Visualization, Writing – review & editing. **Radmila Milačič:** Writing – review & editing. **Janez Ščančar:** Writing – review & editing, Supervision.

Declaration of competing interest

The authors declare that they have no known competing financial interests or personal relationships that could have appeared to influence the work reported in this paper.

Data availability

Data will be made available on request.

Acknowledgements

The authors would like to thank all the volunteers who conducted the $PM_{2.5}$ measurements contributing to this study. This research was

funded by the Slovenian Research Agency, financial support programme groups P2-0273, P1-0143 and P1-0008, EIT Urban Mobility under Subgrant Agreement No. SGA22368.

References

Aleixandre, M., Gerboles, M., 2012. Review of Small Commercial Sensors for Indicative Monitoring of Ambient Gas, 30.

Alfano, B., Barretta, L., Del Giudice, A., De Vito, S., Di Francia, G., Esposito, E., Formisano, F., Massera, E., Miglietta, M.L., Polichetti, T., 2020. A review of low-cost particulate matter sensors from the developers' perspectives. Sensors 20. https://doi.org/10.3390/S20236819. Page 6819 20(23):6819.

ARSO, 2021. "Air Quality in Slovenia in 2021." *Ministry of the Environment, Climate and Energy*. Retrieved April 15, 2023. https://www.arso.gov.si/zrak/kakovostzraka/poročila in publikacije/Letno_porocilo_2021_Final.pdf.

ARSO, 2023. Air Pollution. Retrieved April 10, 2023. https://www.arso.gov.si/en/soer/air_pollution.html.

Benčina, M., Gorenc, T., 2021. POZOR: Tukaj Je Dihanje Nevarno! Ljubljana, Društvo Fokus.

Bergmann, M.L., Andersen, Z.J., Amini, H., Ellermann, T., Hertel, O., Lim, Y.H., Loft, S., Mehta, A., Westendorp, R.G., Cole-Hunter, T., 2021. Exposure to ultrafine particles while walking or bicycling during COVID-19 closures: a repeated measures study in Copenhagen, Denmark. Sci. Total Environ. 791 https://doi.org/10.1016/j.scitotenv.2021.148301.

Bergmann, M.L., Andersen, Z.J., Amini, H., Khan, J., Lim, Y.H., Loft, S., Mehta, A., Westendorp, R.G., Cole-Hunter, T., 2022. Ultrafine particle exposure for bicycle commutes in rush and non-rush hour traffic: a repeated measures study in Copenhagen, Denmark. Environ. Pollut. 294 https://doi.org/10.1016/j.envpol.2021.118631.

Bigazzi, A.Y., Figliozzi, M.A., 2014. Review of urban Bicyclists' intake and uptake of traffic-related air pollution. Transp. Rev. 34 (2), 221–245. https://doi.org/10.1080/01441647.2014.897772.

Boogaard, H., Borgman, F., Kamminga, J., Hoek, G., 2009. Exposure to ultrafine and fine particles and noise during cycling and driving in 11 Dutch cities. Atmos. Environ. 43 (27), 4234–4242. https://doi.org/10.1016/J.ATMOSENV.2009.05.035.

Broach, J., Dill, J., Gliebe, J., 2012. Where do cyclists ride? A route choice model developed with revealed preference GPS data. Transp. Res. A Policy Pract. 46 (10), 1730–1740. https://doi.org/10.1016/J.TRA.2012.07.005.

Castell, N., Dauge, F.R., Schneider, P., Vogt, M., Lerner, U., Fishbain, B., Broday, D., Bartonova, A., 2017. Can commercial low-cost sensor platforms contribute to air quality monitoring and exposure estimates? Environ. Int. 99, 293–302. https://doi.org/10.1016/J.ENVINT.2016.12.007.

Chen, Hong, Goldberg, Mark S., Viileneuve, Paul J., 2008. A systematic review of the relation between long-term exposure to ambient air pollution and chronic diseases. Rev. Environ. Health 23 (4), 243–297. https://doi.org/10.1515/REVEH.2008.23.4.243.

Chen, Z., Chen, D., Zhao, C., Kwan, M., Cai, J., Zhuang, Y., Zhao, B., Wang, X., Chen, B., Yang, J., Li, R., He, B., Gao, B., Wang, K., Xu, B., 2020. Influence of meteorological conditions on PM2.5 concentrations across China: a review of methodology and mechanism. Environ. Int. 139, 105558 https://doi.org/10.1016/J.ENVINT.2020.105558.

Cohen, A.J., Brauer, M., Burnett, R., Anderson, H.R., Frostad, J., Estep, K., Balakrishnan, K., Brunekreef, B., Dandona, L., Dandona, R., Feigin, V., Freedman, G., Hubbell, B., Jobling, A., Kan, H., Knibbs, L., Liu, Y., Martin, R., Morawska, L., Pope, C.A., Shin, H., Straif, K., Shaddick, G., Thomas, M., van Dingenen, R., van Donkelaar, A., Vos, T., Murray, C.J.L., Forouzanfar, M.H., 2017. Estimates and 25-year trends of the global burden of disease attributable to ambient air pollution: an analysis of data from the global burden of diseases study 2015. Lancet 389 (10082), 1907–1918. https://doi.org/10.1016/S0140-6736(17)30505-6.

Cole-Hunter, T., Morawska, L., Stewart, I., Jayaratne, R., Solomon, C., 2012. Inhaled particle counts on bicycle commute routes of low and high proximity to motorised traffic. Atmos. Environ. 61, 197–203. https://doi.org/10.1016/J.ATMOSENV.2012.06.041.

Cole-Hunter, T., Jayaratne, R., Stewart, I., Hadaway, M., Morawska, L., Solomon, C., 2013. Utility of an alternative bicycle commute route of lower proximity to motorised traffic in decreasing exposure to ultra-fine particles, respiratory symptoms and airway inflammation - a structured exposure experiment. Environmental Health: A Global Access Science Source 12 (1). https://doi.org/10.1186/1476-069X-12-29.

Cole-Hunter, T., Morawska, L., Solomon, C., 2015. Bicycle commuting and exposure to air pollution: a questionnaire-based investigation of perceptions, symptoms, and risk management strategies. J. Phys. Act. Health 12 (4). https://doi.org/10.1123/jpah.2013-0122.

Crilley, L.R., Shaw, M., Pound, R., Kramer, L.J., Price, R., Young, S., Lewis, A.C., Pope, F. D., 2018. Evaluation of a low-cost optical particle counter (Alphasense OPC-N2) for ambient air monitoring. Atmos. Meas. Tech. 11 (2) https://doi.org/10.5194/amt-11-709-2018.

Dahl, A., Gharibi, A., Swietlicki, E., Gudmundsson, A., Bohgard, M., Ljungman, A., Blomqvist, G., Gustafsson, M., 2006. Traffic-generated emissions of ultrafine particles from pavement–tire interface. Atmos. Environ. 40 (7), 1314–1323. https://doi.org/10.1016/J.ATMOSENV.2005.10.029.

de Nazelle, A., Fruin, S., Westerdahl, D., Martinez, D., Ripoll, A., Kubesch, N., Nieuwenhuijsen, M., 2012. A travel mode comparison of Commuters' exposures to air pollutants in Barcelona. Atmos. Environ. 59, 151–159. https://doi.org/10.1016/J.ATMOSENV.2012.05.013.

de Nazelle, A., Bode, O., Orjuela, J.P., 2017. Comparison of air pollution exposures in active vs. passive travel modes in European cities: a quantitative review. Environ. Int. 99, 151–160. https://doi.org/10.1016/J.ENVINT.2016.12.023.

Directive 2008/50/EC. n.d. "Directive 2008/50/EC of the European Parliament and of the Council of 21 May 2008 on Ambient Air Quality and Cleaner Air for Europe".

Dominici, F., Peng, R.D., Bell, M.L., Pham, L., McDermott, A., Zeger, S.L., Samet, J.M., 2006. Fine particulate air pollution and hospital admission for cardiovascular and respiratory diseases. JAMA 295 (10), 1127–1134. https://doi.org/10.1001/JAMA.295.10.1127.

European Environmental Agency (EEA). 2022. "Europe's air quality status 2022: Briefing no. 04/2022." European Environmental Agency. Retrieved 15 April 2023. (https://www.eea.europa.eu/publications/status-of-air-quality-in-Europe-2022).

European Environmental Agency (EEA), 2023. Slovenia - air pollution country fact sheet. European Environment Agency. Retrieved 10 April 2023. https://www.eea.europa.eu/themes/air/country-fact-sheets/2021-country-fact-sheets/slovenia-1.

Giordano, M.R., Malings, C., Pandis, S.N., Presto, A.A., McNeill, V.F., Westervelt, D.M., Beekmann, M., Subramanian, R., 2021. From low-cost sensors to high-quality data: a summary of challenges and best practices for effectively calibrating low-cost particulate matter mass sensors. J. Aerosol Sci. 158 https://doi.org/10.1016/j.jaerosci.2021.105833.

Gulliver, J., Briggs, D.J., 2004. Personal exposure to particulate air pollution in transport microenvironments. Atmos. Environ. 38 (1), 1–8. https://doi.org/10.1016/J.ATMOSENV.2003.09.036.

Guzman, L.A., Beltran, C., Morales, R., Sarmiento, O.L., 2023. Inequality in personal exposure to air pollution in transport microenvironments for commuters in Bogotá. Case Stud. Transp. Policy 11, 100963. https://doi.org/10.1016/J.CSTP.2023.100963.

Hofman, J., Samson, R., Joosen, S., Blust, R., Lenaerts, S., 2018. Cyclist exposure to black carbon, ultrafine particles and heavy metals: an experimental study along two commuting routes near Antwerp, Belgium. Environ. Res. 164, 530–538. https://doi.org/10.1016/J.ENVRES.2018.03.004.

Huang, J., Furong, D., Shaowei, W., Xinbiao, G., 2012. Comparisons of personal exposure to PM2.5 and CO by different commuting modes in Beijing, China. Sci. Total Environ. 425, 52–59. https://doi.org/10.1016/J.SCITOTENV.2012.03.007.

Int Panis, L., de Geus, B., Vandenbulcke, G., Willems, H., Degraeuwe, B., Bleux, N., Mishra, V., Thomas, I., Meeusen, R., 2010. Exposure to particulate matter in traffic: a comparison of cyclists and Car passengers. Atmos. Environ. 44 (19), 2263–2270. https://doi.org/10.1016/J.ATMOSENV.2010.04.028.

Karagulian, F., Barbiere, M., Kotsev, A., Spinelle, L., Gerboles, M., Lagler, F., Redon, N., Crunaire, S., Borowiak, A., 2019. Review of the performance of low-cost sensors for air quality monitoring. Atmosphere *10*. https://doi.org/10.3390/ATMOS10090506. *Page 506* 10(9):506.

Kaur, S., Nieuwenhuijsen, M.J., Colvile, R.N., 2007. Fine particulate matter and carbon monoxide exposure concentrations in urban street transport microenvironments. Atmos. Environ. 41 (23), 4781–4810. https://doi.org/10.1016/J.ATMOSENV.2007.02.002.

Kittelson, D.B., 1998. Engines and nanoparticles: a review. J. Aerosol Sci. 29 (5–6), 575–588. https://doi.org/10.1016/S0021-8502(97)10037-4.

Kousis, I., Manni, M., Pisello, A.L., 2022. Environmental Mobile monitoring of urban microclimates: a review. Renew. Sust. Energ. Rev. 169, 112847 https://doi.org/10.1016/J.RSER.2022.112847.

Kumar, P., Morawska, L., Martani, C., Biskos, G., Neophytou, M., Di Sabatino, S., Bell, M., Norford, L., Britter, R., 2015. The rise of low-cost sensing for managing air pollution in cities. Environ. Int. 75, 199–205. https://doi.org/10.1016/J.ENVINT.2014.11.019.

Kuula, J., Mäkelä, T., Aurela, M., Teinilä, K., Varjonen, S., González, O., Timonen, H., 2020. Laboratory evaluation of particle-size selectivity of optical low-cost particulate matter sensors. Atmos. Meas. Tech. 13 (5), 2413–2423. https://doi.org/10.5194/AMT-13-2413-2020.

Kwak, J.H., Kim, H., Lee, J., Lee, S., 2013. Characterization of non-exhaust coarse and fine particles from on-road driving and laboratory measurements. Sci. Total Environ. 458–460, 273–282. https://doi.org/10.1016/J.SCITOTENV.2013.04.040.

Lewis, A., Edwards, P., 2016. Validate personal air-pollution sensors. Nature 2016 535: 7610 535 (7610), 29–31. https://doi.org/10.1038/535029a.

Liu, H.Y., Schneider, P., Haugen, R., Vogt, M., 2019. Performance assessment of a low-cost PM2.5 sensor for a near four-month period in Oslo, Norway. Atmosphere 10. https://doi.org/10.3390/ATMOS10020041. Page 41 10(2):41.

Ljubljana.info, 2021. ZANIMIVI PODATKI: Preverite, Koliko Ljudi Iz Drugih Obči Se Vozi Na Delo v Ljubljano.

Ljubljana.si, 2023. "Ljubljana v Številkah" Mestna Občina Ljubljana. Retrieved May 11, 2023. https://www.ljubljana.si/sl/o-ljubljani/ljubljana-v-stevilkah/.

MacNaughton, P., Melly, S., Vallarino, J., Adamkiewicz, G., Spengler, J.D., 2014. Impact of bicycle route type on exposure to traffic-related air pollution. Sci. Total Environ. 490, 37–43. https://doi.org/10.1016/J.SCITOTENV.2014.04.111.

Malings, C., Tanzer, R., Hauryliuk, A., Saha, P.K., Robinson, A.L., Presto, A.A., Subramanian, R., 2020. Fine particle mass monitoring with low-cost sensors: corrections and long-term performance evaluation. Aerosol Sci. Technol. 54 (2) https://doi.org/10.1080/02786826.2019.1623863.

Miao, Y., Li, J., Miao, S., Che, H., Wang, Y., Zhang, X., Zhu, R., Liu, S., 2019. Interaction between planetary boundary layer and PM2.5 pollution in megacities in China: a review. Curr. Pollut. Rep. 5 (4), 261–271. https://doi.org/10.1007/S40726-019-00124-5/TABLES/2.

Novak, R., Kocman, D., Robinson, J.A., Kanduč, T., Sarigiannis, D., Horvat, M., 2020. Comparing airborne particulate matter intake dose assessment models using low-cost portable sensor data. Sensors 20. https://doi.org/10.3390/S20051406. Page 1406 20(5):1406.

Ono-Ogasawara, M., Smith, T.J., 2004. Diesel exhaust particles in the work environment and their analysis. Ind. Health 42 (4), 389–399. https://doi.org/10.2486/INDHEALTH.42.389.

Pan, L., Xu, J., Tie, X., Mao, X., Gao, W., Chang, L., 2019. Long-term measurements of planetary boundary layer height and interactions with PM2.5 in Shanghai, China. Atmos. Pollut. Res. 10 (3), 989–996. https://doi.org/10.1016/J.APR.2019.01.007.

Qiu, Z., Wang, W., Zheng, J., Lv, Huitao, 2019. Exposure assessment of cyclists to UFP and PM on urban routes in Xi'an, China. Environ. Pollut. 250, 241–250. https://doi.org/10.1016/J.ENVPOL.2019.03.129.

Ramos, M.J., Vasconcelos, A., Faria, M., 2015. Comparison of particulate matter inhalation for users of different transport modes in Lisbon. Transport. Res. Proc. 10, 433–442. https://doi.org/10.1016/J.TRPRO.2015.09.093.

Robinson, J.A., Kontić, D., 2016. Building a wireless sensor network to capture air pollution trends in Ljubljana - added value to the citizens: Pilots, demos and experiment case. In: Smart Cities in Smart Regions 2016. Lahti.

Robinson, J.A., Novak, R., Kanduč, T., Maggos, T., Pardali, D., Stamatelopoulou, A., Saraga, D., Vienneau, D., Flückiger, B., Mikeš, O., Degrendele, C., Sáňka, O., García Dos Santos, S., Visave, J., Gotti, A., Persico, M.G., Chapizanis, D., Petridis, I., Karakitsios, S., Sarigiannis, D.A., Kocman, D., 2021. User-centred design of a final results report for participants in multi-sensor personal air pollution exposure monitoring campaigns. Int. J. Environ. Res. Public Health 18 (23). https://doi.org/10.3390/IJERPH182312544.

Rodrigues, V., Gama, C., Ascenso, A., Oliveira, K., Coelho, S., Monteiro, A., Hayes, E., Lopes, M., 2021. Assessing air pollution in European cities to support a citizen centered approach to air quality management. Sci. Total Environ. 799, 149311 https://doi.org/10.1016/J.SCITOTENV.2021.149311.

Russell, A.G., Bert, B., 2009. A focus on particulate matter and health. Environ. Sci. Technol. 43 (13), 4620–4625. https://doi.org/10.1021/es9005459.

Salma, I., Balásházy, I., Hofmann, W., Záray, G., 2002. Effect of physical exertion on the deposition of urban aerosols in the human respiratory system. J. Aerosol Sci. 33 (7), 983–997. https://doi.org/10.1016/S0021-8502(02)00051-4.

Samad, A., Vogt, U., 2020. Investigation of urban air quality by performing Mobile measurements using a bicycle (MOBAIR). Urban Clim. 33 https://doi.org/10.1016/J.UCLIM.2020.100650.

Samad, A., Melchor Mimiaga, F.E., Laquai, B., Vogt, U., 2021. Investigating a low-cost dryer designed for low-cost PM sensors measuring ambient air quality. Sensors (Basel, Switzerland) 21 (3), 1–18. https://doi.org/10.3390/S21030804.

Statistical Office of the Republic of Slovenia (SURS), 2023a. Dnevna Mobilnost Potnikov, 2021. Retrieved 4 April 2023. https://www.stat.si/StatWeb/News/Index/10324.

Statistical Office of the Republic of Slovenia (SURS), 2023b. Moški v Sloveniji. Retrieved 4 April 2023. https://www.stat.si/statweb/News/Index/6541.

Statistical Office of the Republic of Slovenia (SURS). "Prebivalstvo - Slovenske Regije in Občine v Številkah." Retrieved 4 Aprl 2023. https://www.stat.si/obcine/sl/Theme/Index/PrebivalstvoStarost.

Su, T., Li, Z., Kahn, R., 2018. Relationships between the planetary boundary layer height and surface pollutants derived from Lidar observations over China: regional pattern and influencing factors. Atmos. Chem. Phys. 18, 15921–15935. https://doi.org/10.5194/acp-18-15921-2018.

Terzic, M., 2020. Avtomobili v EU. Dnevnik (May 23).

TIBCO, 2017. Statistica. TIBCO Software Inc.

U.S. Environmental Protection Agency, 1997. Exposure Factors Handbook. Washington, DC.

World Health Organization (WHO), 2023. Physical Activity Slovenia 2022 Country Profile. Retrieved 11 April 2023. https://www.who.int/publications/m/item/physical-activity-svn-2022-country-profile.

Yang, Z., He, Z., Zhang, K., Zeng, L., de Nazelle, A., 2021. Investigation into Beijing Commuters' exposure to ultrafine particles in four transportation modes: bus, Car, bicycle and Subway. Atmos. Environ. 266, 118734 https://doi.org/10.1016/J.ATMOSENV.2021.118734.

Zhu, Y., Smith, T.J., Davis, M.E., Levy, J.I., Herrick, R., Jiang, H.. Comparing gravimetric and real-time sampling of PM2.5 concentrations inside truck cabins. https://doi.org/10.1080/15459624.2011.617234.

Zuurbier, M., Hoek, G., Oldenwening, M., Lenters, V., Meliefste, K., van den Hazel, P., Brunekreef, B., 2010. Commuters' exposure to particulate matter air pollution is affected by mode of transport, fuel type, and route. Environ. Health Perspect. 118 (6), 783–789. https://doi.org/10.1289/EHP.0901622.

Supplementary Information Article 4

Table S1: Summary statistics for measurements across four sampling periods.

Type of monitoring	Monitoring parameters	September (n = 11,250)	October (n = 18,230)	November (n = 9,295)	December (n = 8,170)
LCS SPS30	$PM_{2.5}$ ($\mu g/m^3$)	4.68 ± 4.70	18.40 ± 13.43	17.16 ± 10.63	32.31 ± 18.81
	RH (%)	50.71 ± 16.03	62.28 ± 14.91	67.36 ± 12.11	70.13 ± 17.21
	Temp (°C)	16.31 ± 5.09	13.76 ± 4.76	8.66 ± 3.82	2.06 ± 4.56
AQMS Ljubljana–Bežigrad (ARSO 2023)	$PM_{2.5}$ ($\mu g/m^3$)	6.01 ± 3.32	22.64 ± 12.36	18.02 ± 8.90	21.12 ± 13.57
	RH (%)	74.38 ± 11.33	78.00 ± 3.16	76.00 ± 5.35	84.36 ± 4.62
	Temp (°C)	14.77 ± 3.94	14.33 ± 0.89	11.17 ± 2.72	2.02 ± 2.66
	Wind (m/s)	1.32 ± 0.90	0.54 ± 0.39	0.73 ± 0.61	0.75 ± 0.39
	Precipitation (mm)	20.67 ± 48.52	0.00 ± 0.00	2.64 ± 4.89	11.69 ± 16.33
AQMS Ljubljana–Celovška (ARSO 2023)	$PM_{2.5}$ ($\mu g/m^3$)	5.28 ± 3.16	20.95 ± 11.81	15.54 ± 7.23	18.39 ± 12.88

Mean + standard deviation
$PM_{2.5}$ = particulate matter smaller than 2.5 µm in $\mu g/m^3$, RH = relative humidity in %, Temp = temperature in °C

Table S2: Percentage of data exceeding limit values of AQD and WHO AQG.

Sampling period	$PM_{2.5}$ ≥15 µg/m^3	$PM_{2.5}$ ≥37.5 µg/m^3	$PM_{2.5}$ ≥50 µg/m^3	$PM_{2.5}$ ≥75 µg/m^3
September	3.72	0.17	0.05	0.02
October	46.05	9.06	2.85	0.08
November	52.01	3.56	1.26	0.37
December	79.06	33.98	19.44	1.98

WHO AQG daily interim targets are as follows: 75 µg/m^3, 50 µg/m^3, 37.5 µg/m^3, 25 µg/m^3 and 15 µg/m^3 (EEA 2022).

Table S3: LADD (µg/kg-day) per specific activity type.

Exposure duration	Activity type		September	October	November	December
Average time commuting (h = 52 min)	Cycling	Men	0.005	0.020	0.016	0.032
		Women	0.004	0.016	0.013	0.025
	Walking	Men	0.002	0.006	0.005	0.010
		Women	0.001	0.005	0.004	0.008
Average outdoor activities (h = 106.2 min)	Cycling	Men	0.010	0.041	0.034	0.065
		Women	0.008	0.032	0.027	0.051
	Walking	Men	0.003	0.013	0.011	0.021
		Women	0.003	0.010	0.008	0.016

Table S4: Estimated reference dose (RfD) and toxicological risk (RQ).

RfD (µg/kg-day)	Cycling		Walking	
	Women	Men	Women	Men
	0.348	0.441	0.109	0.141
RQ	September	October	November	December
	0.011	0.045	0.037	0.071

3.5 Article 5: Advances in Sampling and Analytical Approaches for the Determination of Metal(oid)s and Polycyclic Aromatic Hydrocarbons Bound to Size-Fractionated Airborne Particulate Matter: A Review

Authors: Anja Ilenič, Prashant Kumar, Radmila Milačič Ščančar, Marija Đurić, Alenka Mauko Pranjić, Janez Ščančar
Manuscript submitted to Trends in Environmental Analytical Chemistry, Elsevier, under review

Action	Manuscript Number	Title	Initial Date Submitted	Status Date	Current Status
Action Links	TEACM-D-25-00130	Advances in sampling and analytical approaches for the determination of metal(oid)s and polycyclic aromatic hydrocarbons bound to size-fractionated airborne particulate matter: A review	Oct 02, 2025	Dec 10, 2025	Under Review

The review, which included 81 studies from 33 different countries published between 2010 and 2025, evaluated the current state of sampling protocols and analytical methods for the assessment of metal(oid)s and PAHs in size-fractionated PM, with particular emphasis on the gap in the simultaneous multi-pollutant characterisation of ultrafine particulate matter (PM <0.1 µm). Among the reviewed studies, 52% focused on the characterisation of pollutants bound to $PM_{2.5}$, followed by PM_{10} (30%) and PM_1 (13%), while only 5% investigated PM smaller than 0.1 µm, a fraction which can penetrate the deepest into the cell tissues and circulatory system and is highly prevalent in the atmosphere. Simultaneous characterisation of both pollutant groups was rare (14% of studies) and just 32% of studies used certified reference materials for quality control and method validation, most commonly – NIST SRM 1648a. Microwave-assisted digestion and ultrasound-assisted extraction were commonly used for sample preparation prior to the determination of metal(oid)s and PAHs, by inductively coupled plasma mass spectrometry and gas chromatography-mass spectrometry, respectively. The most commonly used filter media were QFFs (65% of studies), followed by PTFE (16%) and GFF (12%), differing in sampling efficiency, mechanical, chemical and temperature stability, blank concentrations, flow resistance and artefacts formation. Both pollutant groups exhibited strong seasonal variability, with elevated concentrations observed during heating periods. Among metal(oid)s, As, Cd, Cr, Ni and Pb were most abundant and traffic-derived pollutants in (ultra)fine PM, showing high bioaccessibility due to their high affinity for adsorption of toxic substances, the occurrence of metals in the free state and their high solubility potential. Smaller PM fractions were mainly associated with anthropogenic sources, such as fossil fuel combustion, traffic emissions, industrial processes and waste incineration, while coarse PM primarily reflected naturally-derived crustal material. Similarly, PM-bound PAHs showed strong seasonal fluctuations, with fine and UFP enriched in HMW PAHs emitted from fossil fuel combustion, biomass burning and traffic. Seasonal and diurnal patterns were influenced by meteorological factors, atmospheric stability and photochemical processes, with BaP, DahA, BaA, BbF and BkF often exceeding health guideline limits, representing high carcinogenic risks. HMW PAHs were more prevalent than LMW PAHs due to their lower volatility corresponding to higher adsorption capacity of toxic substances. Overall, the findings highlight the importance of uniform and comprehensive chemical characterisation

protocols for UFPs, to ensure reliable data and support the development of effective urban air quality control strategies aimed at mitigating emissions.

Advances in sampling and analytical approaches for the determination of metal(oid)s and polycyclic aromatic hydrocarbons bound to size-fractionated airborne particulate matter: A review

Anja Ilenič[1,2*], Prashant Kumar[3,4], Radmila Milačič Ščančar[2,5], Marija Đurić[1], Alenka Mauko Pranjić[1], Janez Ščančar[2,5]

*corresponding author: Anja Ilenič (anja.ilenic@zag.si); Dimičeva ulica 12, 1000 Ljubljana, Slovenia

[1]Slovenian National Building and Civil Engineering Institute (ZAG), Dimičeva ulica 12, 1000 Ljubljana, Slovenia

[2]Jožef Stefan International Postgraduate School, Jamova cesta 39, 1000 Ljubljana, Slovenia

[3]Global Centre for Clean Air Research (GCARE), School of Engineering, Civil and Environmental Engineering, Faculty of Engineering and Physical Sciences, University of Surrey, GU2 7XH Guildford, United Kingdom

[4]Institute for Sustainability, University of Surrey, GU2 7XH Guildford, United Kingdom

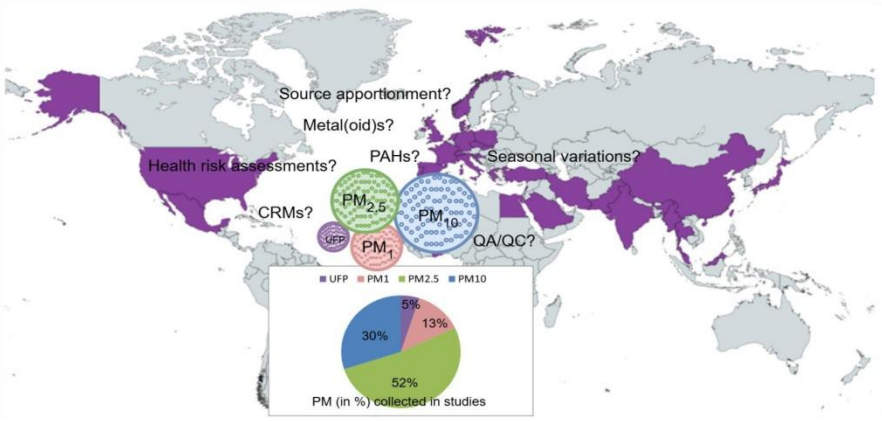
[5]Institute Jožef Stefan, Jamova cesta 39, 1000 Ljubljana, Slovenia

ABSTRACT

This review highlights a significant gap in the simultaneous multi-pollutant characterisation of ultrafine particulate matter (PM <0.1 µm), particularly regarding metal(oid)s and polycyclic aromatic hydrocarbons (PAHs). Fractionation mechanisms, sampling protocols and analytical methods are examined with an emphasis on integrating quality assurance measures to ensure high-quality data and facilitate cross-study comparability. Studies published between 2010 and 2025 demonstrated that research has largely focused on chemical assessment of pollutants bound to $PM_{2.5}$ or PM_{10}. Only 5% of studies addressed ultrafine particles (UFPs), which have the highest toxicological impacts. Simultaneous characterisation of both pollutant groups was rare (14% of studies) and just 32% of studies used certified reference materials for quality control and method validation. Microwave-assisted digestion and ultrasound-assisted extraction were commonly used for sample preparation prior to the determination of metal(oid)s and PAHs, by inductively coupled plasma mass spectrometry and gas chromatography-mass spectrometry, respectively. Both pollutant groups exhibited strong seasonal variability, with elevated concentrations observed during heating periods. They were associated with fine PM and UFPs, fractions that exhibit high bioaccessibility. Smaller PM fractions were mainly associated with anthropogenic sources, including fossil fuel and biomass combustion, traffic emissions and industrial processes, while coarse PM primarily reflected naturally-derived crustal material. Overall, these findings highlight the importance of uniform and comprehensive chemical characterisation protocols for UFPs, to ensure reliable data and support the development of effective urban air quality control strategies aimed at mitigating emissions.

Keywords:

Particulate matter, Sampling protocol, Analytical method, Polycyclic aromatic hydrocarbons, Metal(oid)s



1. Introduction

Particulate matter (PM) is among the most prevalent primary airborne pollutants and represents a significant health and environmental risk, particularly in urban and densely populated areas [1–4]. Its toxicological and environmental implications are strongly dependent on PM size, chemical composition, water affinity and optical properties, such as light scattering and absorption [5]. Both atmospheric and biological behaviour primarily depend on PM chemical composition and particle size [6–8]. Therefore, the systematic classification of particles based on their aerodynamic diameter is considered one of the most important parameters.

Total suspended particles (TSP with aerodynamic diameter 50–100 µm) and coarse particles (PM_{10} with aerodynamic diameter <10 µm) tend to deposit in the upper respiratory tract, in the nasopharynx, while fine particles ($PM_{2.5}$ with aerodynamic diameter <2.5 µm and PM_1 with aerodynamic diameter <1 µm) and ultrafine particles (UFP, PM with aerodynamic diameter <0.1 µm) behave similarly to gas molecules, enabling them to reach terminal bronchioles and alveoli, cross the pulmonary blood-air barrier and translocate further into cell tissue and possibly cause damage to the nervous system [9–12]. The accumulation of PM in the respiratory system is associated with impaired pulmonary and cardiovascular functions, including stroke and lung cancer, neuroinflammation, neurons apoptosis, induced oxidative

stress and dopaminergic neurotoxicity, deterioration of cognitive function and altered brain development [10,13–17]. In addition, increased PM concentrations also disrupt aquatic and terrestrial ecosystems, cause soil acidification, nutrient depletion, eutrophication, reduced biodiversity, crop and forest damage and contribute to acid rain formation [1,4,9,18]. Outdoor air pollution with PM is classified as a Group 1 carcinogen [19,20], with bound PM pollutants, such as metal(oid)s and polycyclic aromatic hydrocarbons (PAHs) representing the greatest risk [21,22].

Metal(oid)s, such as arsenic (As), cadmium (Cd), nickel (Ni) and lead (Pb) are persistent, non-degradable and recognised as genotoxic carcinogens [23]. They accumulate in fatty tissues, have high bioaccumulation potential, can impair organ and endocrine functions and induce DNA mutations [24,25]. Due to their atmospheric stability, certain elemental ratios serve as reliable tracers of emission sources from combustion, non-exhaust traffic emissions and mineral dust re-suspension [7,20,26–31].

PAHs are semi-volatile organic pollutants that exhibit carcinogenic, mutagenic and immunosuppressive properties [12,32,33]. They are formed mostly by incomplete combustion of organic matter (e.g. coal, natural gas or oil) or pyrolysis, with main urban sources associated with municipal and domestic emissions [12,33,34]. In the atmosphere, PAHs partition based on volatility, with low-molecular-weight (LMW) PAHs (2−3 rings) occurring predominantly in the gaseous phase, while high-molecular-weight (HMW) PAHs (4 or more benzene rings) exhibiting lower vapour pressures, absorb to PM, with carcinogenicity increasing with molecular weight [33,35]. More than 95% of HMW PAHs are bound to PM <3 μm [7,36,37]. The United States Environmental Protection Agency (US EPA) has classified 16 unsubstituted PAHs as priority pollutants, of which benzo(a)anthracene (BaA), benzo(a)pyrene (BaP), benzo(b)fluoranthene (BbF), benzo(g,h,i)perylene (BghiP), chrysene (Ch) and indeno(1,2,3-cd)pyrene (IP) are of particular concern [38,39]. HMW PAHs also serve as characteristic markers of local and regional sources, as well as pollutant transport distances [33,40–42].

Particulate aerosol samples in urban areas are typically collected by drawing ambient air through filter materials or using inertial impaction with a pump, followed by the subsequent quantification of particle mass and its chemical components by off-site laboratory analysis [43]. Size-selective inlets in cascade sampling setups allow fractionation, with the most common cut-off points of 10 µm, 2.5 µm and 1 µm [5,18]. Conventional monitoring rely on high-volume samplers placed at fixed location, adhering to standardised quality protocols (e.g. National Ambient Air Quality Standards) to achieve low limits of detection (LOD) [5,44]. However due to easier handling, good collection efficiency and lower costs, portable low-cost and low-volume samplers are increasingly being deployed [12,43,45].

The review of past publications (Table 1) indicates that the majority of atmospheric research focused on the determination of a single-pollutant bound to PM (either metals or PAHs), emphasising their sampling protocols, analytical procedures, potential sources and health effects. However, these studies largely addressed PM_{10} and $PM_{2.5}$, leaving a gap in knowledge on UFP. Moreover, quality assurance and control (QA/QC) were often insufficiently reported, with very few studies routinely reporting the use of certified reference materials (CRMs), raising concerns about data reliability and subsequent cross-study comparability. Therefore, this review provides a comprehensive evaluation of existing sampling protocols and analytical approaches for metal(oid)s and PAHs in size-fractionated PM, with particular emphasis on QA/QC. In addition, it highlights current trends and patterns in their chemical composition, seasonal variations and spatial distribution as well as key metrics for exposure assessment, all of which are essential for evidence-based urban planning for air pollution mitigation.

Table 1: Summary of existing reviews on the sampling protocols and analytical methods for chemical characterisation of size-fractionated PM.

Study focus and topic areas covered	Reference
• Collection methods and analytical procedures for $PM_{2.5}$ and UFP characterisation	[43]
• Sources, composition, transformation processes and environmental effects of major urban aerosols	[46]

• Source apportionment of PM_{10} and $PM_{2.5}$, including metals, water-soluble and carbonaceous components	[47]
• Toxicity and major sources of PM, highlighting traffic-related emissions	[48]
• Characteristics, sources, exposure risks and health impacts of heavy metals bound to PM in Asian cities	[49]
• Characterisation, sampling and analytical methods for organic compounds in air PM samples	[50]
• Sampling, analytical and modelling approaches for health risk evaluation of metals bound to PM	[51]
• Impacts of PM composition and sources on short-term cardiovascular and respiratory health outcomes	[52]
• Sources, exposure pathways, chemical characteristics, health effects and assessment methods of PAHs bound to PM	[53]

2. Methodology

An initial search was conducted in the research database and citation indexing platform Web of Science using the keywords urban air, particulate matter, metals, polycyclic aromatic hydrocarbons. The search covered studies published from January 2010 onwards and yielded a total of 3,948 studies, which selected on the basis of various exclusion criteria (Fig. 1).

The main focus of the review was to provide a comprehensive overview of different sampling protocols, extraction methods and analytical techniques used to characterise the metal(oid)s and PAHs bound to size-fractionated PM. Therefore, studies involving real-time monitoring and receptor modelling were excluded, as well as epidemiological and toxicological studies focusing on *in vitro* effects, oxidative stress and reactions on epithelial cells and DNA changes. In addition, studies focusing exclusively on indoor pollution or using low-cost optical sensors for PM determination were excluded. Another exclusion criteria was studies focusing on phytomonitoring and PM accumulation in various green plants, trees or leaves. Following the exclusion criteria, each individual article was examined for abstract applicability and methodological suitability to fulfil the above requirements.

As a result, 81 research articles written in English were suitable for the discussion in this review. In addition, cross-referenced articles and other relevant articles were included in the manuscript.

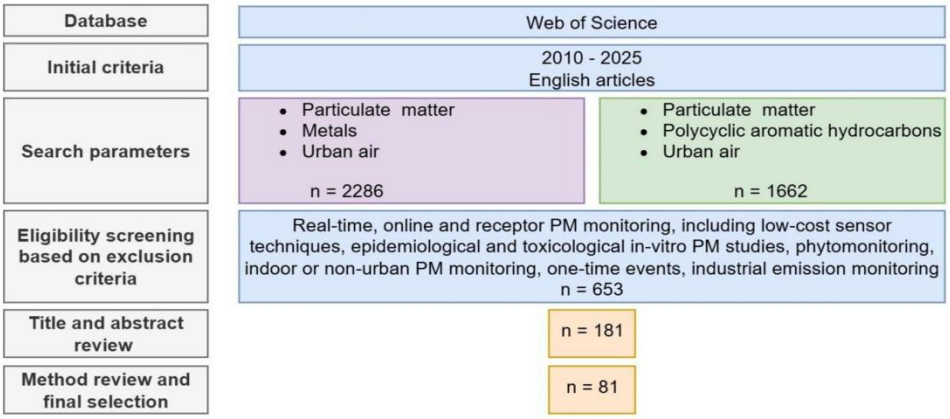


Fig. 1: Flowchart illustrating the systematic literature review process.

3. Results and discussion

3.1. Scope of the study

A total of 81 published studies from 33 different countries were included in this study, of which 62% were conducted in Asia, 32% in Europe, 4% in Africa and 2% in North America. The countries represented were Algeria, China, Croatia, the Czech Republic, Denmark, Egypt, France, Germany, Ghana, Greece, India, Iran, Italy, Japan, Lebanon, Malaysia, Mexico, Myanmar, the Netherlands, Norway, Pakistan, Poland, Portugal, Saudi Arabia, Slovakia, Slovenia, Spain, Switzerland, Taiwan, Thailand, Turkey, the United Kingdom and the United States of America (Fig. 2). The map was created using Map Chart online software.

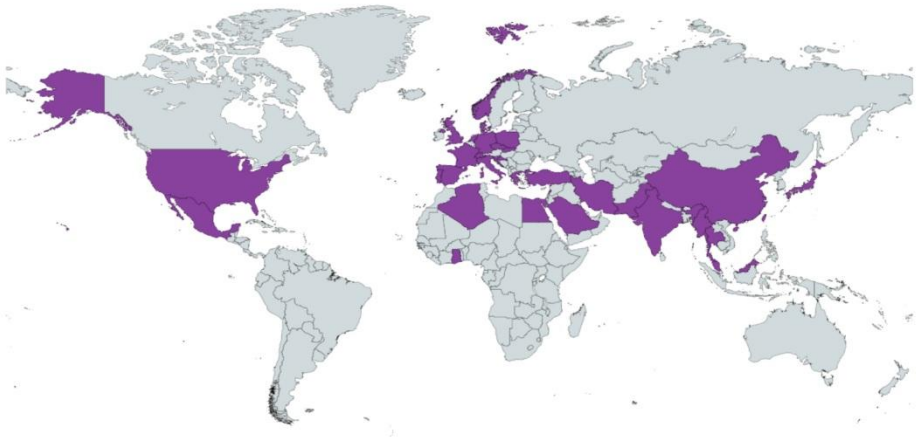


Fig. 2: Map of sampling locations from the selected studies (n = 81).

The main focus of this study was to identify the mechanisms of PM fractionation, in particular the PM fractions collected in different studies, sampling levels, sampler types and their airflow rates, filters types, extraction methods and the analytical techniques used for metal(oid)s and PAHs determination (Table 2).

Table 2: Overview of sampling and analytical techniques.

PM	Location	Sampler elevation	Time (sample number)	Sampler type	Flow rate	Filter type	Pollutant	Analysis	Method	QA/QC	CRM	Calc.	Ref.
PM_{10}, $PM_{2.5}$	Beijing, China	EL	Sep. 2015–Aug. 2016 (572)	MVS	100 L min^{-1}	GFF	Metal	ICP-MS	MAD with HNO_3, $HClO_4$	Rec.: 85–110 %	NIST SRM 1648 a	LADD, HQ, ILCR	[22]
PM_{10}	Agra, Iran	EL	Mar. 2016–Mar. 2017 (*nr*)	HVS	16.7 L min^{-1}	QFF	Metal	ICP-MS	HP with HNO_3	*nr*	*nr*	EF, LADD, DAD, HQ, ILCR, HCA, PCA	[25]
$PM_{2.5}$	Birmingham,	*nr*	Aug. 2012,	HVS	500 L min^{-1}	QFF	PAH	GC-MS	UAE with	Prec.: <10%	NIST SRM	DR	[40]

	United Kingdom		Jan. 2014 (*nr*)						DCM	Acc.: 6–25%	1649a		
PM_{10}–$PM_{<0.1}$	Ljubljana, Dobrova, Maribor, Slovenia	GL	Dec. 2023 (*nr*)	LVS	12 L min^{-1}	PTFE	Metal, PAHs	ICP-MS, GC-MS	MAD with HNO_3, HF, HCl; MS with Pet Eth and Ace	RSD: 6% for metals, 3% for PAHs, Acc.: 2% for metals, 6% for PAHs; Rec.: 96–103 %	NIST SRM 1648a	*nr*	[45]
$PM_{2.5}$	Agra, India	*nr*	Dec. 2015–Feb. 2017 (27)	LVS	16.6 L min^{-1}	QFF	Metal	ICP-OES	HP with HNO_3	RSD: 5–8%	*nr*	PCA, LADD, ILCR, HQ	[54]
$PM_{2.5}$	Bushehr Port, Iran	EL	Dec. 2016–Sep. 2017 (46)	HVS	1.4–1.6 m^3 min^{-1}	QFF	PAH	GC-MS	ASE with DCM, Ace	Rec.: 86–118 %	Yes, not specified	DR, PMF, BTA, BaP_{eq}, LADD, ILCR	[55]
$PM_{2.5}$	Florence, Italy; Athens, Greece; Oporto, Portugal	*nr*	Jan. 2013–Feb. 2014 (*nr*)	LVS, HVS	2.3 m^3 h^{-1}, 1113 L min^{-1}	QFF	PAH	GC-MS	ASE with DCM, Ace	Rec.: 57–154 %	*nr*	BaP_{eq}, ILCR, DR	[26,35,56]
$PM_{2.5}$	Gamharia, Bokaro Steel City, Ranchi, India	*nr*	Jun. 2018–May 2019 (140)	LVS	16.5 L min^{-1}	PTFE	PAH	GC-FID	SOE with DCM	Rec.: >60% RSD: <14%	*nr*	DR, ILCR, LADD, BaP_{eq}, BTA, PCA	[57]
PM_{10}	AUB, Dora, Zouk Mikael, Lebanon	EL	Jan. 2015–Jul. 2015 (36)	HVS, LVS	500 L min^{-1}, *nr*	QFF	PAH	GC-MS	SOE with Eth, Hx, ASE and MS with Tol	Rec.: 65–128% RSD: 1–8%	*nr*	COD, DR	[58]
PM_{10}	Kumasi, Ghana	GL	Jun. 2011–Sep. 2011 (32)	LVS	30 L min^{-1}	QFF	PAH	GC-MS	SOE with Ace, Hx	Rec.: 85–102%	*nr*	BaP_{eq}, ILCR, LADD, CMB, PCA	[59]
PM_{10}	Manlleu, Spain	*nr*	Winter 2013–Dec. 2022 (122)	HVS	30 m^3 h^{-1}	*nr*	Metal, PAHs	ICP-MS, ICP-OES, GC-MS	MAD with HF, HNO_3, $HClO_4$; SOE with	Er.: <10%	*nr*	PMF	[60,61]

									DCM, MeOH				
$PM_{2.5}$	Nanjing, China	EL	Jan. 2015–Dec. 2015	HVS	1000 L min^{-1}	QFF	PAH	GC-MS	ASE with DCM, MeOH	Rec.: >80%	*nr*	DR, BaP_{eq}, LADD, LLE	[62]
PM_{10}–$PM_{0.25}$	Beirut, Lebanon	GL	Jul. 2012–Aug. 2012 (*nr*)	LVS	9 L min^{-1}	QFF, PTFE	PAHs, metal	*nr*	*nr*	*nr*	*nr*	*nr*	[63]
PM_{10}	Naples, Italy	GL	Oct. 2012–Jul. 2013 (140)	LVS	2.3 m^3 h^{-1}	QFF	PAH	GC-MS	UAE with DCM	Rec.: 58–99 %	*nr*	DR, BaP_{eq}, LADD, ILCR, PCA	[64]
$PM_{2.5}$	Beijing, China; Delhi, India	EL	May 2017–Jun. 2018 (115)	HVS	1.33 m^3 min^{-1}	QFF	PAH	GC-Q-TOF-MS	ASE with MeCN	Rec.: 88–107 % RSD: 3–14%	*nr*	DR, BaP_{eq}, ILCR, RC	[65]
PM_{10}	Riyadh, Saudi Arabia	EL	Dec. 2010–Jan. 2011 (21)	HVS	1.2 m^3 min^{-1}	QFF	PAH	GC-MS	ASE with DCM	Rec.: >59%	*nr*	DR	[66]
$PM_{2.5}$	Zouk Mikael, Fiaa village, Lebanon	EL	Dec. 2018–Oct. 2019 (193)	HVS	30 m^3 h^{-1}	QFF	PAH	GC-MS	UAE with Ace, DCM	R^2: 0.93–0.99 Prec.: <14% Rec.: 82% Unc.: 9–30%	*nr*	DR	[67]
$PM_{2.5}$	Giza, Egypt	EL	Nov 2019–Feb. 2020 (59)	HVS	30 m^3 h^{-1}	QFF	PAHs	GC-MS	SOE with Ace, DCM	Rec.: 80–97 %	*nr*	DR	[68]
$PM_{2.5}$	Beijing, China	EL	Nov. 2014–Jun. 2015 (227)	HVS	1 m^3 min^{-1}	QFF	PAH	TD-GC-MS	SOE with DCM, MeOH	RSD: <15% Acc.: ±5% Prec.: <12%	NIST SRM 1649 a	DR, PMF, ILCR	[69,70]
PM_{10}–$PM_{0.05}$	Leipzig, Germany	EL	Winter 2013–Summer 2015 (42)	HVS	75 L min^{-1}	PF	Metal	TXRF	HP with HNO_3	RSD: ±5%	*nr*	EF, CMC	[27,71]
TSP, $PM_{2.5}$	Metropolitan Area of Monterrey,	*nr*	Jan. 2016–Mar. 2016 (*nr*)	HVS	*nr*	GFF	Metal	XPS, ICP-OES	MAD with HNO_3, HCl	Rec.: 85–116 %	*nr*	*nr*	[72]

	Mexico												
PM_{10}, $PM_{2.5}$	Thessaloniki, Greece	EL	Jun. 2011–Apr. 2012 (45)	LVS	2.3 m^3 h^{-1}	PTFE	Metal	ED-XRF	UAE with H_2O, C_3H_8O	Prec.: <5%	NIST SRM 2783	BTA, CMB	[73]
PM_{10}–$PM_{0.25}$	Delhi, India	EL	Jul. 2014–Jul. 2015 (90)	LVS	30 L min^{-1}, 9 L min^{-1}	QFF, PTFE	Metal, PAH	ED-XRF, GC-MS	UAE with CH_2Cl_2	Er.: <10% RSD: 75–86 %	*nr*	PCA, DR, LADD, HQ, HI	[74]
$PM_{2.5}$	Guting, Taipei, Hualien, Chiayi, Siaogang, Taiwan	*nr*	May 2015–Apr. 2018 (*nr*)	LVS	16.7 L min^{-1}	PTFE	Metal	ICP-MS	MAD with HNO_3, HF, H_3BO_3	Rec.: 75–125 % Acc.: ±20%	NIST SRM 2786	PMF, ILCR	[75]
PM_9–$PM_{0.43}$	Chiang Mai, Thailand	*nr*	May 2019–Nov. 2019 (*nr*)	LVS	28.3 L min^{-1}	QFF	PAH	GC-MS	UAE with DCM, Hx	Rec.: 91–126 % RSD: 3–11%	NIST SRM 1649 b	BaP_{eq}, ILCR	[76]
PM_{10}, $PM_{2.5}$, PM_1	Zagreb, Croatia	GL	Jan. 2013–Dec. 2013 (1095)	LVS	*nr*	QFF	PAH	HPLC	UAE with Tol, Chx	Acc.: 73–110 % Rec.: >75%	NIST SRM 1649 b	FA, LRM	[77]
PM_{10}	Kuala Lumpur, Petaling Jaya, Bangi, Malaysia	GL, EL	Sep. 2010–Apr. 2011 (53)	LVS	1.13 m^3 min^{-1}	GFF	PAH	GC-MS	UAE with DCM, MeOH	Rec.: 61–116 %	*nr*	PCA, LADD, ILCR, DR	[78]
PM_{10}, $PM_{2.5}$, PM_1	Žilina, Slovakia	*nr*	Oct. 2010–Jun. 2012 (324)	LVS	2.3 m^3 h^{-1}	NCF	Metal	ICP-MS	MS with HNO_3, HF	*nr*	*nr*	PCA, FA, APCS, MRA	[79]
PM_{10}, $PM_{2.5}$	Oslo, Finland; Helsinki, Turku, Norway; Copenhagen, Denmark; London, Oxford, United Kingdom, Rotterdam, Amsterdam, Groning	*nr*	Oct. 2008–Apr. 2011 (*nr*)	LVS	10 L min^{-1}	PTFE, GFF	PAH	GC-MS	ASE with Tol	*nr*	*nr*	*nr*	[80]

	en, Amersfoort, The Netherlands; Munich, Augsburg, Germany; Paris, France; Rome, Italy; Catalonia, Spain; Athens; Greece												
$PM_{2.5}$	Zhengzhou, China	EL	Dec. 2012–Jul. 2015 (90)	HVS	1.13 m^3 min^{-1}	QFF	Metal, PAH	ICP-MS, GC-MS	MAD with HNO_3, HCl, UAE with DCM	Rec.: 80–120 % for metals, 79–104 % for PAHs	*nr*	LADD, ILCR, DAD, HQ, HI	[81]
$PM_{2.5}$	Belluno, Conegliano, Vicenza, Venezia Mestre, Padua, Rovigo, Italy	*nr*	Apr. 2012–Mar. 2013 (360)	LVS	2.3 m^3 h^{-1}	QFF	PAH	HPLC	UAE with MeCN	Rec.: 72–125 %	ERM-CZ100 PAHs	CPF, DR, BaP_{eq}, ILCR	[82]
$PM_{2.5}$	Ankara, Turkey	*nr*	Jul. 2014–Sep. 2015 (611)	HVS	1.01–1.18 m^3 min^{-1}	QFF	PAH	GC-MS	UAE with DCM	*nr*	NIST SRM 1649 b	DR, CPF	[83,84]
PM_{10}	Volos, Greece	*nr*	Jan. 2014–Dec. 2015 (240)	LVS	2.3 m^3 h^{-1}	QFF	Metals, PAHs	ICP-MS, HPLC-FLD	MAD with HNO_3, H_2O_2; UAE with MeCN	Rec.: 95–111 % for metals, 73–125 % for PAHs	NIST SRM 1648 a	ILCR, LADD, BAP_{eq}, HQ, PCA	[85]
PM_{10}	Ciudad Real, Spain	EL	Nov. 2017–Oct. 2018 (42)	HVS	68 m^3 h^{-1}	GFF	PAH	GC-MS/MS	MAD with DCM	Rec.: 52–134 % Prec.: <30% R^2: >0.99	NIST SRM 1649 b	BaP_{eq}, ILCR, DR	[86]
$PM_{2.5}$, PM_1	Gdynia, Poland	EL	Jan. 2012–Dec. 2012 (*nr*)	LVS	2.3 m^3 h^{-1}	QFF	PAH	LC-FLD	UAE with MeCN, MeOH	Rec.: 83% Unc.: <5%	NIST SRM 2585	*nr*	[87]

PM_{10}–PM_1	Hangzhou, China	EL	Dec. 2017–Dec. 2018	*nr*	*nr*	*nr*	Metal	FAAS	*nr*	*nr*	NIST SRM 981	EF, BTA, PCA	[88]
$PM_{2.5}$	Taiyuan, China	EL	Jan. 2013 (*nr*)	HVS	1.13 m^3 min^{-1}	QFF	PAH	GC-MS	UAE with DCM	RSD: <9% Rec.: 63–128 %	*nr*	DR, BaP_{eq}	[89]
$PM_{2.5}$	Beijing, China	EL	Jan. 2014–Feb. 2014 (98)	HVS	1.03 m^3 min^{-1}	QFF	PAH, metal	GC-MS, ICP-MS	UAE with DCM, MeOH, MAD with HCl, HNO_3, HF	Rec.: >72%	*nr*	BTA, DR, PMF	[90]
$PM_{2.5}$	Beijing, China	EL	Mar. 2012–Mar. 2013 (66)	HVS	1.13 m^3 min^{-1}	QFF	PAH	GC-MS	SOE with Hx, Ace	Rec.: 83±17 %	*nr*	PMF, DR	[91]
$PM_{>9}$–$PM_{<0.4}$	Changsha, China	*nr*	Apr. 2014–May 2014 (36)	LVS	28.3 L min^{-1}	GFF	Metal	ICP-OES	MAD with HCl, HNO_3	*nr*	*nr*	LADD, HQ, ILCR	[92]
PM_{10}	France, Spain, Italy, Switzerland, UK, Portugal, Greece	*nr*	2013–2022 (16864)	*nr*	*nr*	*nr*	Metal	ICP-MS, ICP-MS/MS, PIXE, XRF	*nr*	*nr*	*nr*	*nr*	[93]
$PM_{2.5}$	Yucheng, China	*nr*	Jun. 2013 (*nr*)	MVS	100 L min^{-1}	QFF	PAH	GC-MS	ASE with DCM, Hx	Rec.: 70–125 %	*nr*	ILCR, DR, PCA, BaP_{eq}, BTA	[94]
$PM_{2.5}$	Hong Kong, China	EL	Sep. 2011–Aug. 2012 (56)	HVS	1.13 m^3 min^{-1}	QFF	PAH	GC-MS	SOE with DCM, Hx	Rec.: 80–120 %	*nr*	PMF, BaP_{eq}	[95]
$PM_{2.5}$	Harbin, China	EL	Jun. 2017–May 2018 (82)	HVS	1005 L min^{-1}	QFF	PAH	GC-MS	ASE with Hx, Ace	Rec.: 87–105 % Prec.: 9%	*nr*	DR, PMF, PSCF, ILCR, BaP_{eq}, LLE	[96]
PM_{11}–$PM_{0.54}$	Turin, Italy	EL	Autumn 2011–Winter 2012 (*nr*)	HVS	28.3 L min^{-1}	QFF	Metal	SF-ICP-MS	MAD with HNO_3, H_2O_2	Rec.: 85–115 % RSD: <5% Acc.:	NIST SRM 1648 a	EF, PCA	[97]

										<15%			
PM_{10}, $PM_{2.5}$	Thessaloniki, Greece	EL	Jul. 2011–Mar. 2012 (40)	LVS	2.3 m^3 h^{-1}	QFF	PAH	HPLC/FLD	MAD with DCM, Hx	Rec.: 87–108 % Prec.: <10%	NIST SRM 1647c	BaP_{eq}, CMB, PMF	[98]
$PM_{2.5}$	Rome, Italy	*nr*	Jul. 2013–Feb. 2014 (*nr*)	MVS	2.3 m^3 h^{-1}	PTFE, QFF	Metal	ICP-MS, ICP-OES	MAD with HNO_3, H_2O_2	Rec.: 88–98 %	NIST SRM 1648a	*nr*	[99]
PM_{10}–$PM_{0.03}$	Dunkrik, France	EL	Jan. 2012–Feb. 2012 (*nr*)	HVS	30 L min^{-1}	PF	Metal	ICP-OES, ICP-MS	MAD with HNO_3, HF, H_2O_2	Rec.: 100±15 %	NIST SRM 1648a	EF	[100]
PM_{10}	Gijon, Spain	EL	Jul. 2014 (*nr*)	HVS	30 m^3 h^{-1}	GFF, QFF	Metal	ICP-MS	MAD with HF, HNO_3, $HClO_4$	Er.: <10%	NIST SRM 1648a	BTA	[101]
$PM_{2.5}$	Ostrava - Radvanice, Czech Republic	GL	Jan. 2012–Feb. 2012 (26)	HVS	30 m^3 h^{-1}	QFF	PAH	GC-MS	UAE with DCM, Hx	Rec.: 66–93 %	*nr*	BTA, DR	[102]
PM_{10}	Hamadan, Iran	EL	Jan. 2019–Dec. 2019 (30)	HVS	30 L min^{-1}	FGF	PAH	GC-FID	UAE with MeOH, DCM	Rec.: 75–105 %	*nr*	BaP_{eq}, DR	[103]
PM_{10}, $PM_{2.5}$	Los Angeles, USA	*nr*	Sep. 2019–Feb. 2020 (*nr*)	LVS	5 L min^{-1}	PTFE	Metal	SF-ICP-MS	*nr*	*nr*	*nr*	PCA, EF, RE, LRM	[104]
PM_{10}	Shiraz, Iran	EL	Sep. 2018–Dec. 2018 (30)	HVS	1.42 m^3 min^{-1}	FGF	Metal	ICP-OES	MAD with HNO_3, $HClO_4$	Rec.: 92–105 % RSD: <5% R^2: 0.998–0.99	NIST SRM 1648	ILCR, LADD, HQ, HI, PCA	[105]
PM_{10}	Turin, Borgo San Dalmazzo, Salicento, Druento, Italy	*nr*	Jan. 2011–Dec. 2011 (140)	LVS	2.3 m^3 h^{-1}	QFF	Metal	ICP-MS	MAD with HNO_3, H_2O_2	Rec.: 80–120 %, RSD: <5%	NIST SRM 1648a	PCA, FA, HCA, EF	[106]
PM_{10}	Jalgaon, Bhusaval, Pachora	EL	Mar. 2023 (24)	*nr*	*nr*	*nr*	Metal	ICP-OES	MAD with HNO_3, HCl,	RSD: <10%, Er.: <10%	*nr*	LADD, ILCR, PCA	[107]

	, India												
PM_{10}	Beijing, Tianjin, Jinzhong, Qingdao, China	EL	Apr. 2014–Mar. 2015 (*nr*)	*nr*	*nr*	QFF	Metal	ICP-MS	MAD with HNO_3, HCl, $HClO_4$	Rec.: 78–113 %	SRM GSS 16	LADD, HQ, HI, ILCR, PCA	[108]
$PM_{2.5}$	Gdansk, Diabla Gora, Katowice, Poland	EL	Jan. 2010–Dec. 2010 (1079)	HVS, LVS	*nr*	QFF	Metal, PAH	ETAAS, FAAS, ICP-OES, HPLC	MAD with HNO_3, HF, $HClO_4$, H_2O, HCl; ASE with DCM	Rec.: 91–101 % for metals, 92% for PAHs	NIST SRM 1648 a, NIST SRM 1649 b	BTA, EF	[109]
$PM_{2.5}$	Karachi, Pakistan	EL	Nov. 2010–Jun. 2011 (*nr*)	HVS	16.7 L min^{-1}	PTFE	Metal	ED-XRF	*nr*	*nr*	*nr*	EF, PMF, BTA	[110, 111]
$PM_{2.5}$	Delhi, India	EL	Apr. 2013–Mar. 2014 (*nr*)	LVS	5 L s^{-1}	PTFE	PAH	GS-MS	*nr*	*nr*	*nr*	ILCR, LLE	[112]
PM_{9}–$PM_{0.43}$	Shenyang, Xianghe, Xinglong, Yantai, Fukang, Yucheng, Chongqing, Changsha, Lhasa, Dinghushan, China	*nr*	Jan. 2013–Dec. 2014 (52)	LVS	28.3 L min^{-1}	QFF	PAH	GC-MS	UAE with DCM, MeOH	Rec.: 75–120 % RSD: <10%	*nr*	BaP_{eq}, ILCR	[113]
PM_{10}, $PM_{2.5}$	Chengdu, China	*nr*	2011–2012 (192)	MVS	100 L min^{-1}	QFF	PAH	GC-MS	SOE with Tol	Rec.: 74–113 %	*nr*	BaP_{eq}, UNMIX, DR	[114]
$PM_{2.5}$	Isfahan City, Iran	*nr*	Mar. 2014–Mar. 2015 (*nr*)	HVS	16.6 L min^{-1}	GFF	Metal	ICP-MS	HP with HF, HCl, HNO_3	*nr*	*nr*	PCA	[115]
PM_{10}, $PM_{2.5}$, PM_{1}	Algiers, Algeria	*nr*	Jan. 2015–Nov. 2016 (186)	HVS	1.1 m^3 min^{-1}	GFF	Metal	XRF	*nr*	Rec.: 92–109 % Prec.: <20%	*nr*	PCA, BTA	[116]

$PM_{2.5}$	Lanzhou, China	EL	Dec. 2012–Jul. 2013 (68)	HVS	1.13 m^3 min^{-1}	QFF	Metal, PAH	ICP-MS, ICP-OES; GC-MS	MAD with HCl, HNO_3; UAE with DCM	Rec.: 93–105 %, Prec.: <5%, RSD: 5–10% for PAHs	*nr*	PMF, EF, BTA	[117]
$PM_{2.5}$	Taipei, Taiwan	GL	Jan. 2021–Sep. 2021 (52)	HVS	1.13 m^3 min^{-1}	QFF	PAHs	GC-MS	UAE with DCM, Hx	Rec.: 80–111 %	*nr*	PMF, PSCF, CWT, BTA, BAP_{eq}, ILCR	[118]
$PM_{2.5}$	Thessaloniki, Greece	EL	Jun. 2011–May 2012 (149)	LVS	2.3 m^3 h^{-1}	QFF	Metal, PAH	ETAAS, GC-MS	UAE with DCM; MAD with acids	*nr*	*nr*	BaP_{eq}, DR	[119]
$PM_{2.5}$	Athens, Greece	*nr*	Dec. 2018–Jul. 2021 (217)	HVS	500 L min^{-1}	QFF	PAH	GC-MS	ASE with DCM, Hx	Rec.: 96±10 %	*nr*	PMF, ILCR, DR, BaP_{eq}	[120]
$PM_{2.5}$	Yangon, Myanmar	EL	Dec. 2016–Apr. 2017 (72)	MVS	0.3 m^3 h^{-1}	*nr*	PAH	GC-MS	UAE	Rec: 70–110 %	*nr*	DR, ILCR, BAP_{eq}, PMF	[121]
$PM_{2.5}$	Chendu, China	EL	Jan. 2023–Feb. 2023	HVS	16.7 L min^{-1}	PTFE	Metal	XRF	*nr*	*nr*	*nr*	CMC, WRF-Chem, BTA, CWT, PMF	[122]
$PM_{2.5}$	Tangshan, China	EL	Apr. 2014–Feb. 2015 (39)	HVS	100 L min^{-1}	QFF	PAH	HPLC	UAE with DCM, Hx	Rec.: 58–105 %	*nr*	BaP_{eq}, ILCR, PCA	[123]
$PM_{2.5}$	Jinan, China	EL	Jun. 2015–Jul.2015 (20)	HVS	100 L min^{-1}	QFF	PAH	GC-MS	SOE with DCM	Rec.: 97±15 %	*nr*	DR, BaP_{eq}, ILCR	[124]
$PM_{2.5}$	Beijing, China	EL	Aug. 2014–Dec. 2014 (74)	HVS	100 L min^{-1}	QFF	PAH	HPLC	UAE with MeCN	Rec.: 70–130 %	*nr*	PMF, BaP_{eq}	[125]
$PM_{2.5}$	Guangzhou, China	*nr*	May 2012–May 2013 (24)	HVS	1.05 m^3 min^{-1}	QFF	PAH	GC-MS	SOE	R^2: >0.99 RSD: <15%	*nr*	DR	[126]
PM_{10}, $PM_{2.5}$	Xi'an, China	EL	Dec. 2016–Nov.	HVS	100 L min^{-1}	GFF	PAH	GC-FID	UAE with Hx, Ace	Rec.: 75–111 %	*nr*	DR, PMF, BaP_{eq}	[127]

			2017 (132)									, ILCR	
$PM_{2.5}$	Xi'an, China	*nr*	Jun. 2013–Dec. 2013 (568)	LVS	5 L min^{-1}	QFF	PAH	TD-GC-MS	*nr*	*nr*	NIST SRM 1649 a	BaP_{eq}, ILCR, DR, PMF	[128]
$PM_{>2.1}$, $PM_{<2.1}$	Shanghai, China	EL	Aug. 2013–Jan. 2018 (37)	LVS	28.3 L min^{-1}	QFF	PAH	HPLC	UAE with NaOH, H_2SO_4	Rec.: 80−103 %	*nr*	BaP_{eq}, ILCR, DR, PCA, BTA	[129]
$PM_{2.5}$	Kirishima, Japan	EL	Jul. 2017–Feb. 2018 (*nr*)	LVS	3 L min^{-1}	QFF	PAH	HPLC	UAE	*nr*	*nr*	BaP_{eq}, PCA, DR	[130]
$PM_{>9}$−$PM_{<0.4}$	Beijing, Dunhuang, Hefei, Hailun, Kunming, Qianyanzhou, Sanya, Shapotou, Taiyuan, Tongyu, Wuxi, Xishuangbanna, China	*nr*	Oct. 2012–Sep. 2013 (294)	LVS	28.3 L min^{-1}	QFF	PAH	GC-MS	UAE with DCM, Hx	Rec.: 67−138 %	NIST SRM 1649 b	BaP_{eq}, DR, ILCR, PMF	[131]
$PM_{2.5}$	Wuhan, China	EL	Oct. 2011–Jul. 2012 (168)	MVS	100 L min^{-1}	QFF	Metal, PAH	ICP-OES, GC-MS	HP and UAE with HNO_3, $HClO_4$; UAE with DCM, MeOH	Rec.: 88−95 %for metals, 80−112 % for PAHs	*nr*	BTA, CMB	[132]
$PM_{2.5}$	Xi'an, China	*nr*	Jun. 2013 (72)	LVS	5 L min^{-1}	QFF	PAH	TD-GC-MS	*nr*	RSD: 6−20% R^2: >0.99	*nr*	COD, DR, ILCR, BaP_{eq}	[133]
PM_{10}, $PM_{2.5}$	Hefei, China	EL	Oct. 2016–Jan. 2017 (56)	MVS	*nr*	PTFE	Metal	XRF	*nr*	*nr*	*nr*	EF	[134]

Glossary: nr (not reported), EL – elevated level of the sampler; GL – ground level of the sampler, Calc. (calculations), Ref. (reference), RSD (relative standard deviation), Rec. (recovery), Prec. (precision), Acc. (accuracy), Er. (error), R^2 (coefficient of determination), Unc. (uncertainty).

3.2. Sampling methods for PM collection

Most studies reported sampling of $PM_{2.5}$ (52%), followed by PM_{10} (30%) and PM_1 (13%). Only 5% of the 81 studies reported sampling of PM smaller than 0.1 µm (Fig. 3), despite UFP being the most prevalent fraction, representing approximately 90% of the total PM number, followed by fine particles (~9%) and coarse particles, which contribute less than 1% [135].

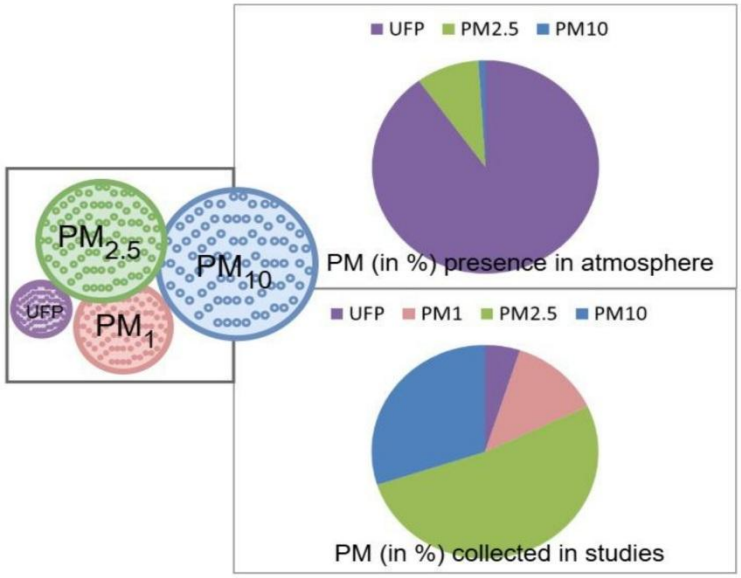


Fig. 3: Comparison of PM fractions present in the atmosphere and those reported studies.

The majority of studies (87%) installed PM samplers at elevated levels (EL; above 2.5 m, e.g. on building roofs), which are not representative of the area and breathing zones where commuters reside. Due to the low mass that accumulates on filters, a constant flow is required for longer periods of time [18]. Therefore, particulate aerosol samplers are categorised as high-volume samplers (HVS; 1000 L min^{-1}), medium-volume samplers (MVS; 100 L min^{-1}) and low-volume samplers (LVS; 20 L min^{-1}). HVS are the most widely used

(51%) as they allow adequate sample deposition on the filter media for detecting compounds at lower LODs, but may reduce the adsorption capacity of filters and increase the likelihood of filter clogging. LVS are therefore recognised as more suitable for quantifying personal emission exposures as their flow rates are more in line with commuter inhalation rates (6 L min^{-1}) [5,136–141].

PAHs were analysed in 56% of the selected studies and metal(oid)s in 31%, while 14% of the studies measured both pollutants simultaneously, indicating on a significant gap in comprehensive PM chemical characterisation.

3.3. Analytical methods for airborne pollutant determination

Prior to PM sample collection, it is essential to identify the nature of the pollutants bound to PM in order to select appropriate analytical procedure, including the types of filter, pollutant extraction methods, solvents used and analytical techniques to obtain reliable data on the chemical composition of size-fractionated PM samples. The main challenges of analytical procedures include the identification and determination of species in the sample, separation of the species, determination of low concentrations with adequate precision and accuracy, and effective elimination of matrix effects [142]. Therefore, ensuring the accuracy of analytical procedures and results by selecting high-resolution and sensitive techniques along with the use of CRMs is essential [47,138,143,144].

Only 32% of studies reported their use, namely National Institute of Standards and Technology (NIST) standard reference material (SRM) 1648a (10 studies), NIST SRM 1649b (6 studies), NIST SRM 1649a (3 studies) and NIST SRM 2783, NIST SRM 2786, ERM-CZ100 PAHs, NIST SRM 2585, NIST SRM 1647c, SRM GSS16, NIST SRM 981, with one study reporting each. Although, the majority of studies included in this review were conducted in Asia, CRMs were predominantly applied in European research, particularly United Kingdom, Greece, Croatia, Spain, Poland, Slovenia, Italy and France. In Asia, CRMs were reported in studies from Iran, China, Taiwan, Turkey and Thailand.

Overall, 82% of studies included QA/QC in their methods. When selecting suitable filter media for compliance measurements, several characteristics are important, including particle sampling efficiency, mechanical, chemical and temperature stability, blank concentrations, flow resistance and loading capacity to obtain the adequate PM deposits, as well as cost efficiency and availability. Potential positive or negative artefacts due to gas adsorption or particle volatilisation may also affect mass balance and chemical composition [5].

In general, membrane filters have a higher flow resistance and a lower loading capacity than fiber filters [5]. The most common filters used are cellulose filters (CF; fibrous, hydrophobic), glass fiber filters (GFF; fibrous, hydrophobic), mixed cellulose filters (MCE; membrane, hydrophilic), polycarbonate filters (PF; membrane, hydrophobic), polyvinyl chloride filters (PVC; membrane, hydrophobic), polytetrafluoroethylene filters (PTFE; membrane, hydrophobic) and quartz fiber filters (QFF; fibrous, hydrophobic) [3].

The choice of filter depends on the nature of the pollutants (organic, inorganic), which in turn determines the subsequent analysis. Overall, QFF were the most commonly used in all selected studies (65%), followed by PTFE (16%) and GFF (12%). The use of PF and fiberglass fabric filters (FGF) was reported in two studies, while nitrocellulose membrane filters (NCF) were employed in a single study for PM filtration. Several studies reported on the simultaneous use of QFF and PTFE or PTFE and GFF. GFF are often used with HVS systems due to their high collection efficiency and low airflow resistance. However, due to their poor chemical stability and relatively high content of certain trace element impurities, their use is limited to areas with relatively high levels of air pollution [5,6,145–147]. CF and PF exhibit the lowest particle sample efficiency, with values below 50% [148,149]. Compared to QFF and PTFE, GFF offer the highest mechanical strength and are the most cost-effective, but also require pre-treatment (baking at >500 ˚C) prior to sampling to remove adsorbed organic vapours [5]. PTFE filters are the most chemically inert, exhibit minimal blank values and low hygroscopicity, but are unsuitable for elemental and organic carbon analysis (EC/OC) due to the high temperatures required. EC/OC is best performed on QFF [150]. Based on the overall properties, PTFE outperforms GFF and QFF [5].

238

239 **3.3.1. Analytical methods for determination of metals bound to PM**

240 Inductively coupled plasma mass spectrometry (ICP-MS; 68% of studies), X-ray analysis
241 (20%) and atomic absorption spectroscopy (AAS; 11%) were the most commonly used
242 spectroscopic techniques used to determine metals in the PM size-fractionated samples
243 (Table 3).

244 ICP-MS was used in 17 studies, including two that employed inductively coupled plasma
245 mass spectrometry with magnetic sector (SF-ICP-MS). Inductively coupled plasma optical
246 emission spectrometry (ICP-OES) was reported in 11 studies. Among the X-ray based
247 techniques, total reflection X-ray fluorescence spectroscopy (TXRF), X-ray photoelectron
248 spectroscopy (XPS), energy dispersive X-ray fluorescence (ED-XRF) and X-ray
249 fluorescence (XRF) were reported in one, one, three and four studies, respectively. In
250 addition, among the AAS techniques, electrothermal atomic absorption spectrometry
251 (ETAAS) and flame atomic absorption spectroscopy (FAAS) were each reported in two
252 studies, while proton induced x-ray emission (PIXE) was reported in one study.

253 The most common sample digestion technique for metal determination was microwave-
254 assisted digestion (MAD; 83% of studies). Total metal concentration was also determined in
255 sample digests after hot plate digestion (HP; 21%), ultrasound-assisted (UAE; 8%) and
256 mechanical shaking extraction (MS; 4%). For these procedures, nitric acid (HNO_3; 51%),
257 hydrofluoric acid (HF; 18%), hydrochloric acid (HCl; 18%) and perchloric acid ($HClO_4$; 14%)
258 were most commonly applied. Some studies also reported the use of hydrogen peroxide
259 (H_2O_2; 10%), boric acid (H_3BO_3; 2%) and isopropyl alcohol (C_3H_8O; 2%).

260

261 Table 3: Consolidated results from selected studies, with corresponding study count.

	Metal(oid)s	PAHs
Analytical technique:		
ICP	30	*n/a*
AAS	4	*n/a*
X-ray	9	*n/a*
GC	*n/a*	46
HPLC	*n/a*	9

Extraction technique:		
HP	5	*n/a*
MAD	20	2
UAE	2	30
MS	1	2
ASE	*n/a*	11
SOE	*n/a*	10

Glossary: n/a (not applicable)

3.3.2. Analytical methods for determination of PAHs bound to PM

Among the analytical techniques for the determination of PAHs, gas chromatography (GC) was predominately used for the separation of PAHs (84% of studies). Other techniques were based on the high performance liquid chromatography (HPLC; 16%). When separated by GC, PAHs are detected with higher sensitivity, speed, selectivity and cost-efficiency. A total of three studies reported the use of GC coupled with flame ionisation detector (GC-FID) and 35 studies used MS (GC-MS). In-injection port thermal desorption GC mass spectrometry (TD-GC-MS) was used in three studies, while one study reported the determination of PAHs using GC coupled with quadrupole time-of flight mass spectrometry system (GC-Q-TOF-MS) and GC coupled to a triple quadrupole mass spectrometer (GC-MS/MS).

HPLC was reported to be used for the separation of PAHs in seven studies and reversed phase HPLC with programmable fluorescence detection (HPLC/FLD) was reported in two studies. Among the selected studies, the most common extraction method for PAHs was UAE (64%), followed by accelerated solvent extraction (ASE; 23%), Soxhlet extraction (SOE; 21%), MAD (4%) and MS (4%). The most commonly used solvents were dichloromethane (DCM) (49%), followed by hexane (Hx; 20%), methanol (MeOH; 13%), acetone (Ace; 12%), toluene (Tl; 6%) and acetonitrile (MeCN; 7%). Some studies (<5%) reported the use of diethyl ether (Eth), methylene chloride (CH_2Cl_2), cyclohexane (Chx), sulphuric acid (H_2SO_4), petroleum ether (Pet Eth) and sodium hydroxide (NaOH).

3.4. Assessment of health and environmental implications and potential source modelling

Health and environmental risks in the reviewed studies were commonly assessed using the incremental lifetime cancer risk (ILCR; 33% of studies), carcinogenic equivalent concentration of BaP (BaP_{eq}; 28%), lifetime daily exposure dose (LADD; 16%), enrichment factor (EF; 10%), hazard quotient (HQ; 8%) and hazard index (HI; 4%). ILCR represents the incremental probability of developing some form of cancer during a lifetime due to pollutant exposure, while BaP_{eq} quantifies the toxicity of the complex PAH mixtures and their mutagenic and carcinogenic potential. LADD estimates the lifetime exposure dose of a chemical compound, while HQ and HI reflect the probability of experiencing adverse non-cancer effects. For health risk assessment, studies also reported the use of loss of life expectancy (LLE), dermal absorption dose (DAD) and relative abundance ratio of an individual PAH to the carcinogenic marker BaP (RC).

The most commonly applied qualitative method for identifying potential sources of air pollution include diagnostic ratios (DR; 43%), principal component analysis (PCA; 25%) and the US EPA's positive matrix factorisation (PMF; 22%). PCA is a statistical technique that reduces the dimensionality of complex data sets and identifies hidden patterns and correlations between identified chemical species, while PMF is a receptor model that quantitatively estimates source contributions [151]. Additionally, the characteristic PAH diagnostic ratios (DRs) are commonly used to distinguish between pyrogenic and petrogenic origins, such as petroleum combustion, biomass or coal combustion, since these ratios remain relatively constant across emission sources [41,152–155]. Source apportionment was addressed using chemical mass balance (CMB), crustal matter contribution (CMC), conditional probability function (CPF), potential source contribution function (PSCF), roadside enrichment (RE), UNMIX multivariate receptor model US EPA, concentration weighted trajectory (CWT), self-organising maps (SOM) and weather research and forecast model with chemistry (WRF-Chem).

Backward trajectory analysis (BTA) was also employed to trace aerosol transport pathways and investigate transport mechanisms. Authors also reported on the use of further statistical approaches, including factor analysis (FA), linear regression models (LRM), absolute

principal component score (APCS), multivariate regression analysis (MRA), hierarchical component analysis (HCA) and coefficient of divergence (COD).

3.5. Distribution and sources of metal(oid)s in urban environments

In China, concentrations of metal(oid)s bound to PM_{10} and $PM_{2.5}$ showed pronounced seasonal fluctuations, with winter peaks and $PM_{2.5}$ concentrations consistently higher than PM_{10}. A significant increase during haze events (1.5 to 11 times higher than on non-haze days), particularly at high relative humidity (>70%), was observed due to enhanced formation of secondary aerosol species and secondary organic compounds [22,156]. Among the measured elements, aluminium (Al), barium (Ba), iron (Fe), magnesium (Mg), manganese (Mn), strontium (Sr) and zinc (Zn) were the most abundant, while Cd, chromium (Cr), Ni and Pb posed the greatest cancer risks [22,81]. Trace element concentrations often exceeded World Health Organisation (WHO) limits, with the highest EFs observed for silver (Ag), As, Cd, Pb, selenium (Se), thallium (Tl) and Zn [117]. Total metal(oid)s concentration in PM_{10} decreased in order: Zn>As>Pb>Mn>Cu>Cr>Ni>Cd>cobalt (Co), with the highest bioaccessibility observed for Mn, Co and Ni. The concentrations of As, Cr, Co, Cd and Pb surpassed precautionary cancer thresholds. The bioaccessibility of heavy metals depends on the source and is higher for traffic-related metal(oid)s than for coal combustion, due to metal(oid)s in vehicles occur in a free state or are adsorbed on the surface and are more soluble in water or other extraction media [108]. Fossil fuel combustion, traffic emissions, industrial emissions and re-suspended dust are considered to be the main sources of PM-bound metal(oid)s in China [108].

In Taiwan, the most abundant elements were Al, Ba, Cr, potassium (K), Mg, Ni and Zn (10−1000 ng m^{-3}), followed by Cu, Mn, Mo, Pb, antimony (Sb), Se, Sr, titanium (Ti) and vanadium (V) (1−10 ng m^{-3}). Elements detected at <1 ng m^{-3} included As, Cd, cerium (Ce), Co, lanthanum (La), neodymium (Nd), praseodymium (Pr), samarium (Sm) and ytterbium (Yb). Five main sources were identified, including traffic, non-ferrous metallurgy, mineral dust and coal [75].

342 In India, similar to China, the highest levels of ILCR values were observed on foggy days,
343 with Cr showing the highest carcinogenic risks and the main sources attributed to industrial
344 processes, fossil fuel combustion, biomass and coal combustion, waste incineration and
345 brake wear [54]. The highest HQ were observed for Al, As, Se, silicon (Si) and Zn, all of
346 which were above the limit values [74]. In Iran, the highest PM_{10} bound metal concentrations
347 were observed at traffic intersections near brick kilns, in the decreasing order:
348 Fe>Zn>Cr>Mn>Pb>Ni>Cu>As>Cd. The highest EFs were observed for Co, Cd, As, Pb and
349 Zn [25]. The calculated cancer risks were the highest for Cr, Co, As and Cd [25,105]. Four
350 main sources were identified, including re-suspension of road dust due to vehicular activity
351 (Fe, Co, Ni, Cu), solid waste incineration (Cr, Mn, Cu), coal combustion and automobile
352 exhaust (Cd, As) and smelters/non-ferrous metal plants (Zn, Pb) [25]. In Pakistan, high
353 seasonal variability was observed, with the highest metal levels observed in winter and fall.
354 Potential non-carcinogenic and carcinogenic risks exhibited highest risks for Pb and Cr
355 through inhalation for children. [111].
356 In Europe, lower $PM_{2.5}/PM_{10}$ ratios were observed in areas with dry climates or in close
357 proximity to deserts [157,158], while higher ratios were reported in urban areas with intense
358 traffic [159]. Crustal elements, such as Al, calcium (Ca), Fe, K, Mg, sodium (Na) and sulfur
359 (S), are predominantly associated with coarse PM, while traffic-related tracers (Ba, Cd, Cr,
360 Cu, Mo, Sb, Zn) indicate tire and brake wear. Diesel and gasoline emissions are
361 characterised by Cu, Mo, Ni, Pd, Co and Zn, which are typically enriched in fine fractions.
362 Additional source markers include V from marine emissions, La and Ce from mineral dust
363 and As, Cd, Pb and Sb from coal combustion [75,91,108,159–163]. Dominance of Zn, Ti and
364 Cu in Europe indicated diverse pollution sources [93]. In general, smaller PM fractions
365 exhibit a higher affinity for adsorption of toxic substances. Metal(oid)s from high-temperature
366 processes are preferentially bound to fine and UFP PM, while coarse particles are mainly
367 derived from natural sources and mechanical abrasion [100,164]. In Germany, the highest
368 metal concentrations occurred in winter, particularly for Ca, Fe, K, Pb and Zn and were
369 accompanied by a shift towards smaller particle fractions. Cr and Cu were mainly present in

370 coarse PM fractions, largely attributed to brake wear, while Ni was enriched in fine PM
371 fraction, reflecting its link to fuel combustion. The highest EF were observed for Zn, Cu, tin
372 (Sn), Pb, As, Sb and Se, all attributed to traffic sources, with notably Zn emissions in
373 particular associated with tyre tread wear from rubber co-polymers [27,31,165,166]. In
374 Slovakia, the highest concentrations of selected metal(oid)s were found in PM_1, primarily
375 originating from non-exhaust traffic emissions and re-suspended road dust [79].
376 In France, the highest concentrations of metals, including As, Cd, Cr, K, Mn, Pb, rubidium
377 (Rb), Sb, V and Zn, were also observed in PM_1, with sources mainly attributed to local
378 combustion sources, traffic emissions and re-suspended road and brake-wear dust [100].
379 Combustion processes in domestic heating and traffic have been shown to contribute to
380 submicronic and UFP [6,167,168]. In Poland, $PM_{2.5}$ levels were 2−3 times higher during the
381 heating period compared to non-heating period, with As, Cd and Pb dominating in winter,
382 while Ni prevailed in summer [109]. In Italy, $PM_{2.5}$ bound Cd and Pb exhibited significant
383 leachability, although most trace elements remained below the threshold levels [99]. The
384 highest concentrations were observed for Cr, Zn and Cd, with Cd, Cr, Cu, Fe, Mn, Mo and
385 Sn predominantly associated with coarse PM and As, Co and Pb enriched in fine PM. Fine
386 particles were mainly emitted from fossil fuel combustion source, while coarse particles were
387 dominated by crustal elements from road dust [97]. The highest EFs were observed for V,
388 Ba, Cr, Ni Cu, As, Zn, Sb, Pb, Mo, Cd and mercury (Hg). Five main sources were identified,
389 including brake and tyre wear (Ba, Cu, Fe, Mo, Zn), non-exhaust vehicular emissions and
390 road dust re-suspension (Al, Mn, Sr, Ce, La), cement plants (Mg, Ca, Ti), industrial
391 emissions (As, Sb), and fossil fuel combustion and biomass burning (K, Ni, V) [106]. In
392 Slovenia, analysis revealed that metal(oid)s and platinum group elements (PGEs) were most
393 abundant in the PM_{10}, largely influenced by soil deposition and re-suspension processes,
394 while those metals (Ba, Cd, Cu, Ni, Pb, palladium (Pd), platinum (Pt), V, Zn) originating from
395 traffic-related sources as well as biomass combustion were also significantly elevated in the
396 $PM_{<0.1}$ [45].

In Algeria, the coarse PM fraction was prevalent due to the lack of vegetation and soil erosion. Concentrations of Ba and Pb were the highest, with higher enrichment in PM_1 and $PM_{2.5}$ in comparison to PM_{10}. Two main sources contributed to elevated metal(oid) concentrations, including exhaust emissions re-suspended road dust and oil combustion. Concentrations were also affected by Saharan dust [116].

In Mexico, metal(oid) contamination was also more dominant in winter, with the highest concentrations observed for Fe, Cu, Zn, As, Ni and Cd [72].

In general, the overview of metal(oid)s bound to PM in different global regions showed great seasonal variations, particularly associated with fine and ultrafine PM fractions. The highest concentrations were observed in winter, especially during haze events. The highest concentrations were observed for As, Cd, Cr, Ni and Pb, with high bioaccessibility observed for traffic-derived metal(oid)s bound to (ultra)fine PM due to their higher affinity for adsorption of toxic substances, the occurrence of metals in the free state and high solubility potential. Smaller PM fractions were associated with anthropogenic sources, such as fossil fuel combustion, traffic emissions, industrial processes and waste incineration, while coarse PM were associated with naturally-derived crustal material.

3.6. Distribution and sources of PAHs in urban environments

In Iran, the highest concentrations of PAHs bound to $PM_{2.5}$ were observed in winter, particularly HMW PAHs [55]. BaP concentrations exceeded the WHO guideline value of 1 ng m^{-3} [23]. The most abundant PAHs in Iran were fluoranthene (Fl), BghiP, acenaphthene (Ace) and IP [103]. A similar seasonal pattern was reported in Lebanon, where winter concentrations were 3−5 times higher than in summer, mainly due to vehicle traffic, diesel generators and nearby power plants [67].

PAHs are typically characterised by strong seasonal variations, primarily due to greater atmospheric stability in winter, enhanced partitioning of HMW PAHs into particulate phase due to reduced volatility and more efficient volatilisation of LMW PAHs into gaseous phase combined with intensified photochemical degradation during summer [57,82,169–174]. PAHs

partitioning to gas phase generally exhibit lower carcinogenic potential [33,171,175]. Elevated temperatures can enhance the evaporation of $PM_{2.5}$-bound PAHs and accelerate their transformation into nitro- and oxy-PAHs, reducing particulate-bound PAHs [176,177]. Moreover, precipitation washout, reduced atmospheric boundary layer depth and stronger winds further dilute and disperse pollutants [57,65,127,178].

In China, PAH concentrations in $PM_{2.5}$ were highest in winter, with levels 14 times higher than in spring, often exceeding the WHO annual limit of 5 μg m^{-3} [123,125,179]. HMW PAH (4–5 ring) bound to PM_{10} and $PM_{2.5}$ were three times more abundant than LMW PAHs, which can be attributed to pyrogenic sources such as fossil fuel combustion, biomass burning and vehicle emissions [96,123,125,127]. Health risks were primarily associated with BaA, BaP, Ch, benzo(b)fluoranthene (BbF), benzo(k)fluoranthene (BkF), IP, dibenzo(a,h)anthracene (DahA) and Fl, with BaP concentrations and ILCR values often above safe levels [62,65,81,89,125,127,180]. Source apportionment attributed PAHs to vehicle exhaust mixed with soot and coke oven emissions, ship emissions, biomass burning and coal combustion [62,81,95,125,127]. The highest concentrations of PAHs were observed in northern China and the lowest in southern China [113]. In addition, the sources of PAH emissions were more dispersed in the suburban areas and were commonly associated with residential cooking using coal, wood and straw [127].

The distribution of PAHs reflects their sources, with specific tracers of BghiP for gasoline vehicles, BbF and BkF for diesel vehicles, and BaA and Ch for natural gas combustion [184–186]. In addition, 2−3 ring PAHs often originate from wood combustion [171,185], 3−4 ring PAHs from coal [171,184], 4−6 ring PAHs from vehicle and petroleum combustion [33,175,184]. The 4−6 ring PAHs contribute to 95% of the total $PM_{2.5}$-bound PAHs [65].

In India, PAH concentrations bound to PM were also highest in winter, with the combustion of biomass, petroleum and coal making the largest contributions. DahA, BaP, BaA, BkF and Ch contributed most to health risks [57,112]. The highest concentrations were observed for PAHs with 5- and 6-rings, which are predominantly associated with fine PM due to their larger surface area and greater absorption capacity [74,112,187]. HMW PAHs exhibit greater

adsorption capacity than LMW PAHs due to their lower volatility and slower adaption to adsorption equilibria. Their pronounced hydrophobicity further promotes association with smaller particles, which provide greater surface area [76].

Similar to China, PAH levels in India were highest in the morning, attributed to morning traffic, lower temperatures, lower atmospheric boundary layer height, weaker turbulence and limited photodecomposition, all of which results in lower pollutant dispersion [65]. In Japan, 4-ring PAHs peaked in winter, with BaP, BaA, BbF, BkF and IP exhibiting the highest concentrations, originating from traffic, coal and biomass combustion [129]. In Thailand, PAH concentrations were significantly higher during the heating period than the non-heating period, with BbF, indicative of biomass emissions, showing the highest concentrations. The ratio of total PAHs to PM decreased with increasing PM size, which can be attributed to ageing process, possible photooxidation of PAHs from secondary organic aerosols or adsorption to pre-existing particles through self-nucleation of gaseous phase partitioning [76]. In Taiwan, both $PM_{2.5}$ and PAHs were elevated during winter, revealing potential impacts of long-range transport and indicating on the dominance of petroleum and fuel combustion [118]. Similarly, in Malaysia, BbF, BkF, BaP, IP and BghiP were the highest, with 80% of the PAHs detected being 5- and 6-ring PAHs. DR indicated on mixed sources of incomplete combustion of petroleum fuel and vehicle emissions together with unburnt crude oil and petroleum products such as gasoline, kerosene and diesel [78].

Similar to the observations in China, PAH concentrations in Europe showed a north-south gradient, with the highest levels reported in southern regions [80]. In Italy, seasonal differences were limited, with BaP, BkF and BbF dominating, mainly originating from engine emissions [64]. In Spain, the highest PAH levels were observed in winter, with strong seasonal variations, and diesel traffic being the main source of BaP, BbF, DahA, IP, BaA, BkF and Ch [35,86]. In Greece, IP, BghiP and Ch were the most abundant, with wood burning and traffic as major sources [98,120]. In Poland, BaP bound to PM_1 was 2.5 times higher than in $PM_{2.5}$ [87], while in Croatia, winter concentrations of BghiP, BaP, BbF and IP were highest, with 80% of PAHs bound to $PM_{2.5}$, mostly from domestic heating [77].

In Slovenia, HMW PAHs were distributed between PM_{10} and $PM_{2.5}$ fractions, with 5- (BaP, BbF) and 6-ring (BghiP, IP) PAH compounds associated more significantly with smaller PM fractions. Contaminant levels were low, indicating minimal health risks for daily commuters [45]. In Portugal, the concentrations were higher than in Italy or Greece, reflecting higher utilisation of fossil fuels and biomass [26]. In the Czech Republic, Fl, Phe, Pyr, BaA and Ch reached peak levels during smog episodes related to coal mining, metallurgy, coke production and residential heating [102]. In the United Kingdom, PAH peaks occurred in the morning and evening, with the evening peaks mainly caused by residential heating [40]. In Turkey, the primary sources of particulate OM were identified as vehicular emissions, coal combustion, and food cooking [84].

In Saudi Arabia, BghiP was the most abundant, mostly released by traffic emissions, with a predominance of local sources [66]. In Ghana, high concentrations of BghiP, Pyr, Phe, IP and BaP were reported, with Phe and Pyr serving as markers of emissions from diesel vehicles and BaP as a marker of gasoline vehicle emissions [59,184,188]. The BaP values remained below the regulatory limit values [59]. Monitoring of PAH concentrations in Egypt revealed the highest levels of IP, BghiP and BaP, primarily originated from combustion sources [68].

In general, the analysis of PAHs bound to PM showed strong seasonal variations, characterised by HMW PAHs being more abundant in (ultra)fine PM during colder moths. The trend is primarily governed by photochemical processes and increased atmospheric stability, and, in certain cases, resulted in exceedances of regulatory limit values for BaP, DahA, BaA, BbF, and BkF. HMW PAHs were more prevalent than LMW PAHs, attributed to their lower volatility corresponding to their higher adsorption capacity of toxic substances. PAH concentrations were also the highest in the mornings, likely due to limited photodecomposition rates, lower temperatures, lower atmospheric boundary layer and weaker turbulence. Additionally, a global north-south gradient was observed, with the highest PAH levels observed in southern regions. Elevated levels of HMW PAHs indicate on

508 a stronger influence of pyrogenic sources, including fossil fuel, biomass and vehicle
509 emissions.
510
511 **4. Conclusions and future prospects**
512 This review, which included 81 studies from 33 different countries, published between 2010
513 and 2025, evaluated the current state of sampling protocols and analytical methods for the
514 assessment of metal(oid)s and PAHs in size-fractionated PM, with particular emphasis on
515 their characteristic chemical composition, seasonal variability and global spatial distribution,
516 emphasising the methods for its data quality assurance.
517 Prior to PM sample collection, it is essential to clearly define the target pollutants to enable
518 the selection of suitable and adequate analytical approaches, including filter material,
519 extraction procedures and high-resolution, sensitive analytical techniques, thereby ensuring
520 data reliability also through the use of CRMs. Nevertheless, only 32% of studies reported
521 employing CRMs, most commonly NIST SRM 1648a. The routine evaluation of analytical
522 method validation for PM determination is uncommon, largely due to the limited availability of
523 standards and their high costs.
524 Among the reviewed studies, 52% focused on the characterisation of pollutants bound to
525 $PM_{2.5}$, followed by PM_{10} (30%) and PM_1 (13%), while only 5% investigated PM smaller than
526 0.1 μm, a fraction which can penetrate the deepest into the cell tissues and circulatory
527 system, is highly prevalent in the atmosphere, and therefore exhibits the most pronounced
528 toxic effects due to high pollutant absorption capacity. In total, 56% of studies identified the
529 chemical composition of PAHs, 31% focused on metal(oid)s, and only 14% addressed both
530 pollutant groups concurrently.
531 ICP-MS was the most widely employed technique (68% of studies) for the determination of
532 metal(oid)s in PM size-fractionated samples, followed by X-ray analysis (20%) and AAS
533 (11%). MAD represented the predominant sample preparation method, used in 83% of
534 studies, followed by HP digestion (21%), UAE (8%) and MS (4%). For PAH analysis, GC-MS
535 was employed in 84% of studies, while HPLC was used in 16%. UAE was the predominant

PAH extraction method, used in 64% of studies, followed by ASE (23%), SOE (21%), MAD (4%) and MS (4%).

The most commonly used filter media were QFFs (65%), followed by PTFE (16% of studies) and GFF (12%), differing in sampling efficiency, mechanical, chemical and temperature stability, blank concentrations, flow resistance and artefacts formation, all relevant for different analytical applications, with PTFE filter outperforming GFF and QFF.

Global PM-bound metal(oid) distribution showed strong seasonal variability, with winter episodes exhibiting the highest concentrations, particularly in (ultra)fine PM. As, Cd, Cr, Ni and Pb were most abundant and traffic-derived pollutants in (ultra)fine PM, showing high bioaccessibility due to their high affinity for adsorption of toxic substances, the occurrence of metals in the free state and their high solubility potential. Smaller PM fractions were mainly associated with anthropogenic sources, such as fossil fuel combustion, traffic emissions, industrial processes and waste incineration, while coarse PM primarily reflected naturally-derived crustal material.

Similarly, PM-bound PAHs showed strong seasonal fluctuations, with fine and UFP enriched in HMW PAHs emitted from fossil fuel combustion, biomass burning and traffic. Seasonal and diurnal patterns were influenced by meteorological factors, atmospheric stability and photochemical processes, with BaP, DahA, BaA, BbF and BkF often exceeding health guideline limits, representing high carcinogenic risks. HMW PAHs were more prevalent than LMW PAHs due to their lower volatility corresponding to higher adsorption capacity of toxic substances. A global north-south gradient was observed, with the highest PAH levels observed in southern regions.

Most studies (87%) deployed PM samplers at elevated sites (above 2.5 m, e.g. rooftops), distant from residential and commuter areas, which may limit the representativeness and thereby reduce the accuracy of exposure assessments. Adequate health and environmental risk assessment, typically based on ILCR (33% of studies), BaP_{eq} (28%) and LADD (16%), is essential for quantifying the potential adverse effects and ensuring public health protection and pollution control. Additionally, the identification of pollutant sources enables more

564 targeted mitigation and more effective regulation, with source apportionment commonly
565 conducted by DR (43% studies), PCA (25%) and the US EPA's PMF (22%).
566 This review highlights a significant gap in the characterisation of the smallest PM fractions,
567 particularly regarding multi-pollutant analysis and the use of CRMs for validating analytical
568 protocols. Future research should prioritise the development and implementation of uniform
569 sampling protocols for UFP collection, with defined methods, instrumentation and extraction
570 procedures to ensure cross-study comparability. Expanding CRM availability will improve
571 data quality, while integrating multi-pollutant analyses into sampling protocols to better
572 capture the complex composition of UFP and their combined toxicological effects,
573 strengthening the scientific basis for environmental policy, regulatory standards and public
574 health protection.
575

576 **5. Funding sources**

577 Marija Đurić and Alenka Mauko Pranjić acknowledge the support of the Slovenian Research
578 Agency financial support programme group P2-0273, Radmila Milačič Ščančar and Janez
579 Ščančar acknowledge the support of the Slovenian Research Agency financial support
580 programme group P1-0143. Prashant Kumar acknowledges the support received through
581 the UKRI-Funded GP4Streets (APP44894), RECLAIM Network Plus (EP/W034034/1),
582 GreenCities (NE/X002799/1), GREENIN Micro Network Plus (APP55977) and UGPN-funded
583 (UGPN-NBS and GREENICON) projects.
584

585 **6. References**

586 [1] A. Daly, S. Zannetti, An Introduction to Air Pollution – Definitions, Classifications, and
587 History, in: Ambient air pollution, The Arab School for Science and Technology and The
588 EnviroComp Institute, 2007. pp. 1–14.

589 [2] OECD, The Economic Consequences of Outdoor Air Pollution OECD.
590 https://www.oecd.org/en/publications/the-economic-consequences-of-outdoor-air-
591 pollution_9789264257474-en.html, 2016 (accessed 4 August 2025).

592 [3] R.F. Phalen, R.N. Phalen, Introduction to Air Pollution Science: A Public Health
593 Perspective, Jones & Bartlett Publishers, 2013.

[4] D.A. Vallero, Fundamentals of Air Pollution, Elsevier, 2008.

[5] J.C. Chow, Measurement methods to determine compliance with ambient air quality standards for suspended particles, J Air Waste Manag Assoc. 45 (1995) 320–82. 10.1080/10473289.1995.10467369.

[6] R. Fernández-Camacho, S. Rodríguez, J. de la Rosa, A.M. Sánchez de la Campa, A. Alastuey, X. Querol, Ultrafine particle and fine trace metal (As, Cd, Cu, Pb and Zn) pollution episodes induced by industrial emissions in Huelva, SW Spain, Atmos Environ, 61 (2012) 507–17. https://doi.org/10.1016/j.atmosenv.2012.08.003.

[7] L. Morawska, Z. Ristovski, E.R. Jayaratne, D.U. Keogh, X. Ling, Ambient nano and ultrafine particles from motor vehicle emissions: Characteristics, ambient processing and implications on human exposure, Atmos Environ 42 (2008) 8113–38. https://doi.org/10.1016/j.atmosenv.2008.07.050.

[8] O. Raaschou-Nielsen, Z.J. Andersen, R. Beelen, E. Samoli, M. Stafoggia, G. Weinmayr, Air pollution and lung cancer incidence in 17 European cohorts: prospective analyses from the European Study of Cohorts for Air Pollution Effects (ESCAPE), Lancet Oncol, 14 (2013) 813–22. 10.1016/S1470-2045(13)70279-1.

[9] F. Gozzi, G.D. Ventura, A. Marcelli, F. Lucci, Current Status of Particulate Matter Pollution in Europe and Future Perspectives: a Review, JMES, 8 (2017) 1901–1909.

[10] N.A. Potter, G.Y. Meltzer, O.N. Avenbuan, A. Raja, J.T. Zelikoff, Particulate Matter and Associated Metals: A Link with Neurotoxicity and Mental Health, Atmosphere, 12 (2021) 425. https://doi.org/10.3390/atmos12040425.

[11] A. Valavanidis, K. Fiotakis, T. Vlachogianni, Airborne Particulate Matter and Human Health: Toxicological Assessment and Importance of Size and Composition of Particles for Oxidative Damage and Carcinogenic Mechanisms, J Environ Sci Health C, 26 (2008) 339–62. 10.1080/10590500802494538.

[12] N. Zioła, K. Słaby, The Content of Selected Heavy Metals and Polycyclic Aromatic Hydrocarbons (PAHs) in PM10 in Urban-Industrial Area, Sustainability, 12 (2020) 5284. https://doi.org/10.3390/su12135284

[13] H. Chen, MS. Goldberg, P.J. Villeneuve, A systematic review of the relation between long-term exposure to ambient air pollution and chronic diseases, Rev Environ Health, 23 (2008) 243–97. 10.1515/reveh.2008.23.4.243.

[14] A.J. Cohen, M. Brauer, R. Burnett, H.R. Anderson, J. Frostad, K. Estep, Estimates and 25-year trends of the global burden of disease attributable to ambient air pollution: an analysis of data from the Global Burden of Diseases Study 2015, Lancet, 389 (2017) 1907–18. 10.1016/S0140-6736(17)30505-6.

[15] F. Dominici, R.D. Peng, M.L. Bell, L. Pham, A. McDermott, S.L. Zeger, Fine Particulate Air Pollution and Hospital Admission for Cardiovascular and Respiratory Diseases, JAMA, 295 (2006) 1127–34. 10.1001/jama.295.10.1127.

[16] S.J. Fan, J. Heinrich, M.S. Bloom, T.Y. Zhao, T.X. Shi, W.R. Feng, 2020, Ambient air pollution and depression: A systematic review with meta-analysis up to 2019, Sci Total Environ, 134721. https://doi.org/10.1016/j.scitotenv.2019.134721.

635 [17] A.G. Russell, B. Brunekreef, A Focus on Particulate Matter and Health, Environ Sci
636 Technol, 43 (2009), 4620–5. https://doi.org/10.1021/es9005459.

637 [18] J. Kuo, Air Pollution Control: Fundamentals and Applications, CRC Press, 2018.

638 [19] IARC, Outdoor Air Pollution. https://publications.iarc.fr/Book-And-Report-Series/Iarc-
639 Monographs-On-The-Identification-Of-Carcinogenic-Hazards-To-Humans/Outdoor-Air-
640 Pollution-2015, 2016 (accessed 18 June 2024).

641 [20] WHO, Outdoor Air Pollution IARC Monographs on the Evaluation of Carcinogenic Risks
642 to Humans. https://publications.iarc.fr/Book-And-Report-Series/Iarc-Monographs-On-
643 The-Identification-Of-Carcinogenic-Hazards-To-Humans/Outdoor-Air-Pollution-2015,
644 2015 (accessed 17 September 2024).

645 [21] EEA, Air quality in Europe — 2012 report.
646 https://www.eea.europa.eu/en/analysis/publications/air-quality-in-europe-2012, 2012.

647 [22] Y. Gao, H. Ji, Microscopic morphology and seasonal variation of health effect arising
648 from heavy metals in PM2.5 and PM10: One-year measurement in a densely populated
649 area of urban Beijing, Atmos Res, 212 (2018), 213–26.
650 https://doi.org/10.1016/j.atmosres.2018.04.027

651 [23] Directive 2004/107/EC of the European Parliament and of the Council of 15 December
652 2004 relating to arsenic, cadmium, mercury, nickel and polycyclic aromatic
653 hydrocarbons in ambient air. http://data.europa.eu/eli/dir/2004/107/oj/eng, 2004
654 (accessed 14 July 2024).

655 [24] J. Briffa, E. Sinagra, R. Blundell, 2020. Heavy metal pollution in the environment and
656 their toxicological effects on humans. Heliyon. 6, e04691.
657 https://doi.org/10.1016/j.heliyon.2020.e04691.

658 [25] D. Sah, P.K. Verma, M.K. Kandikonda, A. Lakhani, Pollution characteristics, human
659 health risk through multiple exposure pathways, and source apportionment of heavy
660 metals in PM10 at Indo-Gangetic site, Urban Clim, 27 (2019) 149–62.
661 https://doi.org/10.1016/j.uclim.2018.11.010.

662 [26] C.A. Alves, A.M. Vicente, D. Custódio, M. Cerqueira, T. Nunes, C. Pio, Polycyclic
663 aromatic hydrocarbons and their derivatives (nitro-PAHs, oxygenated PAHs, and
664 azaarenes) in PM2.5 from Southern European cities, Sci Total Environ, 595 (2017)
665 494–504. https://doi.org/10.1016/j.scitotenv.2017.03.256.

666 [27] K.W. Fomba, D. van Pinxteren, K. Müller, G. Spindler, H. Herrmann, Assessment of
667 trace metal levels in size-resolved particulate matter in the area of Leipzig, Atmos
668 Environ, 176 (2018) 60–70. 10.1016/j.atmosenv.2017.12.024.

669 [28] C. Pio, F. Mirante, C. Oliveira, M. Matos, A. Caseiro, C. Oliveira, Size-segregated
670 chemical composition of aerosol emissions in an urban road tunnel in Portugal. Atmos
671 Environ, 71(2013) 15–25. https://doi.org/10.1016/j.atmosenv.2013.01.037.

672 [29] P. Prati, A. Zucchiatti, F. Lucarelli, P.A. Mandò, Source apportionment near a steel
673 plant in Genoa (Italy) by continuous aerosol sampling and PIXE analysis, Atmos
674 Environ, 34 (2000) 3149–57. https://doi.org/10.1016/S1352-2310(99)00421-5.

675 [30] Y. Qin, C.K. Chan, L.Y. Chan, Characteristics of chemical compositions of atmospheric
676 aerosols in Hong Kong: spatial and seasonal distributions, Sci Total Environ, 206
677 (1997) 25–37. https://doi.org/10.1016/S0048-9697(97)00214-3.

678 [31] A. Thorpe, R.M. Harrison, Sources and properties of non-exhaust particulate matter
679 from road traffic: A review, Sci Total Environ, 400(2008) 270–82.
680 https://doi.org/10.1016/j.scitotenv.2008.06.007.

681 [32] I. Jakovljević, Z. Sever Štrukil, R. Godec, I. Bešlić, S. Davila, M. Lovrić, Pollution
682 Sources and Carcinogenic Risk of PAHs in PM1 Particle Fraction in an Urban Area, Int
683 J Environ Res Public Health, 17(2020) 9587. https://doi.org/10.3390/ijerph17249587.

684 [33] K. Ravindra, R. Sokhi, R. Van Grieken, Atmospheric polycyclic aromatic hydrocarbons:
685 Source attribution, emission factors and regulation, Atmos Environ, 42(2008) 2895–
686 921. https://doi.org/10.1016/j.atmosenv.2007.12.010.

687 [34] K.H. Kim, S.A. Jahan, E. Kabir, R.J.C. Brown, A review of airborne polycyclic aromatic
688 hydrocarbons (PAHs) and their human health effects, Environ Int, 60(2013) 71–80.
689 https://doi.org/10.1016/j.envint.2013.07.019.

690 [35] B.A.M Bandowe, H. Meusel, R.J. Huang, K. Ho, J. Cao, T. Hoffmann, $PM_{2.5}$-bound
691 oxygenated PAHs, nitro-PAHs and parent-PAHs from the atmosphere of a Chinese
692 megacity: seasonal variation, sources and cancer risk assessment, Sci Total Environ,
693 473–474(2014) 77–87. https://doi.org/10.1016/j.scitotenv.2013.11.108.

694 [36] D.M. Agudelo-Castañeda, E.C. Teixeira, Seasonal changes, identification and source
695 apportionment of PAH in PM1.0, Atmos Environ, 96(2014) 186–200.
696 https://doi.org/10.1016/j.atmosenv.2014.07.030.

697 [37] Y. Wei, I.K. Han, M Hu, M. Shao, J. Zhang, X. Tang, Personal exposure to particulate
698 PAHs and anthraquinone and oxidative DNA damages in humans, Chemosphere,
699 81(2010) 1280–5. https://doi.org/10.1016/j.chemosphere.2010.08.055.

700 [38] US EPA, Polycyclic Aromatic Hydrocarbons (PAHs) - Integrated Risk Information
701 System (IRIS). https://www.epa.gov/iris, 2017 (accessed 15 October 2024).

702 [39] WHO, Some Non-heterocyclic Polycyclic Aromatic Hydrocarbons and Some Related
703 Exposures, International Agency for Research on Cancer, 2010.

704 [40] M.S. Alam, I.J. Keyte, J. Yin, C. Stark, A.M. Jones, R.M. Harrison, Diurnal variability of
705 polycyclic aromatic compound (PAC) concentrations: Relationship with meteorological
706 conditions and inferred sources, Atmos Environ, 122(2015) 427–38.
707 https://doi.org/10.1016/j.atmosenv.2015.09.050.

708 [41] N.R. Khalili, P.A. Scheff, T.M. Holsen, PAH source fingerprints for coke ovens, diesel
709 and gasoline engines, highway tunnels, and wood combustion emissions, Atmos
710 Environ, 29(1994) 533–542. https://doi.org/10.1016/1352-2310(94)00275-P.

711 [42] J. Tan, S. Guo, Y. Ma, J. Duan, Y. Cheng, K. He, Characteristics of particulate PAHs
712 during a typical haze episode in Guangzhou, China, Atmos Res, 102 (2011) 91–8.
713 https://doi.org/10.1016/j.atmosres.2011.06.012.

714 [43] P. Kumar, G. Kalaiarasan, A.E. Porter, A. Pinna, M.M. Kłosowski, P. Demokritou, 2021.
715 An overview of methods of fine and ultrafine particle collection for physicochemical

716 characterisation and toxicity assessments. Sci Total Environ. 756, 143553.
717 https://doi.org/10.1016/j.scitotenv.2020.143553.

718 [44] J. Fenger, O. Hertel, F. Palmgren, Urban Air Pollution — European Aspects, in B.J.
719 Alloway, J.T. Trevors (Eds.), Environmental Pollution, Dordrecht, Springer Netherlands,
720 1998.

721 [45] A. Ilenič, R. Milačič Ščančar, M. Đurić, A. Mauko Pranjić, J. Ščančar, An innovative
722 sampling device for size-fractionating airborne particulate matter for improved air
723 pollution control of metal(oid)s and polycyclic aromatic hydrocarbons, Anal Methods, 17
724 (2025) 7184–7199. https://doi.org/10.1039/D5AY00858A.

725 [46] A.I. Calvo, C. Alves, A. Castro, V. Pont, A.M. Vicente, R. Fraile, Research on aerosol
726 sources and chemical composition: Past, current and emerging issues, Atmos Res,
727 120–122(2013) 1–28. https://doi.org/10.1016/j.atmosres.2012.09.021.

728 [47] P.K. Hopke, Q. Dai, L. Li, Y. Feng, 2020. Global review of recent source
729 apportionments for airborne particulate matter. Sci Total Environ. 740, 140091.
730 https://doi.org/10.1016/j.scitotenv.2020.140091.

731 [48] F.J. Kelly, J.C. Fussell, Size, source and chemical composition as determinants of
732 toxicity attributable to ambient particulate matter, Atmos Environ, 60(2012) 504–26.
733 https://doi.org/10.1016/j.atmosenv.2012.06.039.

734 [49] Y. Liu, F. Xu, W. Liu, X. Liu, D. Wang, Characteristics, Sources, Exposure, and Health
735 Effects of Heavy Metals in Atmospheric Particulate Matter, Curr Pollution Rep,
736 11(2025) 16. 10.1007/s40726-025-00344-y.

737 [50] A. Maceira, R.M. Marcé, F. Borrull, 2020. Analytical methods for determining organic
738 compounds present in the particulate matter from outdoor air. TrAC. 122, 115707.
739 https://doi.org/10.1016/j.trac.2019.115707.

740 [51] L.T. Popoola, S.A. Adebanjo, B.K. Adeoye, Assessment of atmospheric particulate
741 matter and heavy metals: a critical review, Int J Environ Sci Technol, 15(2018) 935–48.
742 https://doi.org/10.1007/s13762-017-1454-4.

743 [52] L.W. Stanek, J.D. Sacks, S.J. Dutton, J.J.B. Dubois, Attributing health effects to
744 apportioned components and sources of particulate matter: An evaluation of collective
745 results, Atmos Environ, 45(2011) 5655–63. 10.1016/j.atmosenv.2011.07.023.

746 [53] L. Yang, H. Zhang, X. Zhang, W. Xing. Y. Wang, P. Bai, Exposure to Atmospheric
747 Particulate Matter-Bound Polycyclic Aromatic Hydrocarbons and Their Health Effects: A
748 Review, IJERPH, 18(2021) 2177. 10.3390/ijerph18042177.

749 [54] A. Agarwal, A. Mangal, A. Satsangi, A. Lakhani, K. Maharaj Kumari, Characterization,
750 sources and health risk analysis of PM2.5 bound metals during foggy and non-foggy
751 days in sub-urban atmosphere of Agra, Atmos Res, 197(2017) 121–31.
752 https://doi.org/10.1016/j.atmosres.2017.06.027.

753 [55] R. Akhbarizadeh, S. Dobaradaran, M. Amouei Torkmahalleh, R. Saeedi, R. Aibaghi, F.
754 Faraji Ghasemi, 2021. Suspended fine particulate matter (PM2.5), microplastics (MPs),
755 and polycyclic aromatic hydrocarbons (PAHs) in air: Their possible relationships and
756 health implications. Environ Res. 192, 110339.
757 https://doi.org/10.1016/j.envres.2020.110339.

[56] C. Wei, Y. Han, B.A.M. Bandowe, J. Cao, R.J. Huang, H. Ni, Occurrence, gas/particle partitioning and carcinogenic risk of polycyclic aromatic hydrocarbons and their oxygen and nitrogen containing derivatives in Xi'an, central China, Sci Total Environ, 505(2015) 814–22. 10.1016/j.scitotenv.2014.10.054.

[57] B. Ambade, A. Kumar, A. Kumar, L.K. Sahu, Temporal variability of atmospheric particulate-bound polycyclic aromatic hydrocarbons (PAHs) over central east India: sources and carcinogenic risk assessment, Air Qual Atmos Health, 15(2022) 115–30. https://doi.org/10.1007/s11869-021-01089-5.

[58] R. Baalbaki, J. Nassar, S. Salloum, A.L. Shihadeh, I. Lakkis, N.A. Saliba, Comparison of atmospheric polycyclic aromatic hydrocarbon levels in three urban areas in Lebanon, Atmos Environ, 179(2018) 260–7. https://doi.org/10.1016/j.atmosenv.2018.02.028.

[59] N. Bortey-Sam, Y. Ikenaka, O. Akoto, S.M.M. Nakayama, Y.B. Yohannes, E. Baidoo, Levels, potential sources and human health risk of polycyclic aromatic hydrocarbons (PAHs) in particulate matter (PM10) in Kumasi, Ghana, Environ Sci Pollut Res, 22(2015) 9658–67. 10.1007/s11356-014-4022-1.

[60] A. Canals-Angerri, M. Via, R. Lara, A. Alastuey, M.C. Minguillón, M. Pandolfi, 2024. Causes of the unremitting high ambient levels of PM10 in a suburban background site in NE Spain. Environ Pollut. 363, 125113. https://doi.org/10.1016/j.envpol.2024.125113.

[61] M. Fontal, B.L. Van Drooge, J.F. López, P. Fernández, J.O. Grimalt, Broad spectrum analysis of polar and apolar organic compounds in submicron atmospheric particles, J Chromatogr A, 1404(2015) 28–38. 10.1016/j.chroma.2015.05.042.

[62] Q. Chen, Y. Chen, X.S. Luo, Y. Hong, Z. Hong, Z. Zhao, Seasonal characteristics and health risks of PM2.5-bound organic pollutants in industrial and urban areas of a China megacity, JEM, 245(2019) 273–81. https://doi.org/10.1016/j.jenvman.2019.05.061.

[63] N. Daher, N.A. Saliba, A.L. Shihadeh, M. Jaafar, R. Baalbaki, C. Sioutas, Chemical composition of size-resolved particulate matter at near-freeway and urban background sites in the greater Beirut area, Atmos Environ, 80(2013) 96–106. https://doi.org/10.1016/j.atmosenv.2013.08.004.

[64] P. Di Vaio, B. Cocozziello, A. Corvino, F. Fiorino, F. Frecentese, E. Magli, Level, potential sources of polycyclic aromatic hydrocarbons (PAHs) in particulate matter (PM10) in Naples, Atmos Environ, 129(2016) 186–96. https://doi.org/10.1016/j.atmosenv.2016.01.020.

[65] A. Elzein, G.J. Stewart, S.J. Swift, B.S. Nelson, L.R. Crilley, M.S. Alam, A comparison of $PM_{2.5}$-bound polycyclic aromatic hydrocarbons in summer Beijing (China) and Delhi (India). ACP, 20(2020) 14303–19. https://doi.org/10.5194/acp-20-14303-2020.

[66] A.H. El-Mubarak, A.I. Rushdi, K.F. Al-Mutlaq, A.Y. Bazeyad, S.L.M. Simonich, B.R.T. Simoneit, Identification and source apportionment of polycyclic aromatic hydrocarbons in ambient air particulate matter of Riyadh, Saudi Arabia, Environ Sci Pollut Res, 21(2014) 558–67. 10.1007/s11356-013-1946-9.

[67] M. Fadel, F. Ledoux, M. Farhat, A. Kfoury, D. Courcot, C. Afif, PM2.5 characterization of primary and secondary organic aerosols in two urban-industrial areas in the East Mediterranean, J Environ Sci, 101(2021) 98–116. https://doi.org/10.1016/j.jes.2020.07.030.

[68] E. Farah, M. Fadel, G. Mansour, N. Fakhri, S.K. Hassan, M. Boraiy, 2024. Unveiling the organic chemical composition and sources of organic carbon in PM2.5 at an urban site in Greater Cairo (Egypt): A comprehensive analysis of primary and secondary compounds. Environ Res. 263, 120118. https://doi.org/10.1016/j.envres.2024.120118.

[69] B. Feng, L. Li, H. Xu, T. Wang, R. Wu, J. Chen, PM2.5-bound polycyclic aromatic hydrocarbons (PAHs) in Beijing: Seasonal variations, sources, and risk assessment. J Environ Sci, 77(2019) 11–9. 10.1016/j.jes.2017.12.025.

[70] S.S.H. Ho, J.Z. Yu, J.C. Chow, B. Zielinska, J.G. Watson, E.H.L. Sit, Evaluation of an in-injection port thermal desorption-gas chromatography/mass spectrometry method for analysis of non-polar organic compounds in ambient aerosol samples. J Chromatogr A, 1200(2008) 217–27. 10.1016/j.chroma.2008.05.056.

[71] K.W. Fomba, K. Müller, D. van Pinxteren, H. Herrmann, Aerosol size-resolved trace metal composition in remote northern tropical Atlantic marine environment: case study Cape Verde islands, ACP, 13(2013) 4801–14. https://doi.org/10.5194/acp-13-4801-2013.

[72] L.T. González, F.E. Longoria-Rodríguez, M. Sánchez-Domínguez, C. Leyva-Porras, K. Acuña-Askar, B.I. Kharissov, Seasonal variation and chemical composition of particulate matter: A study by XPS, ICP-AES and sequential microanalysis using Raman with SEM/EDS, J Environ Sci, 74(2018) 32–49. 10.1016/j.jes.2018.02.002.

[73] T. Grigoratos, C. Samara, D. Voutsa, E. Manoli, A. Kouras, Chemical composition and mass closure of ambient coarse particles at traffic and urban-background sites in Thessaloniki, Greece, Environ Sci Pollut Res, 21(2014) 7708–22. 10.1007/s11356-014-2732-z.

[74] N. Hazarika, A. Srivastava, Estimation of risk factor of elements and PAHs in size-differentiated particles in the National Capital Region of India, Air Qual Atmos Health, 10(2017) 469–82. 10.1007/s11869-016-0438-8.

[75] C.Y. Hsu, K.H. Chi, C.D. Wu, S.K. Lin, W.C. Hsu, C.C. Tseng, 2021. Integrated analysis of source-specific risks for PM2.5-bound metals in urban, suburban, rural, and industrial areas. Environ Pollut. 275, 116652. 10.1016/j.envpol.2021.116652.

[76] W. Insian, N. Yabueng, W. Wiriya, S. Chantara, 2022. Size-fractionated PM-bound PAHs in urban and rural atmospheres of northern Thailand for respiratory health risk assessment. Environ Pollut. 293, 118488. 10.1016/j.envpol.2021.118488.

[77] I. Jakovljević, G. Pehnec, V. Vađić, M. Čačković, V. Tomašić, J.D. Jelinić, Polycyclic aromatic hydrocarbons in PM10, PM2.5 and PM1 particle fractions in an urban area, Air Qual Atmos Health, 11(2018) 843–54. https://doi.org/10.1007/s11869-018-0603-3.

[78] A.A. Jamhari, M. Sahani, M.T. Latif, K.M. Chan, H.S. Tan, M.F. Khan, Concentration and source identification of polycyclic aromatic hydrocarbons (PAHs) in PM10 of urban, industrial and semi-urban areas in Malaysia, Atmos Environ, 86(2014) 16–27. https://doi.org/10.1016/j.atmosenv.2013.12.019.

[79] D. Jandacka, D. Durcanska, M. Bujdos, The contribution of road traffic to particulate matter and metals in air pollution in the vicinity of an urban road, Transp Res Part D: Trans Environ, 50(2017) 397–408. https://doi.org/10.1016/j.trd.2016.11.024.

[80] A. Jedynska, G. Hoek, M. Eeftens, J. Cyrys, M. Keuken, C. Ampe, Spatial variations of PAH, hopanes/steranes and EC/OC concentrations within and between European study areas, Atmos Environ, 87(2014) 239–48. https://doi.org/10.1016/j.atmosenv.2014.01.026.

[81] N. Jiang, S. Duan, X. Yu, R. Zhang, K. Wang, Comparative major components and health risks of toxic elements and polycyclic aromatic hydrocarbons of PM2.5 in winter and summer in Zhengzhou: Based on three-year data, Atmos Res, 213(2018) 173–84. https://doi.org/10.1016/j.atmosres.2018.06.008.

[82] M. B. Khan, M. Masiol, C. Bruno, A. Pasqualetto, G.M. Formenton, C. Agostinelli, Potential sources and meteorological factors affecting PM2.5-bound polycyclic aromatic hydrocarbon levels in six main cities of northeastern Italy: an assessment of the related carcinogenic and mutagenic risks, Environ Sci Pollut Res, 25(2018) 31987–2000. https://doi.org/10.1007/s11356-018-2841-1.

[83] E. Koçak, Determination of organic particle composition in Ankara atmosphere and investigation of their contribution to receptor modeling. https://open.metu.edu.tr/handle/11511/27000, 2017 (accessed 24 September 2024).

[84] E. Koçak, S. Aslan, İ. İmamoğlu, G. Tuncel, Multi-group organic pollutants in urban and suburban atmospheric particulate matter (PM2.5): Temporal variation, meteorological impact, and sources, Air Qual Atmos Health, 18(2025) 1359–76. https://doi.org/10.1007/s11869-025-01716-5.

[85] A. Kouras, E. Manoli, A. Avgenikou, A. Paraschaki, D. Voutsa, C. Samara, 2025. Inhalation health risk assessment in the port of Volos, Greece, based on multiannual evolution of PM10-bound polycyclic aromatic hydrocarbons and metals/metalloids: Implications for EU-regulated PM10 pollutants. Atmos Environ. 358, 121348. https://doi.org/10.1016/j.atmosenv.2025.121348.

[86] S. Lara, F. Villanueva, P. Martín, S. Salgado, A. Moreno, P. Sánchez-Verdú, 2022. Investigation of PAHs, nitrated PAHs and oxygenated PAHs in PM10 urban aerosols. A comprehensive data analysis. Chemosphere. 294, 133745. https://doi.org/10.1016/j.chemosphere.2022.133745.

[87] A.U. Lewandowska, M. Staniszewska, A. Witkowska, M. Machuta, L. Falkowska, Benzo(a)pyrene parallel measurements in PM1 and PM2.5 in the coastal zone of the Gulf of Gdansk (Baltic Sea) in the heating and non-heating seasons, Environ Sci Pollut Res, 25(2018) 19458–69. https://doi.org/10.1007/s11356-018-2089-9.

[88] F. Li, G. Zhang, Y. Jinxu, T. Ding, C.Q. Liu, Y. Lang, 2024. Comprehensive source identification of heavy metals in atmospheric particulate matter in a megacity: A case study of Hangzhou. JEM. 366, 121747. https://doi.org/10.1016/j.jenvman.2024.121747.

[89] R.J. Li, X.J. Kou, H. Geng, C. Dong, Z.W. Cai, Pollution characteristics of ambient PM2.5-bound PAHs and NPAHs in a typical winter time period in Taiyuan, CCL, 25(2014) 663–6. https://doi.org/10.1016/j.cclet.2014.03.032.

[90] X. Li, L. Jiang, Y. Bai, Y. Yang, S. Liu, X. Chen, Wintertime aerosol chemistry in Beijing during haze period: Significant contribution from secondary formation and biomass burning emission, Atmos Res, 218(2019) 25–33. https://doi.org/10.1016/j.atmosres.2018.10.010.

887 [91] Y. Lin, Y. Ma, X. Qiu, R. Li, Y. Fang, J. Wang, Sources, transformation, and health
888 implications of PAHs and their nitrated, hydroxylated, and oxygenated derivatives in
889 PM2.5 in Beijing, J Geophys Res Atmos, 120(2015) 7219–28.
890 https://doi.org/10.1002/2015JD023628.

891 [92] X. Liu, Y. Zhai, Y. Zhu, Y. Liu, H. Chen, P. Li, Mass concentration and health risk
892 assessment of heavy metals in size-segregated airborne particulate matter in
893 Changsha, Sci Total Environ, 517(2015) 215–21.
894 https://doi.org/10.1016/j.scitotenv.2015.02.066.

895 [93] X. Liu, X. Zhang, T. Wang, B. Jin, L. Wu, R. Lara, 2024. PM10-bound trace elements in
896 pan-European urban atmosphere. Environ Res. 260, 119630.
897 https://doi.org/10.1016/j.envres.2024.119630.

898 [94] W. Lu, L. Yang, J. Chen, X. Wang, H. Li, Y. Zhu, Identification of concentrations and
899 sources of PM2.5-bound PAHs in North China during haze episodes in 2013, Air Qual
900 Atmos Health, 9(2016) 823–33. https://doi.org/10.1007/s11869-015-0386-8.

901 [95] Y. Ma, Y. Cheng, X. Qiu, Y. Lin, J. Cao, D. Hu, A quantitative assessment of source
902 contributions to fine particulate matter (PM2.5)-bound polycyclic aromatic hydrocarbons
903 (PAHs) and their nitrated and hydroxylated derivatives in Hong Kong, Environ Pollut,
904 219(2016) 742–9. https://doi.org/10.1016/j.envpol.2016.07.034.

905 [96] L. Ma, B. Li, Y. Liu, X. Sun, D. Fu, S. Sun, 2020. Characterization, sources and risk
906 assessment of PM2.5-bound polycyclic aromatic hydrocarbons (PAHs) and nitrated
907 PAHs (NPAHs) in Harbin, a cold city in Northern China. J Clean Prod. 264, 121673.
908 https://doi.org/10.1016/j.jclepro.2020.121673.

909 [97] M. Malandrino, M. Casazza, O. Abollino, C. Minero, V. Maurino, Size resolved metal
910 distribution in the PM matter of the city of Turin (Italy), Chemosphere, 147(2016) 477–
911 89. https://doi.org/10.1016/j.chemosphere.2015.12.089.

912 [98] E. Manoli, A. Kouras, O. Karagkiozidou, G. Argyropoulos, D. Voutsa, C. Samara,
913 Polycyclic aromatic hydrocarbons (PAHs) at traffic and urban background sites of
914 northern Greece: source apportionment of ambient PAH levels and PAH-induced lung
915 cancer risk, Environ Sci Pollut Res, 23(2016) 3556–68. 10.1007/s11356-015-5573-5.

916 [99] S. Mazziotti Tagliani, M. Carnevale, G. Armiento, M.R. Montereali, E. Nardi, M.
917 Inglessis, Content, mineral allocation and leaching behavior of heavy metals in urban
918 PM2.5, Atmos Environ, 153(2017) 47–60.
919 https://doi.org/10.1016/j.atmosenv.2017.01.009.

920 [100] S. Mbengue, L.Y. Alleman, P. Flament, Size-distributed metallic elements in
921 submicronic and ultrafine atmospheric particles from urban and industrial areas in
922 northern France, Atmos Res, 135–136(2014) 35–47.
923 https://doi.org/10.1016/j.atmosres.2013.08.010.

924 [101] L. Megido, L. Negral, L. Castrillón, E. Marañón, Y. Fernández-Nava, B. Suárez-Peña,
925 Traffic tracers in a suburban location in northern Spain: relationship between
926 carbonaceous fraction and metals, Environ Sci Pollut Res, 23(2016) 8669–78.
927 https://doi.org/10.1007/s11356-015-5955-8.

928 [102] P. Mikuška, K. Křůmal, Z. Večeřa, Characterization of organic compounds in the PM2.5
929 aerosols in winter in an industrial urban area, Atmos Environ, 105(2015) 97–108.
930 https://doi.org/10.1016/j.atmosenv.2015.01.028.

[103]A. Nadali, M. Leili, A. Bahrami, M. Karami, A. Afkhami, 2021. Phase distribution and risk assessment of PAHs in ambient air of Hamadan, Iran. EES. 209, 111807. https://doi.org/10.1016/j.ecoenv.2020.111807.

[104]F. Oroumiyeh, M. Jerrett, I. Del Rosario, J. Lipsitt, J. Liu, S.E. Paulson, 2022. Elemental composition of fine and coarse particles across the greater Los Angeles area: Spatial variation and contributing sources. Environ Pollut. 292, 118356. https://doi.org/10.1016/j.envpol.2021.118356.

[105]A. Parvizimehr, A.N. Baghani, M. Hoseini, A. Sorooshian, A. Cuevas-Robles, M. Fararouei, 2020. On the nature of heavy metals in PM10 for an urban desert city in the Middle East: Shiraz, Iran. Microchem J. 154, 104596. https://doi.org/10.1016/j.microc.2020.104596.

[106]E. Padoan, M. Malandrino, A. Giacomino, M.M. Grosa, F. Lollobrigida, S. Martini, Spatial distribution and potential sources of trace elements in PM10 monitored in urban and rural sites of Piedmont Region, Chemosphere, 145(2016) 495–507. https://doi.org/10.1016/j.chemosphere.2015.11.094.

[107]M. Patil, A.S. Jadhav, S.K. Singh, S. Ingle, Urban ambient PM10 analysis: Characterization, sources, health risk and sustainable solutions, J Environ Chem Ecotoxicol, 6(2024) 192–205. https://doi.org/10.1016/j.enceco.2024.05.008.

[108]Y. Ren, Q. Luo, S. Zhuo, Y. Hu, G. Shen, H. Cheng, 2021. Bioaccessibility and public health risk of heavy Metal(loid)s in the airborne particulate matter of four cities in northern China. Chemosphere. 277, 130312. https://doi.org/10.1016/j.chemosphere.2021.130312.

[109]W. Rogula-Kozłowska, K. Klejnowski, P. Rogula-Kopiec, L. Ośródka, E. Krajny, B. Błaszczak, Spatial and seasonal variability of the mass concentration and chemical composition of PM2.5 in Poland, Air Qual Atmos Health, 7(2014) 41–58. https://doi.org/10.1007/s11869-013-0222-y.

[110]H. A. Khwaja, Z. Fatmi, D. Malashock, Z. Aminov, A. Kazi, A. Siddique, Effect of air pollution on daily morbidity in Karachi, Pakistan, J Local Glob Health Sci, 29(2012) 1–13. 10.5339/jlghs.2012.3.

[111]F. Sannoh, Z. Fatmi, D.O. Carpenter, M. Santoso, A. Siddique, K. Khan, 2024. Air pollution we breathe: Assessing the air quality and human health impact in a megacity of Southeast Asia. Sci Total Environ. 942, 173403. 10.1016/j.scitotenv.2024.173403.

[112]B.P. Singh, K. Kumar, V.K. Jain, 2021. Distribution of ring PAHs in particulate/gaseous phase in the urban city of Delhi, India: Seasonal variation and cancer risk assessment. Urban Clim. 40, 101010. https://doi.org/10.1016/j.uclim.2021.101010.

[113]R. Shen, Y. Wang, W. Gao, X. Cong, L. Cheng, X. Li, Size-segregated particulate matter bound polycyclic aromatic hydrocarbons (PAHs) over China: Size distribution, characteristics and health risk assessment, Sci Total Environ, 685(2019) 116–23. https://doi.org/10.1016/j.scitotenv.2019.05.436.

[114]G.L. Shi, X.Y. Zhou, S.Y. Jiang, Y.Z. Tian, G.R. Liu, Y.C. Feng, Further insights into the composition, source, and toxicity of PAHs in size-resolved particulate matter in a megacity in China, Environ Toxicol Chem, 34(2015) 480–7. 10.1002/etc.2809.

973 [115]M. Soleimani, N. Amini, B. Sadeghian, D. Wang, L. Fang, Heavy metals and their
974 source identification in particulate matter (PM2.5) in Isfahan City, Iran, J Environ Sci,
975 72(2018) 166–75. https://doi.org/10.1016/j.jes.2018.01.002.

976 [116]A. Talbi, Y. Kerchich, R. Kerbachi, M. Boughedaoui, Assessment of annual air pollution
977 levels with PM1, PM2.5, PM10 and associated heavy metals in Algiers, Algeria,
978 Environ Pollut, 232(2018) 252–63. https://doi.org/10.1016/j.envpol.2017.09.041.

979 [117]J. Tan, L. Zhang, X. Zhou, J. Duan, Y. Li, J. Hu, Chemical characteristics and source
980 apportionment of PM2.5 in Lanzhou, China, Sci Total Environ, 601–602(2017) 1743–
981 52. https://doi.org/10.1016/j.scitotenv.2017.06.050.

982 [118]Y.C. Ting, Y.X. Zou, S.Y. Pan, Y.R. Ko, Z.J. Ciou, C.H. Huang, 2024. Sources-
983 attributed contributions to health risks associated with PM2.5-bound polycyclic aromatic
984 hydrocarbons during the warm and cold seasons in an urban area of Eastern Asia. Sci
985 Total Environ. 922, 171325. https://doi.org/10.1016/j.scitotenv.2024.171325.

986 [119]E.I. Tolis, D.E. Saraga, M.K. Lytra, A.C. Papathanasiou, P.N. Bougaidis, O.E. Prekas-
987 Patronakis, Concentration and chemical composition of PM2.5 for a one-year period at
988 Thessaloniki, Greece: A comparison between city and port area, Atmos Environ,
989 113(2015) 197–207. https://doi.org/10.1016/j.atmosenv.2015.05.014.

990 [120]I. Tsiodra, G. Grivas, A. Bougiatioti, K. Tavernaraki, C. Parinos, D. Paraskevopoulou,
991 2024. Source apportionment of particle-bound polycyclic aromatic hydrocarbons
992 (PAHs), oxygenated PAHs (OPAHs), and their associated long-term health risks in a
993 major European city. Sci Total Environ. 951, 175416.
994 https://doi.org/10.1016/j.scitotenv.2024.175416.

995 [121]N. Zhang, M.W. Maung, S. Wang, E. Aruffo, J. Feng, 2024. Characterization and health
996 risk assessment of PM2.5-bound polycyclic aromatic hydrocarbons in Yangon and
997 Mandalay of Myanmar. Sci Total Environ. 914, 170034.
998 https://doi.org/10.1016/j.scitotenv.2024.170034.

999 [122]J. Zhang, Y. Su, C. Chen, W. Guo, Q. Tan, M. Feng, Chemical composition, sources
1000 and formation mechanism of urban $PM_{2.5}$ in Southwest China: a case study at the
1001 beginning of 2023, ACP, 24(2024) 2803–20. https://doi.org/10.5194/acp-24-2803-2024.

1002 [123]L. Zhang, H. Xu, B. Fang, H. Wang, Z. Yang, W. Yang, Source Identification and Health
1003 Risk Assessment of Polycyclic Aromatic Hydrocarbon-Enriched PM2.5 in Tangshan,
1004 China, Environ Toxicol Chem, 39(2020) 458–67. 10.1002/etc.4618.

1005 [124]J. Zhang, L. Yang, A. Mellouki, J. Chen, X. Chen, Y. Gao, Diurnal concentrations,
1006 sources, and cancer risk assessments of PM2.5-bound PAHs, NPAHs, and OPAHs in
1007 urban, marine and mountain environments, Chemosphere, 209(2018) 147–55.
1008 https://doi.org/10.1016/j.chemosphere.2018.06.054.

1009 [125]C. Wang, Z. Meng, P. Yao, L. Zhang, Z. Wang, Y. Lv, 2019. Sources-specific
1010 carcinogenicity and mutagenicity of PM2.5-bound PAHs in Beijing, China: Variations of
1011 contributions under diverse anthropogenic activities. Ecotoxicol Environ Saf. 183,
1012 109552. https://doi.org/10.1016/j.ecoenv.2019.109552.

1013 [126]J. Wang, S.S.H. Ho, S. Ma, J. Cao, W. Dai, S. Liu, Characterization of PM2.5 in
1014 Guangzhou, China: uses of organic markers for supporting source apportionment, Sci
1015 Total Environ, 550(2016) 961–71. 10.1016/j.scitotenv.2016.01.138.

[127]L. Wang, S. Dong, M. Liu, W. Tao, B. Xiao, S. Zhang, Polycyclic aromatic hydrocarbons in atmospheric PM2.5 and PM10 in the semi-arid city of Xi'an, Northwest China: Seasonal variations, sources, health risks, and relationships with meteorological factors, Atmos Res, 229(2019) 60–73. https://doi.org/10.1016/j.atmosres.2019.06.014.

[128]J. Wang, J. Cao, Z. Dong, B. Guinot, M. Gao, R. Huang, Seasonal variation, spatial distribution and source apportionment for polycyclic aromatic hydrocarbons (PAHs) at nineteen communities in Xi'an, China: The effects of suburban scattered emissions in winter, Environ Pollut, 231(2017) 1330–43. https://doi.org/10.1016/j.envpol.2017.08.106.

[129]L. Yang, X. Zhang, W. Xing, Q. Zhou, L. Zhang, Q. Wu, Yearly variation in characteristics and health risk of polycyclic aromatic hydrocarbons and nitro-PAHs in urban shanghai from 2010–2018, J Environ Sci, 99(2021) 72–9. https://doi.org/10.1016/j.jes.2020.06.017.

[130]L. Yang, L. Zhang, L. Chen, C. Han, T. Akutagawa, O. Endo, 2021. Polycyclic aromatic hydrocarbons and nitro-polycyclic aromatic hydrocarbons in five East Asian cities: Seasonal characteristics, health risks, and yearly variations. Environ Pollut. 287, 117360. https://doi.org/10.1016/j.envpol.2021.117360.

[131]Q. Yu, X. Ding, Q. He, W. Yang, M. Zhu, S. Li, Nationwide increase of polycyclic aromatic hydrocarbons in ultrafine particles during winter over China revealed by size-segregated measurements, Atmos Chem Phys, 20(2020) 14581–95. https://doi.org/10.5194/acp-20-14581-2020.

[132]Y. Xiong, J. Zhou, J.J. Schauer, W. Yu, Y. Hu, Seasonal and spatial differences in source contributions to PM2.5 in Wuhan, China, Sci Total Environ, 577(2017) 155–65. https://doi.org/10.1016/j.scitotenv.2016.10.150.

[133]H. Xu, S.S.H. Ho, M. Gao, J. Cao, B. Guinot, K.F. Ho, Microscale spatial distribution and health assessment of PM2.5-bound polycyclic aromatic hydrocarbons (PAHs) at nine communities in Xi'an, China, Environ Pollut, 218(2016) 1065–73. https://doi.org/10.1016/j.envpol.2016.08.058.

[134]H. Xue, G. Liu, H. Zhang, R. Hu, X. Wang, Similarities and differences in PM10 and PM2.5 concentrations, chemical compositions and sources in Hefei City, China, Chemosphere, 220(2019) 760–5. https://doi.org/10.1016/j.chemosphere.2018.12.123.

[135]P. Kumar, A. Robins, S. Vardoulakis, R. Britter, A review of the characteristics of nanoparticles in the urban atmosphere and the prospects for developing regulatory controls, Atmos Environ, 44(2010) 5035–52. https://doi.org/10.1016/j.atmosenv.2010.08.016.

[136]S. Karthikeyan, U.M. Joshi, R. Balasubramanian, Microwave assisted sample preparation for determining water-soluble fraction of trace elements in urban airborne particulate matter: evaluation of bioavailability, Anal Chim Acta, 576(2006) 23–30. https://doi.org/10.1016/j.aca.2006.05.051.

[137]C. Marina-Montes, E. Abás, J. Buil-García, J. Anzano, 2023. From multi to single-particle analysis: A seasonal spectroscopic study of airborne particulate matter in Zaragoza, Spain. Talanta. 259, 124550. 10.1016/j.talanta.2023.124550.

1058 [138]D. Salcedo, J.P. Bernal, O. Pérez-Arvizu, E. Lounejeva, Assessment of sample
1059 preparation methods for the analysis of trace elements in airborne particulate matter, J
1060 Anal At Spectrom, 29(2014) 753–61. https://doi.org/10.1039/C3JA50375E.

1061 [139]L. Samek, Z. Stegowski, K. Styszko, L. Furman, J. Fiedor, Seasonal contribution of
1062 assessed sources to submicron and fine particulate matter in a Central European urban
1063 area, Environ Pollut, 241(2018) 406–11. https://doi.org/10.1016/j.envpol.2018.05.082.

1064 [140]D. Saraga, T. Maggos, C. Degrendele, J. Klánová, M. Horvat, D. Kocman, 2021. Multi-
1065 city comparative PM2.5 source apportionment for fifteen sites in Europe: The ICARUS
1066 project. Sci Total Environ. 751, 141855.
1067 https://doi.org/10.1016/j.scitotenv.2020.141855.

1068 [141]J. Szabó, A. Nagy, J. Erdős, Ambient concentrations of PM10, PM10-bound polycyclic
1069 aromatic hydrocarbons and heavy metals in an urban site of Győr, Hungary. Air Qual
1070 Atmos Health. 8(2015) 229–241. https://doi.org/10.1007/s11869-015-0318-7.

1071 [142]R.C. Cornelis, H.M. Crews, J.A. Caruso, K.G. Heumann, Handbook of Elemental
1072 Speciation: Techniques and Methodology, John Wiley & Sons, Ltd, 2003.

1073 [143]V. Celo, E. Dabek, D. Mathieu, I. Okonskaia, Validation of a Simple Microwave-
1074 Assisted Acid Digestion Method Using Microvessels for Analysis of Trace Elements in
1075 Atmospheric PM2.5 in Monitoring and Fingerprinting Studies, The Open Chemical and
1076 Biomedical Methods Journal, 3(2010) 141–50. 10.2174/1875038901003010143.

1077 [144]E. Dabek-Zlotorzynska, Validation of a Simple Microwave-Assisted Acid Digestion
1078 Method Using Microvessels for Analysis of Trace Elements in Atmospheric PM2.5 in
1079 Monitoring and Fingerprinting Studies, TOCBMJ, 3(2010) 143–52.

1080 [145]D.J. Eatough, N. Aghdaie, M. Cottam, T. Gammon, L.D. Hansen, E.A. Lewis, Loss of
1081 Semi-volatile Organic Compounds from Particles During Sampling on Filters.
1082 Transactions: Visibility and Fine Particle, 1990.

1083 [146]J. Marrero, R. Rebagliati, D. Gomez, P. Smichowski, A study of uniformity of elements
1084 deposition on glass fiber filters after collection of airborne particulate matter (PM-10),
1085 using a high-volume sampler, Talanta, 68(2005) 442–7.
1086 https://doi.org/10.1016/j.talanta.2005.09.005.

1087 [147]S.R. McDow, J.J. Huntzicker, Vapor Adsorption Artifact in the Sampling of Organic
1088 Aerosol: Face Velocity Effects, Atmos Enviro, 24(1990) 2563–2571.
1089 https://doi.org/10.1016/0960-1686(90)90134-9.

1090 [148]K.W. Lee, M. Ramamurthi, Filter Collection, in: K. Willeke, P.A. Baron (Eds.), Aerosol
1091 Measurement: Principles, Techniques and Applications, Van Nostrand Reinhold, New
1092 York, 1993, pp. 179–205.

1093 [149]M. Lippmann, Filters and Filter Holders, in J. Lieben (Ed.), Air Sampling Instruments for
1094 Evaluation of Atmospheric Contaminants, Cincinnati, 1995.

1095 [150]J.C. Chow, J.G. Watson, Guideline on speciated particulate monitoring,
1096 https://hero.epa.gov/hero/index.cfm/reference/details/reference_id/24966, 1998
1097 (accessed 23 July 2025).

[151]P. Kumar, L. Pirjola, M. Ketzel, R.M. Harrison, Nanoparticle emissions from 11 non-vehicle exhaust sources – A review, Atmos Environ, 67(2013) 252–77. https://doi.org/10.1016/j.atmosenv.2012.11.011.

[152]M. Akyüz, H. Çabuk, Gas–particle partitioning and seasonal variation of polycyclic aromatic hydrocarbons in the atmosphere of Zonguldak, Turkey, Sci Total Environ, 408(2010) 5550–8. https://doi.org/10.1016/j.scitotenv.2010.07.063.

[153]A.M. Caricchia, S. Chiavarini, M. Pezza, Polycyclic aromatic hydrocarbons in the urban atmospheric particulate matter in the city of Naples (Italy), Atmos Environ, 33(1999) 3731–8. https://doi.org/10.1016/S1352-2310(99)00199-5.

[154]A. Katsoyiannis, E. Terzi, Q.Y. Cai, On the use of PAH molecular diagnostic ratios in sewage sludge for the understanding of the PAH sources. Is this use appropriate?, Chemosphere, 69(2007) 1337–9. https://doi.org/10.1016/j.chemosphere.2007.05.084.

[155]M.B. Yunker, R.W. Macdonald, R. Vingarzan, R.H. Mitchell, D. Goyette, S. Sylvestre, PAHs in the Fraser River basin: a critical appraisal of PAH ratios as indicators of PAH source and composition, Org Geochem, 33(2002) 489–515. https://doi.org/10.1016/S0146-6380(02)00002-5.

[156]J. Hennigan, M.H. Bergin, J.E. Dibb, R.J. Weber, Enhanced secondary organic aerosol formation due to water uptake by fine particles, Geophys Res Lett, 35(2008) https://agupubs.onlinelibrary.wiley.com/doi/10.1029/2008GL035046.

[157]M. Eeftens, M.Y. Tsai, C. Ampe, B. Anwander, R. Beelen, T. Bellander, Spatial variation of PM2.5, PM10, PM2.5 absorbance and PMcoarse concentrations between and within 20 European study areas and the relationship with NO2 – Results of the ESCAPE project, Atmos Environ, 62(2012) 303–17. https://doi.org/10.1016/j.atmosenv.2012.08.038.

[158]X. Querol, A. Alastuey, T. Moreno, M.M. Viana, S. Castillo, J. Pey, Spatial and temporal variations in airborne particulate matter (PM10 and PM2.5) across Spain 1999–2005, Atmos Environ, 42(2008) 3964–79. https://doi.org/10.1016/j.atmosenv.2006.10.071.

[159]F. Amato, A. Alastuey, A. Karanasiou, F. Lucarelli, S. Nava, G. Calzolai, AIRUSE-LIFE+: a harmonized PM speciation and source apportionment in five southern European cities, ACP, 16(2016) 3289–309. https://doi.org/10.5194/acp-16-3289-2016.

[160]A. Bozlaker, N.J. Spada, M.P. Fraser, S. Chellam, Elemental Characterization of PM2.5 and PM10 Emitted from Light Duty Vehicles in the Washburn Tunnel of Houston, Texas: Release of Rhodium, Palladium, And Platinum, Environ Sci Technol, 48(2014) 54–62. https://doi.org/10.1021/es4031003.

[161]R.M. Harrison, A.M. Jones, J. Gietl, J. Yin, D.C. Green, Estimation of the Contributions of Brake Dust, Tire Wear, and Resuspension to Nonexhaust Traffic Particles Derived from Atmospheric Measurements, Environ Sci Technol, 46(2012) 6523–9. https://doi.org/10.1021/es300894r.

[162]P. Pakbin, Z. Ning, M.M Shafer, J.J. Schauer, C. Sioutas, Seasonal and Spatial Coarse Particle Elemental Concentrations in the Los Angeles Area, AST, 45(2011) 949–63. https://doi.org/10.1080/02786826.2011.571309.

[163]S. Wagner, T. Hüffer, P. Klöckner, M. Wehrhahn, T. Hofmann, T. Reemtsma, Tire wear particles in the aquatic environment - A review on generation, analysis, occurrence,

1141 fate and effects, Water Res, 139(2018) 83–100.
1142 https://doi.org/10.1016/j.watres.2018.03.051.

1143 [164]U. Makkonen, H. Hellén, P. Anttila, M. Ferm, Size distribution and chemical
1144 composition of airborne particles in south-eastern Finland during different seasons and
1145 wildfire episodes in 2006, Sci Total Environ, 408(2010) 644–51.
1146 https://doi.org/10.1016/j.scitotenv.2009.10.050.

1147 [165]P. Pant, R.M. Harrison, Estimation of the contribution of road traffic emissions to
1148 particulate matter concentrations from field measurements: A review, Atmos Environ,
1149 77(2013) 78–97. https://doi.org/10.1016/j.atmosenv.2013.04.028.

1150 [166]Y. Wei, P. Kumar, 2024. Beyond the tailpipe: Review of non-exhaust airborne
1151 nanoparticles from road vehicles. EEH. 4, 100130.
1152 https://doi.org/10.1016/j.eehl.2024.11.003.

1153 [167]J. Hitchins, L. Morawska, R. Wolff, D. Gilbert, Concentrations of submicrometre
1154 particles from vehicle emissions near a major road, Atmos Environ, 34(2000) 51–9.
1155 https://doi.org/10.1016/S1352-2310(99)00304-0.

1156 [168]L. Morawska, J.J. Zhang, Combustion sources of particles. 1. Health relevance and
1157 source signatures, Chemosphere, 49(2002) 1045–58. 10.1016/s0045-6535(02)00241-
1158 2.

1159 [169]A. Albinet, E. Leoz-Garziandia, H. Budzinski, E. Villenave, Polycyclic aromatic
1160 hydrocarbons (PAHs), nitrated PAHs and oxygenated PAHs in ambient air of the
1161 Marseilles area (South of France): Concentrations and sources, Sci Total Environ,
1162 384(2007) 280–92. https://doi.org/10.1016/j.scitotenv.2007.04.028.

1163 [170]J. Liu, R. Man, S. Ma, J. Li, Q. Wu, J. Peng, Atmospheric levels and health risk of
1164 polycyclic aromatic hydrocarbons (PAHs) bound to PM2.5 in Guangzhou, China,
1165 Marine Pollut Bull, 100(2015) 134–43. https://doi.org/10.1016/j.marpolbul.2015.09.014.

1166 [171]D. Liu, T. Lin, J.H. Syed, Z. Cheng, Y. Xu, K. Li, 2017. Concentration, source
1167 identification, and exposure risk assessment of PM2.5-bound parent PAHs and nitro-
1168 PAHs in atmosphere from typical Chinese cities. Sci Rep. 7, 10398.
1169 https://doi.org/10.1038/s41598-017-10623-4.

1170 [172]O. Pindado, R.M. Pérez, S. García, M. Sánchez, P. Galán, M. Fernández,
1171 Characterization and sources assignation of PM2.5 organic aerosol in a rural area of
1172 Spain, Atmos Environ, 43(2009) 2796–803.
1173 https://doi.org/10.1016/j.atmosenv.2009.02.046.

1174 [173]H. Song, Y. Zhang, M. Luo, J. Gu, M. Wu, D. Xu, Seasonal variation, sources and
1175 health risk assessment of polycyclic aromatic hydrocarbons in different particle
1176 fractions of PM2.5 in Beijing, China, Atmos Pollut Res, 10(2019) 105–14.
1177 https://doi.org/10.1016/j.apr.2018.06.012.

1178 [174]J. Zhang, L. Yang, A. Mellouki, J. Chen, X. Chen, Y. Gao, Atmospheric PAHs, NPAHs,
1179 and OPAHs at an urban, mountainous, and marine sites in Northern China: Molecular
1180 composition, sources, and ageing, Atmos Environ, 173(2018) 256–64.
1181 https://doi.org/10.1016/j.atmosenv.2017.11.002.

1182 [175]T. Zhao, L. Yang, Q. Huang, Y. Zhang, S. Bie, J. Li, 2020. PM2.5-bound polycyclic
1183 aromatic hydrocarbons (PAHs) and their derivatives (nitrated-PAHs and oxygenated-

PAHs) in a road tunnel located in Qingdao, China: Characteristics, sources and emission factors. Sci Total Environ. 720, 137521. https://doi.org/10.1016/j.scitotenv.2020.137521.

[176]C. Schauer, R. Niessner, U. Pöschl, Polycyclic Aromatic Hydrocarbons in Urban Air Particulate Matter: Decadal and Seasonal Trends, Chemical Degradation, and Sampling Artifacts, Environ Sci Technol, 37(2003) 2861–8. 10.1021/es034059s.

[177]Y. Zhang, J. Chen, H. Yang, R. Li, Q. Yu, Seasonal variation and potential source regions of PM2.5-bound PAHs in the megacity Beijing, China: Impact of regional transport, Environ Pollut, 231(2017) 329–38. https://doi.org/10.1016/j.envpol.2017.08.025.

[178]A. Saffari, S. Hasheminassab, M.M. Shafer, J.J. Schauer, T.A. Chatila, C. Sioutas, Nighttime aqueous-phase secondary organic aerosols in Los Angeles and its implication for fine particulate matter composition and oxidative potential, Atmos Environ, 133(2016) 112–22. https://doi.org/10.1016/j.atmosenv.2016.03.022.

[179]WHO, Air pollution. https://www.who.int/health-topics/air-pollution, 2025 (accessed 23 June 2025).

[180]Y. Wang, L. Xiong, M. Tang, Toxicity of inhaled particulate matter on the central nervous system: neuroinflammation, neuropsychological effects and neurodegenerative disease, J Appl Toxicol, 37(2017) 644–67. 10.1002/jat.3451.

[181]Y.C. Chen, H.C. Chiang, C.Y. Hsu, T.T. Yang, T.Y. Lin, M.J. Chen, Ambient PM2.5-bound polycyclic aromatic hydrocarbons (PAHs) in Changhua County, central Taiwan: Seasonal variation, source apportionment and cancer risk assessment, Environ Pollut, 218(2016) 372–82. https://doi.org/10.1016/j.envpol.2016.07.016.

[182]H. Guo, S.C. Lee, K.F. Ho, X.M. Wang, S.C. Zou, Particle-associated polycyclic aromatic hydrocarbons in urban air of Hong Kong, Atmos Environ, 37(2003) 5307–17. https://doi.org/10.1016/j.atmosenv.2003.09.011.

[183]J. He, S. Fan, Q. Meng, Y. Sun, J. Zhang, F. Zu, Polycyclic aromatic hydrocarbons (PAHs) associated with fine particulate matters in Nanjing, China: Distributions, sources and meteorological influences, Atmos Environ, 89(2014) 207–15. https://doi.org/10.1016/j.atmosenv.2014.02.042.

[184]R.M. Harrison, D.J.T. Smith, L. Luhana, Source Apportionment of Atmospheric Polycyclic Aromatic Hydrocarbons Collected from an Urban Location in Birmingham, U.K, Environ Sci Technol, 30(1996) 825–32. https://doi.org/10.1021/es950252d.

[185]R.K. Larsen, J.E. Baker, Source apportionment of polycyclic aromatic hydrocarbons in the urban atmosphere: a comparison of three methods, Environ Sci Technol, 37(2003) 1873–81. https://doi.org/10.1021/es0206184.

[186]M.F. Simcik, S.J. Eisenreich, P.J. Lioy, Source apportionment and source/sink relationships of PAHs in the coastal atmosphere of Chicago and Lake Michigan, Atmos Environ, 33(1999) 5071–9. https://doi.org/10.1016/S1352-2310(99)00233-2.

[187]H.L. Sheu, W.J. Lee, S.J. Lin, G.C. Fang, H.C. Chang, W.C. You, Particle-bound PAH content in ambient air, Environ Pollut, 96(1997) 369–82. https://doi.org/10.1016/S0269-7491(97)00044-4.

1226 [188]K.F. Ho, S.C. Lee, G.M.Y. Chiu, Characterization of selected volatile organic
1227 compounds, polycyclic aromatic hydrocarbons and carbonyl compounds at a roadside
1228 monitoring station, Atmos Environ, 36(2002) 57–65. https://doi.org/10.1016/S1352-
1229 2310(01)00475-7.

1230

Chapter 4

Conclusions

Particulate aerosol samples in urban environments are typically collected at stationary AQMS, using advanced instrumentation and standardised QA/QC protocols to ensure accurate representation of air quality status in cities. Despite their reliability across a wide range of pollutants and for long-term trend analysis, their high cost and limited spatial coverage presents a major challenge for comprehensive air quality assessment. Furthermore, PM sampling is often conducted at elevated sites (above 2.5 m, e.g. rooftops), distant from residential and commuter areas, limiting the representativeness of personal exposure assessment. Nevertheless, previous research has often used such data to evaluate the exposure of pedestrians and cyclists, who frequently encounter higher pollutant levels than vehicle users. In addition, PM characterisation is often focused on a single pollutant type (organic or inorganic) in size-fractionated PM_{10} or $PM_{2.5}$, with limited information on nano-sized PM, the fraction with the highest toxicological and environmental implications. Therefore, a comprehensive understanding of size-fractionated PM, particularly (ultra)fine fractions and their chemical composition, is essential for high quality data, cross-study comparability and effective air quality control, yet available data remain limited.

This doctoral thesis evaluated the applicability of affordable and portable PM size-fractionating samplers combined with optimised and validated analytical methods for multi-pollutant chemical characterisation, along with the potential of dynamic citizen-participatory LCS campaigns in urban pedestrian and cycling microenvironments to complement AQMS for improved regulatory strategies.

A LVS device was developed consisting of a PTFE membrane filter system (PM_{10}, $PM_{2.5}$, $PM_{0.1}$), connected to an ultrapure water trap that retains the nano-sized fraction ($PM_{<0.1}$). Together with optimised and validated analytical procedures using NIST SRM 1648a, the setup provides a reliable and accurate analytical tool for the determination of metal(oid)s, PGEs and PAHs for residential exposure assessment. Metal(oid)s and PGEs were determined by ICP-MS after MAD using a mixture of acids, while PAHs were extracted with a solvent mixture of C_3H_6O and C_6H_{14}, assisted by MSE and determined by GC-MS. The analytical repeatability and accuracy were 6% and 2% for metal(oid)s and PGEs, and 3% and 6% for PAHs, respectively. SEM analyses were performed to verify the effectiveness of the sampling device in fractionating PM to nano-sized particles and to investigate the morphological characteristics of the particles collected on the PTFE filters. Airborne PM were of geogenic, anthropogenic and biogenic origin, mainly comprising spherules, floccules, biogenic particles, tabular particles, irregularly shaped grains and agglomerate particles. Alumosilicates, magnesium silicates and carbonate particles predominated, indicating soil deposition and re-suspension processes, while carbon-enriched and sulfate particles are commonly associated with biomass burning and

vehicle emissions. Most particles were non-spherical, thereby providing a larger surface area for adsorption of potentially toxic compounds.

The applicability of the PM sampling device was successfully demonstrated in a nationwide, systematic one-year study in Slovenia. Size-fractionated PM was collected in urban, pedestrian and cycling microenvironments in Dobrova, Ljubljana, Maribor, Murska Sobota and Piran, to assess the potential health risks from inhalation exposure to metal(oid)s and PAHs. At all locations, the highest concentrations of metal(oid)s, in descending order, were observed for Zn (6.98 ng m^{-3}), Ba (4.46 ng m^{-3}), Cu (2.81 ng m^{-3}) and Cr (1.52 ng m^{-3}) during the HP, while Ce (0.15 ng m^{-3}), La (0.07 ng m^{-3}), V (0.25 ng m^{-3}) and Ni (0.47 ng m^{-3}) dominated in the NHP. Metal(oid) levels were highest in PM_{10}, with Ba, Cd, Cu, Ni, Pb and Zn also significantly enriched in $PM_{<0.1}$, indicating a strong contribution from vehicle sources. The largest differences between NHP and HP were observed for Co, Mo and Tl, all typically associated with high-temperature fossil fuel combustion. Among PAHs, BbF (0.05 ng m^{-3}), BghiP (0.04 ng m^{-3}) and IP (0.04 ng m^{-3}) exhibited most elevated concentrations, with the total sum of PAHs being highest for PM_{10}, followed by $PM_{0.1}$ and $PM_{2.5}$. Metal(oid)s were mostly influenced by PM size, reflecting the enhanced size-selective adsorption potential of smaller PM due to their larger specific surface area. In contrast, PAH concentrations were significantly affected by seasonal variations, primarily due to greater atmospheric stability in winter, enhanced partitioning of HMW PAHs into the particulate phase due to reduced volatility and more efficient volatilisation of LMW PAHs into the gaseous phase combined with intensified photochemical degradation during summer. The highest concentrations occurred in the more densely populated and higher-traffic cities of Ljubljana and Maribor, where more dispersed pollution sources and unfavourable meteorological conditions allow submicron particles to remain airborne for longer. Source apportionment using PCA, hierarchical clustering, ANOVA and Pearson correlation coefficients, along with DRs and elemental fingerprinting, indicated a dominance of pyrogenic sources, including: vehicle exhausts from diesel engines, deposition and re-suspension of mineral dust and non-exhaust sources, and combustion of coal and biomass during the HP. The carcinogenic risk assessment (LADD, HQ) for pedestrians and cyclists among different demographic groups indicated an overall negligible cancer risk, except for As (2×10^{-7}), Co (1×10^{-6}) and Cr (6×10^{-6}), which showed a low potential risk from inhalation, particularly for child cyclists. The calculated HQ values remained below the threshold, and the European limit values for As, Cd and BaP in PM_{10} were not exceeded.

In addition to gravimetric size-fractionating PM sampling solutions, LCS have recently been employed in citizen-led dynamic monitoring campaigns to assess city's intra-characteristic patterns, enhance understanding of commuters personal exposure and overcome the limitations of sparsely located AQMS. Nevertheless, compared to AQMS, LCS are more susceptible to variations in particle composition and density, hygroscopicity, refractive index, RH and pollutant concentration. Therefore, it is imperative to evaluate these sensors, using laboratory or co-location field assessment methods against reference instruments. The evaluation was performed for a Sensirion SPS30, a real-time OPC, which continuously measures $PM_{2.5}$ concentrations using a laser scattering technique. Under controlled laboratory conditions, R^2 ranged from 0.81−0.99 and RMSE from 0.81−61.72 µg m^{-3}, at an average concentration of 21.5 µg m^{-3}. In contrast, co-location assessment at an average concentration of 9 µg m^{-3} resulted in R^2 = 0.5 and RMSE = 6.82 µg m^{-3}. In addition, $PM_{2.5}$ readings exhibited strong RH sensitivity, with discrepancies attributed to differences in particle composition and concentration. The sensor met micro-environmental monitoring standards (accuracy <25%) and US EPA performance criteria (RMSE ≤7 µg m^{-3}, R^2 >0.7) only at RH <60% and low pollution levels, emphasising the need for RH-dependent data corrections.

Despite inconsistencies, LCS can effectively capture relative spatio-temporal variations and identify air pollution hotspots.

Bicycle-mounted LCS SPS30 were further deployed in two citizen science campaigns. The first campaign, in Ljubljana, Slovenia (September−December 2022) encompassed 312 cycling trips, while the second, in Maribor, Slovenia (October 2023) included 72 cycling trips. The average $PM_{2.5}$ concentrations in Ljubljana ranged 5−32 µg m^{-3}, increasing as temperatures dropped and peaking in December, while in Maribor they ranged 2.9−4.8 µg m^{-3}. In Maribor, the highest $PM_{2.5}$ concentrations were observed during the morning RHT, while in Ljubljana, peak levels occurred at night, with significantly elevated levels also noted during the afternoon RHT. In both cities, $PM_{2.5}$ concentrations were lowest around midday, coinciding with the highest PBL height. Higher winter pollution levels are also associated with frequent thermal inversions and weak vertical air mixing, thus limiting adequate pollutant dispersion. Spatial analysis revealed hotspots clustered near high-traffic areas, intersections with prolonged vehicle waiting times, construction sites and transport hubs. In Slovenia, local emissions – including residential fireplaces and traffic – play a major role in addition to meteorological, topographical, urbanisation and industrialisation factors. Exposure analysis revealed that cyclists were roughly three times more exposed than pedestrians over an equivalent average commute, mainly as a result of increased breathing frequency and greater volume of inhaled air. Men were at greater risk than women, with children recognised as the most vulnerable group. In Maribor, only 0.2% of all $PM_{2.5}$ measurements surpassed the air quality limits, compared to 21% in Ljubljana. However, HQ limits were not exceeded in either city. Moreover, 94% of participants reported willingness to change their travel behaviour to minimise exposure if the infrastructure – such as open cycling lanes, ventilated road junctions and paths separated from roads by vegetation – allowed it.

This thesis provides new insights into the chemical patterns of size-fractionated PM, in particular often overlooked nano-sized fractions, and represents one of Slovenia's first long-term citizen-led LCS campaigns. The findings provide the foundation for future research and regulatory actions, highlighting the need for innovative and cost-effective PM sampling solutions to better characterise pollutant distribution, chemical composition and exposure pathways.

References

Agarwal, A., Mangal, A., Satsangi, A., Lakhani, A., Maharaj Kumari, K. (2017). Characterization, sources and health risk analysis of PM2.5 bound metals during foggy and non-foggy days in sub-urban atmosphere of Agra. *Atmospheric Research*, 197, 121–131. https://doi.org/10.1016/j.atmosres.2017.06.027

Agilent. (2025a, September 9). *ICP-MS Overview*. https://www.agilent.com/en/product/atomic-spectroscopy/inductively-coupled-plasma-mass-spectrometry-icp-ms/what-is-icp-ms-icp-ms-faqs

Agilent. (2025b, September 9). *Gas chromatography mass spectrometry fundamentals*. https://www.agilent.com/en/product/gas-chromatography-mass-spectrometry-gc-ms/gcms-fundamentals

Agudelo-Castañeda, D.M., and Teixeira, E.C. (2014). Seasonal changes, identification and source apportionment of PAH in PM1.0. *Atmospheric Environment*, 96, 186–200. https://doi.org/10.1016/j.atmosenv.2014.07.030

Akhbarizadeh, R., Dobaradaran, S., Amouei Torkmahalleh, M., Saeedi, R., Aibaghi, R., Faraji Ghasemi, F. (2021). Suspended fine particulate matter (PM2.5), microplastics (MPs), and polycyclic aromatic hydrocarbons (PAHs) in air: Their possible relationships and health implications. *Environmental Research*, 192, 110339. https://doi.org/10.1016/j.envres.2020.110339

Akyüz M., Çabuk, H. (2010). Gas–particle partitioning and seasonal variation of polycyclic aromatic hydrocarbons in the atmosphere of Zonguldak, Turkey. *Science of The Total Environment*, 408, 5550–8. https://doi.org/10.1016/j.scitotenv.2010.07.063

Alam, M.S., Keyte, I.J., Yin, J., Stark, C., Jones, A.M., Harrison, R.M. (2015). Diurnal variability of polycyclic aromatic compound (PAC) concentrations: Relationship with meteorological conditions and inferred sources. *Atmospheric Environment*, 122, 427–438. https://doi.org/10.1016/j.atmosenv.2015.09.050

Aleixandre, M., and Gerboles, M. (2012). Review of Small Commercial Sensors for Indicative Monitoring of Ambient Gas. *Chemical Engineering Transactions*, 30, 169–174. https://doi.org/10.3303/CET1230029

Alves, C.A., Vicente, A.M., Custódio, D., Cerqueira, M., Nunes, T., Pio, C., Lucarelli, F., Calzolai, G., Nava, S., Diapouli, E., Eleftheriadis, K., Querol, X., Musa Bandowe, B.A. (2017). Polycyclic aromatic hydrocarbons and their derivatives (nitro-PAHs, oxygenated PAHs, and azaarenes) in PM2.5 from Southern European cities. *Science of The Total Environment*, 595, 494–504. https://doi.org/10.1016/j.scitotenv.2017.03.256

Ambade, B., Kumar, A., Kumar, A., Sahu, L.K. (2022). Temporal variability of atmospheric particulate-bound polycyclic aromatic hydrocarbons (PAHs) over central east India: Sources and carcinogenic risk assessment. *Air Quality, Atmosphere, & Health*, 15(1), 115–130. https://doi.org/10.1007/s11869-021-01089-5

AnaPath Research, S.A.U. (2025, September 18). *Electron Microscopy.* https://anapath.ch/electron-microscopy-2/

Anenberg, S.C., Mohegh, A., Goldberg, D.L., Kerr, G.H., Brauer, M., Burkart, K., Hystad, P., Larkin, A., Wozniak, S., Lamsal, L. (2022). Long-term trends in urban NO2 concentrations and associated paediatric asthma incidence: Estimates from global datasets. *The Lancet Planetary Health*, 6(1), 49–58. https://doi.org/10.1016/S2542-5196(21)00255-2

Appel, B.R., Tanner, R.L., Adams, D.F., Dasgupta, P.K., Knapp, K.T., Kok, G.L., Pierson, W.R., Reiszner, K.D. (1990). Semi-Continuous Determination of Atmospheric Particulate Sulfur, Sulfuric Acid and Ammonium Sulfates. In J.P., Lodge (Ed.), *Methods of Air Sampling and Analysis* (3rd ed., pp. 529–532). New York: Taylor and Francis

Austin, E., Novosselov, I., Seto, E., Yost, M.G. (2015). Laboratory Evaluation of the Shinyei PPD42NS Low-Cost Particulate Matter Sensor. *PLOS ONE*, 10(9), e0137789. https://doi.org/10.1371/journal.pone.0137789

Baalbaki, R., Nassar, J., Salloum, S., Shihadeh, A.L., Lakkis, I., Saliba, N.A. (2018). Comparison of atmospheric polycyclic aromatic hydrocarbon levels in three urban areas in Lebanon. *Atmospheric Environment*, 179, 260–267. https://doi.org/10.1016/j.atmosenv.2018.02.028

Bandowe, B.A.M., Meusel, H., Huang, R.J., Ho, K., Cao, J., Hoffmann, T., Wilcke, W. (2014). PM2.5-bound oxygenated PAHs, nitro-PAHs and parent-PAHs from the atmosphere of a Chinese megacity: Seasonal variation, sources and cancer risk assessment. *The Science of the Total Environment*, 473–474, 77–87. https://doi.org/10.1016/j.scitotenv.2013.11.108

Barkjohn, K.K., Gantt, B., Clements, A. L. (2021). Development and application of a United States-wide correction for PM2.5 data collected with the PurpleAir sensor. *Atmospheric Measurement Techniques*, 14(6), 4617–4637. https://doi.org/10.5194/amt-14-4617-2021

Bergmann, M.L., Andersen, Z.J., Amini, H., Khan, J., Lim, Y.H., Loft, S., Mehta, A., Westendorp, R.G., Cole Hunter, T. (2022). Ultrafine particle exposure for bicycle commutes in rush and non-rush hour traffic: A repeated measures study in Copenhagen, Denmark. *Environmental Pollution*, 294, 118631. https://doi.org/10.1016/j.envpol.2021.118631

Bortey-Sam, N., Ikenaka, Y., Akoto, O., Nakayama, S.M.M., Yohannes, Y.B., Baidoo, E., Mizukawa, H., Ishizuka, M. (2015). Levels, potential sources and human health risk of polycyclic aromatic hydrocarbons (PAHs) in particulate matter (PM10) in Kumasi, Ghana. *Environmental Science and Pollution Research*, 22(13), 9658–9667. https://doi.org/10.1007/s11356-014-4022-1

Breed, C.A., Arocena, J.M., Sutherland, D. (2002). Possible sources of PM10 in Prince George (Canada) as revealed by morphology and in situ chemical composition of particulate. *Atmospheric Environment*, 36(10), 1721–31. https://doi.org/10.1016/S1352-2310(01)00500-3

Briffa, J., Sinagra, E., Blundell, R. (2020). Heavy metal pollution in the environment and their toxicological effects on humans. *Heliyon*, 6(9), e04691. https://doi.org/10.1016/j.heliyon.2020.e04691

Brimblecombe, P. (1999). Air Pollution and Health History. In S.T. Holgate, J.M. Samet, H.S. Koren, R.L. Maynard (Eds.), *Air Pollution and Health* (pp. 5–18). Academic Press. https://doi.org/10.1016/B978-012352335-8/50077-6

Broekaert J.A.C. (2005). Plasma Mass Spectrometry. In J.A.C., Broekaert (Ed.), *Analytical Atomic Spectrometry with Flames and Plasmas* (pp. 284–331). John Wiley & Sons, Ltd. https://doi.org/10.1002/3527606653.ch6

Calvo, A.I., Alves, C., Castro, A., Pont, V., Vicente, A.M., Fraile, R. (2013). Research on aerosol sources and chemical composition: Past, current and emerging issues. *Atmospheric Research*, 120–121, 1–28. https://doi.org/10.1016/j.atmosres.2012.09.021

Canals-Angerri, A., Via, M., Lara, M., Alastuey, A., Minguillón, M.C., Pandolfi, M., van Drooge, B.L., Querol, X. (2024). Causes of the Unremitting High Ambient Levels of PM10 in a Suburban Background Site in NE Spain. *Environmental Pollution*, 363, 125113. doi:10.1016/j.envpol.2024.125113

Caricchia, A.M., Chiavarini, S., Pezza, M. (1999). Polycyclic aromatic hydrocarbons in the urban atmospheric particulate matter in the city of Naples (Italy). *Atmospheric Environment*, 33, 3731–8. https://doi.org/10.1016/S1352-2310(99)00199-5

Carabali, G., Mamani-Paco, R., Castro, T., Peralta, O., Herrera, E., Trujillo, B. (2012). Optical properties, morphology and elemental composition of atmospheric particles at T1 supersite on MILAGRO campaign, *Atmospheric Chemistry and Physics*, 12(5), 2747–55. https://doi.org/10.5194/acp-12-2747-2012

Castell, N., Dauge, F.R., Schneider, P., Vogt, M., Lerner, U., Fishbain, B., Broday, D., Bartonova, A. (2017). Can commercial low-cost sensor platforms contribute to air quality monitoring and exposure estimates? *Environment International*, 99, 293–302. https://doi.org/10.1016/j.envint.2016.12.007

Cecinato, A., Balducci, C., Mastroianni, D., Perilli, M. (2012). Sampling and analytical methods for assessing the levels of organic pollutants in the atmosphere: PAH, phthalates and psychotropic substances: a short review. *Environmental Science and Pollution Research International*, 19(6), 1915–1926. https://doi.org/10.1007/s11356-012-0959-0

Celo, V., Dabek, E., Mathieu, D., Okonskaia, I. (2010). Validation of a Simple Microwave-Assisted Acid Digestion Method Using Microvessels for Analysis of Trace Elements in Atmospheric PM2.5 in Monitoring and Fingerprinting Studies. *The Open Chemical and Biomedical Methods Journal*, 3, 141–150. https://doi.org/10.2174/1875038901003010143

Chen, H., Goldberg, M.S., Villeneuve, P.J. (2008). A systematic review of the relation between long-term exposure to ambient air pollution and chronic diseases. *Reviews on Environmental Health*, 23(4), 243–297. https://doi.org/10.1515/reveh.2008.23.4.243

Chen, Q., Chen, Y., Luo, X.S., Hong, Y., Hong, Z., Zhao, Z., Chen, J. (2019). Seasonal characteristics and health risks of PM2.5-bound organic pollutants in industrial and urban areas of a China megacity. *Journal of Environmental Management*, 245, 273–281. https://doi.org/10.1016/j.jenvman.2019.05.061

Choi, B., and Hummel, M.A. (2025). Spatiotemporal air quality prediction using stochastic advection–diffusion model for multimodal data fusion. *Environmental Research Letters*, 20(1), 014065. https://doi.org/10.1088/1748-9326/ada397

Choi, E., Yi, S.M., Lee, Y.S., Jo, H., Baek, S.O., Heo, J.B. (2022). Sources of airborne particulate matter-bound metals and spatial-seasonal variability of health risk potentials in four large cities, South Korea. *ESPR*, 29, 28359–74. https://doi.org/10.1007/s11356-021-18445-8

Chong, C.Y., and Kumar, S.P. (2003). Sensor networks: Evolution, opportunities, and challenges. *Proceedings of the IEEE*, 91(8), 1247—1256. 10.1109/JPROC.2003.814918

Chow, J.C. (1995). Measurement methods to determine compliance with ambient air quality standards for suspended particles. *Journal of the Air & Waste Management Association*, 45(5), 320–382. https://doi.org/10.1080/10473289.1995.10467369

Chow, J.C., and Watson, J.G. (1998). *Guideline on speciated particulate monitoring* (technical report 24966, pp. 15–21). United States Environmental Protection Agency. https://hero.epa.gov/hero/index.cfm/reference/details/reference_id/24966

Cohen, A.J., Brauer, M., Burnett, R., Anderson, H.R., Frostad, J., Estep, K., Balakrishnan, K., Brunekreef, B., Dandona, L., Dandona, R., Feigin, V., Freedman, G., Hubbell, B., Jobling, A., Kan, H., Knibbs, L., Liu, Y., Martin, R., Morawska, L., … Forouzanfar, M.H. (2017). Estimates and 25-year trends of the global burden of disease attributable to ambient air pollution: An analysis of data from the Global Burden of Diseases Study 2015. *Lancet*, 389(10082), 1907–1918. https://doi.org/10.1016/S0140-6736(17)30505-6

Cornelis, R.C., Crews, H.M., Caruso, J.A., Heumann, K.G. (2003). *Handbook of Elemental Speciation: Techniques and Methodology.* John Wiley & Sons, Ltd. https://doi.org/10.1002/0470868384.ch1

Coufalík, P., Mikuška, P., Matoušek, T., Večeřa, Z. (2016). Determination of the bioaccessible fraction of metals in urban aerosol using simulated lung fluids. *Atmospheric Environment*, 140, 469—475. https://doi.org/10.1016/j.atmosenv.2016.06.031

Crilley, L.R., Shaw, M., Pound, R., Kramer, L.J., Price, R., Young, S., Lewis, A.C., Pope, F.D. (2018). Evaluation of a low-cost optical particle counter (Alphasense OPC-N2) for ambient air monitoring. *Atmospheric Measurement Techniques*, 11(2), 709–720. https://doi.org/10.5194/amt-11-709-2018

Croghan, W., Egeghy, P. (2009). Methods of dealing with values below the limit of detection using SAS

Dabek Zlotorzynska, E. (2010). Validation of a Simple Microwave-Assisted Acid Digestion Method Using Microvessels for Analysis of Trace Elements in Atmospheric PM2.5 in Monitoring and Fingerprinting Studies. *The Open Chemical and Biomedical Methods Journal*, 3(1), 143–152. https://doi.org/10.2174/1875038901003010143

Daher, N., Saliba, N.A., Shihadeh, A.L., Jaafar, M., Baalbaki, R., Sioutas, C. (2013). Chemical composition of size-resolved particulate matter at near-freeway and urban background sites in the greater Beirut area. *Atmospheric Environment*, 80, 96–106. https://doi.org/10.1016/j.atmosenv.2013.08.004

Daly, A., Zannetti, S. (2007). An Introduction to Air Pollution – Definitions, Classifications, and History. In P. Zannetti, D. Al-Ajmi, S. Al-Rashied (Eds), *Ambient air pollution* (1st ed., pp. 1–14). The Arab School for Science and Technology and The EnviroComp Institute

Deabji, N., Fomba, K.W., dos Santos Souza, E.J., Mellouki, A., Herrmann, H. (2024). Influence of anthropogenic activities on metals, sugars and PAHs in PM10 in the city of Fez, Morocco: Implications on air quality. *Environmental Science and Pollution Research*, 31(17), 25238–57. https://link.springer.com/article/10.1007/s11356-024-32740-0

Decree on ambient air quality (Uredba o kakovosti zunanjega zraka). (2011). Official Gazette of the Republic of Slovenia no. 9/11, 8/15, 66/18, 14/22 – ZVO-2. https://pisrs.si/pregledPredpisa?id=URED5493

Decree on arsenic (As), cadmium (Cd), mercury (Hg), nickel (Ni) and polycyclic aromatic hydrocarbons (PAHs) in the ambient air (Uredba o arzenu, kadmiju, živem srebru, niklju in policikličnih aromatskih ogljikovodikih v zunanjem zraku). (2011). Official Gazette of the Republic of Slovenia no. 56/06, 44/22 – ZVO-2. https://pisrs.si/pregledPredpisa?id=URED4057

Decree on the classification of areas, agglomerations and sub-areas according to ambient air pollution (Odredba o razvrstitvi območij, aglomeracij in podobmočij glede na onesnaženost zunanjega zraka). (2017). Official Gazette of the Republic of Slovenia no. 38/17, 3/20, 152/20, 203/21, 44/22 – ZVO-2, 30/23. https://pisrs.si/pregledPredpisa?id=ODRE2387

Decree on the rules of assessment of ambient air quality (Pravilnik o ocenjevanju kakovosti zunanjega zraka). (2011). Official Gazette of the Republic of Slovenia no. 55/11, 6/15, 5/17, 44/22 – ZVO-2. https://pisrs.si/pregledPredpisa?id=PRAV10250

deSouza, P., Wang, A., Machida, Y., Duhl, T., Mora, S., Kumar, P., Kahn, R., Ratti, C., Durant, J.L., Hudda, N. (2023). Evaluating the Performance of Low-Cost PM2.5 Sensors in Mobile Settings. *Environmental Science & Technology*, 57(41), 15401–15411. https://doi.org/10.1021/acs.est.3c04843

Dettmer Wilde, K., and Engewald, W. (2014). *Practical Gas Chromatography, A Comprehensive Reference*. Berlin, Heidelberg: Springer. https://doi.org/10.1007/978-3-642-54640-2

Di Vaio, P., Cocozziello, B., Corvino, A., Fiorino, F., Frecentese, F., Magli, E., Onorati, G., Saccone, I., Santagada, V., Settimo, G., Severino, B., Perissutti, E. (2016). Level, potential sources of polycyclic aromatic hydrocarbons (PAHs) in particulate matter (PM10) in Naples. *Atmospheric Environment*, 129, 186–196. https://doi.org/10.1016/j.atmosenv.2016.01.020

Directive (EU) 2016/2284 of the European Parliament and of the Council of 14 December 2016 on the reduction of national emissions of certain atmospheric pollutants, amending Directive 2003/35/EC and repealing Directive 2001/81/EC. http://data.europa.eu/eli/dir/2016/2284/oj

Directive 2004/107/EC of the European Parliament and of the Council of 15 December 2004 relating to arsenic, cadmium, mercury, nickel and polycyclic aromatic hydrocarbons in ambient air. http://data.europa.eu/eli/dir/2004/107/oj/eng

Directive 2008/50/EC of the European Parliament and of the Council of 21 May 2008 on Ambient Air Quality and Cleaner Air for Europe. https://eur-lex.europa.eu/eli/dir/2008/50/oj/eng

Directive 2024/2881 of the European Parliament and of the Council of 23 October 2024 on ambient air quality and cleaner air for Europe. https://eur-lex.europa.eu/eli/dir/2024/2881/oj/eng

Dominici, F., Peng, R.D., Bell, M.L., Pham, L., McDermott, A., Zeger, S.L., Samet, J.M. (2006). Fine Particulate Air Pollution and Hospital Admission for Cardiovascular and Respiratory Diseases. *JAMA*, 295(10), 1127–1134. https://doi.org/10.1001/jama.295.10.1127

Drventić, I., Šala, M., Vidović, K., Kroflič, A. (2023). Direct quantification of PAHs and nitro-PAHs in atmospheric PM by thermal desorption gas chromatography with electron ionization mass spectroscopic detection. *Talanta*, 251, 123761. https://doi.org/10.1016/j.talanta.2022.123761

El-Mubarak, A.H., Rushdi, A.I., Al-Mutlaq, K.F., Bazeyad, A.Y., Simonich, S.L.M., Simoneit, B.R.T. (2014). Identification and source apportionment of polycyclic aromatic hydrocarbons in ambient air particulate matter of Riyadh, Saudi Arabia. *Environmental Science and Pollution Research*, 21(1), 558–567. https://doi.org/10.1007/s11356-013-1946-9

Elzein, A., Stewart, G.J., Swift, S.J., Nelson, B.S., Crilley, L.R., Alam, M.S., Reyes-Villegas, E., Gadi, R., Harrison, R.M., Hamilton, J.F., Lewis, A.C. (2020). A comparison of PM2.5-bound polycyclic aromatic hydrocarbons in summer Beijing (China) and Delhi (India). *Atmospheric Chemistry and Physics*, 20(22), 14303–14319. https://doi.org/10.5194/acp-20-14303-2020

European Commission. (2025, August 4). *Biodiversity strategy for 2030.* https://environment.ec.europa.eu/strategy/biodiversity-strategy-2030_en

European Council, Council of the European Union. (2024, August 4). *Euro 7: Council adopts new rules on emission limits for cars, vans and trucks.*

https://www.consilium.europa.eu/en/press/press-releases/2024/04/12/euro-7-council-adopts-new-rules-on-emission-limits-for-cars-vans-and-trucks/

European Environment Agency (EEA). (2013). *Air quality in Europe—2013 report*. European Environmental Agency. https://www.eea.europa.eu/publications/air-quality-in-europe-2013

European Environmental Agency (EEA). (2012). *Air quality in Europe—2012 report* (Report No 4/2012). European Environmental Agency. https://www.eea.europa.eu/en/analysis/publications/air-quality-in-europe-2012

European Environmental Agency (EEA). (2022). *Europe's air quality status 2022* (Briefing no. 04/2022). European Environmental Agency. https://www.eea.europa.eu/publications/status-of-air-quality-in-Europe-2022

European Parliament. (2024, August 4). *Zero pollution action plan for water, air and soil*. https://www.europarl.europa.eu/legislative-train/theme-a-european-green-deal/file-zero-pollution-action-plan

Evagelopoulos, V., Charisiou, N.D., Zoras, S. (2022). Dataset of Polycyclic aromatic hydrocarbons and trace elements in PM2.5 and PM10 atmospheric particles from two locations in North-Western Greece. *Data in Brief*, 42, 108266. https://doi.org/10.1016/j.dib.2022.108266

Fadel, M., Ledoux, F., Farhat, M., Kfoury, A., Courcot, D., Afif, C. (2021). PM2.5 characterization of primary and secondary organic aerosols in two urban-industrial areas in the East Mediterranean. *Journal of Environmental Sciences*, 101, 98–116. https://doi.org/10.1016/j.jes.2020.07.030

Fan, S.J., Heinrich, J., Bloom, M.S., Zhao, T.Y., Shi, T.X., Feng, W.R., Sun, Y., Shen, J.C., Yang, Z.C., Yang, B.Y., Dong, G.H. (2020). Ambient air pollution and depression: A systematic review with meta-analysis up to 2019. *The Science of the Total Environment*, 701, 134721. https://doi.org/10.1016/j.scitotenv.2019.134721

Farah, E., Fadel, M., Mansour, G., Fakhri, N., Hassan, S.K., Boraiy, M. (2024). Unveiling the organic chemical composition and sources of organic carbon in PM2.5 at an urban site in Greater Cairo (Egypt): A comprehensive analysis of primary and secondary compounds. *Environmental Research*, 263, 120118. https://doi.org/10.1016/j.envres.2024.120118

Feng, B., Li, L., Xu, H., Wang, T., Wu, R., Chen, J., Zhang, Y., Liu, S., Ho, S.S.H., Cao, J., Huang, W. (2019). PM2.5-bound polycyclic aromatic hydrocarbons (PAHs) in Beijing: Seasonal variations, sources, and risk assessment. *Journal of Environmental Sciences*, 77, 11–19. https://doi.org/10.1016/j.jes.2017.12.025

Fenger, J., Hertel, O., Palmgren, F. (1998). *Urban Air Pollution—European Aspects*. Netherlands: Springer Netherlands. https://doi.org/10.1007/978-94-015-9080-8

Fernández Camacho, R., Rodríguez, S., de la Rosa, J., Sánchez de la Campa, A.M., Alastuey, A., Querol, X., González-Castanedo, Y., Garcia-Orellana, I., Nava, S. (2012). Ultrafine particle and fine trace metal (As, Cd, Cu, Pb and Zn) pollution episodes induced by

industrial emissions in Huelva, SW Spain. *Atmospheric Environment*, 61, 507–517. https://doi.org/10.1016/j.atmosenv.2012.08.003

Fomba, K.W., Müller, K., van Pinxteren, D., Herrmann, H. (2013). Aerosol size-resolved trace metal composition in remote northern tropical Atlantic marine environment: Case study Cape Verde islands. *Atmospheric Chemistry and Physics*, 13(9), 4801–4814. https://doi.org/10.5194/acp-13-4801-2013

Fomba, K.W., van Pinxteren, D., Müller, K., Spindler, G., Herrmann, H. (2018). Assessment of trace metal levels in size-resolved particulate matter in the area of Leipzig. *Atmospheric Environment*, 176, 60–70. https://doi.org/10.1016/j.atmosenv.2017.12.024

Fontal, M., Van Drooge, B.L., López, J.F., Fernández, P., Grimalt, J.O. (2015). Broad Spectrum Analysis of Polar and Apolar Organic Compounds in Submicron Atmospheric Particles. *Journal of Chromatography A*, 1404, 28–38. doi:10.1016/j.chroma.2015.05.042

Fowler, D., Brimblecombe, P., Burrows, J., Heal, M.R., Grennfelt, P., Stevenson, D.S., Jowett, A., Nemitz, E., Coyle, M., Liu, X., Chang, Y., Fuller, G.W., Sutton, M.A., Klimont, Z., Unsworth, M.H., Vieno, M. (2020). A chronology of global air quality. Philosophical Transactions of the Royal Society A: Mathematical, *Physical and Engineering Sciences*, 378(2183), 20190314. https://doi.org/10.1098/rsta.2019.0314

Gaberšek, M., Watts, M.J., Gosar, M. (2022). Attic dust: an archive of historical air contamination of the urban environment and potential hazard to health? *Journal of Hazardous Materials*, 432, 128745. https://doi.org/10.1016/j.jhazmat.2022.128745

Gao, Y., and Ji, H. (2018). Microscopic morphology and seasonal variation of health effect arising from heavy metals in PM2.5 and PM10: One-year measurement in a densely populated area of urban Beijing. *Atmospheric Research*, 212, 213–226. https://doi.org/10.1016/j.atmosres.2018.04.027

Gatari, M.J., Boman, J., Wagner, A., Janhäll, S., Isakson, J. (2006). Assessment of inorganic content of PM2.5 particles sampled in a rural area north-east of Hanoi, Vietnam. *Science of The Total Environment*, 368(2), 675–685. https://doi.org/10.1016/j.scitotenv.2006.04.004

Giordano, M.R., Malings, C., Pandis, S.N., Presto, A.A., McNeill, V.F., Westervelt, D.M., Beekmann, M., Subramanian, R. (2021). From low-cost sensors to high-quality data: A summary of challenges and best practices for effectively calibrating low-cost particulate matter mass sensors. *Journal of Aerosol Science*, 158, 105833. https://doi.org/10.1016/j.jaerosci.2021.105833

González, L.T., Longoria-Rodríguez, F.E., Sánchez-Domínguez, M., Leyva-Porras, C., Acuña-Askar, K., Kharissov, B.I., Arizpe-Zapata, A., Alfaro-Barbosa, J. M. (2018). Seasonal variation and chemical composition of particulate matter: A study by XPS, ICP-AES and sequential microanalysis using Raman with SEM/EDS. *Journal of Environmental Sciences*, 74, 32–49. https://doi.org/10.1016/j.jes.2018.02.002

Gozzi, F., Ventura, G.D., Marcelli, A., Lucci, F. (2017). Current Status of Particulate Matter Pollution in Europe and Future Perspectives: A Review. *Journal of Materials and Environmental Sciences*, 8(6), 1901−1909

Grigoratos, T., Samara, C., Voutsa, D., Manoli, E., Kouras, A. (2014). Chemical composition and mass closure of ambient coarse particles at traffic and urban-background sites in Thessaloniki, Greece. *Environmental Science and Pollution Research*, 21(12), 7708–7722. https://doi.org/10.1007/s11356-014-2732-z

Grob, R.L., and Barry, E.F. (2004). *Modern Practice of Gas Chromatography*. John Wiley & Sons. DOI: 10.1002/0471651141

Guaita, R., Pichiule, M., Maté, T., Linares, C., Díaz, J. (2011). Short-term impact of particulate matter (PM(2.5)) on respiratory mortality in Madrid. *International Journal of Environmental Health Research*, 21(4), 260–274. https://doi.org/10.1080/09603123.2010.544033

Halonen, J.I., Lanki, T., Yli-Tuomi, T., Tiittanen, P., Kulmala, M., Pekkanen, J. (2009). Particulate air pollution and acute cardiorespiratory hospital admissions and mortality among the elderly. *Epidemiology*, 20(1), 143–153. https://doi.org/10.1097/EDE.0b013e31818c7237

Harrison, R.M., and Msibi, I.M. (1994). Validation of Techniques for Fast Response Measurement of HNO4 and NH3 and Determination of the [NH3] [HNO4] Concentration Product. *Atmospheric Environment*, 2(28), 247–255. https://doi.org/10.1016/1352-2310(94)90099-X

Harrison, R.M., Smith, D.J.T., Luhana, L. (1996). Source apportionment of atmospheric polycyclic aromatic hydrocarbons collected from an urban location in Birmingham, U.K. *Environmental Science & Technology*, 30, 825–32. https://doi.org/10.1021/es950252d

Hazarika, N., and Srivastava, A. (2017). Estimation of risk factor of elements and PAHs in size-differentiated particles in the National Capital Region of India. *Air Quality, Atmosphere & Health*, 10(4), 469–482. https://doi.org/10.1007/s11869-016-0438-8

Ho, S.S.H., Yu, J.Z., Chow, J.C., Zielinska, B., Watson, J.G., Sit, E.H.L., Schauer, J.J. (2008). Evaluation of an in-injection port thermal desorption-gas chromatography/mass spectrometry method for analysis of non-polar organic compounds in ambient aerosol samples. *Journal of Chromatography A*, 1200(2), 217–227. https://doi.org/10.1016/j.chroma.2008.05.056

Hofman, J., Samson, R., Joosen, S., Blust, R., Lenaerts, S. (2018). Cyclist exposure to black carbon, ultrafine particles and heavy metals: an experimental study along two commuting routes near Antwerp, Belgium. *Environmental Research*, 164, 530–8. https://doi.org/10.1016/j.envres.2018.03.004

Hopke, P.K., Dai, Q., Li, L., Feng, Y. (2020). Global review of recent source apportionments for airborne particulate matter. *Science of The Total Environment*, 740, 140091. https://doi.org/10.1016/j.scitotenv.2020.140091

Hsu, C.Y., Chi, K.H., Wu, C.D., Lin, S.L., Hsu, W.C., Tseng, C.C., Chen, M.J., Chen, Y.C. (2021). Integrated analysis of source-specific risks for PM2.5-bound metals in urban, suburban, rural, and industrial areas. *Environmental Pollution*, 275, 116652. https://doi.org/10.1016/j.envpol.2021.116652

Ilenič, A., Mauko Pranjić, A., Ščančar, J., Milačič Ščančar, R., Kumar, P. (2025). Can low-cost sensors (LCS) enhance air quality monitoring for personal pollution exposure assessment? *Environmental Research Communication*, 7(9), 095007. DOI 10.1088/2515-7620/ae02ef

Ilenič, A., Mauko Pranjić, A., Zupančič, N., Milačič, R., Ščančar, J. (2024). Fine particulate matter (PM2.5) exposure assessment among active daily commuters to induce behaviour change to reduce air pollution. *Science of The Total Environment*, 912, 169117. https://doi.org/10.1016/j.scitotenv.2023.169117

Ilenič, A., Milačič Ščančar, R., Đurić, M., Mauko Pranjić, A., Ščančar, J. (2025). An innovative sampling device for size-fractionating airborne particulate matter for improved air pollution control of metal(oid)s and polycyclic aromatic hydrocarbons. *Analytical Methods*, 17 7184-7199. DOI https://doi.org/10.1039/D5AY00858A

Inglič, R.T., Pirnat, U., Stare, M. (2023). *Household energy efficiency.* Statistical Office, Republic of Slovenia. https://www.stat.si/StatWeb/en/News/Index/12783?utm_source=chatgpt.com

Insian, W., Yabueng, N., Wiriya, W., Chantara, S. (2022). Size-fractionated PM-bound PAHs in urban and rural atmospheres of northern Thailand for respiratory health risk assessment. *Environmental Pollution*, 293, 118488. https://doi.org/10.1016/j.envpol.2021.118488

Int Panis, L., de Geus, B., Vandenbulcke, G., Willems, H., Degraeuwe, B., Bleux, N., Mishra, V., Thomas, I., Meeusen, R. (2010). Exposure to particulate matter in traffic: a comparison of cyclists and car passengers. *Atmospheric Environment*, 44, 2263–70. https://doi.org/10.1016/j.atmosenv.2010.04.028

International Agency for Research on Cancer (IARC). (2016). *Outdoor Air Pollution.* https://publications.iarc.fr/Book-And-Report-Series/Iarc-Monographs-On-The-Identification-Of-Carcinogenic-Hazards-To-Humans/Outdoor-Air-Pollution-2015

International Organization for Standardization. (2011). Water quality — Determination of 16 polycyclic aromatic hydrocarbons (PAH) in water — Method using gas chromatography with mass spectrometric detection (GC-MS) (ISO 28540:2011)

Jakovljević, I., Pehnec, G., Vađić, V., Čačković, M., Tomašić, V., Jelinić, J.D. (2018). Polycyclic aromatic hydrocarbons in PM10, PM2.5 and PM1 particle fractions in an urban area. *Air Quality, Atmosphere & Health*, 11(7), 843–854. https://doi.org/10.1007/s11869-018-0603-3

Jakovljević, I., Sever Štrukil, Z., Godec, R., Bešlić, I., Davila, S., Lovrić, M., Pehnec, G. (2020). Pollution Sources and Carcinogenic Risk of PAHs in PM1 Particle Fraction in an Urban Area. *International Journal of Environmental Research and Public Health*, 17(24), 9587. https://doi.org/10.3390/ijerph17249587

Jamhari, A.A., Sahani, M., Latif, M.T., Chan, K.M., Tan, H.S., Khan, M.F., Mohd Tahir, N. (2014). Concentration and source identification of polycyclic aromatic hydrocarbons (PAHs) in PM10 of urban, industrial and semi-urban areas in Malaysia. *Atmospheric Environment*, 86, 16–27. https://doi.org/10.1016/j.atmosenv.2013.12.019

Jandacka, D., Durcanska, D., Bujdos, M. (2017). The contribution of road traffic to particulate matter and metals in air pollution in the vicinity of an urban road. *Transportation Research Part D: Transport and Environment*, 50, 397–408. https://doi.org/10.1016/j.trd.2016.11.024

Jedynska, A., Hoek, G., Eeftens, M., Cyrys, J., Keuken, M., Ampe, C., Beelen, R., Cesaroni, G., Forastiere, F., Cirach, M., de Hoogh, K., De Nazelle, A., Madsen, C., Declercq, C., Eriksen, K.T., Katsouyanni, K., Akhlaghi, H.M., Lanki, T., Meliefste, K., … Kooter, I.M. (2014). Spatial variations of PAH, hopanes/steranes and EC/OC concentrations within and between European study areas. *Atmospheric Environment*, 87, 239–248. https://doi.org/10.1016/j.atmosenv.2014.01.026

Jerrett, M., Arain, A., Kanaroglou, P., Beckerman, B., Potoglou, D., Sahsuvaroglu, T., Morrison, J., Giovis, C. (2005). A review and evaluation of intraurban air pollution exposure models. *Journal of Exposure Analysis and Environmental Epidemiology*, 15(2). https://doi.org/10.1038/sj.jea.7500388

Jiang, N., Duan, S., Yu, X., Zhang, R., Wang, K. (2018). Comparative major components and health risks of toxic elements and polycyclic aromatic hydrocarbons of PM2.5 in winter and summer in Zhengzhou: Based on three-year data. *Atmospheric Research*, 213, 173–184. https://doi.org/10.1016/j.atmosres.2018.06.008

Kanaroglou, P.S., Jerrett, M., Morrison, J., Beckerman, B., Arain, M.A., Gilbert, N.L., Brook, J.R. (2005). Establishing an air pollution monitoring network for intra-urban population exposure assessment: A location-allocation approach. *Atmospheric Environment*, 39(13), 2399–2409. https://doi.org/10.1016/j.atmosenv.2004.06.049

Karagulian, F., Barbiere, M., Kotsev, A., Spinelle, L., Gerboles, M., Lagler, F., Redon, N., Crunaire, S., Borowiak, A. (2019). Review of the Performance of Low-Cost Sensors for Air Quality Monitoring. *Atmosphere*, 10(9). https://doi.org/10.3390/atmos10090506

Karthikeyan, S., Joshi, U.M., Balasubramanian, R. (2006). Microwave assisted sample preparation for determining water-soluble fraction of trace elements in urban airborne particulate matter: Evaluation of bioavailability. *Analytica Chimica Acta*, 576(1), 23–30. https://doi.org/10.1016/j.aca.2006.05.051

Katsoyiannis, A., Terzi, E., Cai, Q.Y. (2007). On the use of PAH molecular diagnostic ratios in sewage sludge for the understanding of the PAH sources. Is this use appropriate? *Chemosphere*, 69, 1337–9. https://doi.org/10.1016/j.chemosphere.2007.05.084

Keith, L.H. (2015). The Source of U.S. EPA's Sixteen PAH Priority Pollutants. *Polycyclic aromatic hydrocarbons*, 35(2−4), 147−160. https://doi.org/10.1080/10406638.2014.892886

Kelly, F.J., and Fussell, J.C. (2012). Size, source and chemical composition as determinants of toxicity attributable to ambient particulate matter. *Atmospheric Environment*, 60, 504–526. https://doi.org/10.1016/j.atmosenv.2012.06.039

Kelly, K.E., Whitaker, J., Petty, A., Widmer, C., Dybwad, A., Sleeth, D., Martin, R., Butterfield, A. (2017). Ambient and laboratory evaluation of a low-cost particulate

matter sensor. *Environmental Pollution*, 221, 491–500. https://doi.org/10.1016/j.envpol.2016.12.039

Khalili, N.R., Scheff, P.A., Holsen, T.M. (1995). PAH source fingerprints for coke ovens, diesel and gasoline engines, highway tunnels, and wood combustion emissions. *Atmospheric Environment*, 29. https://doi.org/10.1016/1352-2310(94)00275-P

Khan, B., Masiol, M., Bruno, C., Pasqualetto, A., Formenton, G.M., Agostinelli, C., Pavoni, B. (2018). Potential sources and meteorological factors affecting PM2.5-bound polycyclic aromatic hydrocarbon levels in six main cities of northeastern Italy: An assessment of the related carcinogenic and mutagenic risks. *Environmental Science and Pollution Research*, 25(32), 31987–32000. https://doi.org/10.1007/s11356-018-2841-1

Khwaja, H.A., Fatmi, Z., Malashock, D., Aminov, Z., Kazi, A., Siddique, A. (2012). Effect of air pollution on daily morbidity in Karachi, Pakistan. *Journal of Local and Global Health Science*, 29, 1—13. 10.5339/jlghs.2012.3

Kim, H., Kim, W.H., Kim, Y.Y., Park, H.Y. (2020). Air Pollution and Central Nervous System Disease: A Review of the Impact of Fine Particulate Matter on Neurological Disorders. *Frontiers in Public Health*, 16(8), 575330. 10.3389/fpubh.2020.575330

Kim, K.H., Jahan, S.A., Kabir, E., Brown, R.J.C. (2013). A review of airborne polycyclic aromatic hydrocarbons (PAHs) and their human health effects. *Environment International*, 60, 71–80. https://doi.org/10.1016/j.envint.2013.07.019

Kingham, S., Longley, I., Salmond, J., Pattinson, W., Shrestha, K. (2013). Variations in exposure to traffic pollution while travelling by different modes in a low density, less congested city. *Environmental Pollution*, 181, 211–218. https://doi.org/10.1016/j.envpol.2013.06.030

Koçak, E. (2017). *Determination of organic particle composition in Ankara atmosphere and investigation of their contribution to receptor modeling.* https://open.metu.edu.tr/handle/11511/27000

Koçak, E., Aslan, S., İmamoğlu, İ., Tuncel, G. (2025). Multi-group organic pollutants in urban and suburban atmospheric particulate matter (PM2.5): Temporal variation, meteorological impact, and sources. *Air Quality, Atmosphere & Health*, 18, 1359–76. https://doi.org/10.1007/s11869-025-01716-5

Kosmopoulos, G., Salamalikis, V., Pandis, S.N., Yannopoulos, P., Bloutsos, A.A., Kazantzidis, A. (2020). Low-cost sensors for measuring airborne particulate matter: Field evaluation and calibration at a South-Eastern European site. *Science of The Total Environment*, 748, 141396. https://doi.org/10.1016/j.scitotenv.2020.141396

Kouras, A., Manoli, E., Avgenikou, A., Paraschaki, A., Voutsa, D., Samara, C. (2025). Inhalation health risk assessment in the port of Volos, Greece, based on multiannual evolution of PM10-bound polycyclic aromatic hydrocarbons and metals/metalloids: Implications for EU-regulated PM10 pollutants. *Atmospheric Environment*, 358, 121348. https://doi.org/10.1016/j.atmosenv.2025.121348

Kousis, I., Manni, M., Pisello, A.L. (2022). Environmental mobile monitoring of urban microclimates: A review. *Renewable and Sustainable Energy Reviews*, 169, 112847. https://doi.org/10.1016/j.rser.2022.112847

Kukutschová, J., Moravec, P., Tomášek, V., Matějka, V., Smolík, J., Schwarz, J., Seidlerová, J., Šafářová, K., Filip, P. (2011). On airborne nano/micro-sized wear particles released from low-metallic automotive brakes. *Environmental Pollution*, 159(4), 998–1006. https://doi.org/10.1016/j.envpol.2010.11.036

Kumar, P., Kalaiarasan, G., Porter, A.E., Pinna, A., Kłosowski, M.M., Demokritou, P., Chung, K.F., Pain, C., Arvind, D.K., Arcucci, R., Adcock, I.M., Dilliway, C. (2021). An overview of methods of fine and ultrafine particle collection for physicochemical characterisation and toxicity assessments. *Science of The Total Environment*, 756, 143553. https://doi.org/10.1016/j.scitotenv.2020.143553

Kumar, P., Morawska, L., Martani, C., Biskos, G., Neophytou, M., Di Sabatino, S., Bell, M., Norford, L., Britter, R. (2015). The rise of low-cost sensing for managing air pollution in cities. *Environment International*, 75, 199–205. https://doi.org/10.1016/j.envint.2014.11.019

Kumar, P., Robins, A., Vardoulakis, S., Britter, R. (2010). A review of the characteristics of nanoparticles in the urban atmosphere and the prospects for developing regulatory controls. *Atmospheric Environment*, 44(39), 5035–5052. https://doi.org/10.1016/j.atmosenv.2010.08.016

Kuo, J. (2018). *Air Pollution Control: Fundamentals and Applications*. Boca Raton: CRC Press. https://doi.org/10.1201/9780429185793

Kuula, J., Mäkelä, T., Aurela, M., Teinilä, K., Varjonen, S., González, Ó., Timonen, H. (2020). Laboratory evaluation of particle-size selectivity of optical low-cost particulate matter sensors. *Atmospheric Measurement Techniques*, 13(5), 2413–2423. https://doi.org/10.5194/amt-13-2413-2020

Lara, S., Villanueva, F., Martín, P., Salgado, S., Moreno, A., Sánchez-Verdú, P. (2022). Investigation of PAHs, nitrated PAHs and oxygenated PAHs in PM10 urban aerosols. A comprehensive data analysis. *Chemosphere*, 294, 133745. https://doi.org/10.1016/j.chemosphere.2022.133745

Lawes, G. (1987). *Scanning Electron Microscopy and X-Ray Microanalysis*. Wiley.

Leavey, A., Fu, Y., Sha, M., Kutta, A., Lu, C., Wang, W., Drake, B., Chen, Y., Biswas, P. (2015). Air quality metrics and wireless technology to maximize the energy efficiency of HVAC in a working auditorium. *Building and Environment*, 85, 287–297. https://doi.org/10.1016/j.buildenv.2014.11.039

Lewandowska, A.U., Staniszewska, M., Witkowska, A., Machuta, M., Falkowska, L. (2018). Benzo(a)pyrene parallel measurements in PM1 and PM2.5 in the coastal zone of the Gulf of Gdansk (Baltic Sea) in the heating and non-heating seasons. *Environmental Science and Pollution Research*, 25(20), 19458–19469. https://doi.org/10.1007/s11356-018-2089-9

Li, F., Zhang, G., Jinxu, Y., Ding, T., Liu, C.Q., Lang, Y. (2024). Comprehensive source identification of heavy metals in atmospheric particulate matter in a megacity: A case study of Hangzhou. *JEM*, 366, 121747. https://doi.org/10.1016/j.jenvman.2024.121747

Li, R.J., Kou, X.J., Geng, H., Dong, C., Cai, Z.W. (2014). Pollution characteristics of ambient PM2.5-bound PAHs and NPAHs in a typical winter time period in Taiyuan. *Chinese Chemical Letters*, 25(5), 663–666. https://doi.org/10.1016/j.cclet.2014.03.032

Li, W., and Shao, L. (2009). Transmission electron microscopy study of aerosol particles from the brown hazes in northern China, *Journal of Geophysical Research: Atmospheres*, 114(D9). https://doi.org/10.1029/2008JD011285

Li, X., Jiang, L., Bai, Y., Yang, Y., Liu, S., Chen, X., Xu, J., Liu, Y., Wang, Y., Guo, X., Wang, Y., Wang, G. (2019). Wintertime aerosol chemistry in Beijing during haze period: Significant contribution from secondary formation and biomass burning emission. *Atmospheric Research*, 218, 25–33. https://doi.org/10.1016/j.atmosres.2018.10.010

Lin, W., Zhang, H., Lai, Y., Zhuang, S., Wei, Q., Fu, S., Mai, D., Yuan, L., Wei, Q., Yue, D., Hu, Q. (2024). Source-Specific Ecological Risk of Atmospheric PM2.5-Bound Metals and Implications for Air Pollution Control: A Regional Perspective from China. *Exposure and Health*, 16, 745−757. https://link.springer.com/article/10.1007/s12403-023-00589-2

Lin, Y., Ma, Y., Qiu, X., Li, R., Fang, Y., Wang, J., Zhu, Y., Hu, D. (2015). Sources, transformation, and health implications of PAHs and their nitrated, hydroxylated, and oxygenated derivatives in PM2.5 in Beijing. *Journal of Geophysical Research: Atmospheres*, 120(14), 7219–7228. https://doi.org/10.1002/2015JD023628

Lippmann, M. (1998). The 1997 US EPA Standards for Particulate Matter and Ozone. In R.E. Hester and R.M. Harrison (Eds.). *Air Pollution and Health, Issues in Environmental Science & Technology* (pp. 75–99). Cambridge: Royal Society of Chemistry

Littlewood, A.B. (2013). *Gas Chromatography: Principles, Techniques, and Applications*. Elsevier. https://doi.org/10.1016/C2013-0-11096-3

Liu, D., Lin, T., Syed, J.H. Cheng, Z., Xu, Y., Li, K., Zhang, G., Li, J. (2017). Concentration, Source Identification, and Exposure Risk Assessment of PM2.5-Bound Parent PAHs and Nitro-PAHs in Atmosphere from Typical Chinese Cities. *Scientific Reports*, 7(1), 10398. doi:10.1038/s41598-017-10623-4

Liu, X., Zhai, Y., Zhu, Y., Liu, Y., Chen, H., Li, P., Peng, C., Xu, B., Li, C., Zeng, G. (2015). Mass concentration and health risk assessment of heavy metals in size-segregated airborne particulate matter in Changsha. *Science of The Total Environment*, 517, 215–221. https://doi.org/10.1016/j.scitotenv.2015.02.066

Liu, X., Zhang, X., Wang, T., Jin, B., Wu, L., Lara, R. (2024). PM10-bound trace elements in pan-European urban atmosphere. *Environmental Research*, 260, 119630. https://doi.org/10.1016/j.envres.2024.119630

Lu, W., Yang, L., Chen, J., Wang, X., Li, H., Zhu, Y., Wen, L., Xu, C., Zhang, J., Zhu, T., Wang, W. (2016). Identification of concentrations and sources of PM2.5-bound PAHs in

North China during haze episodes in 2013. *Air Quality, Atmosphere & Health*, 9(7), 823–833. https://doi.org/10.1007/s11869-015-0386-8

Logar M. (2023, August 18). *Izpusti delcev v zrak.* Okoljski kazalci. https://kazalci.arso.gov.si/sl/content/izpusti-delcev-v-zrak-8?tid=2

Ma, L., Li, B., Liu, Y., Sun, X., Fu, D., Sun, S., Thapa, S., Geng, J., Qi, H., Zhang, A., Tian, C. (2020). Characterization, sources and risk assessment of PM2.5-bound polycyclic aromatic hydrocarbons (PAHs) and nitrated PAHs (NPAHs) in Harbin, a cold city in Northern China. *Journal of Cleaner Production*, 264, 121673. https://doi.org/10.1016/j.jclepro.2020.121673

Ma, Y., Cheng, Y., Qiu, X., Lin, Y., Cao, J., Hu, D. (2016). A quantitative assessment of source contributions to fine particulate matter (PM2.5)-bound polycyclic aromatic hydrocarbons (PAHs) and their nitrated and hydroxylated derivatives in Hong Kong. *Environmental Pollution*, 219, 742–749. https://doi.org/10.1016/j.envpol.2016.07.034

MacNee, W., and Donaldson, K. (2003). Mechanism of lung injury caused by PM10 and ultrafine particles with special reference to COPD. *European Respiratory Journal*, 21(40), 47–51. https://doi.org/10.1183/09031936.03.00403203

Malandrino, M., Casazza, M., Abollino, O., Minero, C., Maurino, V. (2016). Size resolved metal distribution in the PM matter of the city of Turin (Italy). *Chemosphere*, 147, 477–489. https://doi.org/10.1016/j.chemosphere.2015.12.089

Malings, C., Knowland, K.E., Pavlovic, N., Coughlin, J.G., King, D., Keller, C., Cohn, S., Martin, R.V. (2024). Air Quality Estimation and Forecasting via Data Fusion With Uncertainty Quantification: Theoretical Framework and Preliminary Results. *Journal of Geophysical Research: Machine Learning and Computation*, 1(4), e2024JH000183. https://doi.org/10.1029/2024JH000183

Malings, C., Tanzer, R., Hauryliuk, A., Saha, P.K., Robinson, A.L., Presto, A.A., Subramanian, R. (2020). Fine particle mass monitoring with low-cost sensors: Corrections and long-term performance evaluation. *Aerosol Science and Technology*, 54(2), 160–174. https://doi.org/10.1080/02786826.2019.1623863

Manoli, E., Kouras, A., Karagkiozidou, O., Argyropoulos, G., Voutsa, D., Samara, C. (2016). Polycyclic aromatic hydrocarbons (PAHs) at traffic and urban background sites of northern Greece: Source apportionment of ambient PAH levels and PAH-induced lung cancer risk. *Environmental Science and Pollution Research*, 23(4), 3556–3568. https://doi.org/10.1007/s11356-015-5573-5

Marina Montes, C., Abás, E., Buil García, J., Anzano, J. (2023). From multi to single-particle analysis: A seasonal spectroscopic study of airborne particulate matter in Zaragoza, Spain. *Talanta*, 259, 124550. https://doi.org/10.1016/j.talanta.2023.124550

Marrero, J., Rebagliati, R., Gomez, D., Smichowski, P. (2005). A study of uniformity of elements deposition on glass fiber filters after collection of airborne particulate matter (PM-10), using a high-volume sampler. *Talanta*, 68(2), 442–447. https://doi.org/10.1016/j.talanta.2005.09.005

Mazziotti Tagliani, S., Carnevale, M., Armiento, G., Montereali, M.R., Nardi, E., Inglessis, M., Sacco, F., Palleschi, S., Rossi, B., Silvestroni, L., Gianfagna, A. (2017). Content, mineral allocation and leaching behavior of heavy metals in urban PM2.5. *Atmospheric Environment*, 153, 47–60. https://doi.org/10.1016/j.atmosenv.2017.01.009

Mbengue, S., Alleman, L.Y., Flament, P. (2014). Size-distributed metallic elements in submicronic and ultrafine atmospheric particles from urban and industrial areas in northern France. *Atmospheric Research*, 135–136, 35–47. https://doi.org/10.1016/j.atmosres.2013.08.010

McDow, S.R., and Huntzicker, J.J. (1990). Vapor Adsorption Artifact in the Sampling of Organic Aerosol: Face Velocity Effects. *Atmospheric Environment. Part A. General Topics*, 24(10), 2563−2571. https://doi.org/10.1016/0960-1686(90)90134-9

McNair, H.M., Miller, J.M., Snow, N.H. (2019). *Basic Gas Chromatography*. John Wiley & Sons. 10.1002/9781119450795

Megido, L., Negral, L., Castrillón, L., Marañón, E., Fernández-Nava, Y., Suárez-Peña, B. (2016). Traffic tracers in a suburban location in northern Spain: Relationship between carbonaceous fraction and metals. *Environmental Science and Pollution Research*, 23(9), 8669–8678. https://doi.org/10.1007/s11356-015-5955-8

Meyer, M.B., Lijek, J., Ono, D.M. (1992). Continuous PM10 Measurements in a Woodsmoke Environment. In J.C. Chow and D.M. Ono (Eds.) *Transactions: PMHI Standards and Nontraditional Particulate Source Controls* (pp. 24–38). Pittsburgh: AWMA

Mikuška, P., Křůmal, K., Večeřa, Z. (2015). Characterization of organic compounds in the PM2.5 aerosols in winter in an industrial urban area. *Atmospheric Environment*, 105, 97–108. https://doi.org/10.1016/j.atmosenv.2015.01.028

Milačič, R., Leskovšek, H., Dolinšek, F., Hrček, D. (1995). A complex study of air pollution with cadmium, lead, polycyclic aromatic hydrocarbons, sulfur dioxide, and black smoke in the Zasavje industrialized urban region in Slovenia, *Analytica Chimica Acta*, 85, 131−148

Morawska, L., Ristovski, Z., Jayaratne, E.R., Keogh, D.U., Ling, X. (2008). Ambient nano and ultrafine particles from motor vehicle emissions: Characteristics, ambient processing and implications on human exposure. *Atmospheric Environment*, 42(35), 8113–8138. https://doi.org/10.1016/j.atmosenv.2008.07.050

Morawska, L., Thai, P., Liu, X., Asumadu Sakyi, A., Ayoko, G., Bartonova, A., Bedini, A., Chai, F., Christensen, B., Dunbabin, M., Gao, J., Hagler, G., Jayaratne, R., Kumar, P., Lau, A., Louie, P., Mazaheri, M., Ning, Z., Motta, N., … Williams, R. (2018). Applications of low-cost sensing technologies for air quality monitoring and exposure assessment: How far have they gone? *Environment International*, 116, 286–299. https://doi.org/10.1016/j.envint.2018.04.018

Mosley, S. (2014). Environmental History of Air Pollution and Protection. In M. Agnoletti and S. Neri Serneri (Eds.), *The Basic Environmental History* (1st ed., pp. 143–169). Switzerland: Springer International Publishing. https://doi.org/10.1007/978-3-319-09180-8_5

Nadali, A., Leili, M., Bahrami, A., Karami, M., Afkhami, A. (2021). Phase distribution and risk assessment of PAHs in ambient air of Hamadan, Iran. *Ecotoxicology and Environmental Safety*, 209, 111807. https://doi.org/10.1016/j.ecoenv.2020.111807

Nelms, S.M. (2005*). ICP Mass Spectrometry Handbook*. Oxford, UK: Blackwell Publishing Ltd

Negral, L., Suárez Peña, B., Zapico, E., Fernández Nava, Y., Megido, L., Moreno, J., Marañón, E, Castrillón, L. (2020). Anthropogenic and meteorological influences on PM10 metal/semi-metal concentrations: implications for human health. *Chemosphere*. 243, 125347. https://doi.org/10.1016/j.chemosphere.2019.125347

Okano, Y. (2018). Scanning Electron Microscopy. In The Surface Science Society of Japan (Ed.), *Compendium of Surface and Interface Analysis* (pp. 563–569). Springer. https://doi.org/10.1007/978-981-10-6156-1_91

Ono Ogasawara, M., Smith, T.J. (2004). Diesel exhaust particles in the work environment and their analysis. *Ind. Health*, 42, 389–99. https://doi.org/10.2486/indhealth.42.389

OriginLab Corporation. (2021). Origin [Computer software]

Orosa, J.A. (2011). *Indoor and Outdoor Air Pollution*. IntechOpen

Oroumiyeh, F., Jerrett, M., Del Rosario, I., Lipsitt, J., Liu, J., Paulson, S.E., Ritz, B., Schauer, J.J., Shafer, M.M., Shen, J., Weichenthal, S., Banerjee, S., Zhu, Y. (2022). Elemental composition of fine and coarse particles across the greater Los Angeles area: Spatial variation and contributing sources. *Environmental Pollution*, 292, 118356. https://doi.org/10.1016/j.envpol.2021.118356

Padoan, E., Malandrino, M., Giacomino, A., Grosa, M.M., Lollobrigida, F., Martini, S., Abollino, O. (2016). Spatial distribution and potential sources of trace elements in PM10 monitored in urban and rural sites of Piedmont Region. *Chemosphere*, 145, 495–507. https://doi.org/10.1016/j.chemosphere.2015.11.094

Pandey, S.K., Kim, K.H., Brown, R.J.C. (2011). A review of techniques for the determination of polycyclic aromatic hydrocarbons in air. *TrAC Trends in Analytical Chemistry*, 30(11), 1716–1739. https://doi.org/10.1016/j.trac.2011.06.017

Pant, P., and Harrison, R.M. (2013). Estimation of the contribution of road traffic emissions to particulate matter concentrations from field measurements: A review. *Atmospheric Environment*, 77, 78–97. https://doi.org/10.1016/j.atmosenv.2013.04.028

Parvizimehr, A., Baghani, A.N., Hoseini, M., Sorooshian, A., Cuevas-Robles, A., Fararouei, M., Dehghani, M., Delikhoon, M., Barkhordari, A., Shahsavani, S., Badeenezhad, A. (2020). On the nature of heavy metals in PM10 for an urban desert city in the Middle East: Shiraz, Iran. *Microchemical Journal*, 154, 104596. https://doi.org/10.1016/j.microc.2020.104596

Pascal, M., Corso, M., Chanel, O., Declercq, C., Badaloni, C., Cesaroni, G., Henschel, S., Meister, K., Haluza, D., Martin-Olmedo, P., Medina, S. (2013). Assessing the public health impacts of urban air pollution in 25 European cities: Results of the Aphekom

project. *Science of The Total Environment*, 449, 390–400. https://doi.org/10.1016/j.scitotenv.2013.01.077

Patashnick, H., and Rupprecht, E.G. (1991). Continuous PM10 Measurements Using the Tapered Element Oscillating Microbalance. *Journal of the Air & Waste Management Association*, 41, 1079–1083. https://www.osti.gov/biblio/5067192

Patil, M., Jadhav, A.S., Singh, S.K., Ingle, S. (2024). Urban ambient PM10 analysis: Characterization, sources, health risk and sustainable solutions. *Journal of Environmental Chemistry and Ecotoxicology*, 6, 192–205. https://doi.org/10.1016/j.enceco.2024.05.008

Pénard-Morand, C., and Annesi-Maesano, I. (2004). Air pollution: From sources of emissions to health effects. *Breathe*, 1(2), 108–119. https://doi.org/10.1183/18106838.0102.108

Perez, L., Tobías, A., Querol, X., Pey, J., Alastuey, A., Díaz, J., Sunyer, J. (2012). Saharan dust, particulate matter and cause-specific mortality: A case-crossover study in Barcelona (Spain). *Environment International*, 48, 150–155. https://doi.org/10.1016/j.envint.2012.07.001

Phalen, R.F., and Phalen, R.N. (2013). *Introduction to Air Pollution Science: A Public Health Perspective*. Jones & Bartlett Publishers

Pindado, O., Pérez, R.M., García, S., Sánchez, M., Galán, P., Fernández, M. (2009). Characterization and Sources Assignation of PM2.5 Organic Aerosol in a Rural Area of Spain. *Atmospheric Environment*, 43(17), 2796–2803. doi:10.1016/j.atmosenv.2009.02.046

Pio, C., Mirante, F., Oliveira, C., Matos, M., Caseiro, A., Oliveira, C., Querol, X., Alves, C., Martins, N., Cerqueira, M., Camões, F., Silva, H., Plana, F. (2013). Size-segregated chemical composition of aerosol emissions in an urban road tunnel in Portugal. *Atmospheric Environment*, 71, 15–25. https://doi.org/10.1016/j.atmosenv.2013.01.037

Potter, N.A., Meltzer, G.Y., Avenbuan, O.N., Raja, A., Zelikoff, J.T. (2021). Particulate Matter and Associated Metals: A Link with Neurotoxicity and Mental Health. *Atmosphere*, 12(4). https://doi.org/10.3390/atmos12040425

Prati, P., Zucchiatti, A., Lucarelli, F., Mandò, P.A. (2000). Source apportionment near a steel plant in Genoa (Italy) by continuous aerosol sampling and PIXE analysis. *Atmospheric Environment*, 34(19), 3149–3157. https://doi.org/10.1016/S1352-2310(99)00421-5

Qin, Y., Chan, C.K., Chan, L.Y. (1997). Characteristics of chemical compositions of atmospheric aerosols in Hong Kong: Spatial and seasonal distributions. *Science of The Total Environment*, 206(1), 25–37. https://doi.org/10.1016/S0048-9697(97)00214-3

Raaschou-Nielsen, O., Andersen, Z.J., Beelen, R., Samoli, E., Stafoggia, M., Weinmayr, G., Hoffmann, B., Fischer, P., Nieuwenhuijsen, M.J., Brunekreef, B., Xun, W.W., Katsouyanni, K., Dimakopoulou, K., Sommar, J., Forsberg, B., Modig, L., Oudin, A., Oftedal, B., Schwarze, P.E., … Hoek, G. (2013). Air pollution and lung cancer incidence in 17 European cohorts: Prospective analyses from the European Study of Cohorts for Air Pollution Effects (ESCAPE). *The Lancet. Oncology*, 14(9), 813–822. https://doi.org/10.1016/S1470-2045(13)70279-1

Rai, A.C., Kumar, P., Pilla, F., Skouloudis, A.N., Di Sabatino, S., Ratti, C., Yasar, A., Rickerby, D. (2017). End-user perspective of low-cost sensors for outdoor air pollution monitoring. *The Science of the Total Environment*, 607–608, 691–705. https://doi.org/10.1016/j.scitotenv.2017.06.266

Ravindra, K., Sokhi, R., Van Grieken, R. (2008). Atmospheric polycyclic aromatic hydrocarbons: Source attribution, emission factors and regulation. *Atmospheric Environment*, 42(13), 2895–2921. https://doi.org/10.1016/j.atmosenv.2007.12.010

Regulation on national upper limits of ambient air pollutant emissions (Uredba o nacionalnih zgornjih mejah emisij onesnaževal zunanjega zraka). (2018). Official Gazette of the Republic of Slovenia no. 48/18, 44/22 – ZVO-2, 95/24. https://pisrs.si/pregledPredpisa?id=URED7668

Ren, Y., Luo, Q., Zhuo, S., Hu, Y., Shen, G., Cheng, H., Tao, S. (2021). Bioaccessibility and public health risk of heavy Metal(loid)s in the airborne particulate matter of four cities in northern China. *Chemosphere*, 277, 130312. https://doi.org/10.1016/j.chemosphere.2021.130312

Rogula-Kozłowska, W., Klejnowski, K., Rogula-Kopiec, P., Ośródka, L., Krajny, E., Błaszczak, B., Mathews, B. (2014). Spatial and seasonal variability of the mass concentration and chemical composition of PM2.5 in Poland. *Air Quality, Atmosphere & Health*, 7(1), 41–58. https://doi.org/10.1007/s11869-013-0222-y

Romano, S. (2023). Bioaerosols: Composition, Meteorological Impact, and Transport. *Atmosphere*, 14(3), 590. https://doi.org/10.3390/atmos14030590

Rouessac, F., and Rouessac, A. (2013). *Chemical Analysis: Modern Instrumentation Methods and Techniques*. John Wiley & Sons

Roy, R., Jan, R., Gunjal, G., Bhor, R., Pai, K., Satsangi, P.G. (2019). Particulate matter bound polycyclic aromatic hydrocarbons: Toxicity and health risk assessment of exposed inhabitants. *Atmospheric Environment*, 210, 47–57. https://doi.org/10.1016/j.atmosenv.2019.04.034

Russell, A.G., and Brunekreef, B. (2009). A Focus on Particulate Matter and Health. *Environmental Science & Technology*, 43(13), 4620–4625. https://doi.org/10.1021/es9005459

Sah, D., Verma, P.K., Kandikonda, M.K., Lakhani, A. (2019). Pollution characteristics, human health risk through multiple exposure pathways, and source apportionment of heavy metals in PM10 at Indo-Gangetic site. *Urban Climate*, 27, 149–162. https://doi.org/10.1016/j.uclim.2018.11.010

Salcedo, D., Bernal, J.P., Pérez Arvizu, O., Lounejeva, E. (2014). Assessment of sample preparation methods for the analysis of trace elements in airborne particulate matter. *Journal of Analytical Atomic Spectrometry*, 29(4), 753–761. https://doi.org/10.1039/C3JA50375E

Samad, A., and Vogt, U. (2020). Investigation of urban air quality by performing mobile measurements using a bicycle (MOBAIR). *Urban Climate*, 33, 100650. https://doi.org/10.1016/j.uclim.2020.100650

Samek, L., Stegowski, Z., Styszko, K., Furman, L., Fiedor, J. (2018). Seasonal contribution of assessed sources to submicron and fine particulate matter in a Central European urban area. *Environmental Pollution*, 241, 406–411. https://doi.org/10.1016/j.envpol.2018.05.082

Samoli, E., Peng, R., Ramsay, T., Pipikou, M., Touloumi, G., Dominici, F., Burnett, R., Cohen, A., Krewski, D., Samet, J., Katsouyanni, K. (2008). Acute effects of ambient particulate matter on mortality in Europe and North America: Results from the APHENA study. *Environmental Health Perspectives*, 116(11), 1480–1486. https://doi.org/10.1289/ehp.11345

Sánchez-Piñero, J., Moreda-Piñeiro, J., Concha-Graña, E., Fernández-Amado, M., Muniategui-Lorenzo, S., López-Mahía, P. (2021). Inhalation bioaccessibility estimation of polycyclic aromatic hydrocarbons from atmospheric particulate matter (PM10): Influence of PM10 composition and health risk assessment. *Chemosphere*, 263, 127847. https://doi.org/10.1016/j.chemosphere.2020.127847

Sanderson, P., Delgado-Saborit, J.M., Harrison, R.M. (2014). A review of chemical and physical characterisation of atmospheric metallic nanoparticles. *Atmospheric Environment*, 94, 353–365. https://doi.org/10.1016/j.atmosenv.2014.05.023

Sannoh, F., Fatmi, Z., Carpenter, D.O., Santoso, M., Siddique, A., Khan, K. (2024). Air pollution we breathe: Assessing the air quality and human health impact in a megacity of Southeast Asia. *Science of the Total Environment*, 942, 173403. 10.1016/j.scitotenv.2024.173403

Saraga, D., Maggos, T., Degrendele, C., Klánová, J., Horvat, M., Kocman, D., Kanduč, T., Garcia Dos Santos, S., Franco, R., Gómez, P.M., Manousakas, M., Bairachtari, K., Eleftheriadis, K., Kermenidou, M., Karakitsios, S., Gotti, A., Sarigiannis, D. (2021). Multi-city comparative PM2.5 source apportionment for fifteen sites in Europe: The ICARUS project. *Science of The Total Environment*, 751, 141855. https://doi.org/10.1016/j.scitotenv.2020.141855

Sarkar, S.L., Aimin, X., Jana, D. (2001). Scanning Electron Microscopy, X-Ray Microanalysis of Concretes. In V.S. Ramachandran, J.J. Beaudoin (Eds.). *Handbook of Analytical Techniques in Concrete Science and Technology* (pp. 231–274). William Andrew Publishing. https://doi.org/10.1016/B978-081551437-4.50010-2

Sarti, E., Pasti, L., Rossi, M., Ascanelli, M., Pagnoni, A., Trombini, M, Remelli, M. (2015). The composition of PM1 and PM2.5 samples, metals and their water soluble fractions in the Bologna area (Italy). *Atmospheric Pollution Research*, 6(4), 708–18. https://doi.org/10.5094/APR.2015.079

Schauer, C., Niessner, R., Pöschl, U. (2003). Polycyclic aromatic hydrocarbons in urban air particulate matter: Decadal and seasonal trends, chemical degradation, and sampling artifacts. *Environment Science Technology*, 37, 2861–8. https://doi.org/10.1021/es034059s

Schorran, D.E., Fought, C., Miller, D.F., Coulombe, W.C., Keislar, R.E., Benner, R., Stedman, D. (1994). Semicontinuous Method for Monitoring SO2 at Low Parts-per-Trillion Concentrations. *Environmental Science & Technology*, 28(7), 1307–1311

Scrivener, K., Snellings, R., Lothenbach, B. (2018). *A Practical Guide to Microstructural Analysis of Cementitious Materials*. Boca Raton: CRC Press. https://doi.org/10.1201/b19074

Shen, R., Wang, Y., Gao, W., Cong, X., Cheng, L., Li, X. (2019). Size-segregated particulate matter bound polycyclic aromatic hydrocarbons (PAHs) over China: Size distribution, characteristics and health risk assessment. *The Science of the Total Environment*, 685, 116–123. https://doi.org/10.1016/j.scitotenv.2019.05.436

Shetaya, W.H., El-Mekawy, A., Hassan, S.K. (2024). Tempo-Spatial Variability and Health Risks of PM2.5 and Associated Metal(loid)s in Greater Cairo, Egypt. *Expo Health*, 16(4), 973−988. 10.1007/s12403-023-00603-7

Shi, G.L., Zhou, X.Y., Jiang, S.Y., Tian, Y.Z., Liu, G.R., Feng, Y.C., Chen, G., Liang, Y.K.X. (2015). Further insights into the composition, source, and toxicity of PAHs in size-resolved particulate matter in a megacity in China. *Environmental Toxicology and Chemistry*, 34(3), 480–487. https://doi.org/10.1002/etc.2809

Sicard, P., Agathokleous, E., Anenberg, S.C., De Marco, A., Paoletti, E., Calatayud, V. (2023). Trends in urban air pollution over the last two decades: A global perspective. *Science of The Total Environment*, 858, 160064. https://doi.org/10.1016/j.scitotenv.2022.160064

Singh, B.P., Kumar, K., Jain, V.K. (2021). Distribution of ring PAHs in particulate/gaseous phase in the urban city of Delhi, India: Seasonal variation and cancer risk assessment. *Urban Climate*, 40, 101010. https://doi.org/10.1016/j.uclim.2021.101010

Slovenian Environment Agency (ARSO). (2021). *Air Quality in Slovenia in 2021*. Ministry of the Environment, Climate and Energy. https://www.arso.gov.si/zrak/kakovost zraka/poročila in publikacije/Letno_porocilo_2021_Final.pdf

Slovenian Environment Agency (ARSO). (2023). *Kakovost zraka v Sloveniji v letu 2023*. Ministry of the Environment, Climate and Energy. https://www.gov.si/novice/2024-11-27-kakovost-zraka-v-sloveniji-v-letu-2023/

Slovenian Institute for Standardization. (2008). *Air quality - Standard method for the measurement of the concentration of benzo[a]pyrene in ambient air* (SIST EN 15549:2008)

Slovenian Institute for Standardization. (2009). *Characterization of waste - Determination of polycyclic aromatic hydrocarbons (PAH) in waste using gas chromatography mass spectrometry (GC/MS)* (SIST EN 15527:2009)

Slovenian Institute for Standardization. (2019). *Soil quality - Determination of polycyclic aromatic hydrocarbons (PAH) - Gas chromatographic method with mass spectrometric detection (GC-MS)* (SIST ISO 18287:2019)

Soleimani, M., Amini, N., Sadeghian, B., Wang, D., Fang, L. (2018). Heavy metals and their source identification in particulate matter (PM2.5) in Isfahan City, Iran. *Journal of Environmental Sciences*, 72, 166–175. https://doi.org/10.1016/j.jes.2018.01.002

Song, H., Zhang, Y., Luo, M., Gu, J., Wu, M., Xu,D., Xu, G., Ma, L. (2019). Seasonal Variation, Sources and Health Risk Assessment of Polycyclic Aromatic Hydrocarbons in Different Particle Fractions of PM2.5 in Beijing, China. *Atmospheric Pollution Research*, 10(1), 105–14. doi:10.1016/j.apr.2018.06.012

Statistical Office of the Republic of Slovenia (SURS). (2024, August 15). *Prebivalstvo* https://www.stat.si/StatWeb/Field/Index/17

Suwa, T., Hogg, J.C., Quinlan, K.B., Ohgami, A., Vincent, R., van Eeden, S.F. (2002). Particulate air pollution induces progression of atherosclerosis. *Journal of the American College of Cardiology*, 39(6), 935–942. https://doi.org/10.1016/s0735-1097(02)01715-1

Szabó, J., Nagy, A., Erdős, J. (2015). Ambient concentrations of PM10, PM10-bound polycyclic aromatic hydrocarbons and heavy metals in an urban site of Győr, Hungary. *Air Quality, Atmosphere & Health*, 8. https://doi.org/10.1007/s11869-015-0318-7

Talbi, A., Kerchich, Y., Kerbachi, R., Boughedaoui, M. (2018). Assessment of annual air pollution levels with PM1, PM2.5, PM10 and associated heavy metals in Algiers, Algeria. *Environmental Pollution*, 232, 252–263. https://doi.org/10.1016/j.envpol.2017.09.041

Tan, J., Guo, S., Ma, Y., Duan, J., Cheng, Y., He, K., Yang, F. (2011). Characteristics of particulate PAHs during a typical haze episode in Guangzhou, China. *Atmospheric Research*, 102(1–2), 91–98. https://doi.org/10.1016/j.atmosres.2011.06.012

Tan, J., Zhang, L., Zhou, X., Duan, J., Li, Y., Hu, J., He, K. (2017). Chemical characteristics and source apportionment of PM2.5 in Lanzhou, China. *Science of The Total Environment*, 601–602, 1743–1752. https://doi.org/10.1016/j.scitotenv.2017.06.050

Teffahi, A., Kerchich, Y., Moussaoui, Y., Romagnoli, P., Balducci, C., Malherbe, C., Kerbachi, R., Eppe, G., Cecinato, A. (2021). Exposure levels and health risk of PAHs associated with fine and ultrafine aerosols in an urban site in northern Algeria. *Air Quality, Atmosphere and Health*, 14(9), 1375—1391. 10.1007/s11869-021-01028-4

Terzič, M. (2020). *Avtomobili v EU.* https://www.dnevnik.si/nedeljski/prosti-cas/svet-vozil/avtomobili-v-eu-2224578/

The Organisation for Economic Cooperation and Development (OECD). (2015). *Air Pollution and Urban Structure Linkages: Evidence from European Cities.* OECD Publishing. https://doi.org/10.1787/5jrp6w9xlbq6-en

The Organisation for Economic Cooperation and Development (OECD). (2016). *The Economic Consequences of Outdoor Air Pollution.* OECD Publishing. http://dx.doi.org/10.1787/9789264257474-en

Thomas, R. (2008). *Practical Guide to ICP-MS: A Tutorial for Beginner*. CRC Press. https://doi.org/10.1201/9781420067873

Thorpe, A., and Harrison, R.M. (2008). Sources and properties of non-exhaust particulate matter from road traffic: A review. *Science of The Total Environment*, 400(1), 270–282. https://doi.org/10.1016/j.scitotenv.2008.06.007

TIBCO Software Inc. (2017). Statistica [Data analysis software system], version 13. http://statistica.io

Tian, Y., Jia, B., Zhao, P., Song, D., Huang, F., Feng, Y. (2022). Size distribution, meteorological influence and uncertainty for source-specific risks: PM2.5 and PM10-bound PAHs and heavy metals in a Chinese megacity during 2011–2021. *Environmental Pollution*, 312, 120004. https://doi.org/10.1016/j.envpol.2022.120004

Ting, Y.C., Zou, Y.X., Pan, S.Y., Ko, Y.R., Ciou, Z.J., Huang, C.H. (2024). Sources-attributed contributions to health risks associated with PM2.5-bound polycyclic aromatic hydrocarbons during the warm and cold seasons in an urban area of Eastern Asia. *Science of the Total Environment*, 922, 171325. https://doi.org/10.1016/j.scitotenv.2024.171325

Tolis, E.I., Saraga, D.E., Lytra, M.K., Papathanasiou, A.Ch., Bougaidis, P.N., Prekas-Patronakis, O.E., Ioannidis, I.I., Bartzis, J.G. (2015). Concentration and chemical composition of PM2.5 for a one-year period at Thessaloniki, Greece: A comparison between city and port area. *Atmospheric Environment*, 113, 197–207. https://doi.org/10.1016/j.atmosenv.2015.05.014

Tsiodra, I., Grivas, G., Bougiatioti, A., Tavernaraki, K., Parinos, C., Paraskevopoulou, D. (2024). Source apportionment of particle-bound polycyclic aromatic hydrocarbons (PAHs), oxygenated PAHs (OPAHs), and their associated long-term health risks in a major European city. *Science of the Total Environment*, 951, 175416. https://doi.org/10.1016/j.scitotenv.2024.175416

Turpin, B.J., and Huntzicker, J.J. (1991). Secondary Formation of Organic Aerosol in the Los Angeles Basin: A Descriptive Analysis of Organic and Elemental Carbon Concentrations. *Atmospheric Environment. Part A. General Topics*, 25(2), 207-215. https://doi.org/10.1016/0960-1686(91)90291-E

United Nations (UN). (2024, June 17). *The 17 goals for sustainable development.* https://sdgs.un.org/goals

United States Environmental Protection Agency (US EPA). (1997). *Exposure factors handbook*. https://cfpub.epa.gov/ncea/risk/recordisplay.cfm?deid=12464

United States Environmental Protection Agency (US EPA). (2009). *Risk assessment guidance for superfund volume I: human health evaluation manual* (Part F, Supplemental guidance for inhalation risk assessment). Office of Superfund Remediation and Technology Innovation

United States Environmental Protection Agency (US EPA). (2011). *Exposure factors handbook*. https://www.epa.gov/expobox/exposure-factors-handbook-2011-edition

United States Environmental Protection Agency (US EPA). (2016). *Particulate Matter (PM) Basics*. https://www.epa.gov/pm-pollution/particulate-matter-pm-basics

United States Environmental Protection Agency (US EPA). (2017). *Polycyclic Aromatic Hydrocarbons (PAHs)—Integrated Risk Information System (IRIS)*. https://www.epa.gov/iris

United States Environmental Protection Agency (US EPA). (2019). *Integrated Science Assessment (ISA) for Particulate Matter*. https://cfpub.epa.gov/ncea/isa/recordisplay.cfm?deid=347534

United States Environmental Protection Agency (US EPA). (2024). *Regional screening level (RSL) resident ambient air table as of November 2024*. https://www.epa.gov/risk/regional-screening-levels-rsls-generic-tables

Usman, F., Zeb, B., Alam, K., Huang, Z., Shah, A., Ahmad, I., Ullah, S. (2022) In-Depth Analysis of Physicochemical Properties of Particulate Matter (PM10, PM2.5 and PM1) and Its Characterization through FTIR, XRD and SEM–EDX Techniques in the Foothills of the Hindu Kush Region of Northern Pakistan. *Atmosphere*, 13(1), 124. https://doi.org/10.3390/atmos13010124

Valavanidis, A., Fiotakis, K., Vlachogianni, T. (2008). Airborne Particulate Matter and Human Health: Toxicological Assessment and Importance of Size and Composition of Particles for Oxidative Damage and Carcinogenic Mechanisms. *Journal of Environmental Science and Health, Part C*, 26(4), 339–362. https://doi.org/10.1080/10590500802494538

Vallero, D.A. (2008). *Fundamentals of Air Pollution*. Durham, North Carolina: Elsevier

Viskup, R. (2020). Comparison of Different Techniques for Measurement of Soot and Particulate Matter Emissions from Diesel Engine. In R. Viskup (Ed.) *Introduction to Diesel Emissions*. DOI: 10.5772/intechopen.91186

Vogt, M., Schneider, P., Castell, N., Hamer, P. (2021). Assessment of Low-Cost Particulate Matter Sensor Systems against Optical and Gravimetric Methods in a Field Co-Location in Norway. *Atmosphere*, 12(8). https://doi.org/10.3390/atmos12080961

Wang, C., Meng, Z., Yao, P., Zhang, L., Wang, Z., Lv, Y., Tian, Y., Feng, Y. (2019). Sources-specific carcinogenicity and mutagenicity of PM2.5-bound PAHs in Beijing, China: Variations of contributions under diverse anthropogenic activities. *Ecotoxicology and Environmental Safety*, 183, 109552. https://doi.org/10.1016/j.ecoenv.2019.109552

Wang, J., Cao, J., Dong, Z., Guinot, B., Gao, M., Huang, R., Han, Y., Huang, Y., Ho, S.S.H., Shen, Z. (2017). Seasonal variation, spatial distribution and source apportionment for polycyclic aromatic hydrocarbons (PAHs) at nineteen communities in Xi'an, China: The effects of suburban scattered emissions in winter. *Environmental Pollution*, 231, 1330–1343. https://doi.org/10.1016/j.envpol.2017.08.106

Wang, J., Ho, S.S.H., Ma, S., Cao, J., Dai, W., Liu, S., Shen, Z., Huang, R., Wang, G., Han, Y. (2016). Characterization of PM2.5 in Guangzhou, China: Uses of organic markers for

supporting source apportionment. *Science of The Total Environment*, 550, 961–971. https://doi.org/10.1016/j.scitotenv.2016.01.138

Wang, L., Dong, S., Liu, M., Tao, W., Xiao, B., Zhang, S., Zhang, P., Li, X. (2019). Polycyclic aromatic hydrocarbons in atmospheric PM2.5 and PM10 in the semi-arid city of Xi'an, Northwest China: Seasonal variations, sources, health risks, and relationships with meteorological factors. *Atmospheric Research*, 229, 60–73. https://doi.org/10.1016/j.atmosres.2019.06.014

Wang, Y., Xiong, L., Tang, M. (2017). Toxicity of inhaled particulate matter on the central nervous system: neuroinflammation, neuropsychological effects and neurodegenerative disease. *Journal of Applied Toxicology*, 37(6), 644−667. 10.1002/jat.3451

Wang, Z., Zhang, L., Zhang, Y., Zhao, Z., Zhang, S. (2008). Morphology of single inhalable particle in the air polluted city of Shijiazhuang, China. *Journal of Environmental Sciences*, 20(4), 429–35. https://doi.org/10.1016/S1001-0742(08)62075-6

Wedding, J.B., and Weigand, M.A. (1993). An Automatic Particle Sampler with Beta Gauging. *Journal of the Air & Waste Management Association*, 43, 475–479. https://doi.org/10.1080/1073161X.1993.10467146

Wei, C., Han, Y., Bandowe, B.A.M., Cao, J., Huang, R.J., Ni, H., Tian, J., Wilcke, W. (2015). Occurrence, gas/particle partitioning and carcinogenic risk of polycyclic aromatic hydrocarbons and their oxygen and nitrogen containing derivatives in Xi'an, central China. *Science of The Total Environment*, 505, 814–822. https://doi.org/10.1016/j.scitotenv.2014.10.054

Wei, Y., Han, I.K., Hu, M., Shao, M., Zhang, J., Tang, X. (2010). Personal exposure to particulate PAHs and anthraquinone and oxidative DNA damages in humans. *Chemosphere*, 81(10), 1280–1285. https://doi.org/10.1016/j.chemosphere.2010.08.055

Wilson, J.G., Kingham, S., Pearce, J., Sturman, A.P. (2005). A review of intraurban variations in particulate air pollution: implications for epidemiological research. *Atmospheric Environment*, 39, 6444–62. https://doi.org/10.1016/j.atmosenv.2005.07.030

Williams, R., Duvall, R., Kilaru, V., Hagler, G., Hassinger, L., Benedict, K., Rice, J., Kaufman, A., Judge, R., Pierce, G., Allen, G., Bergin, M., Cohen, R.C., Fransioli, P., Gerboles, M., Habre, R., Hannigan, M., Jack, D., Louie, P., … Ning, Z. (2019). Deliberating performance targets workshop: Potential paths for emerging PM2.5 and O3 air sensor progress. *Atmospheric Environment: X*, 2, 100031. https://doi.org/10.1016/j.aeaoa.2019.100031

Wise, S.A., and Watters, R.L. (2020). Standard reference material 1648A – urban particulate matter, Certificate Analysis, Gaithersburg

World Health Organisation (WHO). (2010). *Some Non-heterocyclic Polycyclic Aromatic Hydrocarbons and Some Related Exposures*. International Agency for Research on Cancer. https://pubmed.ncbi.nlm.nih.gov/21141735/

World Health Organisation (WHO). (2015). *Outdoor Air Pollution IARC Monographs on the Evaluation of Carcinogenic Risks to Humans* (volume 109). IARC Monographs.

https://publications.iarc.fr/Book-And-Report-Series/Iarc-Monographs-On-The-Identification-Of-Carcinogenic-Hazards-To-Humans/Outdoor-Air-Pollution-2015

World Health Organisation (WHO). (2010). *Some non-heterocyclic polycyclic aromatic hydrocarbons and some related exposures (Vol. 92).* International Agency for Research on Cancer

World Health Organisation (WHO). (2025, June 23). *Air pollution.* https://www.who.int/health-topics/air-pollution

Wu, Y., Zhang, N., Shi, Y., Chen, Z., Zhang, H., Yin, J., Zeng, T., Yuan, Z., Li, N., Ren, Y., Cai, L., Li, Y., Du, S. (2023). PAH Pollution in Particulate Matter and Risk in Chinese Cities. *Exposure and health*, 16, 401—415. https://link.springer.com/article/10.1007/s12403-023-00562-z

Xie, X., Semanjski, I., Gautama, S., Tsiligianni, E., Deligiannis, N., Rajan, R.T., Pasveer, F., Philips, W. (2017). A Review of Urban Air Pollution Monitoring and Exposure Assessment Methods. *ISPRS International Journal of Geo-Information*, 6(12), 389. https://doi.org/10.3390/ijgi6120389

Xing, W., Zhang, L., Yang, L., Zhou, Q., Zhang, X., Toriba, A., Hayakawa, K., Tang, N. (2020). Characteristics of PM2.5-Bound Polycyclic Aromatic Hydrocarbons and Nitro-Polycyclic Aromatic Hydrocarbons at A Roadside Air Pollution Monitoring Station in Kanazawa, Japan. *International Journal of Environmental Research and Public Health*, 17(3), 805. https://pmc.ncbi.nlm.nih.gov/articles/PMC7037384/

Xiong, Y., Zhou, J., Schauer, J.J., Yu, W., Hu, Y. (2017). Seasonal and spatial differences in source contributions to PM2.5 in Wuhan, China. *Science of The Total Environment*, 577, 155–165. https://doi.org/10.1016/j.scitotenv.2016.10.150

Xu, H., Ho, S.S.H., Gao, M., Cao, J., Guinot, B., Ho, K.F., Long, X., Wang, J., Shen, Z., Liu, S., Zheng, C., Zhang, Q. (2016). Microscale spatial distribution and health assessment of PM2.5-bound polycyclic aromatic hydrocarbons (PAHs) at nine communities in Xi'an, China. *Environmental Pollution*, 218, 1065–1073. https://doi.org/10.1016/j.envpol.2016.08.058

Xue, H., Liu, G., Zhang, H., Hu, R., Wang, X. (2019). Similarities and differences in PM10 and PM2.5 concentrations, chemical compositions and sources in Hefei City, China. *Chemosphere*, 220, 760–765. https://doi.org/10.1016/j.chemosphere.2018.12.123

Yang, L., Zhang, L., Chen, L., Han, C., Akutagawa, T., Endo, O., Yamauchi, M., Neroda, A., Toriba, A., Tang, N. (2021). Polycyclic aromatic hydrocarbons and nitro-polycyclic aromatic hydrocarbons in five East Asian cities: Seasonal characteristics, health risks, and yearly variations. *Environmental Pollution*, 287, 117360. https://doi.org/10.1016/j.envpol.2021.117360

Yang, L., Zhang, X., Xing, W., Zhou, Q., Zhang, L., Wu, Q., Zhou, Z., Chen, R., Toriba, A., Hayakawa, K., Tang, N. (2021). Yearly variation in characteristics and health risk of polycyclic aromatic hydrocarbons and nitro-PAHs in urban shanghai from 2010–2018. *Journal of Environmental Sciences*, 99, 72–79. https://doi.org/10.1016/j.jes.2020.06.017

Yao, S., Li, H., Pang, S., Zhu, B., Zhang, X., Fatikow, S. (2021). A Review of Computer Microvision-Based Precision Motion Measurement: Principles, Characteristics, and Applications. *IEEE Transactions on Instrumentation and Measurement*, 70, 1–28. https://doi.org/10.1109/TIM.2021.3065436

Yu, Q., Ding, X., He, Q., Yang, W., Zhu, M., Li, S., Zhang, R., Shen, R., Zhang, Y., Bi, X., Wang, Y., Peng, P., Wang, X. (2020). Nationwide increase of polycyclic aromatic hydrocarbons in ultrafine particles during winter over China revealed by size-segregated measurements. *Atmospheric Chemistry and Physics*, 20(23), 14581–14595. https://doi.org/10.5194/acp-20-14581-2020

Yunker, M.B., Macdonald, R.W., Vingarzan, R., Mitchell, R.H., Goyette, D., Sylvestre, S. (2002). PAHs in the Fraser River basin: a critical appraisal of PAH ratios as indicators of PAH source and composition. *Organic Geochemistry*, 33, 489–515. https://doi.org/10.1016/S0146-6380(02)00002-5

Zeb, B., Alam, K., Sorooshian, A., Blaschke, T., Ahmad, I., Shahid, I. (2018). On the Morphology and Composition of Particulate Matter in an Urban Environment. *Aerosol and Air Quality Research*, 18(6), 1431–47. 10.4209/aaqr.2017.09.0340

Zereini, F., Alsenz, H., Wiseman, C.L.S., Püttmann, W., Reimer, E., Schleyer, R., Bieber, E., Wallasch, M. (2022). Platinum group elements (Pt, Pd, Rh) in airborne particulate matter in rural vs. urban areas of Germany: Concentrations and spatial patterns of distribution. *Science of The Total Environment*, 416, 261—268. https://doi.org/10.1016/j.scitotenv.2011.11.070

Zereini, F., Alt, F., Messerschmidt, J., von Bohlen, A., Liebl, K., Püttmann, W. (2004). Concentration and distribution of platinum group elements (Pt, Pd, Rh) in airborne particulate matter in Frankfurt am Main, Germany. *Environmental Science & Technology*, 38(6), 1686–92. DOI: 10.1021/es030127z

Zhang, J., Su, Y., Chen, C., Guo, W., Tan, Q., Feng, M. (2024). Chemical composition, sources and formation mechanism of urban PM2.5 in Southwest China: a case study at the beginning of 2023. *Atmospheric Chemistry and Physics*, 24, 2803–20. https://doi.org/10.5194/acp-24-2803-2024

Zhang, J., Yang, L., Mellouki, A., Chen, J., Chen, X., Gao, Y., Jiang, P., Li, Y., Yu, H., Wang, W. (2018). Diurnal concentrations, sources, and cancer risk assessments of PM2.5-bound PAHs, NPAHs, and OPAHs in urban, marine and mountain environments. *Chemosphere*, 209, 147–155. https://doi.org/10.1016/j.chemosphere.2018.06.054

Zhang, L., Wang, Y., Liu, Y., Li, Z., Li, X. (2019). Variation of platinum group elements (PGE) in airborne particulate matter (PM2.5) in the Beijing urban area, China: A case study of the 2014 APEC summit. *Atmospheric Environment*, 198, 70—76. https://doi.org/10.1016/j.atmosenv.2018.10.044

Zhang, L., Xu, H., Fang, B., Wang, H., Yang, Z., Yang, W., Hao, Y., Wang, X., Wang, Q., Wang, M. (2020). Source Identification and Health Risk Assessment of Polycyclic Aromatic Hydrocarbon-Enriched PM2.5 in Tangshan, China. *Environmental Toxicology and Chemistry*, 39(2), 458–467. https://doi.org/10.1002/etc.4618

Zhang, N., Maung, M.W., Wang, S., Aruffo, E., Feng, J. (2024). Characterization and health risk assessment of PM2.5-bound polycyclic aromatic hydrocarbons in Yangon and Mandalay of Myanmar. *Science of the Total Environment*, 914, 170034. https://doi.org/10.1016/j.scitotenv.2024.170034

Zimmerman, N. (2022). Tutorial: Guidelines for implementing low-cost sensor networks for aerosol monitoring. *Journal of Aerosol Science*, 159, 105872. https://doi.org/10.1016/j.jaerosci.2021.105872

Zioła, N., and Słaby, K. (2020). The Content of Selected Heavy Metals and Polycyclic Aromatic Hydrocarbons (PAHs) in PM10 in Urban-Industrial Area. *Sustainability*, 12(13). https://doi.org/10.3390/su12135284

Zupančič, N. (2017). Influence of climate factors on soil heavy metal content in Slovenia. *JSS*, 17, 1073–83. https://doi.org/10.1007/s11368-016-1614-z

Bibliography

Publications Related to the Thesis

Journal Articles

Ilenič, A., Mauko Pranjić, A., Ščančar, J., Milačič Ščančar, R., Kumar, P. (2025). Can low-cost sensors (LCS) enhance air quality monitoring for personal pollution exposure assessment? *Environmental Research Communication*, 7(9), 095007. DOI 10.1088/2515-7620/ae02ef

Ilenič, A., Milačič Ščančar, R., Đurić, M., Mauko Pranjić, A., Ščančar, J. (2025). An innovative sampling device for size-fractionating airborne particulate matter for improved air pollution control of metal(oid)s and polycyclic aromatic hydrocarbons. *Analytical Methods*, 17, 7184-7199. DOI https://doi.org/10.1039/D5AY00858A

Ilenič, A., Mauko Pranjić, A., Zupančič, N., Milačič, R., Ščančar, J. (2024). Fine particulate matter (PM2.5) exposure assessment among active daily commuters to induce behaviour change to reduce air pollution. *Science of The Total Environment*, 912, 169117. https://doi.org/10.1016/j.scitotenv.2023.169117

Ilenič, A., Milačič Ščančar, R., Mauko Pranjić, A., Zupančič, N., Đurić, M., Ščančar, J. (submitted manuscript). Size-fractionated Airborne Particulate Matter-Bound Metal(oid)s and Polycyclic Aromatic Hydrocarbons in Urban Pedestrian and Cycling Microenvironments: Seasonal Trends, Source Apportionment and Health Risk Assessment

Ilenič, A., Kumar, P., Milačič Ščančar, R., Đurić, M., Mauko Pranjić, A., Ščančar, J. (submitted manuscript). Advances in sampling and analytical approaches for the determination of metal(oid)s and polycyclic aromatic hydrocarbons bound to size-fractionated airborne particulate matter: A review

Published Scientific Conference Contribution

Ilenič, A., Đurić, M., Milačič Ščančar, R., Mauko Pranjić, A., Ščančar, J. (2025, April 27−May 2). *Size-fractionation of airborne particulate matter: chemical properties, distribution and health risk assessment – a one year study in Slovenia, Central Europe.* [Conference presentation]. EGU General Assembly 2025, Vienna, Austria & online. https://meetingorganizer.copernicus.org/EGU25/EGU25-6515.html

Ilenič, A., Mauko Pranjić, A., Milačič Ščančar, R., Ščančar, J. (2023, May 31−June 2). *Validating affordable bicycle-mounted sensors for behaviour change to reduce air*

pollution. [Conference presentation]. 15th Jožef Stefan International Postgraduate School Students' Conference, Kamnik, Slovenia. http://ipssc.mps.si/auxiliary_material/BoA%20IPSSC%202023.pdf

Other Conference Contributions

Ilenič, A., Mauko Pranjić, A., Milačič Ščančar, R., Ščančar, J. (2024, November 22). *Izpostavljenost onesnaženemu zraku v prometu v Ljubljani*. [Conference presentation]. 11. srečanje o kemijski varnosti: zdravstvena tveganja zaradi onesnaženja zraka in vode, ki jih povzročajo gospodarske javne službe in promet, Ljubljana, Slovenia

Ilenič, A., Ščančar, J., Milačič Ščančar, R., Zupančič, N., Mauko Pranjić, A. (2023, September 3—8). *Utilisation of portable, low-cost air quality sensors as a monitoring tool for assessing air pollution in urban environment*. European Aerosol Conference, Málaga, Spain

Ilenič, A. (2022, June 14—17). *EIT Urban Mobility RIS Hub Slovenia – engaging cycling community in Slovenia*. Velo-city 2022, Ljubljana, Slovenia

Professional and Expert Papers

Ilenič, A. (2024, May 23). *Odkrivanje nevidnega – zmanjševanje onesnaženosti zraka v urbanih okoljih s pomočjo prebivalcev*. Alternator: misliti znanost. https://www.alternator.science/sl/daljse/odkrivanje-nevidnega-zmanjsevanje-onesnazenosti-zraka-v-urbanih-okoljih-s-pomocjo-prebivalcev/

Ilenič, A., Mauko Pranjić, A. (2023). *Analiza meritev PM2,5: Kakšen zrak dihajo kolesarji v Mariboru?* Mariborska kolesarska mreža: MKM: novosti in dobre prakse na slovenskih cestah. https://ibikemaribor.com/analiza-meritev/

Ilenič, A., Mauko Pranjić, A., Mladenovič, A. (2021). Kolesarjenje v mestih in kvaliteta zraka. *Gradbenik: revija za gradnjo, sanacije in gradbene materiale*. 25(10), 54—55.

Interviews, Podcasts, Radio or Television Broadcasts

Ilenič, A. (2024, December 16). *Vemo ali mislimo, da vemo? : onkraj zmotnih predstav z Anjo Ilenič*. Strašno hudi: podkast o ljudeh, ki ustvarjajo presežke, navdihe in predvsem strašno hude zgodbe. https://www.strasnohudi.si/novice/vemo-ali-mislimo-da-vemo-anja-ilenic

Ilenič, A. (2024, December 14). *Nevidni delci, veliki problem: grožnja onesnaženega zraka*. Večer.com. https://vecer.com/v-soboto/intervju-anja-ilenic-nevidni-delci-veliki-problemi-groznja-onesnazenega-zraka-10371986#google_vignette

Ilenič, A. (2024, October 28). *S kolesom v službo v prometni konici: kako varno je?* 24.ur. https://www.caszazemljo.si/ekologija/kolesarjenje-v-onesnazenem-zraku.html

Ilenič, A. (2024, October 17). *V delo vključuje tudi občansko znanost.* Delo.si. https://www.delo.si/novice/znanoteh/v-delo-vkljucuje-tudi-obcansko-znanost

Ilenič, A., Škrinjar, K., Čakarić, M. (2024). *Anja Ilenič : geologinja, ki opozarja na skrite grožnje trdnih delcev in kaže, kako lahko sami prispevamo k reševanju težav z onesnaženjem zraka.* Strašno hudi. https://www.strasnohudi.si/podkasti/anja-ilenic

Ilenič, A., Močnik, G., Benčina, M., Pohar, M., Koleša, T., Bolte, T. (2023). *Onesnažen zrak ubija - kako dolgo še?* Radiotelevizija Slovenija. https://prvi.rtvslo.si/podkast/studio-ob-1700/87/174944463

Other Publications

Patents

Oprčkal, P., Mauko Pranjić, A., Mladenovič, A., Meža, S., Ilenič, A., Šprinzer, M. (2024). *Construction composite from the residue of mixed municipal waste after mechanical treatment, process of its preparation and installation = Bauverbundwerkstoff aus den Rückständen gemischter Siedlungsabfälle nach mechanischer Aufbereitung, Verfahren zu dessen Herstellung und Einbau = Matériau composite de construction préparé à partir de déchets municipaux ayant subi un pré-traitement mécanique, procédé pour sa fabrication et mise en place dudit matériau* (European patent specification EP 4 132 731 B1, 2024-08-07. European Patent Office. https://worldwide.espacenet.com/patent/search/family/080448858/publication/EP 4132731B1?q=pn%3DEP4132731B1

Journal Articles

Ilenič, A., Lojen, S., Župan, I., Šarić, T., Šikić, Z., Vrhovnik, P., Dolenec, M. (2018). Is the Kornati National Park still an acceptable reference area for environmental studies? Geosciences, 18(11). DOI 10.3390/geosciences8110385

Published Scientific Conference Contribution

Ilenič, A., Mauko Pranjić, A., Kokot, D., Mladenović, A. (2022, March 28). *EIT Urban Mobility RIS Hub Slovenia – supporting innovative mobility community in Slovenia.* [Conference presentation]. ISEP 2022: 30th International Symposium on Electronics in Transport, Ljubljana, Slovenia

Other Conference Contributions

Ilenič, A., Mauko Pranjić, A., Kokot, D., Mladenović, A. (2022, March 28). *EIT Urban Mobility RIS Hub Slovenia – supporting innovative mobility community in Slovenia.* [Conference presentation]. ISEP 2022: 30th International Symposium on Electronics in Transport, Ljubljana, Slovenia

Mauko Pranjić, A., Ilenič, A. (2021, October 7−8). *EIT urban mobility – Solving the mobility challenges facing our cities.* 19th European Transport Congress of the EPTS Foundation, Maribor, Slovenia

Editorial

Ilenič, A. (editor), Košir, M. (editor), Šolc, U., (editor), Marinič, D. (editor). (2022, October, 24). *Surovinske potrebe za zagotavljanje prehoda na trajnostno in pametno mobilnost* (Proceedings of Conference Abstracts). EIT Open Day Slovenija, Ljubljana, Slovenia

Professional and Expert Papers

Ilenič, A., Mauko Pranjić, A., Kokot, D., Mladenovič, A., Košir, M. (2021). Skupnost znanja in inovacij EIT Urbana mobilnost – prijetnejše in bolj trajnostno bivanje v evropskih mestih z uporabo inovativnih rešitev. Urbani izziv. 32(2), 68−72, 136−140. http://urbani-izziv.uirs.si/Portals/urbaniizziv/Clanki/2021/urbani-izziv-2021-32-02-07.pdf, http://urbani-izziv.uirs.si/en-us/Summary_r?id=84&id_k=r&idc=8

Biography

Anja Ilenič is a research assistant at the Slovenian National Building and Civil Engineering Institute (ZAG). In September 2020, she completed her master's degree at the University of Ljubljana, where her thesis focused on assessing the anthropogenic pollution in soil and sediment from a lagoon contaminated by wastewater sewage. In October 2021, she enrolled in doctoral studies in the Ecotechnologies programme at the Jožef Stefan International Postgraduate School. Her current research focuses on air pollution assessment, primarily on the chemical characterisation of metal(oid)s and polycyclic aromatic hydrocarbons bound to size-fractionated airborne particulate matter, source apportionment and health risk exposure assessment. She is also actively involved in engaging citizens in air quality data acquisition through participatory approaches that utilise low-cost mobile sensors. During her doctoral studies, she received two research awards and participated in two Erasmus+ and one PROM research exchanges at the University of Surrey, United Kingdom and Wrocław University of Environmental and Life Sciences, Poland. She has over 38 contributions in the SICRIS database, including four scientific articles as a first author, accounting for over 51 citations according to Google Scholar database, five expert articles, one European patent and various publications in general media. She is a founding member of the Youth Council ZAG and is actively engaged in various international and national research projects aimed at integrating circular strategies into the built environment.